Investigating alterations in autophagy in Alzheimer's disease using human brain tissue and skin-derived fibroblasts

Diana-Madalina Stan

University of
Salford
MANCHESTER

School of Environment and Life Sciences

University of Salford

University of Salford, UK

Submitted in partial fulfilment of the requirements of the

Degree of Doctor of Philosophy, 2018

Table of Contents

List of Figures

List of Tables

ACKNOWLEDGMENTS

ABBREVIATIONS

Ach= Acetylcholine

AchE=Acetylcholinesterase

AD= Alzheimer's disease

AICD= amyloid intracellular domain

Ala= alanine

AMP= adenosine monophosphate

AMPK= adenosine monophosphate-activated protein kinase

ApoE= Apolipoprotein E

APP= Amyloid precursor protein

APS= ammonium persulfate

ATG= Autophagy-related genes

Bcl= B-cell lymphoma

BSA= bovine serum albumin

CA=Cornu Ammonis

CAA= cerebral amyloid angiopathy

ChAT= Choline acetyltransferase

CMA= Chaperone-mediated autophagy

CoA= Coenzyme A

CTF= C-terminus fragment

DAB= diaminobenzidine

DMSO=Dimethyl sulfoxide

EC= entorhinal cortex

ECL= electrochemiluminescence

EDTA= ethylenediaminetetraacetic acid

FAD=familial Alzheimer's disease

Glu= glutamine

GrDG= granular layer of dentate gyrus

H_2O_2= hydrogen peroxide

HRP= horseradish peroxidase

Hsc70=Heat shock cognate 70

Hsp70= Heat shock protein 70

LAMP2A= Lysosomal-associated membrane protein 2A

LC3= microtubule-associated protein 1A/1B light chain 3

LEC= lateral entorhinal cortex

LIR=LC3-interacting region

MA= Macroautophagy

MEC= medial entorhinal cortex

MoDG= molecular layer of dentate gyrus

mTOR= mammalian target of Rapamycin

NFT= Neurofibrillary tangles

NMDA- N-methyl-D-aspartate

PAS= phagofore assembly site

PD= Parkinson's disease

PE= phosphoethanolamine

PoDG= polymorphic layer of dentate gyrus

PSC=pluripotent stem cells

PSEN= presenilin

PtdIns3K= phosphatidylinositol 3-kinase complex

RIPA= radioimmunoprecipitation assay

SB= sample buffer

SDS= sodium dodecyl sulphate

SN= substantia nigra

TBS= tris-buffered saline

TC= temporal cortex

TEMED= tetramethylethylenediamine

ULK1= Unc-51like kinase 1

ULK2= Unc-51like kinase 2

Vps= vacuolar protein sorting

WM= white matter

ABSTRACT

Alzheimer's disease (AD) is the main cause of dementia, affecting 500,000 people in the UK. Pathology of AD is characterised by the accumulation of abnormally phosphorylated tau protein within neurofibrillary tangles and plaques containing amyloid-β (Aβ). Autophagy is a normal intracellular mechanism that functions to degrade damaged cellular proteins. Studies have shown that there is an association between the dysfunction of the two main autophagy pathways-macroautophagy (MA) and chaperone-mediated autophagy (CMA) - and AD. However, it is unclear how the autophagic pathway activity changes during disease progression and how this relates to the accumulation of abnormal protein deposits in the brain.

This study aimed to explore alterations in different autophagy pathway linked proteins with AD progression and find the relationship between MA and CMA. Immunohistochemical/double labelling techniques were performed on post-mortem human brain tissue from 45 cases. Three brain regions were used including the hippocampus, the frontal cortex and the occipital cortex. Autophagy was investigated via the assessment of cellular distribution of LC3, Beclin-1 (markers of MA) and LAMP2A, Hsp70 (markers of CMA). Neurofibrillary tangles and amyloid plaques were also assessed via immunohistochemistry. Skin-derived fibroblasts from AD patients were also used to test the cells potency to become eventual markers in the assessment of autophagy impairment in living patients with AD via Western blotting.

The results showed that the autophagy levels decline with increasing Braak, suggesting impairments in both MA and CMA. Also, the results showed that CMA markers were significantly lower in the hippocampus while MA changes were most prevalent in the frontal cortex. The hippocampal region CA1 had increased tau/amyloid-β deposition and decreased autophagy markers, while region CA4 had decreased tau/amyloid-β and increased autophagy markers. Western blotting revealed significant differences in LAMP2A and Beclin-1 expression between the control cells and the AD mutated cells.

Identifying cell models such as skin-derived fibroblasts from patients with AD and targeting the autophagy pathays dysregulated at particular disease stages could offer potential for novel therapeutic strategies to prevent AD pathogenesis.

Chapter 1   INTRODUCTION

1.1   Alzheimer's disease: a tremendous impact on society

1.1.1   Dementia prevalence

Dementia is a set of symptoms, caused by brain disease or injury and it is generally described as a slow, progressive decline in memory and cognition (Dobranici, 2010). Alzheimer's disease (AD) is the most common cause of dementia; it accounts for approximately two-thirds of all the cases of dementia worldwide (Karantzoulis, 2011). In 2015, AD International reported that there were 46.8 million people suffering from dementia with the number increasing to 50 million at present, according to Alzheimer's Research UK. The global number will increase to 152 million in 2050, a 204% increase (dementiastatistics.org).   In the UK, Alzheimer's Society outlines an estimation of 800,000 with dementia, of which 500,000 people suffering of AD, a number which is expected to increase to 1 million by 2025 and 2 million by 2051 (Thies and Bleiler, 2012). Alzheimer's Research UK also reports that the economic impact of dementia is greater than cancer and heart disease combined, currently costing the NHS £26 billion.

1.1.2 Symptoms of Alzheimer's disease

AD is characterized by symptoms that relate to impaired cognition leading to functional impairment in advanced stages. In early stages, the first signs are short term memory loss, difficulty in planning, solving problems, depression and apathy (Bäckman, 2004). Later on, in moderate stages of AD, patients experience long-term memory loss, irritability, aphasia, disorientation (DeFina, 2013). In advanced stages, the AD patients lose their ability to move independently and to communicate.

1.1.3 Historical background

AD was named after Bavarian psychiatrist Aloysius (Alois) Alzheimer (A.A.), one of the founders of the field of neuropathology and the doctor who first described the disorder.

In 1906, Alzheimer became famous by giving a lecture on his new discoveries which related to what was thought to be an uncommon disease of the cerebral cortex affecting a middle-age woman, Auguste Deter. She presented memory loss, hallucinations, disorientation and died at the age of 55. The post-mortem studies showed various abnormalities of the brain, where A.A. used the reduced silver staining method, described by Max Bielschowsky (Bielschowsky, 1902) to show abnormal protein aggregates such as senile plaques and neurofibrillary tangles which were evident in the shrunken cerebral cortex (see figure 1.1) (Goedert and Ghetti, 2007). Later on, Emil Kraepelin decided to name this unusual disease, Alzheimer's

disease as A.A.'s case was the first one to describe these unusual features associated with senile plaques and tangles, which opened a new area of neurodegeneration research (Swerdlow, 2007).

1.1.4 Molecular biology of Alzheimer's disease

From the early 1900s until present, the neuropathology of AD has been described by the presence of various microscopic lesions including neurofibrillary tangles, senile/amyloid plaques, granulovacuoles and eosinophilic rod like inclusions (Hirano bodies), cerebral amyloid angiopathy and glial responses (Serrano-Pozo, 2011). However, the two main physical hallmarks of AD are the amyloid plaques and the neurofibrillary tangles, by which a conclusive diagnosis is made (Perl, 2010; Tanghe, 2010) (see figure 1.1).
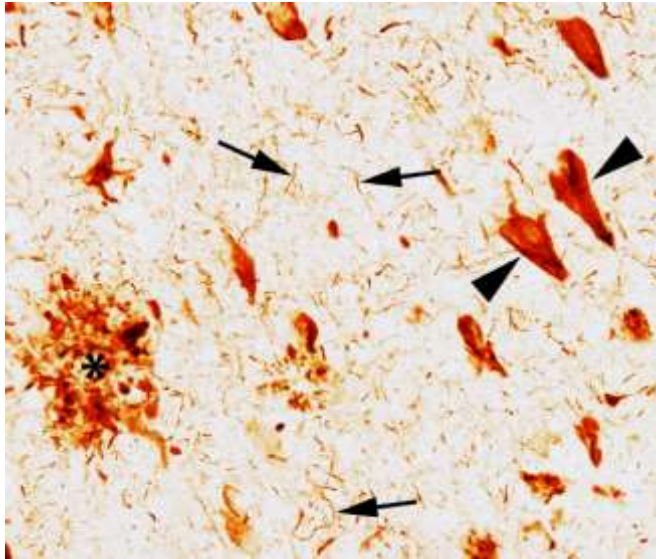
Figure 1.1 Alzheimer's disease pathology

Immunohistochemistry of an AD post-mortem brain section presenting neurofibrillary tangles (arrowheads), senile plaques (asterisk) and neuropil threads (arrows) (Kanaan, 2012).

At a structural level, abnormal intracellular neurofibrillary tangles consist of pairs of fibrils (paired helical filaments-PHF) made of hyperphosphorylated microtubule-associated protein tau. Formation of neurofibrillary tangles is proposed to result in extensive neuronal loss and impaired cognitive and memory functions (Nelson, 2012; Di, 2016). They are not specifically associated with AD but occur in numerous other neurodegenerative disorders called tauopathies which include fronto-temporal dementia with tau mutation on chromosome 17, Pick's disease, progressive supranuclear palsy and corticobasal degeneration (Wang, 2016; Wolfe, 2012).

The adult human brain expresses tau protein in 6 different isoforms depending on their number of binding domains, due to the inclusion/exclusion of the repeat region coded for by exon 10 and they are either three 3R or three 4R repeat domains (Goedert *et al*. 1989; Himmler *et*

al. 1989). Researchers have widely investigated tauopathies, including exploring the most predominant aggregation of the isoforms, either the 4R tau or 3R tau (Chen, 2010). Studies suggest structural and functional differences between the two tau splicing isoforms. There are similar expressed levels of 3R tau and 4R tau in the normal adult human brain however, the 3R/4R ratio is altered in the brains affected by tauopathies, suggesting that the tau aggregates can be either 3R or 4R specific (Liu, 2008). A study from 2014, relates how the two isoforms dominance relates to different neurodegenerative disorders (Sanders, 2014). They describe 3R to be specific to Pick bodies in Pick's disease, 4R to be associated to tau lesions in argyrophilic grain disease, progressive supranuclear palsy and corticobasal degeneration, while neurofibrillary tangles in AD have similar levels of 3R and 4R tau (Sanders, 2014).

Regarding structural differences, there is one study on human neuroblastoma SH-SY5Y cell lines overexpressing either human 4R tau or 3R tau which reported structural differences at 2N inclusion of tau isoforms (Chen, 2010). The most recent studies emphasize the functional difference of tau isoforms as they quantified and compared the ratio of 3R and 4R tau in mutant mice models and conclude that 4R overexpression leads to tauopathy pathology resulting in behaviour changes in MAPT N296H tau mouse model (Kathleen, 2016; Wobst, 2017).

Apart from conformational changes of tau and its truncation, the most well founded cause of defective tau in neurodegenerative disorders is the hyperphosphorylation of this microtubule protein which has been extensively explored over the past 3 decades (Alonso, 1994; Grundke-Iqbal,

1986). Aggregated tau protein, which undergoes hyperphosphorylation, changes the microtubule stability, the primary function of this protein. As a consequence, the cellular integrity as well as the cytoskeletal maintenance is altered and tau dysfunction could contribute to toxicity through various mechanisms such as axonal transport defects or synaptic damage (Jadhav, 2015). The altered microtubule stability due to tau hyperphosphorylation, as a result of kinase and phosphatase imbalances (Boutajangout, 2011), causes tau to dissociate from the microtubules which result in formation of insoluble oligomeric forms, altering the microtubule stability (Mietelska-Porowska, 2014). Neurotoxicity has been reported to arise from the direct toxic effect of free tau oligomers as evidence suggests an alternation of the mitochondrial membrane, minimization in complex I levels, and activation of the apoptotic-related caspase-9, resulting in toxicity (Churcher, 2006). Hyperphosphorylation and abnormal tau aggregation leads to neurofibrillary degeneration through cellular cytoskeletal changes as a consequence of abnornal tau which depolymerize the microtubule and leads to insoluble PHF formation (Šimić, 2016). Hyperphosphorylation has been explained to be an early and crucial event in the AD pathogenesis (Šimić, 2002), being clearly described by Braak as the neurofibrillary lesions develop across different brain regions at different stages of the disease.

Cytotoxicity of hyperphosphorylated tau could be explained as it has been shown to sequester normal tau into abnormal tangles of filaments stimulating microtubule alteration (Alonso, 1996). Moreover, an example of studies exploring conformational changes and abnormal aggregation of aberrant proteins is prion disease focused studies where structural changes

are explained through polymerization of a functional protein into an aberrant structured protein that is highly likely to have cytotoxic effects which could explain cytotoxicity of abnormal tau aggregates (Avila, 2006).

Existing tau species including oligomeric tau and soluble tau are known to be cytotoxic to the neurons and to the synapses in AD, with the oligomeric tau form being extensively investigated and proposed as a potential diagnostic biomarker for early detection of AD (Cárdenas-Aguayo, 2014; Guerrero-Muñoz, 2015; Sengupta, 2017). In 2009, an *in vivo* study on AD like tauopathy transgenic mouse model suggested an increase of insoluble tau fractions with ageing, in contrast to reduced soluble tau fractions and lower levels of hyperphosphorylation (Hirata-Fukae, 2009). Despite these findings, recent studies demonstrate that soluble tau species are highly toxic to the neurons and to the synapses in AD brains as injection of human soluble tau into the dentate gyrus of mice hippocampus showed reduction of synapses and synaptic vesicles, affecting the morphology and the connectivity of granule cells (Kopeikina, 2012; Bolós, 2017; Stern, 2018).

Since over two decades ago, it has been described that neurofibrillary tangles are a sign of cell death that results in neurodegeneration and directly correlates with the dementia status in AD in contrast to the plaque deposition (Bierer, 1995; Nelson, 2012; Di, 2016). The abnormal accumulation of tau is highly damaging to the brain and therefore a rapidly developing area of research is trying to find a way to clear defective proteins before cell death is initiated (Kayed, 2010; Herrmann, 2014; Funk, 2015). Phospho-tau AT8 monoclonal antibody is widely used to visualize

the abnormal hyperphosphorylation, targeting PHF-tau (Ser202/Thr205) and enables researchers to assess the severity in AD (Goedert *et al*, 1995). At first instance, in AD, neurofibrillary tangles seem to occur in regions such as hippocampus, limbic structures and the basal nucleus of Meynert and then spread to the parietal cortex, the frontal and the occipital cortex (Lace, 2009).

The other lesions, found in AD post-mortem brain tissue, are the senile/neuritic plaques, located extracellularly between the neurons. These are abnormal accumulations of insoluble misfolded amyloid proteins that result in a toxic amyloid form called beta amyloid (Aβ) (Perl, 2010). Over the past 25 years, there have been numerous clinical and genetic studies describing the role of Aβ and the accumulation of the toxic plaques in AD (Kirkitadze and Kowalska, 2005). Aβ peptide is a 4kDa protein, which results form the proteolytic processing of amyloid precursor protein (APP), and is the main component of the amyloid plaques in AD (Murphy and LeVine, 2010). APP is highly expressed in the brain and it is cleaved by enzymes called α- and γ-secretases, resulting in toxic Aβ fragments such as C99 and APPβ (O'Brien, 2011). A more in-depth description of APP processing to Aβ is described in section 1.1.7. After formation of Aβ fragments, a complex process takes place and through fibrillization of Aβ fragments, senile plaques are formed (Walsh *et al*, 2010). Aβ fragments can be found bound to proteins such as apolipoprotein E albumin or complement proteins (Ma *et al*, 2011), but it can also be present as soluble dimers, which were detected in brain homogenates and cell culture media (Enya *et al*, 1999). In young and healthy brains, Aβ is fully catabolised after

it is secreted with no deposition taking place, however, in the ageing brain, Aβ production is enhanced, leading to deposition and reduced clearance (Kirkitadze and Kowalska, 2005). Studies have identified three types of Aβ oligomers such as very short oligomers (dimers to hexamers), small oligomers between 17kDa and 42 kDa, called Aβ-derived diffusible ligands, and protofibrils between 8nm and 150nm (Kirkitadze and Kowalska, 2005). Another study identified a stronger relationship between oligomers and altered neuronal viability, compared with the fibrils, emphasizing the importance of the regulation of oligomers and protofibrils formation in AD (Dahlgren *et al*, 2002).

Aβ40 and Aβ42 are the main Aβ isoforms, present in AD pathology and have been found to have different oligomerization pathways, as Aβ42 forms fibrils faster than Aβ40 and is more neurotoxic due to an extra Asp23-Lys28 salt-bridge in its structure (Kirkitadze et al, 2002; Ahmed, 2010). Presenilin proteins, PSEN1 and PSEN2, are known to regulate γ-secretase proteoytic function, therefore mutations in the presenilins can affect the enzyme funtional rate and lead to an increase production of Aβ (Ridge *et al,* 2013). Besides neurotoxicity, Aβ in high concentrations can also alter the blood flow, resulting in neuronal dysfunction due to Aβ accumulation in the cerebral blood vessels, known as cerebral amyloid angiopathy and considered a hallmarks of AD (Attems, 2010). Vascular accumulation of Aβ can cause vasoconstriction and impairment of the vascular tone, causing alteration of neuronal projections (Harkany, 2010).

Considering all AD hallmarks, it has been very challenging to develop the perfect transgenic animal model – in particular, a mouse model – due to the

complexity of the disease and replicating all pathological characteristics (Saraceno, 2013). Most of the transgenic models that have been developed exhibit some of the AD hallmarks, including Aβ plaques (Platt, 2013). Researchers have mainly focused on the amyloid cascade hypothesis – which is described in detail in Section 1.1.7 – based on which amyloid deposition is the key contributor to pathogenesis and neurodegeneration. One of the first AD transgenic model was reported in 1995 and expressed high levels of mutant APP that could generate extracelular neurotoxic Aβ (Spires, 2005). Different types of mutations determine the nature of the neurotoxic fragments. For example, mutations at the N terminus of Aβ results in mutant Aβ40 and Aβ42, however, mutations at the C terminus lead to Aβ1-42 isoform (Xu, 2016). There are numerous AD studies, decribing such models that focus on amyloid deposition and these models are further described in Section 1.5.

In 1986, the Consortium to Establish a Registry for Alzheimer's disease (CERAD) was funded by the National Institute on Aging (NIA) (Fillenbaum, 2008) due to a need of standardized and reliable diagnostic criteria for AD and it has been used in neuropathological clinical studies to evaluate the presence of tau tangles or neuritic plaques (NP) and determine the stage of the disease (Murayama, 2004). Based on CERAD criteria, the cortical density of beta-amyloid plaques is measured from 0 (none) to C (abundant) (Mirra, 1991) (see Section 1.2).

1.1.5   Environmental risk factors

Age is one of the major factors of AD (Guerreiro, 2015) in both males and females (Ruitenberg, 2001). The prevalence of the neurodegenerative disorder doubles every 5 years after the age of 65. It is known to occur in 1 in 10 individuals aged 65+ and in 1 in 3 people aged 85+ in developed countries (Qiu *et al.*, 2009).

Cardiovascular disease is another major AD risk factor with smoking being known to increase the chance of cardiovascular diseases. Therefore, smokers have 45% greater risk of developing dementia, in particular AD by accelerating the brain ageing and its cortical reduction (Cataldo, 2010; Durazzo, 2014). Smoking is also known to be a high risk of developing atherosclerosis, mainly affecting the endothelial cells and resulting in tissue remodelling and activation of inflammatory responses (Messner, 2014). This leads to changes in the vessel walls resulting in cerebral small vessel disease which interconnects with AD (Fitzgerald, 2014). Moreover, tobacco, the main component of smoking cigarettes contains several neurotoxins such as nicotine alkaloids and acetylaldehydes, which directly damage the neuronal cells, event seen in AD (Treweek, 2009).

It is well known that obesity has negative effects on the cardiovascular system, leading to insulin resistance, hypertension and type 2 diabetes (Pi-Sunyer, 2009). There is a lot of research evidence that links obesity and diabetes as risk factors of AD (Alford, 2018), as resistance to insulin overstimulates the pancreas to produce insulin, accelerating its failure (Cerf, 2013). Excessive insulin levels in the blood are also reported to interfere with the brain glucose levels by passing the blood brain barrier and binding

to insulin receptors on neurons and glial cells, resulting in impaired cognition and memory loss (Banks, 2012; Gray, 2014)

1.1.6   Genetic risk factors

Familial AD (FAD) or early onset AD (EOAD refers to the disease starting at earlier ages than usual, between 30-65 years old and it accounts for 1-2% of all AD cases, arising from one of the three mutations in either APP gene, Presenilin 1 (PSEN 1) or Presenilin 2 (PSEN 2) genes, components of the γ–secretase enzyme, responsible in cleavage of beta-amyloid (Zhu, 2015). EOAD cases with APP mutations account for 10-15% of all EOAD cases, while PSEN1 mutations are more common, being found in 18-50% of EOAD cases (Bekris, 2010). Bekris's review from 2010, also reported that PSEN2 mutations in FAD, found in only 6 families, by that time, were much rarer than PSEN1 mutations seen in 390 families (Bekris, 2010). The mechanisms by which APP mutations lead to neurodegeneration are explained through the amyloid hypothesis which is described in detail in the next subsection 1.1.6. FAD is strongly linked to the family history of neurodegeneration, diabetes status, vascular diseases and ApoE4 variant, the largest genetic risk factor in late-onset sporadic AD (Blennow, 2006; Harold, 2009).

Apolipoprotein E (ApoE) is a lipid transport protein, carrying cholesterol and phospholipids, being encoded by genes located on chromosome 19 and is known to supports injury repair in the brain (Liu, 2013). ApoE is polymorphic with different allelic variants such as ε2, ε3 and ε4 (Figure 1.2) (Ghebranious, 2005). It has been shown that individuals carrying the ε4

allele have a higher risk of developing AD compared with those carrying ε3 allele, found more frequently (Farrer, 1997), whilst ε2 allele is shown in population based studies to decrease the risk of AD (Figure 1.3) (Farrer, 1997; Verghese, 2012; Liu, 2013).

ApoE4 genotype together with atherosclerosis, diabetes and peripheral vascular disease contribute to a high risk of AD (Haan, 1999). ApoE4 allele and cerebrovascular disease also contribute to cognitive decline in patients with AD (Liu, 2013). Diabetes plays a crucial role amongst risk factors with a strong link of people carrying the ApoE4 allele with diabetes and AD (Irie, 2008; Matsuzaki, 2010). AD pathogenesis is worsen by diabetes complications such as neuropathy and vascular damage (Yagihashi, 2011). Studies have shown that carriers of ApoE4 that suffer from diabetes can present AD pathology including neurofibrillary tangles, amyloid plaques and cerebral amyloid angiopathy (CAA) (Peila, 2002). Neuritic plaque deposition is promoted by ApoE4 allele and diabetes factors such as hyperglycaemia, insulin resistance and hyperinsulinaemia (Matsuzaki, 2010). Other studies demonstrated that ApoE4 can trigger inflammation related events, independently from Aβ, leading to neuronal damage, neurovascular dysfunction, reduction in the length of small vessels, blood brain barrier breakdown resulting in leakage of toxic proteins into the brain (Bell, 2012).

ApoE$_4$ has also been linked to prevalence of coronary artery disease and cerebrovascular ischemia with increased risk of cerebral amyloid angiopathy (a condition in which amyloid spreads and deposits the blood vessels), which are all significant risk factors in AD (Eichner, 2002). ApoE$_3$

could also relate to the amyloid cascade hypothesis as previous, biochemical assays confirmed interaction between ApoE3 and Aβ, as ApoE3 is thought to mediated the clearance of Aβ (Carter, 2005; Kanekiyo, 2014), however it is not associated with increased AD risk. ApoE3 was also shown to protect the neuronal cells from the toxic effects and oxidation by the presence of Aβ (Parihar and Hemnani, 2004).

Some researchers are describing the post-traumatic brain injury to be linked to ApoE4, thus a risk factor in AD (Fleminger, 2003; Verghese, 2011). There is a study suggesting that AD pathology increases by 35% in ApoE4 allele carrier patients as a results of traumatic brain damage, 6 months post head injury, resulting in post-mortem abundant Aβ plaque deposition (Nicoll, 1995). On the other hand, only 10% of ApoE4 noncarriers with brain injury presented Aβ pathology (Nicoll, 1995), suggesting that ApoE4 allele is linked to increased risk of AD after head injury. The post injury outcomes are thought to be declined due to reduced repair ability of the nervous tissue and post-trauma reduced synapse remodelling (Bu, 2009).
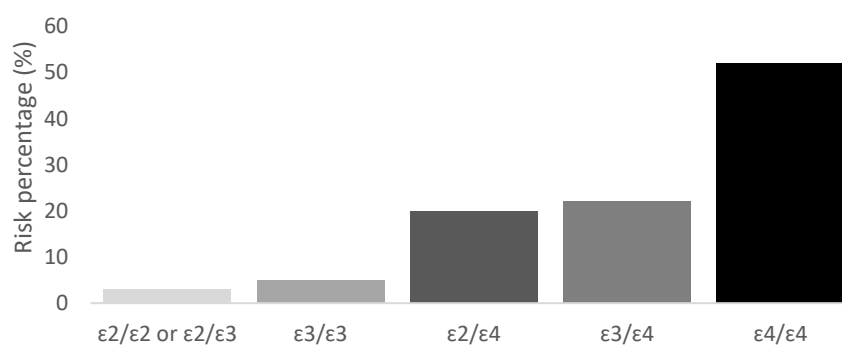
Figure 1.2 ApoE risk factor. Percentage of lifetime risk of developing Alzheimer's disease based on ApoE genotype comprising of the three alleles.
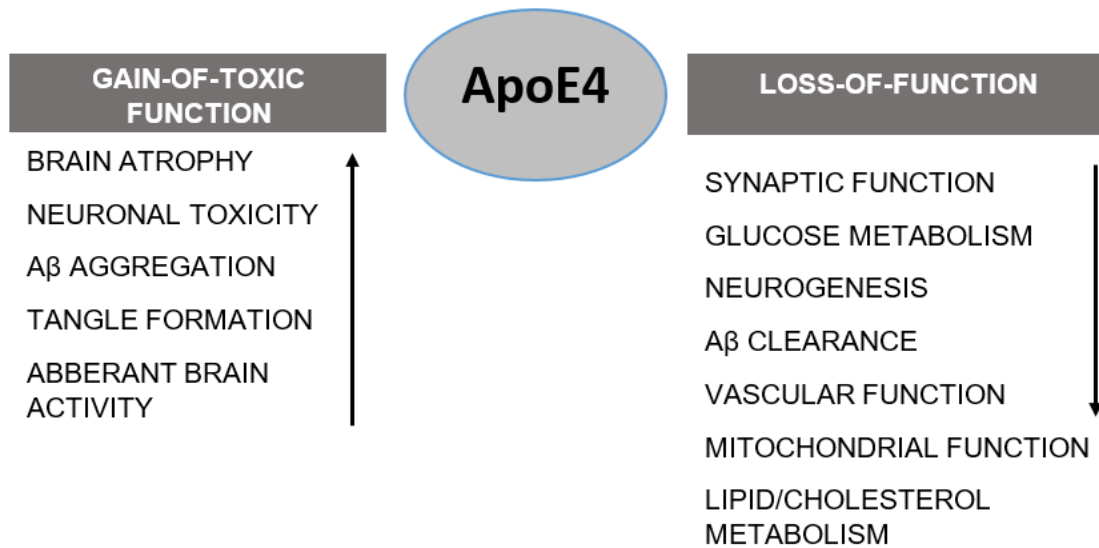
Figure 1.3 ApoE functions. Apolipoprotein E4 roles in Alzheimer disease pathogenesis. ApoE4 confers toxic gain of function, loss of neuroprotective function or both in the pathogenesis of Alzheimer disease.

There is also evidence of education playing an important role in the risk factors of AD as a recent paper, based on an American study, the Framingham Heart Study which is a longitudinal cohort, community based initiative, comprising of over 5000 people from Framingham, Massachutes, states that there is a decline in the risk of developing dementia in the higher educated people (Satizabal *et al*, 2016). Persons who had at least a high school diploma shown a temporal decline over three decades with an improvement in the cardiovascular health suggesting that higher education levels could have contributed to the onset delay which was observed in the study (Satizabal *et al*, 2016).

The Framingham Heart study which has had patients under dementia surveillance since 1975 offered data which has been considered to be reliable by the Alzheimer's Association using them for educational purposes (Seshadri, 2007). However, the study had some limitations as worldwide there are millions of people suffering from AD and the study has only used 5000 participants which are of European ancestry. Therefore, it is unclear whether the study can be replicated within groups of participants belonging to other ethnic background and races (Satizabal *et al*, 2016). Despite these findings of declining dementia incidence, the worldwide dementia number will continue to increase rapidly as estimations suggest, especially in the economically vulnerable and developing countries, where life expectancy and higher education rate are lower (Wu, 2015; Chan, 2013; George-Carey, 2012). There is also a European study, from Switzerland emphasizing how lifestyle and higher education amongst people can reduce the burden of AD pathology, in particular the amyloid plaques found in the diseased brains, which declined over a time of three decades (1972-2006) (Kövari, 2014). Similarly to Framingham Heart Study, the findings might relate to changes in lifestyle, diet, physical activity and high education as Switzerland is a highly developed country.

These studies are thought to have a crucial role in explaining and understanding the importance of risk factors and how they impact on the prevention and the disease delay, despite the small number of participants in the studies, compared to the millions of AD sufferers worldwide and considering the increasing number projections over the next decades (Prince, 2013).

1.1.7   Historical hypotheses of Alzheimer's disease

There are two main historical hypotheses which describe the molecular events that may lead to AD and attempt to explain the comprehensive pathogenesis of this disorder: the cholinergic hypothesis and the amyloid cascade hypothesis (Parihar and Hemnani, 2004). Though neither offer a full explanation of the disease pathogenesis, both offer same insight to the disease process and are useful for highlighting the key early research findings in this field.

The cholinergic hypothesis

The cholinergic hypothesis suggests that a defective cholinergic system and loss of cholinergic neurons in the basal forebrain is linked to memory loss and neurodegeneration (Mufson, 2008). Importantly, this hypothesis suggests that cholinergic cells are characterized by selective vulnerability in the AD pathogenesis (Mufson, 2008). However, more recent studies argue that pathogenesis spread is impacting a variety of cells including the CNS immune cells: astrocytes, microglia and others (Kurosinky, 2002; Serrano-Pozo, 2011; Van Eldik, 2016). Cholinergic neurons are specialized nerve cells that produce the neurotransmitter acetylcholine and are involved in the cortical activation of the brain during wakefulness but also during the sleep state (Deurveilher, 2011). Impairment in the acetylcholine-based pathway (Ach) was suggested to occur as a result of reduction in both the

synthesizing enzyme choline acetyltransferase (ChAT) and the metabolizing enzyme acetyl cholinesterase (AchE which converts Ach into inactive choline and acetate). This was proposed to lead to a cascade of molecular events including depletion of Ach neurotransmitter, essential in sending signals between the neurons of the parasympathetic nervous system (Parihar and Hemnani, 2004).

In the early 1970s, researchers initiated a biochemical investigation of post-mortem AD brains, hoping that they would identify a neurochemical imbalance that could be to treat AD (Francis, 1999). In the following years, studies have identified deficits of ChAT enzyme in the neocortex and reduced levels of Ach, confirming a cholinergic impairment (Bowen, 1976; Davies, 1976; Perry, 1977).

Ever since then, researchers took the theory into consideration for a potential therapeutic approach to target and correct the neurochemical alterations found in the samples (Contestabile, 2011). Current drugs such as cholinesterase inhibitors that aim to enhance the cholinergic neurotransmission already exist such as donepezil, rivastigmine, galantamine and tacrine (described later on in section 1.1.4). They ameliorate the symptoms, but cannot repair or reverse the neurodegenerative mechanisms, lacking efficacy once the cells die. Currently, the main treatment of AD, works by aiming to enhance the cholinergic transmission, however it does not cure or slow AD progression, demonstrating that the hypothesis has limitations as it does not explain the underlying cell death or formation of abnormal protein aggregates.

The amyloid cascade hypothesis

Another theory of AD pathogenesis, which was proposed by John Hardy in 1992, the amyloid cascade hypothesis, is based on explaining neurodegeneration as a result of excessive production and accumulation of extracellular β-amyloid (Aβ) plaques (Figure 1.1) which eventually leads to deposition of intracellular neurofibrillary tangles (NFT) (see figure 1.4) (Hardy and Higgins, 1992; Reitz, 2012).

The β-amyloid protein occurs as a result of proteolytic processing of its parent protein, APP, which lies on chromosome 21 (Selkoe, 1988; Korenberg, 1989). Its importance has not been clearly emphasized, however it is thought to be essential for neuronal growth, thus cerebral development (Swerdlow, 2007; O'Brien, 2011; Müller, 2012). More recent papers support that APP controls cholesterol homeostasis, promotes the cell survival and the formation of the synapses between neurons as well as being involved in neurons maturation as a result of APP being expressed at early stages of nervous system development (Dawkins, 2014; Kant, 2015). One of the most recent papers reviews the findings on *in vivo* APP knockout mouse studies, focusing on the function of the APP protein and the APP fragments in the development of the nervous system, synaptogenesis, neuroprotection, brain injury and ageing (Müller, 2017).

Amyloid precursor protein is a transmembrane protein which consists of 770 amino acid residues (Matsui, 2007). Its amino-terminal domain is hydrophilic and it is situated extracellularly. The transmembrane domain is hydrophobic continuing with a small carboxyl-terminal cytoplasmic domain

(Parihar and Hemnani, 2004) (see figure 1.5). Secretases α, β and γ are essential enzymes involved in the production of Aβ from APP parent molecule (Hartmann, 2013) (see figure 1.5).
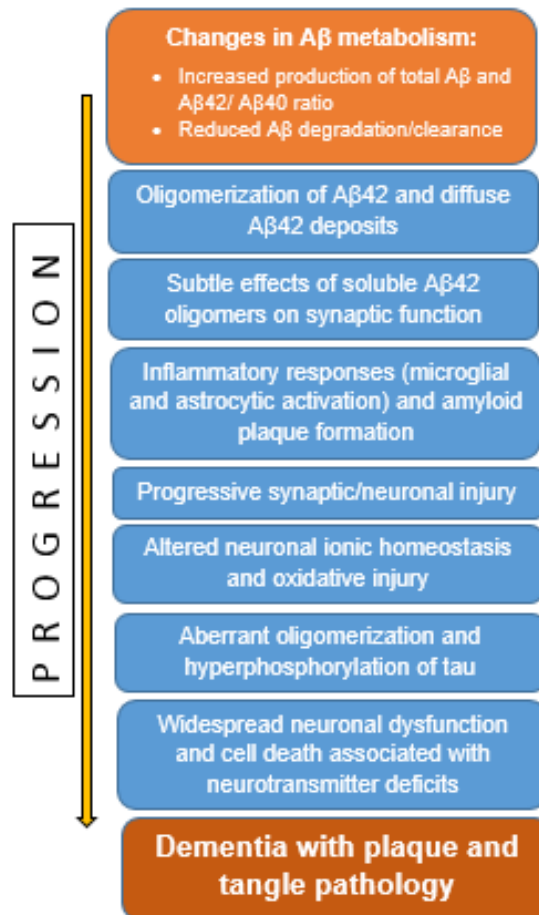
Figure 1.4 The amyloid cascade hypothesis. This hypothesis describes the events that lead to dementia pathology showing that the hypotheses can coexist with abnormal accumulation of plaques, hyperphosporylation of tau and reduction of neurotransmitters in the brain.

Secretases α, β and γ cleave the APP molecule at different positions, respectively at residue 687 by α-secretase and at residue 671 by β-secretase, resulting in large soluble N-terminus fragments, sAPPα and sAPPβ (see figure 1.5). In addition, smaller C-terminus fragments are released: C83 and C99, which are further cleaved by γ-secretase. Cleavage of C83 results into Aβ40 and Aβ42 whereas C99 peptide fragment results into Aβ40 (more common and soluble form) and Aβ42, having two more amino acids on the tail end of the peptide (see figure 1.5). One of these, amino acid 42 is represented by alanine, which extends, resulting in a salt bridge with amino acid 35, and methionine. This makes Aβ42 less soluble and more toxic (Kowalska, 2004; Kazuhiro, 2005).

In this hypothesis, the Aβ plaque accumulation is proposed to act as a pathological trigger for a cascade of neurotoxic events such as free radicals release, inflammatory responses in the neurons within the brain, neuritic injury, disruption of Ca^{2+} channels (Kowalska, 2004), all leading to irreversible neuronal damage, cell death and shrinkage of the brain (Figure 1.4) (Parihar and Hemnani, 2004).
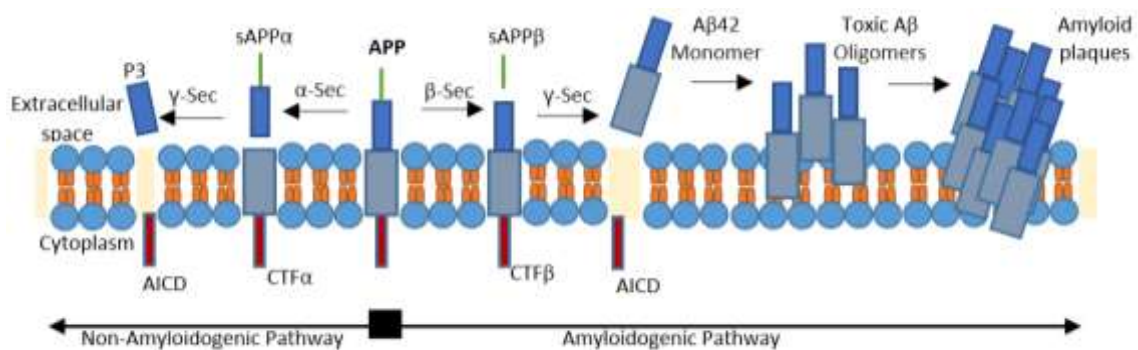
Figure 1.5 APP processing. Diagram describing the processing of amyloid precursor protein (APP) via the non-amyloidogenic and the amyloidogenic pathways leading to Aβ plaques formation that trigger AD pathology. APP molecule is cleaved by α-secretase (α-sec) resulting in sAPPα fragment and a C-terminus fragment (CTFα or C83), which is further cleaved by γ-secretase to P3 peptide and AICD (amyloid intracellular domain) which are non-plaque fragments. The amyloidogenic pathway starts with APP being cleaved by β-secretase releasing sAPPβ and CTFβ or C99 which is then cleaved by γ-secretase, resulting in monomers of Aβ38-42 which fold into the toxic plaques.

This hypothesis was supported by human genetic studies (Goate *et al*, 1991). In the early 1990s, the amyloid cascade hypothesis was formulated after a case of APP gene mutation was discovered in a family with autosomal dominant, early onset AD. At this point, the hypothesis was only sustained by the idea that the mutation in the APP gene causes alteration in the β-amyloid production, giving rise to senile plaques formation and dementia related symptoms (Goate *et al*., 1991). Later on, further research studies failed to prove that this was the only cause of AD but researchers

continued the genetic analysis finding results that contributed to the consolidation of the hypothesis (Swerdlow, 2007).

Two important gene mutations were found on chromosome 14 in presenilin 1 gene and on chromosome 1, in gene presenilin 2. These were shown to cause early onset of autosomal dominant hereditary AD (Levy-Lehad *et al.*, 1995). Understanding of presenilin proteins functions was poor; however it was found that the mutations increased the production of a long 42 amino acid APP C-terminal product Aβ42. This product manifests toxicity to cells grown in culture and it is found within the plaques specific to AD pathology, due to its aggregation properties (Scheuner *et al.*, 1996). However, as more studies were done on the key AD protein, tau, researchers, began to argue the compentence of this protein as well as β-amyloid. This was particularly after tau mutations were found to underlie FTDP-17 (Gpedert, 1999).

Additionally, amyloidocentric drugs were not proven successful in clinical trials (Tarenflurbil, Bapineuzumab, etc.-see Table 1.1) suggesting that β-amyloid build-up alone, might not fully underlie AD pathogenesis (Karran, 2016). The amyloidocentric drugs have been described through programs that involved patients with mild to moderate AD, reaching Phase II and III clinical trials, however most of them were terminated or discontinued (see Table 1.1) (Morris, 2014).

A review paper from 2009 describes the missing gaps in the amyloid cascade hypothesis supporting research (Hardy, 2009). The paper debates animal studies on Aβ toxicity, one of the main hypothesis events, suggesting that although there is evidence on behavioural improvements such as enhancing memory and learning after passive immunization with

anti β-amyloid monoclonal antibody, there is no convincing evidence to reduce the massive cell loss seen in AD brains, thus slow the disease progression (Morgan *et al*, 2000; Dodart *et al*, 2002). A second aspect debated in the paper is based on tau pathology developing as a secondary effect in the amyloid cascade events. Cell studies suggest that tau pathology can modulate β-amyloid toxicity (Roberson *et al*, 2007), however the actual relationship between β-amyloid and tau protein has been described to be very complex in human studies (Mudher and Lovestone, 2005). Although β-amyloid deposition is thought to occur prior to the neurofibrillary tangles, tau pathology has been described to be more related to cellular death and neuronal loss (Hanger *et al*, 2009). Numerous papers review experimental evidence from AD patients' studies or from *in vivo* and *in vitro* animal studies, suggesting that the two AD pathological hallmarks, tau and β-amyloid interact with each other, as β-amyloid expresses its toxicity via tau (Wray, 2009; Nisbet, 2014; Stancu, 2014). Some papers suggest that β-amyloid plaques form in neocortical areas that receive afferent projections from NFT containing neurons, which could indicate a link between the presynaptic NFT and the postsynaptic plaques (Ittner, 2011; Musiek, 2015). In the most recent study, aiming to explore the relationship between tau and β-amyloid in AD, researchers performed *in vivo* PET scans on β-amyloid positive and negative AD patients. Results suggested that tau accumulation was locally associated to plaque burden in the frontal, cortex and the occipital cortices (Iaccarino, 2018).

There is plenty of evidence that both tau and β-amyloid have neurotoxic effects in AD brains and as a result, a successful treatment approach would

be to establish new ways of clearing both abnormal protein aggregates (Bloom, 2014; Lansdall, 2014; Lloret, 2015; Nisbet, 2015).

Table 1.1 AD clinical trials in 2014. Amyloid hypothesis-based trials that tested different amyloidocentric drugs that reached phases II and III, however most of them were discontinued or terminated (adapted from Morris, 2014).

Mechanism of action	Drug name	Clinical Phase	Key results from each trial	Current status (August 2014)
Active immunisation with Aβ	AN1792	2	Plaque cleared. NFT reduced in neuronal processes, but not cell bodies. Very few antibody responders (25/239). Reports of encephalitis	Discontinued
	CAD106	2	Favourable safety profile. Prolonged antibody titre in responders.	Ongoing
	ACC001	2	Co-administration of adjuvant required for strong antibody response. Generally safe and well-tolerated, no adverse-related events.	Discontinued
	AD02	2	Favourable safety and tolerability profile. Did not reach primary or secondary outcomes measures in phase 2.	Ongoing
Passive immunisation with Aβ	Solanezumab	3	Worsening cognition compared to placebo, multiple adverse events.	Terminated
	Babinezmab	3	Engaged target. Reduction in cerebrospinal fluid phospho-tau in APOE4 carriers. Decreased rate of amyloid accumulation in APOE4 carriers. No improvement in clinical outcomes in carriers or non-carriers of APOE4. Negative amyloid scans in 36% of non-carriers.	Discontinued
	Gantenerumab	2 and 3	Safe and well-tolerated at phase 1. Focal inflammation in areas with amyloid reduction a concern. Amyloid reductions compared to placebo.	Recruiting for Phase 3 DIAN trial

	Crenezumab	2	Did not meet co-primary endpoints. Trend of improved cognition in people with mild disease.	Ongoing
	Ponezumab	2	Safe and well-tolerated at phase 1. Plasma Aβ40 increased at phase 2. No effect on primary endpoints in phase 2.	Recruiting for further Phase 2 trials
γ-Secretase inhibitors	Avagacestat	2	Gastrointestinal and dermatological side effects at phase 1. Also dose-dependent pharmacodynamics effects on CSF biomarkers in some patients. Trend towards worsening cognition at higher doses compared to placebo. Amyloid related imaging abnormalities.	Discontinued
	Semagestat	3	Dose-dependent reduction in Aβ synthesis at phase 1. Reduced plasma Aβ at Phase 2, but no differences in cognition. No improvement in cognition and worsening cognition at higher doses compared to controls at Phase 3.	Discontinued
γ-Secretase modulators	CHF5074	2	Anti-inflammatory at Phase 2. Trend towards improved function in APE4 carrier.	Ongoing
	EVP-0962	2	Does not inhibit cleavage of γ-secretase substrate other than APP.	Ongoing
	Tarenflurbil	3	Small functional benefit at higher doses in mild AD but no cognitive benefit at Phase 2. No changes in CSF Aβ42. Failed to meet primary and secondary endpoits at phase 3.	Discontinued
β-Secretase modulatos	MK-8931	3	Reduced CSF Aβ compared to controls. Safe and tolerable at Phase 2.	Recruiting for Phase 3
	CTS-21166	1	Dose dependent reduction in plasma Aβ.	Completed

According to Karran and Hardy, most of the drugs tested failed to replicate their benefits which were previously proved in the research laboratories, into the clinical science on patients (Karran and Hardy, 2014). As an example, Solanezumab appeared to improve cognition in Phase II clinical trials in mild stages of the disease but failed in phase III revealing multiple adverse effects (Siemers *et al.,* 2016). According to Morris and co-workers, there are still many gaps in the research field of amyloid hypothesis, with poorly explained Aβ presence in cognitively healthy people, weak correlation between how cognition is affected by the plaques and many unresolved questions regarding the chemical nature, presence and importance of the Aβ oligomeric fragments. Reviewing the existing evidence, it was concluded that it is necessary for the AD pathogenesis research to go beyond the existing hypothesis including Aβ and tau pathology (Morris, 2014). A more recent paper, from 2016, is reviewing the amyloid cascade hypothesis, at 25 years, after it has become one of the most important AD related theories, covering the treatment development and the latest findings (Selkoe, 2016). It suggests a novel antibody against β-amyloid, aducanumab, which has demonstrated slowing effects on cognitive decline in 165 patients with mild AD. Selkoe mentions that the human monoclonal antibody BIIB-037 (aducanumab) passed Phase 1b trial in 2014 and the studies show that it has entered Phase 3 trial in 2015 (Selkoe, 2016). The limitations of the study described how the antibody was binding to the plaques and the oligomers but not to the monomers, despite the cognitive improvement in the AD patients. According to the U.S. National Library of Medicine, aducanumab was still in Phase III

immunotherapy trial in September 2017, targeting Aβ in early and mild to moderate AD subjects (Cummings, 2017).

Selkoe's paper describes that although there are many contributing factors to AD pathogenesis, β-amyloid approach remains the most proven theory contributing to the disease progression that could target potential therapeutics (Selkoe, 2016). Nevertheless, the amyloid cascade hypothesis has been useful to contribute to both academia and industry science and the field has established that amyloid deposition occurs many years before the first AD symptoms resulting in a preclinical asymptomatic amyloidosis phase (Sperling *et al.*, 2011). Many researchers argue that anti-Aβ drugs would only be beneficial if given at pre-clinical stages of AD but practically this would be very difficult to conduct (Hardy, 2011; Selkoe, 2016). This research based on Aβ clearing is still very popular (Ries, 2016; Wood, 2017; Zuroff, 2017), however neither fully explain AD biochemical and histopathological lesions which might explain the limitations in developing effective drugs to cure AD (Roy, 2005; Morris, 2014; Selkoe, 2016; Harrison, 2016).

As previously mentioned, abnormal tau and β-amyloid, characterized by neurotoxicity, become damaging to the healthy brain cells, disrupting the functioning of the synapses and altering the axon transportation. As a result, neuronal injury and cell loss lead to plaque and tangle pathology and lastly to neurodegeneration (Bloom, 2014; Lloret, 2015; Nisbet, 2015). All these mechanisms have been intensively investigated by researchers and one of the main focuses targerted the clearance of the abnormal tau and β-amyloid aggregates (Lansdall, 2014; Tarasoff-Conway, 2015). More recent

studies support defective protein clearance pathways in AD, which could lead to abnormal accumulation of tau and β-amyloid (Nixon, 2005; Pickford, 2008; Son, 2012, Nixon, 2013; Talboom, 2015).

Nixon was one of the first researchers to explain how electron microscopy revealed increased immature autophagic vacuoles within the lysosomes of the AD brain cells, as well as finding high autophagic levels in the cell bodies of the damaged neurons containing NFT (Nixon *et al*, 2005). Nixon's study suggested how impaired autophagy, due to incomplete development of autophagic vacuoles, altered their transportation to the lysosomes enabling a normal autophagy functioning. These findings were supported by another study which described how immunolabeling detected immature autophagy vacuoles, in the human brain, which were found to be abundant in beta-cleaved APP, complete APP or presenilin proteins (Yu *et al*, 2005).

Restoring the function of protein degradation pathways could potentially clear the abnormal protein aggregates found in AD brains, however there are still gaps in this relatively new area of research. This will be fully explained in Section 1.4.

In continuation to Table 1.1, the status of the ongoing drugs in Phase II and III trials has been updated and the latest data regarding all current clinical trials has been published in September 2017 (See Table 1.2).

Table 1.2 Ongoing AD clinical trials in 2017. (A) Phase I trials; (B) Phase II trials; (C) Phase III trials.

A

AGENT	AGENT MECHANISM CLASS	MECHANISM OF ACTION	STATUS	START DATE	END DATE
AC-1204	Methylphenidate	Ketogenic agent	Active, not recruiting	Mar-13	Oct-17
Aducanumab	Anti-amyloid	Monocloncal antibody	Recruiting	Sep-15	Feb-22
Albumin + immunoglobulin	Anti-amyloif	Polyclonal antibody	Recruiting	Aug-15	Feb-22
ALZT-OP1a + ALZT-OP1b	Anti-amyloid	Anti-amyloid combination, inhibits neuroinflammation	Recruiting	Mar-12	Dec-16
Aripiprazole	Neurotransmitter based	Atypical anti-psychotic (dopamine partial agonist)	Recruiting	Sep-15	Mar-18
AVP-786	Neurotransmitter based	Mixed transmitter effect; agitation therapy	Recruiting	Jun-14	Jul-17
AZD3293 (LY3314814)	Anti-amyloid	BACE1 inhibitor	Recruiting	Sep-15	Jul-18
Brexpiprazole (OPC-34712)	Neurotransmitter based	Atypical anti-psychotic (dopamine partial agonist)	Recruiting	Dec-15	Jul-19
CAD106	Anti-amyloid	Amyloid vaccine	Recruiting	Sep-14	Aug-19
CNP520	Anti-amyloid	BACE inhibitor	Recruiting	Jul-16	Apr-21
Crenezumab	Anti-amyloid	Monoclonal antibody	Recruiting	Mar-16	Jul-21
E2609	Anti-amyloid	BACE inhibitor	Recruiting	Oct-16	Jun-20
Gantenerumab	Anti-amyloid	Monoclonal antibody	Active, not	Mar-14	Nov-19

			recruiting		
Idalopirdine (Lu AE58054)	Neurotransmitter based	5-HT6 antagonist	Recruiting, extension	Apr-14	Oct-17
Insulin (humulin)	Metabolic	Metabolic agent	Active, not recruiting	Sep-13	Feb-17
ITI-007	Neurotransmitter based	5-HT2A antagonist, dopamine receptor modulator	Recruiting	Jun-16	Aug-18
JNJ-54861911	Anti-amyloid	BACE inhibitor	Recruiting	Nov-15	May-23
Methylphenidate	Neurotransmitter based	Dopamine reuptake inhibitor	Recruiting	Oct-15	Aug-20
MK-8931 (verubecestat)	Anti-amyloid	BACE inhibitor	Active, not recruiting	Nov-13	Mar-21
MK-4305 (suvorexant)	Neurotransmitter based	Dual orexin receptor antagonist	Recruiting	May-16	Jul-17
Nabilone	Neurotransmitter based	Cannabinoid (receptor agent)	Recruiting	Jan-15	Dec-17
Nilvadipine	Anti-amyloid	Calcium channel blocker	Active, not recruiting	Oct-12	Dec-17
Pioglitazone	Metabolic	PPAR-gamma agonist, anti-amyloid effect	Recruiting, extension	Feb-15	Apr-21
RVT-101 (interpirdine)	Neurotransmitter based	5-HT6 antagonist	Recruiting	Oct-15	Oct-17
Sodium Oligo-mannurarate (GV-971)	Anti-amyloid	Anti-amyloid agent	Recruiting, extension	Apr-14	May-17
Solanezumab	Anti-amyloid	Monoclonal antibody	Active, not recruiting	Dec-12	Dec-19
TRx0237	Anti-tau	Tau protein aggregation inhibitor	Recruiting, extension	Aug-14	Sept-17
TTP488	Anti-amyloid	Anti-amyloid RAGE	Recruiting	Apr-15	Jan-19

AGENT		MECHANISM OF ACTION	STATUS		
(azeliragon)		antagonist			

AGENT	AGENT MECHANISM CLASS	MECHANISM OF ACTION	STATUS	START DATE	END DATE
AADvac1	Anti-tau	Monoclonal antibody	Recruiting	Dec-15	Feb-19
ABBV-8E12	Anti-tau	Monoclonal antibody	Recruiting	Oct-16	Mar-21
ATP	Anti-amyloid	Inhibits amyloid misfolding and toxicity	Activr, but not recruiting	Nov-14	Nov-16
AD-SVF cells	Regenerative	AD-SVF cell infustion	Recruiting	Nov-15	Dec-17
ANAVEX 2-73	Neuroprotective	Sigma-1 receptor agonist	Active, but not recruiting	Dec-14	Oct-16
Atomoxetine	Anti-amyloid	Adrenergic uptale inhibitor, SNRI	Active, but not recruiting	Mar-12	Dec-17
AVP-786	Neurotransmitter based	Mixed transmitter mechanism	Recruiting	Oct-15	Mar-18
AZD0530	Anti-amyloid	Kinade inhibitor	Active, but not recruiting	Dec-14	Dec-17
BAN2401	Anti-amyloid	Monoclonal antibody	Recruiting	Dec-12	Jul-18
Benfotiamine	Metabolic	Antioxidant	Recruiting	Nov-14	Nov-19
BI409306	Neuroprotective	Phosphodiesterase 9A inhibitor	Recruiting	Jan-15	Oct-17
Bryostatin 1	Neuroprotective	Protein kinase C modulator	Recruiting	Jul-15	May-17

Candesartan	Neuroprotective	Angiotensis receptor blocker	Active, but not recruiting	Jun-16	Sept-21
CB-AC-02	Regenerative	Stem cell therapy	Not yet recruiting	Sept-16	Jun-18
Cilostazol	Neuroprotective	Phosphodiesterase 3 antagonist	Recruiting	Jul-15	Jul-18
CPC-201	Neuroprotective	Cholinesterase inhibitor + peripheral cholinergic antagonist	Recruiting	Oct-15	Dec-16
Crenezumab	Anti-amyloid	Monoclonal antibody	Recruiting	Dec-13	Sep-20
CT1812	Anti-amyloid	Sigma-2 receptor modulator	Recruiting	Sep-16	Jun-17
DAOIB	Neurotransmitter based	NMDA enhancer	Recruiting	Feb-14	Sep-17
Dronabinol	Neurotransmitter based	CB1 and CB2 endocannabinoid receptor partial agonist	Not yet recruiting	Aug-14	Dec-20
E2609	Anti-amyloid	BACE inhibitor	Recruiting	Nov-14	Jan-18
Formoterol	Neuroprotective	Beta-2 adrenergic receptor agonist	Recruiting	Jan-15	Jul-16
hUCB-MSCs	Regenerative	Stem cell therapy	Recruiting	Feb-14	Feb-18
Insulin detemir (intranasal)	Metabolic	Increases insulin signalling in the brain	Active, not recruiting	Aug-15	Sep-17
Insulin glulisine	Metabolic	Increases insulin signalling in the brain	Recruiting	Aug-15	Sep-17
JNJ-54861911	Anti-amyloid	BACE inhibitor	Active, not recruiting, extension	Jul-15	Oct-22
Levetiracetam	Neurotransmitter based	Anticonvulsant	Recruiting	Jun-14	Mar-19

Liraglutide	Metabolic	Glucagon-like peptide 1 receptor agonist	Recruiting	Jan-14	Mar-19
Lithium	Neurotransmitter based	Ion channel modulator	Recruiting	Jun-14	Apr-19
LY3202626	Anti amyloid	BACE inhibitor	Recruiting	Jun-16	Aug-18
Methylene blue	Anti-tau	Tau inhibitor, neuronal stimulant	Recruiting	Jul-15	Jul-18
NewGam 10% IVIG	Anti-amyloid	Polyclonal antibody	Active, not recruiting	Jan-11	Nov-17
Nicotine	Neurotransmitter based	Nicotinic acetylcholine receptor agonist	Not yet recruiting	Dec-16	Dec-19
Nilotinib	Anti-tau	Tyrosine kinase inhibitor	Not yet recruiting	Nov-16	Mar-18
ORM-12741	Neurotransmitter based	Alpha-2c adrenergic receptor	Recruiting	Jun-15	Jul-17
Pimavanserin	Neurotransmitter based	5-HT2A inverse agonist	Active, not recruiting	Nov-16	Jun-19
Piromelatine	Neurotransmitter based	Melatonin receptor agonist; 5-HT 1A and 1D receptor agonist	Recruiting	Nov-15	Mar-18
Posiphen	Anti-amyloid	Selective inhibitor of APP production	Not yet recruiting	Dec-16	Dec-18
PQ912	Anti-amyloid	Glutaminyl-peptide cyclotransferase inhibitor	Recruiting	Mar-15	Mar-17
Probucol	Neuroprotective	Anti-hyperlipidemic	Not yet recruiting	Apr-16	May-18
Rasagiline	Neuroprotective	Monoamine oxidase B inhibitor	Recruiting	Feb-15	May-17
Riluzole	Neuroprotective	Glutamate receptor anatagonist; glutamate	Recruiting	Apr-13	Nov-18

		release inhibitor			
RVT-101	Neurotransmitter based	5-HT6 antagonist	Recruiting	Oct-16	Sep-17
S47445	Neurotransmitter based	AMPA receptor agonist; nerge growth factor stimulant	Active, not recruiting	Feb-15	Dec-17
Sargramostim (GM-CSF)	Anti-amyloid	Granulocyte colony stimulator; amyloid removal	Recruiting	Mar-11	Jan-17
Simvastatin + L-Arginine + Tetrahydrobiopterin	Neuroprotective	HMG-CoA reductase inhibitor and antioxidant	Recruiting	Nov-11	Dec-16
STA-1	Neuroprotective	Antioxidant properties of echinascoside	Not yet recruiting	Dec-15	Dec-18
SUVN-502	Neurotransmitter based	5-HT6 antagonist	Recruiting	Sep-15	Jun-17
T-817 MA	Neurotransmitter based	Neurotrophic agent	Active, not recruiting	Mar-14	Mar-17
Telmisartan	Neuroprotective	Angiotensin II receptor blocker	Recruiting	Mar-14	Aug-18
UB-311	Anti-amyloid	Monoclonal antibody	Recruiting	Oct-15	Dec-17
Valacyclovir	Anti-amyloid, anti-tau	Antiviral agent	Recruiting	Dec-16	Dec-17
VX-745	Neuroprotective	P38 mitogen-activated protein kinase inhibitor	Active, not recruiting	Apr-15	Nov-16
Xanamema	Neuroprotective	Blocks 11-HSD1 enzyme activity, decreasing cortisol in the brain	Not yet recruiting	Apr-15	Sep-16

C

AGENT	AGENT MECHANISM CLASS	MECHANISM OF ACTION	STATUS	START DATE	END DATE
AADvac1	Anti-tau	Monoclonal antibody	Active, not recruiting	Jan-14	Dec-16
Aducanumab	Anti-amyloid	Monocloncal antibody	Active, not recruiting	Oct-12	Oct-19
Allopregnanolone	Regenerative	GABA receptor modulator	Active, not recruiting	May-15	Dec-16
BI409306	Neurotransmitter based	Phosphodiesterase 9A inhibitor	Active, not recruiting	Apr-15	May-17
Bisnorcymserine	Neurtransmitter based	Butyrylycholinesterase inhibitor	Recruiting	Nov-12	Jul-17
BPN14770	Neuroprotective	Negative allosteric modulator of phosphodiesterase 4D	Recruiting	Jun-16	Dec-16
Crenezumab	Anti-amyloid	Monoclonal antibody	Recruiting	Feb-15	May-17
E2609	Anti-amyloid	BACE inhibitor	Not yet recruiting	Aug-16	Jan-17
HTL0009936	Neurotransmitter based	Muscarinic M1 receptor agonist	Recruiting	Sep-15	Sep-16
Insulin Apart Intranasal	Metabolic	Increases insulin signalling in the brain	Recruiting	May-15	Dec-16
KHK6640	Anti-amyloid	Amyloid aggregation inhibitor	Active, not recruiting	Jul-14	Apr-17
HMSCs	Regenerative	Stem cell therapy	Recruiting	Jan-16	Oct-19
Lu AF20513	Anti-amyloid	Polyclonal antibody	Recruiting	Mar-15	May-17
LY2599666 + solanezumab	Anti-amyloid	Monoclonal antibody combination	Active, not recruiting	Dec-15	Sep-17

LY3002813	Anti-amyloid	Monoclonal antibody	Active, not recruiting	May-13	Jan-17
LY3303560	Anti-amyloid	Monoclonal antibody	Recruiting	Dec-15	Jun-20
MK-8931 (vrubecestat)	Anti-amyloid	BACE inhibitor	Recruiting	Apr-16	Apr-17
NGP 555	Anti-amyloid	Gamma-secretase modulator	Recruiting	Oct-16	Apr-17
Oxaloacetate	Metabolic	Mitochondrial enhancer	Recruiting	Oct-15	Oct-17
PF-06751979	Anti-amyloid	Undisclosed mechanism	Recruiting	Jun-16	Jan-17
RGN1016	Undisclosed	Undisclosed mechanism	Recruiting	Jun-16	Feb-17
RO7105705	Anti-tau	Anti-tau antibody	Recruiting	Jun-16	May-17
TAK-071	Neurotransmitter based	Muscarinic M1 receptor modulator	Recruiting	May-16	Mar-17
Telmisartan	Neuroprotective. Anti-inflammatory	Angiotensin II receptor blocker, PPAR-gamma agonist	Recruiting	Apr-15	Mar-18
TPI-287	Anti-tau	Microtubule protein modulator	Active, not recruiting	May-14	Nov-17

1.1.8   Drug treatment

A number of medications are currently prescribed to AD patients to temporarily help improve some symptoms and enhance cognitive functions. The already approved palliative drugs treat symptoms that affect memory, thinking, learning and communication and they are called cholinesterase inhibitors (Wilkinson, 2004; Pepeu, 2010). One of the first drugs introduced on the marker was donepezil (Aricept) approved in 1996, to treat all stages of AD. It is the most common used in patients with AD, followed by rivastigmine (Exelon) approved in 2000, to treat mild to moderate AD, galantamine (Razadyne) approved in 2001, to treat mild to moderate AD and tacrine (Cognex), approved in 1993, to treat mild to moderate AD (Birks, 2006). The mechanism by which they work is based on the cholinergic hypothesis by preventing the breakdown of acetylcholine (Ach), the key neurotransmitter, and essential in sending signals between the neurons of the parasympathetic nervous system (Čolović, 2013). By keeping continuous and healthy communication between the nervous cells, cognitive symptoms may be improved (Birks, 2006). Donepezil, the leading cholinesterase inhibitor drug, used in the treatment of AD, was reported to have the best pharmacological profile regarding the cognitive improvement, showing efficacy in 40-58% of patients, with only 6-13% side effects (Cacabelos, 2007), whereas other studies suggest that rivastigmine exhibit a higher rate of adverse effects (Hansen, 2008).

In 2003, a drug was approved to treat moderate to severe conditions of AD. It is called memantine (Namenda), an NMDA (N-methyl-D-aspartate) receptor antagonist, which works by a different molecular mechanism than the others (Wang, 2015). It regulates the activity of glutamate, a key neurotransmitter in the brain (Nedergaard, 2002). Glutamate attaches to specific sites on the nerve cell surfaces called NMDA receptors allowing Ca^{2+} to enter the cell (Korde, 2012). This process is important for cell signalling, enhancing learning and memory. Glutamate has excitatory functions, being the main excitatory brain neurotransmitter (Petroff, 2002). It is present in over 50% of the nervous tissue and it interacts with receptors at the surface of a neuron resulting in an action potential (Shigetomi, 2004), which is known as an impulse triggered by ion molecules crossing the neuron membrane. This impulse passes from the cell body down the axon to send information which is crucial in learning and memory formation (Barnett, 2007). Therefore, when glutamate binds to the NMDA receptors on the neurons, Ca^{2+} goes in the cell and an action potential is fired. In AD, however, glutamate is excessively released from altered cells, leading to calcium overexposure, which enhances cell alteration (Danysz, 2012). Memantine drug targets the NMDA receptors, blocking them and preventing this destructive series of events by stopping the glutamate to bind to the receptors, thus reducing the Ca^{2+} flow (Wang, 2015).

All of these current drugs help ameliorate the AD patients' symptoms, but they do not succeed in treating the actual disease or cannot postpone its progression. A perfect, successful drug would be able to treat the

fundamental disease by reversing it or by delaying the cellular damage and preventing the cell death that leads to pathogenesis.

One of the most important category of AD drugs, in clinical trials, comprises of those that target the amyloid plaques and reduce amyloid plaques production or increase their removal from the system. As Aβ is produced by secretase enzymes, inhibition agents are used to reduce or block the activity of the proteases that cleave the APP molecules and lead to the more toxic Aβ fragments. These amyloid drugs such as semagacestat, solanezmab, avagacestat, tarenflurbil etc have gone to either phase II or phase III clinical trials to assess their effectiveness and safety but some have failed due to poor outcome (see table 1.1 and table 1.2). Enzyme γ-secretase is involved in processing Notch3 protein, essential for maintenance and development of the brain (Rusanescu, 2014; Wang, 2014). Thus, altering the protein balance in this pathway can result into dementia and cerebral autosomal dominant arteriopathy condition, followed by subcortical infarcts (Panza, 2011; Rutten, 2014). It was therefore very important to define the cellular action sites of γ-secretase for APP processing and Notch3, as γ-secretase is a key target for drug development in AD. Previous studies have used small molecule approaches, utilizing γ-secretase inhibitors (L-685, 458, MRL505 and MRL631) and found that there are at least two cellular sites for γ-secretase action: one for Notch3, which is blocked by MRL631 and the other for APP which is not inhibited by MRL631. Therefore, Notch and APP have distinct γ-secretase pathways (Tarassishin, 2004).

An example of drug induced side effect would be the phase III clinical trials of semagacestat, which failed in mild to moderate AD patients due to damaging effects on cognition and brain function (Panza, 2011).

Immunotherapies that aim to clear amyloid plaques are also under evaluation in clinical trials and include aducanumab, CAD106, crenezumab, solanezumab and many others (Table 1.2). Passive immunization is desired, by using antibodies against Aβ, without triggering adverse immune responses that involve inflammation like encephalitis (Relkin et al., 2005).

In addition to drugs targeting Aβ pathology, therapeutic approaches towards tau pathology have also evolved as disruption of tau protein contributes as well to the neurotoxicity events that lead to neuronal death (Mietelska-Porowska, 2014). In a normal healthy brain cell, phosphatase and kinase activities regulate the phosphorylation of tau. Imbalances in these activities result in hyperphosphorylation of tau that leads to microtubule instability and cell homeostasis disruption in AD cells (Martin, 2013). Research on pharmacological targets that restore kinase and phosphatase activities and inhibit tau hyperphosphorylation include drugs that target glycogen synthase kinase (GSK-3), MAPK family members (extracellular signal-regulated kinsases Erk1 and Erk 2), cyclin-dependant kinase-5 (Cdk-5), calcium calmodulin-dependant kinase II (CaMK-II), casein kinase, microtubule affinity regulating kinase (MARK) and others (Churcher, 2006). Therapeutics also aim to promote microtubule stability and most importantly to reduce aggregation of tau and enhance NFT clearance by administrating specific drugs of immunotherapies against the

tangles. (Boutajangout, 2011). As seen in Table 1.2, there are numerous tau therapies in phase II and III clinical trials that work through various agents: either monoclonal antibodies targeting pathogenic tau (AADvac1, ABBV-8E12, RO7105705), kinase inhibitors that aim to halt hyperphosphorylation (Nilotinib) or modulators for microtubule stability (TP1-287).

The most recent tau study, published in October 2017, presents the use of Leuco-Methylthioninium Bis(Hydromethanesulphonate) (LMTM), a tau aggregation inhibitor used in the treatment of mild AD in a phase III clinical trial (Wischik, 2017). An initial phase III clinical trial, from 2016, using LMTM, used high doses of the drug (175mg) along with AD cholinesterase inhibitors and memantine. The study revealed no benefits when LMTM is taken in combination with other drugs however the second phase III clinical trial and the most recent study on monotherapy with LMTM, used doses of 4mg and 100mg which showed improvements such as slowing the cognitive decline in the AD patients, increasing the brain glucose and lowering the rate of brain tissue waste (Wischik, 2017). After the two phase III clinical trials, they concluded that LMTM is an effective monotherapy that needs further investigation.

Considering all Aβ and tau ongoing clinical trials and their previous individual proven benefits, their relationship is still poorly understood in how they cause AD. This suggests that an ideal combination therapy between amyloid and tau-targeting treatments would be essential, especially in moderate and severe stages of AD, were tau and amyloid pathology is very abundant in more than one brain region, as well as

treating at the right stage to prevent the build-up of toxic proteins (Lansdall, 2014).
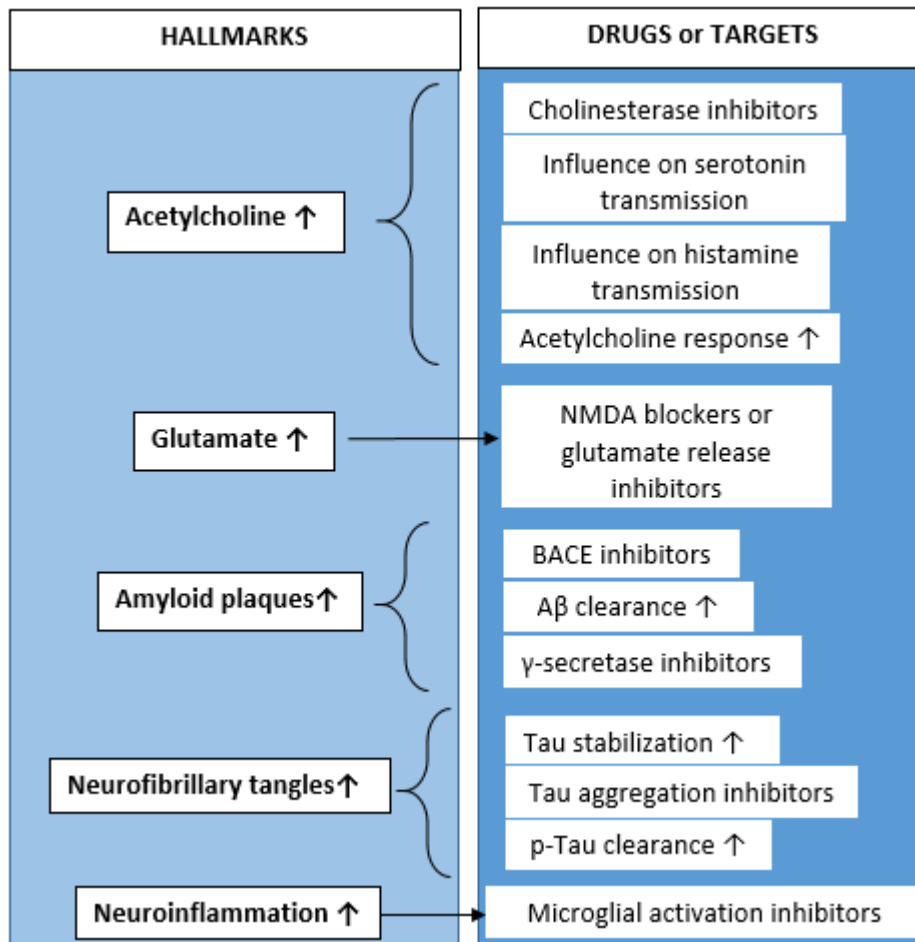
Figure 1.6 Therapeutic strategies and specific drugs in the treatment of AD, based on different hallmarks such as neuritic plaques, neurofibrillary tangles and neurotransmitters reduction (adapted from Hung, 2017).

Current drugs ameliorate the symptoms in patients with AD, however they cannot slow down, reverse or stop the progression of the disease. Therefore, it is very important to prevent the build-up of toxic proteins that lead to a cascade of neurotoxic events which result in neuronal death and neurodegeneration (see figure 1.4).

Thus, drugs that enhance protein degradation in the brain, could have a potential as a new treatment for AD by preventing the build-up of abnormal proteins. Protein degradation pathways are very complex, characterized by numerous steps at which various regulatory proteins participate and despite the existing impairment, the location and the nature of these defects are still unclear.

Autophagy is an intracellular degradation mechanism that functions to clear abnormal or dysfunctional cellular components such as abnormal proteins in order to maintain homeostasis and under stress conditions (Glick, 2010) (see chapter 1.3 and 1.4). In AD brains, the abnormal deposits of amyloid and tau fail to be cleared and there has been a lot of evidence over the past decade, describing impaired autophagy in AD patients (see Chapter 1.4) (Nixon, 2005; Yu, 2005; Wang; 2009; Pickford, 2008; Son, 2012).

One example of autophagy related drug is rapamycin which is known to be involved in rescuing autophagy and helps reduce AD pathology in both human and mice models (Cai, 2013). Rapamycin, a macrolide compound, produced by the soil bacterium *Streptomyces hygroscopicus* has beneficial uses in cancer having immunosuppressant and anti-tumour properties, preventing organ rejection after transplant by inhibition of T and B cell proliferation (Khanna, 2000; Law, 2005). Rapamycin is also shown to have neuroprotective effects in 3xTg-AD mice after enhancing autophagy that facilitates the clearance of abnormal proteins tau and amyloid, resulting in cognitive improvement (Santos, 2011; Majumder, 2011). Aβ can be degraded by autophagy-lysosome systems in normal

ageing brains, however if autophagy clearance pathways are impaired, Aβ seems to abnormally accumulate and the lysosomal systems fail to degrade it (Nixon, 2007). A study from 2010, suggests that rapamycin has cleared abnormal Aβ in a transgenic mouse model, facilitating the autophagy-lysosome systems (Spilman, 2010). Three years later, an *in vitro* study suggested that Rapamycin could enhance autophagy and clear abnormal tau after showing potential of reduction in tau hyperphosphorylation in human neuroblastoma SH-SY5Y cells (Liu, 2013). There are several types of autophagy, including macroautophagy, chaperone-mediated autophagy and microautophagy which are fully described in section 1.3 (Haidar, 2017). It has not been established how these different pathways interact in disease and if there is a shift in pathway recruitment to compensate for any deficit. Studies have not yet shown how autophagy impairment in AD brains manifests in different brain regions and whether the impairment varies across different stages of the disease. Levels of significance might differ from mild to moderate to severe cases which could influence the necessary amount of drug that needs to be administered to regulate autophagy. The brain is a very complex and evolved organ which differs from individual to individual, hence some therapeutic drugs might show improvement in one pathway and be damaging to the others. Moreover, different types of dementia with different abnormal proteins may need drugs to target different autophagy pathways. Previous studies on transgenic mouse models (SOD1G93A) have suggested that treatment with Rapamycin, a commonly drug used to enhance autophagy, can increase the neuropathology in the mice brains

while the symptoms worsen (Zhang, 2011). As a result, switching on the whole autophagy machinery can have irreversible damaging effects in some cases and the most suitable therapeutic intervention would be a highly specific drug that could target the defected step within the pathway (Zhang, 2011). In order to develop successful autophagy based therapeutics, more understanding is needed regarding the exact nature of the deficit, how this impacts other protein degradation pathways and how this varies across different neurodegenerative diseases. Autophagy pathways and their role in neurodegeneration are covered in chapter 1.4. Therefore, if there is an impairment in the autophagic process, an ideal drug would specifically target the deficit which lies within the pathway and restore its function leading to clearance of the abnormal proteins in the AD brains (Liu, 2014). As previously mentioned, there is evidence that restoring the whole autophagy system may not be beneficial in all diseases as it might lead to degradation of normal cellular components.

1.1.9 Alternative treatment approaches

An alternative treatment considered by researchers was antioxidant-based and has been tested in AD clinical trials. One example is a study from 1997, when high doses of ascorbic acid (vitamin C) and α- tocopherol (vitamin E) were tested and were reported to have potential in slowing AD progression by delaying loss of ability to carry out daily tasks (Evans, 2014). Nevertheless, study groups showed side effects such as increased risk of death in people with coronary artery disease, a risk of AD whilst the groups tested with memantine only were not shown to have high risk of

death (Evans, 2014). Vitamin E was then thought to be effective in combination with other AD drugs and as a result in a study group with 613 individuals, results showed improvements in patients with moderately severe AD however in mild stages, the evidence was limited (Dysken, 2014). In another study, 341 patients, with moderate AD, were administered vitamin E and selegiline, treatment which also demonstrated a potential to slow the progression of AD by significantly delaying the time to hospitalization (585 days in the vitamin E and selegiline treatment group vs 440 days in the placebo group, p=0.049), loss of the ability to perform basic activities of daily living or to death (Sano, 1997). A few years later, a contradictory study, on 769 patients, demonstrated that vitamin E does not change the progression of AD with no benefits to the cognitive decline (Petersen, 2005).

Oestrogen hormone showed its properties to modulate neurotransmission and act as a free radical scavenger (Razmara, 2007; Hayes, 2012; Zhu, 2012). Oestrogen plays a role in cell signalling within the cell and it has been suggested to prevent Aβ formation by promoting the non amyloidogenic α-secretase processing APP (Parihar and Hemnani, 2004). Most studies with oestrogen hormone treatment in the assessment of the cognitive function have been performed on female subjects (Asthana, 2001; Sherwin, 2003; Hampson, 2013), however there are some studies on animal models which test both males and females (Razmara, 2007).

A study from 2001 showed that treatment with high dosage of oestrogen may benefit menopausal women with AD by enhancing attention and memory (Asthana, 2001). Similarly, a more recent pilot study

demonstrated that both oestrogen and progesterone have beneficial effects on cognition with respect to visual and verbal functions when tested on menopausal women however this needs further investigation as they used a small sample size (Berent-Spillson, 2015).

1.2   Neuropathology

In Alzheimer's disease, the hippocampus is one of the first area of the brain to suffer damage, causing early symptoms such as short-term memory loss and disorientation (Dhikav, 2011). The hippocampus is a neural structure of the brain, situated in the medial temporal lobe. It is particularly differentiated from other structures by its specific circular seahorse shape. It belongs to the limbic system, playing a crucial role in spatial navigation, learning and forming short-term memories and long-term memories (Rajmohan, 2007). The hippocampus subregions exhibit histological differences regarding the cell size and morphology (see Figure 1.7).
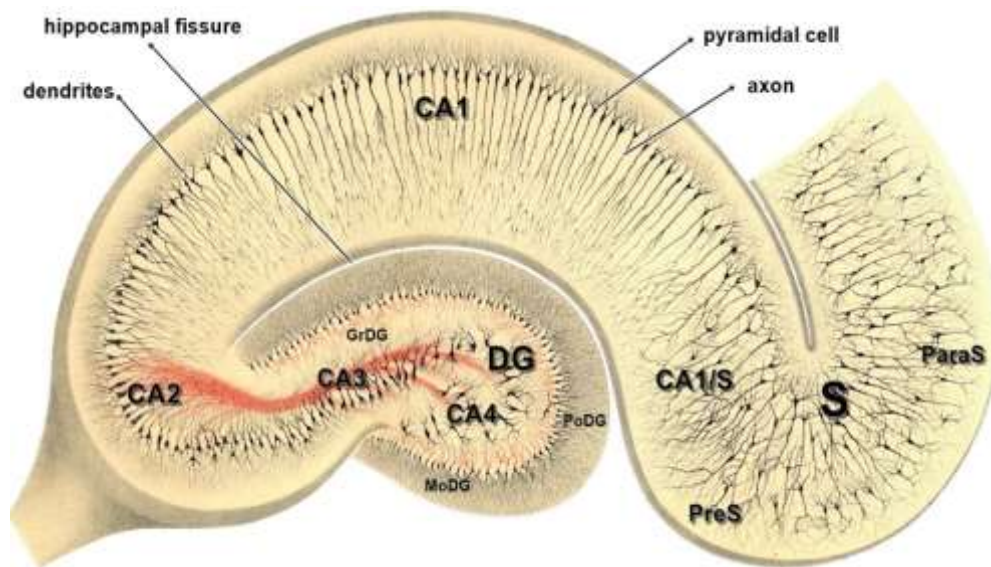
Figure 1.7 Anatomical structure of the hippocampus

This figure shows a cross section of the hippocampus, which extends to the subiculum (S). The three layers of the dentate gyrus (DG) are the polymorphic layer (PoDG), the molecular layer (MoDG) and the granular layer (GrDG). Cornu Ammonis 3 (CA3) and Cornu Ammonis 2 (CA2) differ from Cornu Ammonis 1 (CA1) by higher density of the pyramidal cells, which are more dispersed in CA1. The subiculum is an extension of the DG, with two subdivisions: presubiculum (PreS) and parasubiculum (ParaS). CA1/S is the border between CA1 and S. *Drawing by C. Golgi* (1894)

Understanding the anatomy of the hippocampus is important as the subregions are differentially affected at different stages of AD (Lace, 2009). The dentate gyrus (DG) is a separate, tightly dense packed layer of small granule/polymorphic/pyramidal cells, which surrounds a C-shaped structure called the hippocampus proper or Cornu Ammonis (CA). This

area extends to the subiculum (S) and finally to the parahippocampal gyrus, comprising of the entorhinal cortex (El Falougy, 2008) (Figure 1.7). CA divides into 4 subregions, CA4, CA3, CA2 and CA1, due to cell body location, size and shape, proximal terminations and afferent/efferent projections (Dekeyzer, 2017). The dominant neurons in the hippocampus proper and the subiculum are the pyramidal cells which vary in density and size depending on the subregion. The CA subregions are made up of densely packed pyramidal cells similar to those found in the neocortex (El Falougy, 2008).

The subiculum is the area that lies between CA1 in the hippocampus proper and the medial entorhinal cortex. The ending area of the hippocampus is the entorhinal cortex (EC), the interconnecting network between two major brain areas, the hippocampus and the neocortex.

The degree of pathology in AD is assessed by pathologists using a scheme called Braak staging firstly described in 1991, according to which Braak I and II stages represent the presence of neurofibrillary tangles in the transentorhinal cortex, Braak III-IV when the hippocampus and other limbic structures get involved and Braak V-VI are associated with isocortical regions (Braak *et al*, 1991; Braak *et al*, 1997).

AD specific tau deposition follows a spatiotemporal pattern of neurofibrillary degeneration that initially appears in the transentorhinal cortices, CA1 and EC subregions in stages I-II, then in the limbic cortices (subiculum, amygdala, and thalamus) in stages III-IV and lastly in the isocortical regions, in stages V-VI (Serrano-Pozo, 2011) (Figure 1.8 A). According to Lace, regions such as EC, TEC (transentorhinal cortex) and

CA1 are primarily affected by tau pathology in Braak 0-II; CA2 and CA3 in Braak III; S in Braak IV and lastly late Braak stages affect DG and CA4 tau deposition, resulting in a tau staging system 0-5 (Lace, 2009) (Figure 1.8 B).

In 1986, the Consortium to Establish a Registry for Alzheimer's disease (CERAD) was funded by the National Institute on Aging (NIA) (Fillenbaum, 2008) due to a need of standardized and reliable diagnostic criteria for AD and it has been used in neuropathological clinical studies to evaluate the presence of tau tangles or neuritic plaques (NP) and determine the stage of the disease (Murayama, 2004). Based on CERAD criteria, the cortical density of beta-amyloid plaques is measured from 0 (none) to C (abundant) (Mirra, 1991). On the other hand, Braak staging measures the density of tau tangles (NFT) characterized by entorhinal spread (Braak I-II), limbic spread (III-IV) and neocortical spread (V-VI), corresponding to normal cognition, impaired cognition and dementia (Braak, 1991; Serrano-Pozo, 2011). NIA and Ronald and Nancy Reagan Institute of Alzheimer's Association proposed the two scoring systems to merge and result in three categories: Braak V-VI and NP C (highly likely AD diagnosis), Braak III-IV and NP B (probable AD diagnosis) and Braak I-II and NP A (low AD probability) (Boluda, 2014).

Considering the existing literature on hippocampal subregions differential involvement in the disease, CA regions as well as DG, S and EC regions were chosen for this study since they capture cells and regions that become affected by AD pathology at the earliest stages, as well as the late

stages of disease. This allows for an assessment of cells, both burdened and cleared of AD pathology, within the same case.
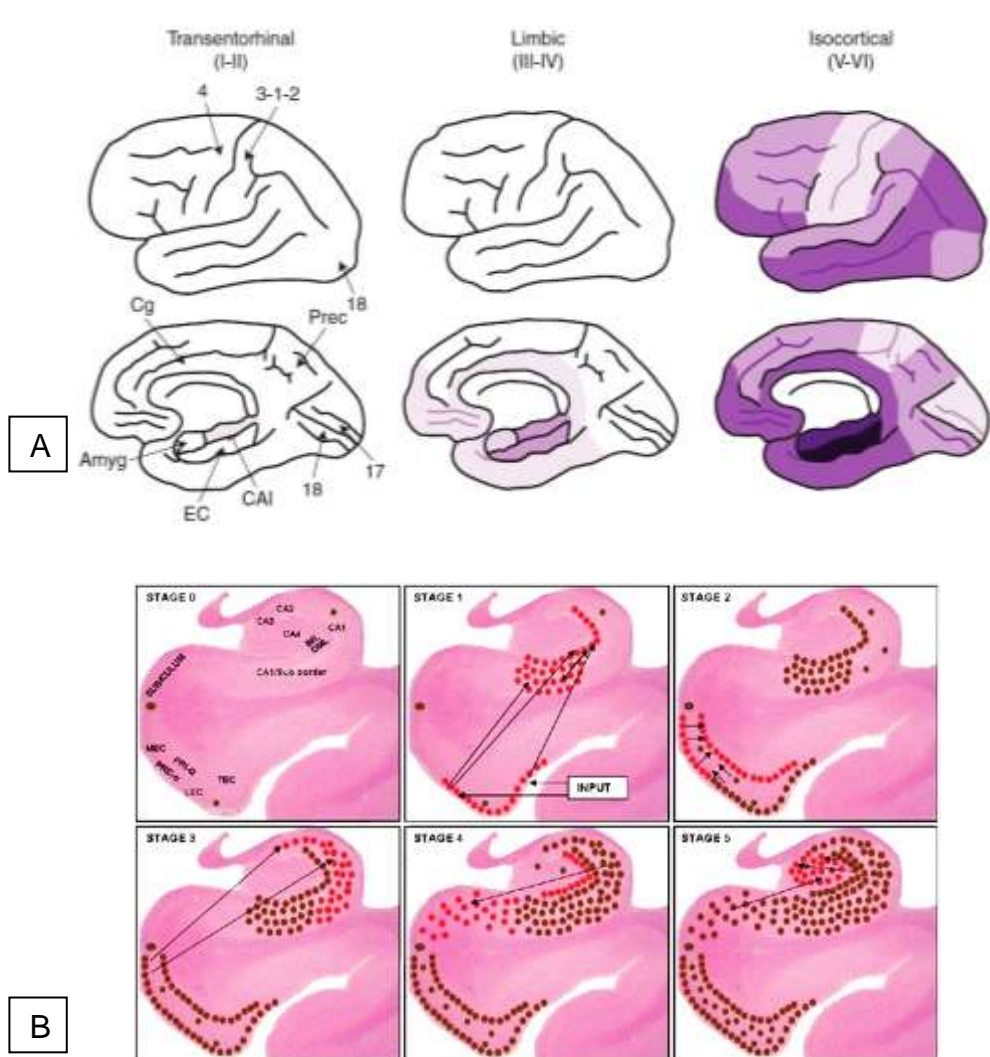
Figure 1.8 Tau pathology distribution. (A) Neurofibrillary tangles distribution pattern in the brain regions with AD progression. The areas of darker colour shades represent increased pathological densities; Amyg =Amygdala; Cg =Cingulate cortex; Prec = Precuneus; 3-1-2 = Primary sensory cortex; 4 = Primary motor cortex; 17 = Primary visual cortex; 18 = Associative visual cortex (Serrano-Pozo, 2011); (B) Tau pathology distribution in the hippocampus across tau stages 0-5; arrows indicate the hippocampus connectivity and their associated areas; red dots represent the new areas of involvement in each tau stage and the brown dots show tau deposition from previous stage (Lace *et al*, 2009).

1.3   Autophagy pathways

In order for a healthy cell to grow and develop, it is necessary to maintain a well-controlled balance between protein/organelle synthesis and degradation that takes place in the cell (Rothman, 2010). Autophagy is the mechanism that maintains cellular homeostasis and balance, essential in cellular development and maintenance under certain environmental stress conditions (Glick, 2010). There are three main autophagy pathways: macroautophagy, chaperone mediated autophagy (CMA) and microautophagy, mediated by specific genes and their associated proteins/enzymes described in more detail in the following sections including figure 1.9 (Haidar, 2017).
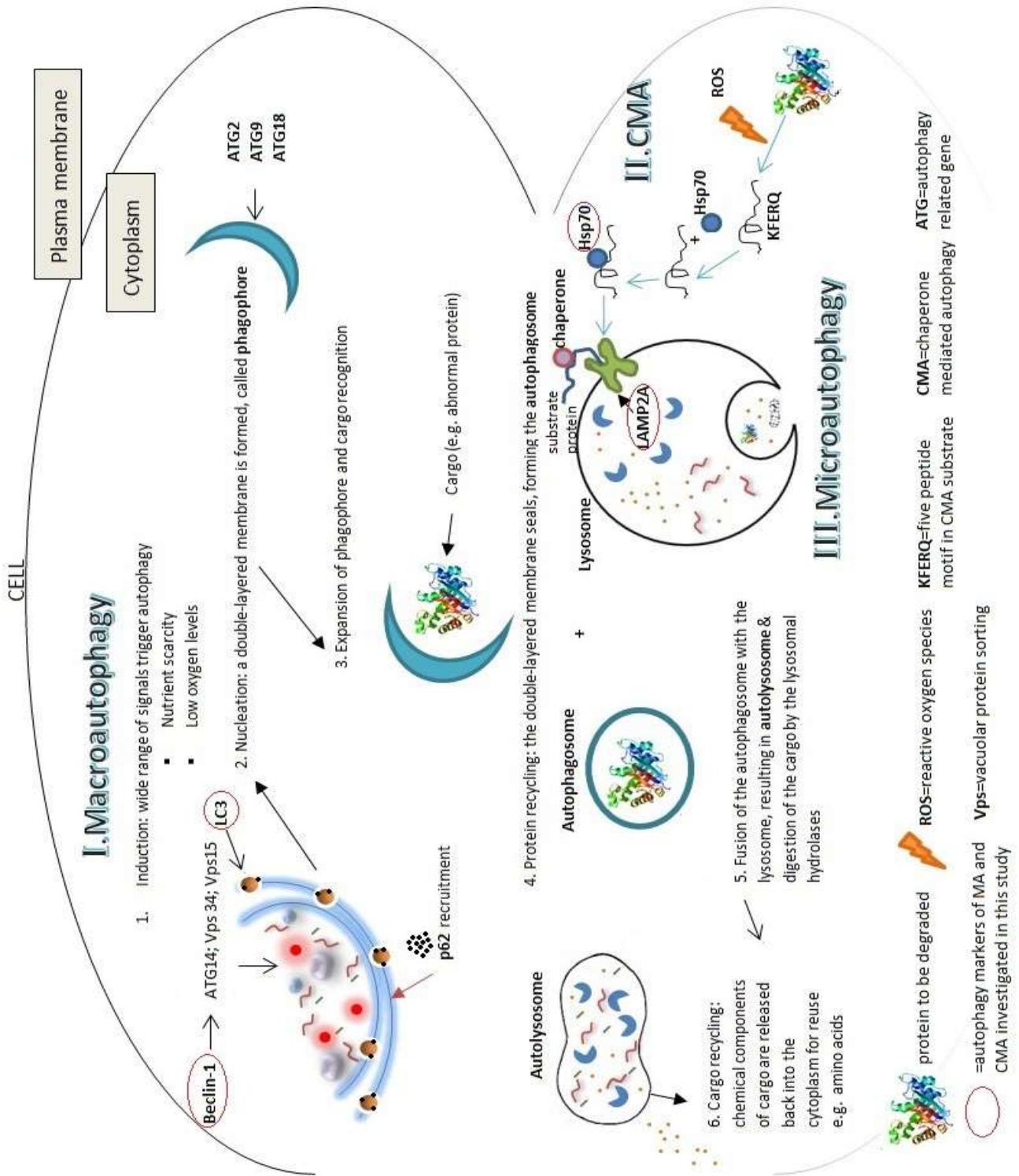
Figure 1.9 Autophagy pathway.
Diagram illustrating all three autophagy pathways: MA (I), CMA (II) and

macroautophagy (III); MA steps 1-6 are described in detail starting with the induction, nucleation and formation of the phagophore which expands, recognizes the substrate that needs to be degraded resulting in a closed autophagosome vesicle. This binds to the lysosome forming the autolysosome. Here acidic lysosomal enzymes degrade the proteins in amino acids, which are released back in the cytosol to be reused. *Key biomarkers of MA and CMA are highlighted within a red circle.*

1.3.1   Macroautophagy

Macroautophagy, the main pathway of autophagy takes place to eliminate damaged   cell organelles or protein   aggregates. In   the   1950s, autophagosomes were firstly observed in mammalian cells, a few years after autophagy started being investigated. The research began with genetic assays in a specific species of yeast: *Saccharomyces cerevisiae* and resulted in a discovery of 31 different autophagy-related genes (ATG). The proteins processed from ATG have different functions at different stages of autophagy such as cargo recognition, packing of cargo or vesicle formation (Klionsky, 2007).

In eukaryotic cells, the lysosome is the main organelle used for degradation through acid hydrolases, enzymes that facilitate degradation of various types of macromolecules, such as proteins, lipids, complex sugars or nucleic acids (Schneider, 2014). After engulfment of cargo, the fusion takes place between the outer-membrane of the autophagosome with the membrane of the lysosome (Figure 1.9). Here, the inner vesicle, containing the cargo, is degraded (Yorimitsu, 2005). The process involves the sequestration of cellular matter by a specialized component, a double-membrane autophagosome that fuses with the lysosome (Figure 1.9).

Here, there are various hydrolases, known as cathepsins, specialized in degradation of the autophagy substrates (Lee, 2012). They can be divided based on the catalytic residue in the active site such as serine, cysteine and aspartic enzymes (Kaminskyy, 2012).

Extracellular and intracellular stress signals (endoplasmic reticulum stress, cell starvation, infections) are both triggers for autophagy upregulation. When autophagy is defective, it has been associated with diseases such as cancer, neurodegeneration and infectious diseases as a consequence of autophagy alteration since clearance of unnecessary or damaged components maintains a good functioning of the cell (see Chapter 1.4) (Chen, 2011).

1.3.1.1 Induction of macroautophagy

Levels of macroautophagy are kept low under normal physiological conditions (He, 2009). Under stress or starvation autophagy is induced and the levels are amplified in order to provide sufficient nutrients for survival and homeostasis under scarcity conditions (Shang, 2011). Numerous genetic studies have shown that the yeast ATG1 kinase with its essential regulatory component ATG13, have an essential role in autophagy induction (Scott, 2007; Cebollero, 2009; Chang, 2009; Kamada, 2010; Jung, 2010; Papinski, 2016).

Phosphatidylinositol 3-phosphate is produced from the phosphatidylinositol 3-kinase complex and is important in targeting yeast ATG proteins (ATG18, 20, 21, 24) that bind to phosphatidylinositol 3-

phosphate. This proteins interaction is a mediator in autophagy induction. Nevertheless, in mammals, some of these proteins have not been identified or are poorly understood (ATG 20, 24) (Stromhaug, 2004; Yang, 2009; Popelka, 2017).

Unc-51 like kinase 1 (ULK1) and unc-51 like kinase 2 (ULK2) are serine/threonine protein kinases, the homologues of yeast ATG1 and are known to regulate the induction of autophagy in human cells (Figure 1.11) (Ro, 2013). Autophagy is also enhanced by adenosine monophosphate-activated protein kinase (AMPK), a key enzyme that regulates the cell metabolism to ensure healthy homeostasis (Zhao, 2011). On the other hand, the mammalian target of Rapamycin (mTOR), which is a growth factor regulator, inhibits autophagy. When mTOR is inhibited by either Rapamycin or starvation, ULKs are activated and contribute to a well-functioning mechanism of autophagy (Figure 1.11) (Hara, 2008). When the cells undergo glucose starvation, AMPK kinase activates ULK kinases by phosphorylation resulting in activating macroautophagy (Figure 1.11). An example is a study on human embryonic kidney cells which demonstrated that cell starvation activates signalling mechanisms of regulatory ULK1 leading to macroautophagy induction (Kim, 2011). Another study from 2009 describes a binding protein called ATG101 that attaches to ATG13 interacting with ULK1 and leading to the induction of macroautophagy in mammalian cells (Mercer, 2009).

Studies of autophagy relate that clearance of abnormal proteins is characterized by selectivity through mediators such as protein p62/ sequestrome 1 (SQSTM1) (Hewitt, 2016). Protein p62 was initially reported to play a role in signalling and regulatory pathways of cell growth and proliferation and later on, it was described to get involved in detecting ubiquitinylated proteins in macroautophagy (Moscat, 2009). LC3 (microtubule-associated protein 1 light chain 3) along with mono and poly-ubiquitin-associated domain, are shown to bind to protein p62 (figure 1.10) and contribute to the cargo being tagged, processed and degraded (He, 2009). Ubiquitinylated proteins, recognized by p62/SQSMT1, are tagged through ubiquitin receptors that have binding domains (Pankiv, 2007). The specific structure of p62 allows the binding of key proteins of the pathway, such as LC3 through a short LC3-interacting region (LIR) found on p62 as well as ubiquitin binding to a binding domain found on the C-terminal of p62 (Pankiv, 2007). Studies on knockout mouse models showed that deletion of p62 gene, inhibits the formation of ubiquitinylated protein aggregated for degradation, thus emphasizing the importance of p62 in the autophagic clearance (Komatsu, 2007). Specialized autophagy receptors such as p62/SQSTM1, NBR1 and NDP52 selectively tag misfolded proteins, damaged mitochondria, intracellular pathogens and other substrates, mediating their engulfment into the autophagosome (Muhlinen, 2010; Mizushima, 2015; Wang, 2015). Atg8/LC3 protein complex is required in mediating macroautophagy via the recruitment of

LIR-containing autophagy receptors that recognize and select cargo (Lippai, 2014).

Once the double membrane is formed and elongated, free cytosolic LC3I is recruited and binds to the autophagosome, becoming membrane bound LC3II (see figure 1.10). P62, previously attached to the ubiquitin cargo that needs to be degraded, will bind to LC3II protein. After the autophagosome and the lysosome fuse to form the autolysosome, LC3II dissociates from the membrane and is released back into the cytosol. P62 with the cargo are degraded by lysosomal acid hydrolases resulting into release of amino acids and fatty acids back into the cytosol that are ready to be used later on (see figure 1.10). LC3 and p62 proteins are often found in the autophagy related research among the most used proteins of macroautophagy as they actively participate into numerous steps of the protein degradation including the membrane elongation (see figure 1.7), the formation of the autophagosome and the autolysosome (see figure 1.7). Most research investigating MA pathway considers both LC3 and p62 key markers since p62 binds to LC3 to form a complex which actively participate in the recognition and the tagging of the protein to degraded, resulting in autophogosome formation.
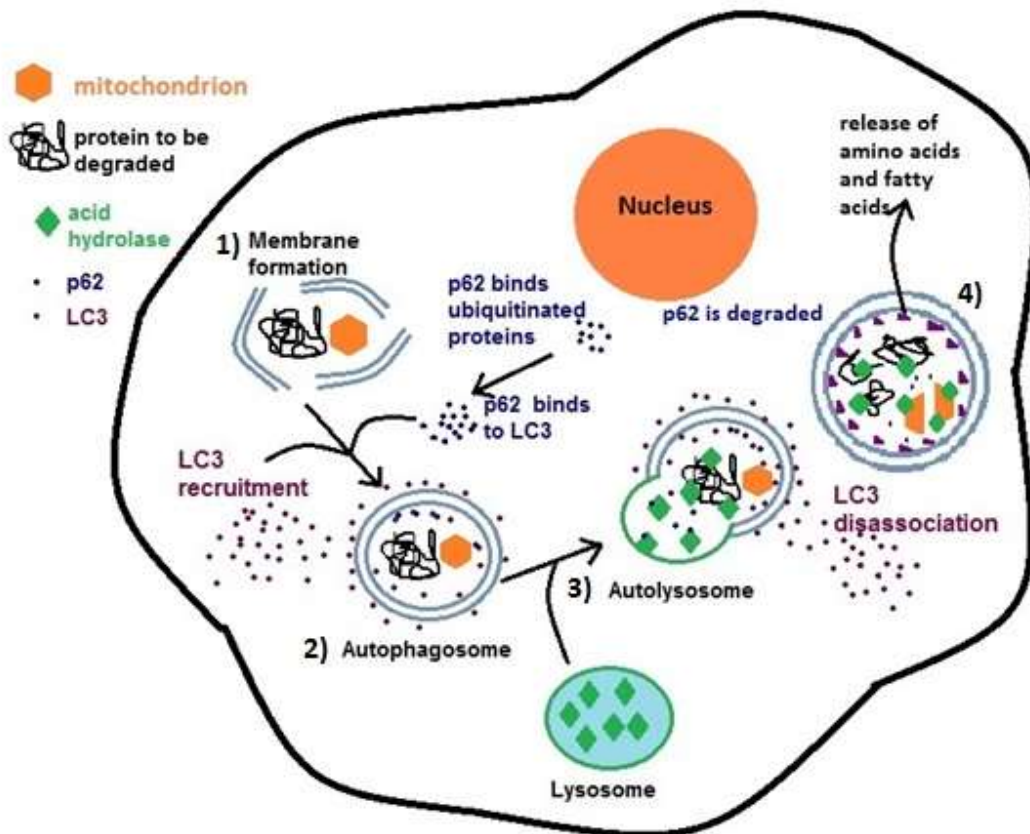
Figure 1.10 LC3 interaction with p62. This diagram illustrates the interaction of p62 to LC3 in macroautophagy, where p62 molecules bind to cytosolic LC3I which is then recruited to the autophagosome membrane.

1.3.1.3 Autophagosome formation

The phagophore assembly site (PAS) is known as the initial site where autophagy-related proteins are recruited and double-membrane autophagosomes are assembled. It is the most complex molecular event of the autophagy mechanism, by which vesicles form to sequester material for degradation. Numerous ATG proteins are required and recruited to the phagophore site to participate in the formation of the autophagosome (see figure 1.11). This step is crucial with respect to very well-balanced

regulation of all ATG proteins (He, 2009). The process of self-assembly and nucleation of the phagophore membrane involves the class III phosphatidylinositol 3-kinase complex (PtdIns3K), which comprises of the PtdIns3K Vps34 (vacuolar protein sorting 34), a serine/threonine kinase Vps15, mATG14 and Beclin-1. Beclin-1 is known to be regulated by an antiapoptotic protein called Bcl-2 (B-cell lymphoma-2) which inhibits autophagy by binding to Beclin-1. Autophagy is induced if Bcl-2 dissociates from Beclin-1 (Liang, 1999) (see figure 1.11). Beclin-1 and LC3 are commonly used in autophagy related studies as macroautophagy proteins, especially in cancer studies (He, 2014). They are involved in the most important and complex steps of the pathway, promoting membrane nucleation (Beclin-1), membrane elongation (LC3) and autophagosome formation (LC3) (He, 2009).

The ATG proteins in partnership with the phosphatidylinositol 3-kinase complex recruit other two ubiquitin-like conjugation systems, ATG5-12-16 and ATG8- phosphatidylethanolamine (PE), to the phagophore which is vital in membrane the regulation of elongation and expansion of the forming autophagosome (see figure 1.11). ATG8 is mainly found free in the cytosol; after autophagic induction, it can be found in a lipid-conjugated form, bound to the phagophore. This protein is important in controlling autophagosome size and its membrane shaping. ATG8 lipidation, LC3 protein, p62, ubiquitin and Beclin-1, are extensively used to assess macroautophagy activity (He, 2009).
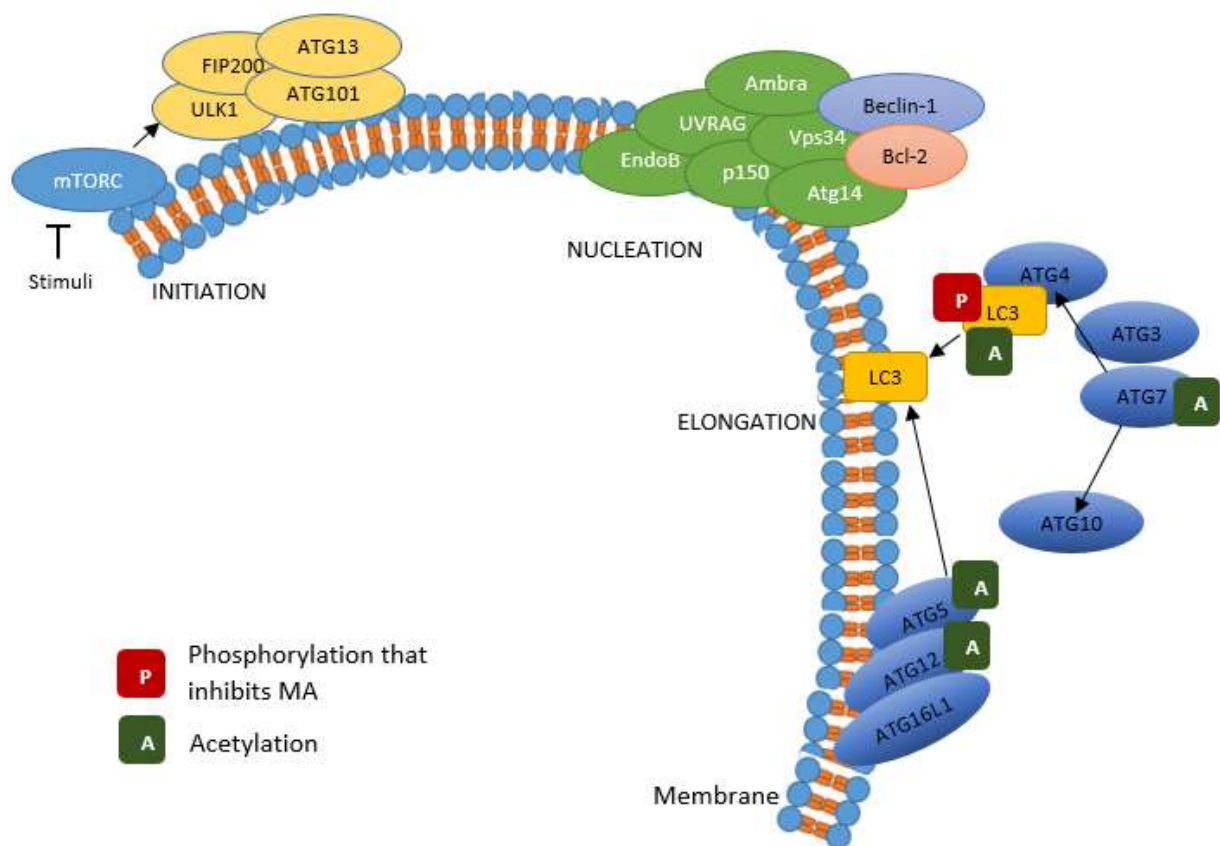
Figure 1.11 Molecular regulation of autophagosome formation in macroautophagy. The ULK protein complex comprising ULK1, ATG13, FIP200 and ATG101 dissociates from mTORC1 and binds to the membrane to initiate autophagosome formation under stress such as starvation. Membrane nucleation involves the formation of Beclin-1/PI3K complex, coordinated by the interactions between Beclin-1, UVRAG, ATG14, Bcl-2, p150, ambra1, endophilin B1 and Vps34. For the membrane elongation, ATG3, ATG4, ATG7, ATG10, and an ATG5–ATG12–ATG16L1 complex are recruited to conjugate PE to LC3 (cytosolic LC3I), leading to the translocation of LC3 from cytoplasm to the autophagosome membrane (bound form LC3II). Also, phosphorylation and acetylation of macroautophagy key proteins enhance autophagosome formation.

1.3.1.4 Vesicle fusion and autophagosome breakdown

Finally, the autophagosome is completely formed and ATG8 protein, which lies on the surface of the membrane, is cleaved by ATG4 and released back into the cytosol. The same mechanism that regulates the autophagic vacuole membrane fusion mediates the fusion between autophagosome and lysosome, resulting in autolysosome formation which requires the lysosomal membrane protein isoform B (LAMP2B) (Nishino, 2000). This has been reported to be used as a biomarker of macroautophagy measuring the rate of autolysosome formation as previously described (Massey, 2006; Pérez, 2016). After fusion is completed, the inner vesicle has to be degraded by numerous lysosomal acid hydrolases such as proteinases A and B. This degradation process results in smaller compounds, particularly amino acids that are transported back into the cellular cytosol for further protein synthesis. This continuous cycle maintains vital cellular functions and assures nourishment during cellular stress such as starvation (He, 2009).

Macroautophagy is usually measured by looking at the levels of autophagic markers either by immunohistochemical studies using antibodies against proteins of interest, by immunofluorescence or by immunoblotting, looking at immunoreactive bands for proteins of interest (Martinet, 2013). As previously mentioned, the most common used markers of macroautophagy are LC3, p62, beclin-1 and ubiquitin proteins (Pickford *et al*, 2008; Spencer *et al*, 2009; Jaeger *et al*, 2010; Liu, 2014; Guo, 2016; Hewitt, 2016). Macroautophagy stimulation has been shown to

enhance clearance of tau and beta-amyloid aggregated in AD, providing neuronal protection in cellular and animal models which suggests potential therapeutic benefits (Jiang, 2014). However, it is necessary to explore and identify at which parts of the macroautophagy pathway, the protein degradation is failing. This will allow development of more targeted therapeutic strategies.

1.3.2   Chaperone-mediated autophagy

CMA is the most specific autophagy pathway. It differs from the other two as it transfers proteins one by one, being highly selective with the substrates that pass into the lysosome (Kaushik, 2012). The protein to be translocated, requires a chaperone, Hsc70 (heat shock-cognate protein 70), which is part of Hsp70 family (heat-shock protein70), a group of 70kDa molecular weight proteins produced by cells when exposed to stress, forming the CMA- substrate/chaperone complex. Subsequently, the complex will travel to the lysosome where it will bind with the CMA receptor, LAMP2A, allowing entrance in the lysosome (figure 1.12). Due to recognition, the substrate protein becomes unfolded and it is transferred across the lysosome membrane with the aid of the hsc70 chaperone (Lee, 2012). It has been stated that the CMA rate is regulated by the rate of assembly and disassembly of the translocation complex (Cuervo, 1996).

CMA does not require vesicles for engulfment, thus substrates are recognized in the cytosol and directly enter the lysosome by crossing the membrane. The substrate selectivity is highly specific, removing certain

proteins without interference with other healthy ones. Chaperones are indispensable in this cellular pathway and in 2000, their dependence led to the name of the autophagic pathway (Cuervo, 2000).

CMA is a complex process with four main cellular steps: protein/substrate recognition and lysosomal targeting; substrate binding followed by its unfolding; substrate translocation and substrate degradation in the lumen of the lysosome (Cuervo, 2014). The first step takes place in the cytosol when a specific chaperone, hsc70, binds to a motif made of five peptides, present in the amino acid sequence of all CMA substrates (see Figure 1.12a). This motif (e.g. KFERQ) consists of a glutamine residue (Q) either at the beginning or at the end of the sequence, one of the two positively charged amino acids, lysine (K) or arginine (R), one of the non-polar hydrophobic amino acids, phenylalanine (F), leucine, isoleucine and valine and lastly, one negatively charged amino acids, either glutamic acid (E) or aspartic acid (Jackson, 2016). The second step takes places after the chaperone-substrate binding, when the complex is targeted to the lysosome (Figure 1.12). Here, the substrate interacts with the membrane through the cytosolic tail of a specific transmembrane protein called lysosome-associated membrane protein type 2A (LAMP-2A).

LAMP2A is present in a monomeric form at the surface of the lysosome, but in association proteins such as the substrate-chaperone complex, it results in the formation of a multimeric protein complex that is required for substrate translocation in step 3 (Cuervo, 1996). The binding of the chaperone-substrate complex to LAMP2A, at the surface of the lysosome (see Figure 1.12b), takes places while the substrate is still in an unfolded

state, however, it requires unfolding processes in order to cross the lysosomal membrane. Translocation also requires the presence of hsc70 which is normally found in the lysosomes. The last step of CMA is the degradation of the substrate by disassembling the multimeric LAMP-2A complex into monomers that can be reused in further CMA pathways (Figure 1.12).
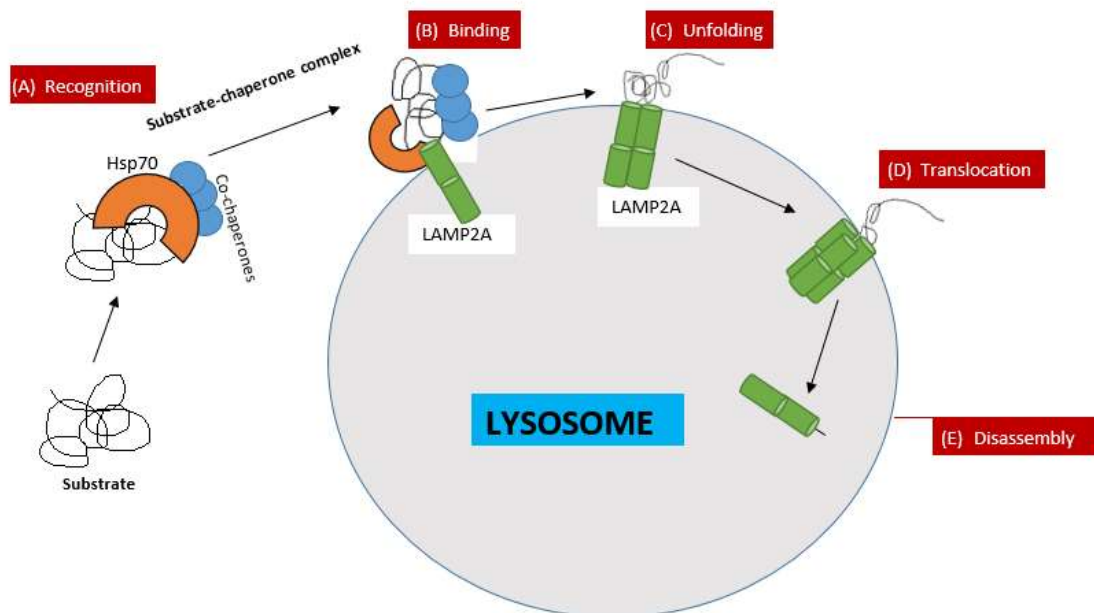
Figure 1.12 Chaperone-mediated autophagy. Chaperone-mediate autophagy steps describing the recognition of the substrate in the cytosol, with the help of chaperones, followed by formation of a complex substrate-chaperone, which will migrate to the cell surface where the substrate will be translocated, through a transmembrane protein, into the cell to be degraded.

As previously mentioned, CMA rate is regulated by the rate of assembly and disassembly of the translocation complex (Cuervo, 1996). CMA rate is also dependent on the LAMP2A present in the lysosomal membrane. According to Kaushik, LAMP2A is exclusively associated with CMA, although hsc70 chaperones are involved in both CMA and microautophagy (Kaushik, 2009). While LAMP2A is a widely used marker of CMA, measuring the rate of substrate translocation in the lysosome in order to be degraded, the other different isoform of this protein, LAMP2B, has been described to be a potential marker exclusively in macroautophagy pathway measuring the rate of autolysosome formation (Nishino, 2000).

Similar to macroautophagy, CMA is measured by looking at the levels of CMA markers either by immunohistochemical studies, by immunofluorescence or by immunoblotting. The most commonly used markers of CMA are LAMP2A (the only isoform associated with CMA), which measures the translocation rate of the abnormal or defective proteins to be degraded, through the lysosomal membrane and Hsp70 which indicates the rate of recognition of KFERQ motif on the protein that is cleared and the rate of binding to it. Under hypoxic and ischemic stress, dysfunction of CMA, has been shown to result in accumulation of abnormal proteins in the brain therefore exploration of CMA impairments is crucial in AD (Koga, 2011; Cuervo, 2014). A decrease in both lysosomal LAM2A and hsc70 indicate a reduced CMA rate, while increased levels of LAMP2A would suggest overexpression of LAMP2A (Patel, 2015), however, if LAMP2A production is upregulated but lys-Hsc70 is

41

insufficient, substrate uptake would become limited, resulting in CMA defects (Cuervo, 1995; Cuervo, 2000).

1.3.3 Microautophagy

The third type of autophagy, called microautophagy differs as it involves a direct engulfment of the protein to be degraded into the lysosome. This action takes place by a process called invagination and involves the inward budding of the lysosomal membrane (figure 1.9) (Lee, 2012).

Similarly to macroautophagy, microautophagy role is important in cell survival during oxygen starvation and nutrient scarcity. Microautophagy is activated by stress conditions such as short-term starvation or prolonged starvation but also by glucagon and cyclic AMP administration, cortisone acetate treatment and albumin injection (Mijaljica, 2011). Microautophagy does not respond to most commonly used autophagy enhancers (Cuervo, 2004).

The major limitations of microautophagy investigation are the incomplete understanding of its physiological roles and its contribution to specific diseases along with the methods of detection such as the electron microscopy. Microautophagy investigation is represented by the morphological analysis of the lysosomes with the electron microscope which is expensive and yields minimal information regarding lysosomal content. Previous studies which investigated abnormalities seen in the lysosomal morphology of the microautophagy have reported that these changes are associated to the final steps of the pathway however the

initiation steps of microautophagy were unclear (Dice, 2000). Microautophagy research is not as popular as MA and CMA research due to high costs of electron microscopy facilities and due to its biochemical and molecular events that take place at a much lower scale than the other autophagy pathways.

1.4 Autophagy in neurodegenerative disorders

Over the last decade, there has been emerging evidence linking impairments of autophagy pathway to neurodegenerative disorders such as AD, resulting in failure of abnormal proteins clearance (Nixon, 2005; Nikon, 2007; Pickford, 2008; Son, 2012). Generally, autophagy cannot complete digestion unless functional and dynamic communications between all stages of the autophagic pathways work. Studies have shown that when these particular interactions are disrupted, neuronal cells are prone to become vulnerable, especially with age (Cuervo, 2008; Martinez-Lopez, 2015).

The substantial dependency of neurons on autophagy is demonstrated by brain studies in lysosomal disorders and studies of autophagy-related gene mutations (Platt, 2012). Neurons are atypical cells in the body as they have dendrites and axonal cytoplasm and as a result these cells meet a higher degree of difficulty in eliminating accumulations of dysfunctional organelles and protein aggregates (Misgeld, 2017). Young neurons manage to efficiently clear all damaged components, despite the significant distances that the many vacuoles, containing organelles and proteins, generated in axons must travel to reach lysosomes (Carmona-

Gutierrez, 2016). Nevertheless, studies suggest that lysosomal-based autophagy pathways including macroautophagy and CMA are involved in the clearance of both AD deposits: Aβ and tau suggesting that both protein degradation pathways could be important in neurodegeneration (Wang, 2009; Wang, 2012; Lee, 2013).

Over two decades ago, electron microscopy studies on AD brain revealed a possible link between neurodegeneration and impaired macroautophagy (Nixon *et al.*, 2005). A significant increased level of autophagic vacuoles was observed within the lysosome of AD neurons, after it fused with the autophagosomes, suggesting an accumulation of immature vacuoles leading to incompletion of macroautophagy in AD. Also, the damaged neurons, containing neurofibrillary tangles, showed high autophagic levels in the cell bodies, measured by immunoblotting and immunofluorescent labelling (Yu *et al*, 2005). Impaired macroautophagy was suggested due to incomplete development of macroautophagic vacuoles by immunolabeling, affecting their transport to the lysosomes. Surprisingly, immature vacuoles were discovered to be a considerable Aβ-containing site while APP molecules (either complete or cleaved), γ–secretase complex and presenilin-1 were found abundantly in autophagic vacuoles, suggesting that macroautophagy is linked to AD pathology however, it failed to clear Aβ molecules, resulting in impaired macroautophagy (Yu *et al.*, 2005). Based on this study, we could hypothesize that macroautophagy gets impaired in AD at the autophagosome formation step, suggesting a possible target for therapeutics.

According to Nixon, transport and development of autophagolysosomes is impaired in AD, leading to significant accumulation of immature autophagic vacuoles in the neuron cell bodies. Upregulation of autophagy induction, combined with faulty mechanisms of Aβ clearance was reported to result in accumulation of toxic protein aggregates and alteration of neuronal cells (Nixon, 2007). Beclin-1 protein is a key regulator of macroautophagy pathway initiation. It was shown that this protein expression decreases with age, thus reducing the levels of autophagy in the human brain (Pickford *et al.*, 2008). AD transgenic mouse model experiments revealed that deletion of Beclin-1 gene causes decline in neuronal autophagy leading to neurodegeneration pathology (Pickford *et al.*, 2008). In addition, beclin-1 depletion in age brain causes damage to the autophagosome and lysosome degradation, altering APP metabolism, too. It is still unclear how Beclin-1 levels relate to protein accumulation in individual neurons. Considering the beclin-1 findings, its increase may play a role in therapeutic potential in Alzheimer's disease (Jaeger *et al.*, 2010). Age-related diseases such as AD and PD have been shown to demonstrate a decline in the well-functioning of the lysosome and a decline in lysosomal lifespan, resulting in compromised efficient clearance of abnormal accumulations in the ageing neurons, however the cause of lysosomal malfunction is unclear (Carmona-Gutierrez, 2016).

Neuronal cells become vulnerable to decline in the proteolytic clearance of lysosomal material. If autophagy fails to function, ubiquitinated protein aggregates accumulate within neurons and they start to degenerate, losing vital functions and integrity (Nixon, 2013).

Substantial evidence suggests that impaired CMA leads to pathogenesis and one example is neurodegeneration by failure of proteolytic systems to remove abnormal aggregates that cause toxicity (Koga, 2011). Impaired CMA levels are associated with AD, as studies in mouse neuroblastoma N2a cell model suggest that tau protein contains the CMA recognizing motif, interacting with Hsc70 facilitating mutant tau to translocate to the lysosomes, therefore being degraded by CMA (Wang, 2009). Other studies have reported APP to contain the KFERQ motif, meaning that Hsc70 could target it and degrade beta-amyloid aggregated via CMA (Koga, 2011). Considering this, there is sufficient evidence to warrant further investigation of CMA in AD since enhancing this pathway could be a viable therapeutic target.

In addition, autophagy-mediated mTOR kinase complex has been proposed to contribute to neurodegeneration in AD (Talboom, 2015). Post-mortem brain studies revealed mTOR signalling hyperactivity and dysregulation, was associated with the presence of soluble Aβ and hyperphosphorylated tau proteins (Rosner, 2008). Therefore, another therapeutic target is mTOR complex, by inhibiting its signalling pathways. A regulator of cell metabolism and survival, mTOR emerges as a novel therapeutic target for Parkinson's disease (PD), which is explained, in more detail, in the following section. The mTOR complex was shown to modulate cognitive functions including memory and learning (Lan, 2017). Some studies on rat models suggest that activation of autophagy involving autophagy-related proteins such as Beclin-1 and mTOR are involved in

the pathology of vascular dementia leading to impaired cognition and learning functions (Liu, 2014; Guo, 2016).

Rapamycin treatment on mice models aimed to inhibit mTOR signalling and as a result, this pharmacological approach improved some neurodegenerative symptoms and reduced senile plaque pathology (Caccamo *et al.*, 2010). Regarding all these findings, mTOR signalling inhibition plays an important role of amelioration in cognitive impairment and confirms that the result of increased autophagy is directly linked to Aβ reduction. Previous studies have suggested that in AD there is an impairment of MA in the pathway initiation, autophagosome formation and maturation, as well as a CMA impairment associated to reduced levels of LAMP2A and Hsc70 (Nixon, 2005; Yu, et al 2005; Koga, 2011; Cuervo, 2014). However, it is unclear at what stage in disease this occurs, how the impairments relate to AD protein aggregation and if alterations vary between brain regions.

Macroautophagy and CMA are also implicated in the clearance of other neurodegenerative diseases associated with aggregated proteins such as Lewy bodies (Vogiatzi *et al.*, 2008; Tanik, 2013). Formation of Lewy bodies is the main pathological feature of PD, inclusions which are composed of ubiquitin and α-synuclein (Spillatini, 1998).

Initially, brain studies on PD patients revealed increased apoptosis and decreased autophagy in the substantia nigra neurons, primarily affected in PD (Anglade *et al.*, 1997). This was shown by inhibitory experiments of the two pathways, showing that CMA and macroautophagy inhibition results in accumulation of α-synuclein species (Vogiatzi *et al.*, 2008).

Over a decade ago, links between PD and autophagy pathways were established by finding that α-synuclein is degraded by macroautophagy and CMA (Cuervo *et al.*, 2004). More recent studies suggest that PD abnormal protein aggregates fail to degrade resulting in impairment of the autophagy pathways (Lynch-Day, 2012; Giacoppo, 2017; Karabiyik, 2017). There is a study on parkinsonian Sprague-Dawley rat models suggesting that there is decreased tyrosine hydroxylase, an important enzyme for dopamine synthesis, and increased LAMP2A and Hsp90, in the PD rats, suggesting a link of CMA activation and neurodegeneration (Marin, 2011). Other studies have shown that CMA impairment is associated with neurodegeneration in familial and sporadic Parkinson's disease cases. Experiments using mouse models, which included lysosome extraction, neuronal-differentiated induced pluripotent stem cells and cell culture based models, suggested lysosomal degradation of specific PD proteins such as alpha-synuclein (Wang, 2009). While Beclin-1, which regulates macroautophagy pathway, was shown to be important in AD, experimental studies, on transgenic mice, proved the same for PD. This was accomplished by injecting Beclin-1 expressing lentivirus into the mice brain and the results suggested reduced α-synuclein abnormal deposition (Spencer *et al.*, 2009).

Studies in PD post-mortem brain sections showed that Lewy bodies contained autophagy-related proteins and decreased levels of LAMP2A and Hsc70 in the dopaminergic neurons of human PD brains when compared to control brain samples, suggesting a reduced CMA activity in PD (Alvarez-Erviti, 2010).

Although, the majority of the PD cases are sporadic, in familial cases, studies revealed that mutant variants of the α-synuclein gene, such as A53T and A30P have inhibitory effects on CMA with mutant A53T and A30P α-synuclein being shown to bind with high affinity to LAMP2A (Sala, 2016). Several studies on post-mortem PD brains with genetic mutations, have proved an important role of macroautophagy mechanism which contributes to dopaminergic neuronal cell death. For instance, Anglade's paper reported active cell death in the final stages of the disease, in substantia nigra of PD patients. Oxidative stress was reported to induce toxicity of dopamine, resulting in an increase of autophagic vacuoles. (Anglade *et al.,* 1997). In PD, oxidative stress is a common pathogenic mechanism and neuroprotective protein Oxi-α is shown to be reduced in dopaminergic neurons (Yoo, 2004). Researcher found that Oxi-α protein can protect dopamine neurons by activating mTOR kinase involved in autophagy. Therefore, downregulation of this protein inhibits mTOR kinase and activated oxidative stress responses in the brain. Moreover, the same study demonstrated that treatment with Rapamycin, an autophagy enhancer, aggravated cell death due to enhanced oxidative stress whereas treatment with 3-methyladenine, an autophagy inhibitor, showed neuroprotective properties on the neurons (Choi *et al*, 2010).

Other studies using ALS transgenic mouse models (SOD1G93A) have suggested that after treatment with Rapamycin, the neuropathology and the symptoms worsened (Zhang, 2011). This suggests that switching on the whole autophagy machinery may, in some cases, have irreversible, damaging effects so the most suitable therapeutic intervention would be a

highly specific drug that could target the defected step within the different protein degradation pathways.

1.5   Models of Alzheimer's disease

The mechanisms that lead to AD pathogenesis and irreversible brain damage have been described extensively, providing potential tools of generating AD models including invertebrate, rodent and cell models. Yet, the biggest challenge is to produce a disease model that includes all pathological aspects of AD (Saraceno, 2013).

1.5.1   *Drosophila* and *C. elegans*

Drosophila and C. elegans have been used in many studies as they have conserved AD proteins enabling researchers to understand the molecular functions of their genes and the associated proteins. Examples are Apl-1 protein, equivalent to human APP protein, expressed in the cortical region of nervous system (Hornsten *et al.*, 2007), kuzbanian gene in Drosophila, ortholog of human α-secretase (Tan *et al.*, 2017) or sup17 and adm-4 genes in C. elegans, equivalent to human α-secretase (Ewald, 2010). Presenilin 1 and 2 are also conserved in the two species, along with tau protein (Iijima-Ando, 2010; Prüßing, 2013).

These models pose some limitations, despite contributing with knowledge to the AD field. One example is that Apl-1, the APP drosophila ortholog, lacks the human Aβ42 domain, making this key protein difficult to study (Figure

1.13) (Prüßing, 2013). Similarly, in C. elegans, Apl-1 does not contain the Aβ domain (Figure 1.13), although the Apl-1 extracellular domain is approximately 50% similar to the human APP extracellular domain, while the transmembrane and the cytosolic domains share 71% sequence similarity to human APP (Alexander, 2014).

1.5.2   Zebrafish models

Zebrafish (*Danio rerio*) have become a potent model in the research of AD exhibiting neuropathological and behavioural phenotypes that are quantifiable in experimental studies (Newman, 2011). Zebrafish have numerous advantageous, offering physiological complexity, high rates of reproduction and longer lifespan than rodent models enable zebrafish to model neurodegeneration (Santana, 2012; Leitner, 2014). Investigating neurodegeneration by exploring molecular and genetic mechanisms on zebrafish are costly effective and less time consuming compared to other models (Leitner, 2014). Zebrafish models have a fully characterized genome (Barbazuk, 2000), with physiological homology to humans with a high conservation of the basic brain organization including the hypothalamus, the olfactory bulb and the lateral pallium, which is thought to be the homologous of the mammalian hippocampus (Mueller, 2004). Moreover, zebrafish have been shown to produce neurotransmitters crucial for the glutaminergic and GABAergic systems, including GABA, dopamine, acetylcholine, glutamate, serotonin, histamine and others (Panula, 2006; Rico, 2011).

Studies reported that zebrafish express presenilin genes and others orthologous to the human genes in familial AD (Newman, 2014). Other studies suggest that zebrafish models could be used in studying the underlying mechanisms of tauopathies (Bai, 2011). Two genes equivalent to human MAPT have been indentified as mapta and maptb, however they need further investigation (Chen, 2009). Twenty years ago, scientists started to describe the presence of AD major genes in zebrafish, such as APP, PSEN1, PSEN2, APOE (Babin, 1997; Leimer, 1999; Musa, 2001; Groth, 2002), which are crucial in understanding the molecular biology of AD. More recent studies on APP gene in zebrafish (homologous appa and appb), demonstrated that APP transgenic models exhibit appb protein in the brain, spinal cord, thalamus and cerebellum (Lee, 2007) and that knocking down the appa and appb genes results in body structural deformities, movement impairment and mild synophtalmia, with no Aβ plaques present (Joshi *et al*, 2009).

Limitations in zebrafish models include a need for developing more effective transgenic zebrafish AD models, for a better understanding of the key genes and their corresponding proteins as well as the need to develop APOE zebrafish transgenic models (Figure 1.13) (Saraceno, 2013). Another limitation is that studies of neurodegenerative diseases on zebrafish have limited understanding in the neuronal cell death, process crucial in human neurodegeneration (Fontana, 2013). Moreover, scientists describe pharmacological limitation of using zebrafish models in neuroscience research, as drug manipulation is simply performed by administering chemical compounds to the aqueous environment (Tran, 2015), however

there is no fully controlled drug dose absorption as it quickly passes through the skin (Rubinstein, 2006). Despite the limitations, zebrafish models are still a good model for investigating genetic, molecular and pharmacological aspects of neurodegeneration (Kalueff, 2013; Norton, 2013).

```
┌─────────────────────┐              ┌─────────────────┐
│     DROSOPHILA      │◄────────────►│    ZEBRAFISH    │
│                     │              │                 │
│   CAENORHABDITIS    │              └─────────────────┘
└─────────────────────┘                       │
           │                                   ▼
           ▼                          ┌─────────────────────┐
┌─────────────────────────┐          │ ADVANTAGES          │
│ ADVANTAGES              │          │ -Faster development │
│ -Easy to work with      │          │ and longer lifespan │
│ -Short generation time  │          │ compared with mice  │
│ -High fertility         │          │ -High reproductive  │
│ -Low cost of maintenance│          │ rate                │
│ -Readily available      │          │ -Embryos transparent│
│ techniques for          │          └─────────────────────┘
│ genetic manipulation    │                    │
│ -Ease of feeding        │                    ▼
│ therapeutics            │          ┌─────────────────────┐
└─────────────────────────┘          │ DISADVANTAGES       │
           │                          │ -Expensive to       │
           ▼                          │ maintain            │
┌─────────────────────────┐          │ -More difficult to  │
│ DISADVANTAGES           │          │ modify genetically  │
│ -Not all human genes    │          └─────────────────────┘
└─────────────────────────┘
```

Figure 1.13 Advantages and disadvantages of the use of the invertebrate (left) and vertebrate (right) models used in the study of AD**.**

1.5.3 <u>Mouse models</u>

One of the most popular animal model used in the study of neurodegenerative disorders including AD is the transgenic mouse (Platt, 2013). Unfortunately, a mouse model to capture all AD aspects has not yet

been produced, however each mouse model allows researchers to explore certain genes, proteins or pathways by wither genetic of drug manipulation, reducing the ethical and other limitations in human cells or brain tissue (Saraceno, 2013). Transgenic mouse models have widely been used, being generated by using the APP gene mutations which have been identified, with Swedish double mutation K670N/M671L being present in almost half of the APP transgenic mice (Sasaguri, 2017). Over time, knockout mice models including widely used APP23Tg, Tg2576, APP/PS1, 3xTg-AD, PS19, Htau, rTg4510 as well as double transgenic mice allowed understanding of mechanisms that lead to AD pathogenesis, the disease progression and potential therapeutic treatments (Arnim, 2006; Sterniczuk, 2010; Iba, 2015; Song, 2015). Tg2576 transgenic mouse model has been one of the most commonly used rodent model, presenting the Swedish mutation at APP695 and expressing amyloid protein in the spinal cord and the forebrain regions (Hsiao, 1995). Staining with thioflavin-s have showed that these mice exhibit pathology and express amyloid plaques starting at the age of 10 months, as well as producing oligomeric beta-amyloid, which is known to be more toxic than aggregated beta-amyloid in the plaques (Lesne, 2006). Despite plaque deposition, this mouse model failed to demonstrate neuronal loss which is commonly observed in AD brains (Irizarry, 1997), however later on, studies on Tg2576 mice demonstrated a significant loss in synapses in the hippocampal entorhinal cortex at the age of 15 months (Dong, 2007). APP23 mouse model has successfully showed that besides expression of tau and beta-amyloid, key AD hallmarks, seen in transgenic mice, there is also glial cell activation, seen around the plaques,

which is known to play an important role in the neuroinflammatory responses, seen in human AD (Sturchler-Pierrat, 1997; Stalder, 1999; Bornemann, 2001). This model has also successfully demonstrated extensive neuronal loss in CA1, of the APP23 mice hippocampi (Calhoun, 1998).

Along with APP mutated mice, transgenic models expressing human wildtype tau have also been generated in laboratories in order to investigate pathological changes in neurodegeneration (Kitazawa, 2012; Platt, 2013). One of the first transgenic mouse model, expressing tau 40, either 1N4R or 0N3R isoform, demonstrated PHF-1 positive phopsho-tau in the cell bodies and the dendrites of neurons, however neurofibrillary tangles were absent (Götz, 1995; Brion, 1999). At that time, these studies provided useful insight on neuropathology, as transgenic mice showed evidence that intracellular tangles can aggregate in the absence of amyloid plaques, however more recent studies suggest that Aβ fibrils and plaques can enhance the formation of tangle pathology in mutant tau mice such as P301L, rTg3696AB and APPKOTg30 mice (Götz, 2001; Götz, 2004; Paulson, 2008; Vandes Dries, 2017).

For a better and complete understanding of the neuropathological changes in AD, scientists have created transgenic models to express both amyloid plaques and tau tangles as single mutations in the rodent models, as described above, are insufficient to generate all the specific pathological changes observed in the human AD brains (Kitazawa, 2012).

Lewis and collegues have developed the first dual mutated mouse model, by crossing JNPL3 with Tg2576 transgenic lines (Lewis *et al*, 2001). The

key findings of their study were that amyloid plaque formation is generated similarly as seen in the parental Tg2576 mice, however NFT deposition, seen in the entorhinal cortex, amygdala and the subiculum of these mice, was accelerated, when compared to JNPL3 line suggesting that the amyloid pathology enhances formation of tau tangles in the double transgenic mice models (Lewis *et al*, 2001)

Despite all advantages of using mouse models in AD studies, there are also papers that debate this using these models, suggesting that human studies are still very limited in comparison to mice studies and that key findings in transgenic mice studies fail to successfully translate and apply into human clinical trials that could find a cure for AD (Franco, 2014). One of the most important aspects to be considered regarding the discrepancies between research and clinical practise is that the extensive neuronal loss reported in the brains of AD patients is not always present in the AD mouse models (Cuadrado-Tejedor, 2014). Moreover, when patients are diagnosed with moderate and severe AD, they already have substantial synaptic and neuronal loss with cognitive impairment (Serrano-Pozo, 2011).

Most of the research that uses transgenic mice focused on mutations that result in plaque and tangle pathology, however patients with AD have been described to have more pathologies than just plaques and tangles (Scheinder, 2007; Scheinder, 2009). Mouse models represent the pathology of AD, exclusively, therefore potential therapies on these mice may not prove total efficacy (Kitazawa, 2012).

Besides AD pathology, the complexity of the disease arises from numerous processes such as neuroinflammation, neurotoxicity, mitochondrial and

oxidative stress. Thus, no transgenic line is able to cover all aspects of the disease, suggesting that the mouse models fail to fully reproduce the human disease mechanisms that can take decades to develop specific pathology resulting in symptoms that are primarily involved in the higher cognitive function (Gama, 2012).

1.5.4   Cell models

Another important AD model, based on growing amount of evidence, suggests that studies using cell models such as embryonic stem cells, human induced pluripotent stem cells (iPSC) and neuronal cells are important in revealing normal (control) and pathological conditions in the research of AD through a different approach (Saraceno, 2013). A study from 2011, explained the use of familial AD fibroblasts with mutations in the PSEN 1 and PSEN2 genes, which were differentiated into iPSC leading to neurons that revealed increased Aβ accumulation, illustrating the specific pathological characteristics of familial AD (Yagi *et al.*, 2011). This study demonstrated the potential of familial AD-iPSC-derived neurons in the research of AD to identify novel therapeutic strategies. In the following year, another study which explored iPSC in both familial AD and sporadic AD, revealed that in some of the sporadic cases, the cells showed increased Aβ generation and tau hyperphosphorylation (Israel *et al.*, 2012). The same study also emphasized the importance of studying AD pathology only in these iPSC-derived neurons as the initial fibroblast cells did not exhibit the same AD pathology features (Israel *et al.*, 2012). These two studies as well as other numerous studies demonstrate the potential of iPSC-derived

neurons as a good AD model to explore the disease progression and to guide the drug development in the hope of finding the cure (Zhang, 2014; Nieweg, 2015; Ortiz-Virumbrales, 2017).

Nevertheless, researchers also consider the limitations of this model as growing certain iPSC cell lines could not be time or cost effective due to prolonged time required for developing the cells until they reach adult phenotype (D'Antonio, 2017; Wray, 2017). Moreover, there is a recent paper suggesting that the cell culture models may not represent the variety of tau isoforms seen in the adult brain and the necessity of this to the development of tau pathology is not known (Arber, 2017).

Considering the above discussed advantages and disadvantages of AD models which allow mimicking AD specific phenotypes at different stages of the disease progression, they represent an important tool of investigating AD, however a constant need for more accurate potent models is required to overcome all challenges of finding the best AD model.

1.5.5   Skin-derived fibroblasts

As previously mentioned in Section 1.1.7, a new high throughout model is needed to study abnormal Aβ and tau deposits from the brains of AD patients. Although altered autophagy pathway, in animal models and human autopsy tissue, has been described, it is still unclear whether pathogenic alterations extend to peripheral cells such as skin-derived fibroblasts. The idea of using fibroblasts as a potential resource came after many of the neuronal changes that take place in AD brains, such as toxic protein

accumulation, increased oxidative stress and mitochondrial abnormalities have also been reported in fibroblasts derived from AD patients (Citron *et al.*, 1994, Magini *et al.*, 2010, Ramamoorthy *et al.*, 2012; Mocali, 2014). *In vitro* culture cell models using human skin-derived fibroblasts could explore whether AD deposits extend to peripheral cells such as the skin fibroblasts based on the previous studies on AD patients fibroblasts.

Peripheral fibroblasts, obtained from AD patients, are a potentially useful tool to investigate the progression of molecular events throughout various stages of AD. These cells have many advantages, from which they are commercially available and avoid many of the ethical and methodological issues associated with the use of animal or human post-mortem tissue. Also, there are several cell banks worldwide from which they can be ordered and cultured *in vitro*, fed with suitable medium, stored (at -80° or in liquid nitrogen) and recovered when needed for experiments (Connolly, 1998).

Once, research will identify specific targets within the autophagy machinery, novel strategies to prevent and treat AD could revolutionize the neurodegeneration research. Thus, these cells could prove invaluable in identifying and assessing new therapeutic approaches, as well as for the identification of new diagnostic biomarkers, which are scarce at the moment.

1.6   Aims and objectives

There are numerous studies on animal models investigating autophagy impairment in demented brains however human studies are minimal and there are still gaps to the research.

This study will aim to characterize macroautophagy and CMA deficits in post-mortem human brain tissue across different subregions of three brain regions and at different AD stages (as defined by Braak stage). This investigation also aims to understand macroautophagy and CMA deficits in relationship to each other and identify which steps in these complex pathways seem to be most significantly impacted in disease. This study also aims to test skin-derived fibroblasts and explore the autophagy levels that are found within these cells. Another aim is to explore whether there are variations in autophagy marker expression across the three brain regions differentially affected in AD, the hippocampus, the frontal cortex and the occipital cortex. The study also aimed to compare the levels of autophagy markers to pathological tau and beta-amyloid in the three brain regions to understand how the two pathways relate to significant pathological protein aggregates.

1.7 <u>Hypotheses</u>

We propose that MA and CMA pathways become impaired with advancing AD and that autophagy markers distribution vary between subregions of brain areas. We hypothesize that with excessive accumulation of pathological proteins such as tau, there will be a decrease in autophagy markers found within the brain regions. We also propose that MA and CMA become defective at a cellular level, in skin-derived fibroblasts from patients with AD.

HUMAN BRAIN

Early stage of AD   **Moderate stage of AD**   **Severe stage of AD**

Healthy cell   Cellular alteration

SKIN FIBROBLASTS
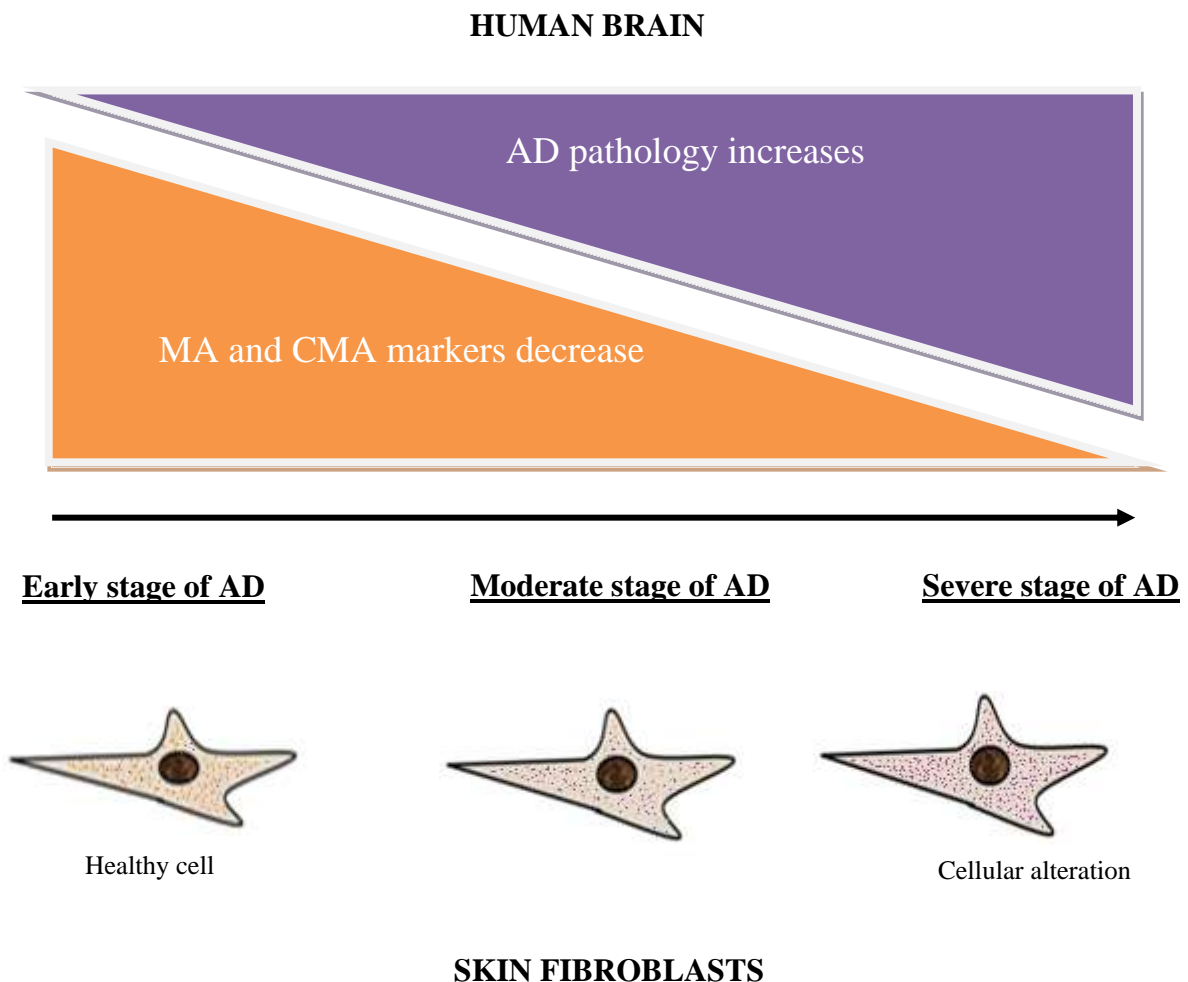
Chapter 2 MATERIALS AND METHODS

2.1 Human brain tissue

2.1.1 Post-mortem human brain tissue

The human brain tissue used for this studies was supplied by the Manchester Brain Bank. The Newcastle & North Tyneside 1 Research Ethics Committee approved the collection, storage and distribution of this brain tissue on 29th of June, 2009 (REC reference 09/H0906/52). Under conditions agreed with the REC, The Manchester Brain Bank supplied tissue or data to the researchers, without requirement for researchers to apply individually to the REC for approval. This work was also approved by the University of Salford Ethics Committee.

A total of 45 cases were used from formalin-fixed, wax embedded brain tissue sections (6μm) were provided from the Manchester Brain Bank. Tissue from three different brain regions including those demonstrating an early pathological involvement (hippocampus and temporal cortex) and regions that become involved with advancing disease progression (frontal and occipital lobe) for each case were provided. The 45 cases consist of 17 cases of Braak stage 0-II (minimal pathology, highly unlikely Alzheimer's disease), 15 cases Braak stage III-IV (probable AD, moderate pathology and 13 cases Braak stage V-VI (highly likely AD). Braak staging had been previously performed by the Brain Bank pathologists and data was supplied regarding this.

2.1.2 Patient demographics

Data associated with gender, age at death, main clinical feature, principal pathology and Braak stage was provided (Table 1).

Table 2.1 Patients demographic

	Braak 0-II	Braak III-IV	Braak V-VI
Mean age at death	87	86.2	79.5
% females	47	73	69
% males	53	27	31

Brain pH data was only available from a subset of more recent samples that were collected fresh and therefore, amenable to pH testing. Thus, minimal pH data was available on a few cases (n=11) used in this study: four Braak 0-II cases had average brain pH 5.63–6.27, four Braak III-IV cases had pH 6.08–6.63 and three Braak V-VI cases had Ph 5.41–6.27. Post-mortem delay (PMD) data was also collected for all cases (n=44; data missing for one case) and reported in hours: Braak 0-II, 12–144; Braak III-IV, 6–134; and Braak V-VI, 25–176. All 45 cases manifested as sporadic AD; dementia status was considered based on the patients' clinical diagnosis and it was recorded for 41 cases (data missing for four cases). In Braak 0-II group, a total of 15 patients had available dementia status and were considered: cognitively normal (n=11), diagnosed with vascular dementia (n=2) or found with a history of stroke (n=2). In Braak III-IV, a total of 11 patients were: cognitively normal (n=3), diagnosed with AD (n=2), diagnosed with vascular dementia (n=2) or other type of dementia (n=4). In Braak V-VI, 12 patients

were diagnosed with: AD (n=10), vascular dementia (n=1) and other type of dementia (n=1).

2.1.3   Tissue processing

The tissue was obtained post-mortem at the Manchester Brain Bank and tissue was formalin fixed and wax-embedded to preserve it's the cellular and molecular contents for further analysis. Tissue was then sectioned at 6µm, attached to glass slides for further analysis. Tissue processing was performed by staff at the Manchester Brain Bank.

2.2   Immunohistochemistry

The experiments in this study use methods to investigate alterations in autophagy related to neurodegeneration and to explore the correlation between autophagy biomarkers and AD pathological hallmarks. Methods include immunohistochemistry, microscopy, image analysis, staining scoring and stats analysis.

2.2.1   Antibodies

The optimal staining dilution and conditions were achieved for all the antibodies (see table 2.1.4). These conditions were used for all 45 sections including the positive and the negative controls for each antibody.

Polyclonal anti-human LAMP2A antibody, purchased from Abcam is a lysosome associated membrane protein, present at the surface of the cell

and plays a crucial role in the chaperone mediated autophagy pathway, being highly selective on the cargo that enters the cell. This antibody is used as a biomarker to assess impaired chaperone mediated autophagy in the 45 cases of temporal cortex and hippocampal neurodegeneration (Cuervo, 2014).

Polyclonal anti-human LC3 antibody, purchased from the MBL (Medical and Biological Laboratories), is an autophagosome biomarker, associated with the levels of formation of a double-layered membrane which engulfs the cargo that needs to be degraded. LC3 antibody was used to assess macroautophagy pathway in the 45 cases of temporal cortex and hippocampal neurodegeneration.

Monoclonal anti-human Beclin-1 antibody, purchased from Abcam, is a key regulator in macroautophagy, involved in nucleation of the phagophore and the formation of the autophagosome and it is often used in studies to assess macroautophagy.

Monoclonal anti-human Hsp70 antibody, purchased from Santa Cruz Biotechnology, is a protein with many functions such as being a chaperone to facilitate the assembly of multi-protein complexes and aiding in the transport of polypeptides across cell membranes or to reach the nucleus. Hsp70 was used to assess chaperone mediated autophagy being the biomarker

Monoclonal anti-human AT8 antibody, purchased from Pierce, stains tau protein which a microtubule-associated protein that gets hyperphosphorylated and results in the pathological neurofibrillary tangles that are found in AD brains.

Monoclonal anti-human beta-amyloid (clone 6F/3D), purchased from Dako, stains deposits of beta-amyloid, found in plaques specific to AD brains. The antibody was manufactured to label human beta-amyloid containing the N-terminal epitope.

Table 2.2 **Antibodies for immunohistochemistry.** Table of optimal antibody dilutions and staining conditions for each antibody

Primary Antibody	Host species	Cat no	Brand	Dilution	Pre-treatment
LAMP2A	Rabbit	Ab18528	Abcam	1:500	H_2O_2 in methanol
LC3	Rabbit	PM036	MBL	1:5000	H_2O_2 in methanol
Beclin-1	Mouse	Ab114071	Abcam	1:2000	H_2O_2 in methanol
Hsp70/ Hsc70	Mouse	W27/sc-24	SantaCruz Biotechnology	1:4000	H_2O_2 in methanol
AT8	Mouse	MN1020	Thermo Fisher	1:750	H_2O_2 in methanol
Aβ	Mouse	M0872	Dako	1:100	H_2O_2 in methanol and formic acid

2.2.2   Immunohistochemistry

Using two separate histoclear (National Diagnostics) pots, the brain sections were dewaxed, for 5 mins incubation in each solution. The tissue followed sequential rehydration in 100%, 100%, 95% and 75% ethanol, for 5 mins each. Many types of tissue, in particular the brain tissue contains endogenous peroxidase. This may result in high, non-specific background

staining which can be reduced by adding a pre-treatment step. In order to block the endogenous peroxidase activity, LAMP2A, AT8 and Aβ sections were incubated in 3% H_2O_2 (Sigma-Aldrich) in methanol, for 20 mins whereas LC3, Hsp70 and Beclin-1 slides which required 1 hour incubation in 3% H_2O_2 in methanol. Formalin-fixed tissue sections required an antigen retrieval step before immunohistochemical staining was performed. The reason for this is the formation of methylene bridges during fixation, which cross-link proteins and therefore mask antigenic sites. One method of antigen retrieval is heat-mediated or heat-induced epitope retrieval. Thus, LAMP2A sections were microwaved for 10 minutes, set at 800W, in 0.01M Tri-sodium citrate buffer (pH 6.5). LC3, Beclin-1, Hsp70, AT8 and Aβ sections required pre-treatment in the Lab Vision™ PT Module (Thermo Scientific) which involved a cycle of heating the slides for 20min in 0.01M Tri-sodium citrate at 98°C (Scientific Laboratory Supplies) buffer (pH 6.5). Aβ required a 4 hour incubation, in 99% formic acid (Scientific Laboratory Supplies) to enhance antigen unmasking after heat induced epitope retrieval. The incubation was done before the endogenous peroxidase was blocked.

The following step involved blocking non-specific sites on LAMP2A and LC3 sections by using 1.5% goat normal blocking serum (diluted in Tris-buffered saline/TBS), contained in the Vectastain ABC kit (Elite Vectastain rabbit ABC kit (Avidin-biotinylated enzyme complex; Elite PK-6102 Rabbit IgG, Vector Laboratories), for 30min incubation (LAMP2A) and 1h (LC3) at room temperature. Beclin-1, Hsp70, AT8 and Aβ sections were blocked by using 1.5% (150μl in 10ml) horse normal blocking serum from the Vectastain ABC

kit, for 30min (AT8 and Aβ) and 1h (Beclin-1 and Hsp70) at room temperature.

LAMP2A and LC3 antibodies were diluted in 1.5% goat normal blocking serum (1:500 antibody dilution and 1:5000, respectively) and incubated for 1h at room temperature. AT8 and beta-amyloid antibodies were diluted in 1.5% horse normal blocking serum (1:750 and 1:100, respectively) for 1 hour at room temperature. Beclin-1 and Hsp70 required overnight primary antibody incubation in 1.5% (150µl in 10ml) horse normal blocking serum (1:2000 and 1:4000, respectively) at 4°C, in a humid box to avoid evaporation.

After the incubations, sections were washed with TBS-T (Tris-buffered saline + 0.1% Tween 20). A biotinylated anti-rabbit IgG secondary antibody (Elite Vectastain ABC rabbit kit) was made up as per manufacturer instructions, then applied to the LAMP2A and LC3 sections for 30 mins at room temperature. For Beclin-1, Hsp70, AT8 and Aβ, a biotinylated anti-mouse IgG secondary antibody (Elite Vectastain ABC mouse kit) was prepared as per manufacturer instructions, then applied to the sections for 30 mins at room temperature. Sections were again washed with TBS-T and incubated with ABC (Elite Vectastain ABC kit, Avidin-Biotin complex, made up as per manufacturer instructions) for 30 mins at room temperature.

Peroxidase activity was developed for 1 min (LAMP2A, Beclin-1, Hsp70); 4 mins (LC3); 5 mins (AT8); 6 mins (Aβ) at room temperature with 3,3-diaminobenzidine (DAB) kit and the reaction was stopped by washing slides in tap water for 5 mins.

The DAB (3,3-diaminobenzidine DAB ImmPACT™ peroxidase substrate kit from Vector Laboratories and DAB tablets from Sigma-Aldrich) developing times were decided after the positive controls for each staining were monitored under the light microscope to observe the positive staining (brown colouration) and when there was sufficient staining (to avoid overexposure) , the reaction was stopped, leading to the optimal chosen time for each antibody. Haematoxylin (Vector Laboratories) counterstain was applied for 2-3 seconds with the being excess rinsed off with tap water for 2-3 mins. Lastly, sections were dehydrated in 75%, 95%, 100% and 100% ethanol, 5 mins each, followed by 5 mins incubation in a clearing histoclear. Sections were mounted in DPX mounting media (Sigma-Aldrich) to be further analysed under the light microscope.

2.2.3   Microscopy analysis

Leica AirLab software was used from a tablet connected to a Leica ICC50W Wi-Fi Camera attached to Leica Microscope DM500. 100x and 400x magnifications were used to capture the autophagy markers staining and the AD pathological features in all sections.

All sections were scored, based on the region with most intense staining (one field within the region of interest), on a semi-quantitative scale, for positive staining in both grey and white matter, using 0-3 scale and + scoring system as previously described (Lace *et al*, 2009). Stained sections were scored according to the number of cells stained positive (0=no cells stained; 1=<20% cells stained; 2=21-69% cells stained; 3=70-100% cells stained). Also, the cells were scored according to the intensity of the

staining (0=no staining present; +=mild/pale brown colour; ++=moderate brown colour; +++=severe, intense colour) (Figure 2.1*). Positive controls for AT8 and Aβ antibodies were chosen based on high Braak. Other positive controls for LAMP2A, LC3, Beclin-1 and Hsp70 antibodies were chosen based on low Braak stage since these should demonstrate minimal disruption to autophagy pathways and previous studies have suggested that these markers are present in a normal brain. All negative controls involved implementing the immunohistochemistry staining protocols described above in absence of the primary antibody incubations.
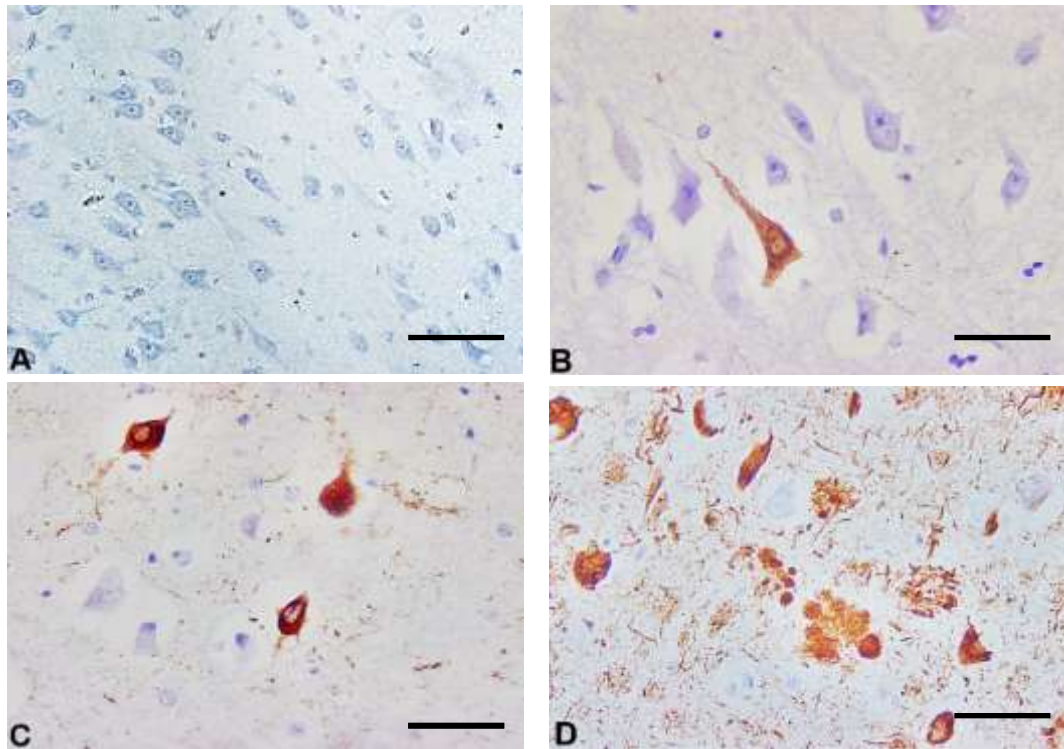
Figure 2.1 Scoring scheme of immunohistochemistry

Sections within the hippocampus region of 4 cases which were scored according to the number of the cells stained: 0=no staining (A); +=mild (B); ++ moderate (C); +++ severe (D); Magnification: 100x (A) and 400x (B-D); Scale bars 50µm.
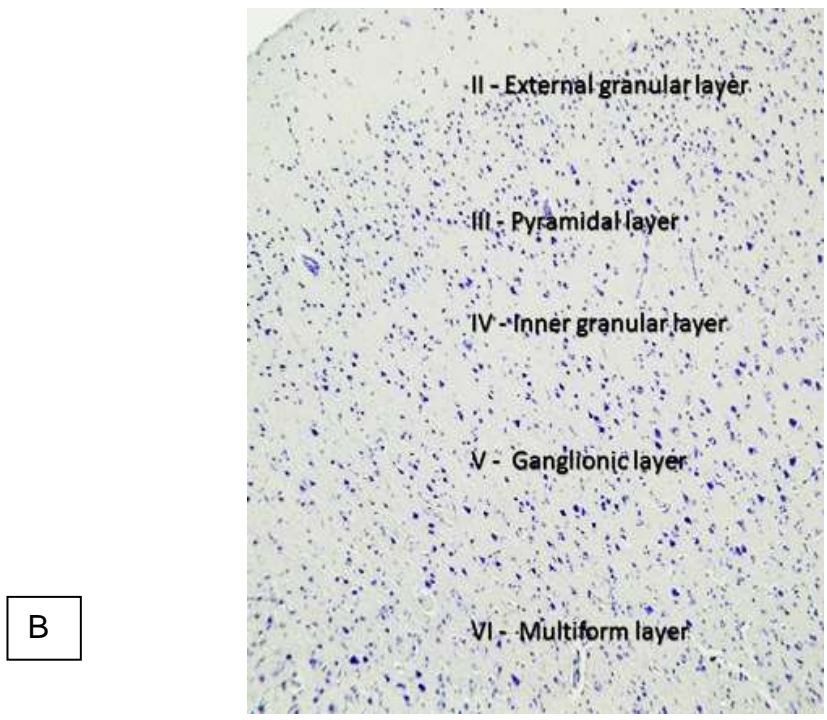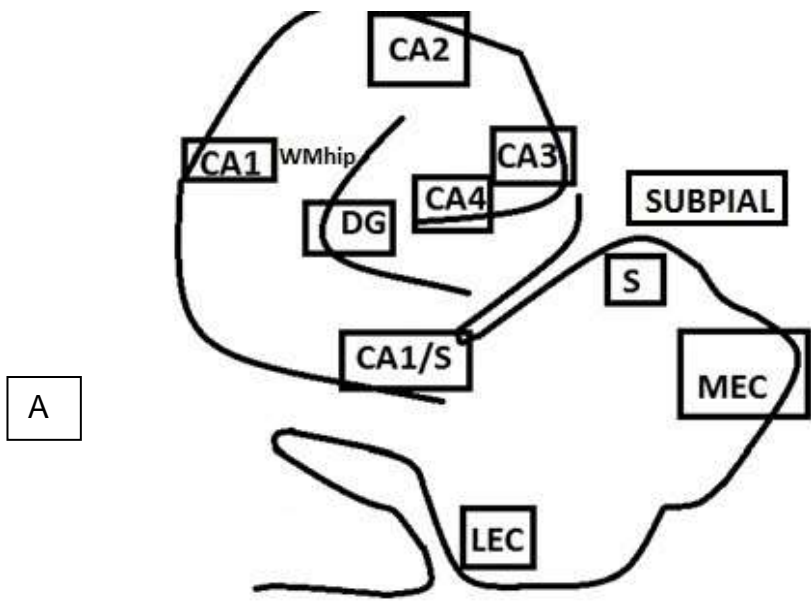
Figure 2.2 Immunohistochemical scores areas. Diagram illustrating the areas of choice by which the scoring was targeted A) in the hippocampus and B) in the frontal/occipital cortices (Layers I-VI).
WM=white matter; CA=cornu ammonis; DG=dentate gyrus; S=subiculum; MEC=medial entorhinal cortex; LEC=lateral entorhinal cortex.

In the hippocampus, the scored areas comprised chosen fields of view with the highest staining levels (most intense staining) for each subregion including DG, CA4, CA3, CA2, CA1 and the subiculum as indicated in Figure 2.2. LEC (lateral entorhinal cortex) and MEC (medial entorhinal cortex) layers were also scored, along with the temporal cortex (TC) and the white matter (WM) regions (figure 2.2). The chosen regions are known to have different pathological involvement in AD with disease progression mentioned in section 1.2. A separate region, the CA1/Subiculum border was scored independently, due to slightly different pathology as previously described (Lace *et al.*, 2009). Also, the subpial region within the entorhinal cortex was take into consideration for astrocytic positivity, being given scores of 0 (negative staining) and 1 (positive staining).

Glial cells morphologies were identified in the AT8 stained sections (Figure 2.3). Various morphologies of astrocytes were seen in the hippocampus sections, including thorn-shaped astrocytes, fuzzy astrocytes with fine granular processes, ramified astrocytes, stellate astrocytes and globular astroglial inclusions. Microglia and coiled bodies were also seen in the brain sections (Figure 2.3). An in-depth analysis of various AT8 lesions (Supplementary figures 1–4) and autophagy markers could be explored in the future.
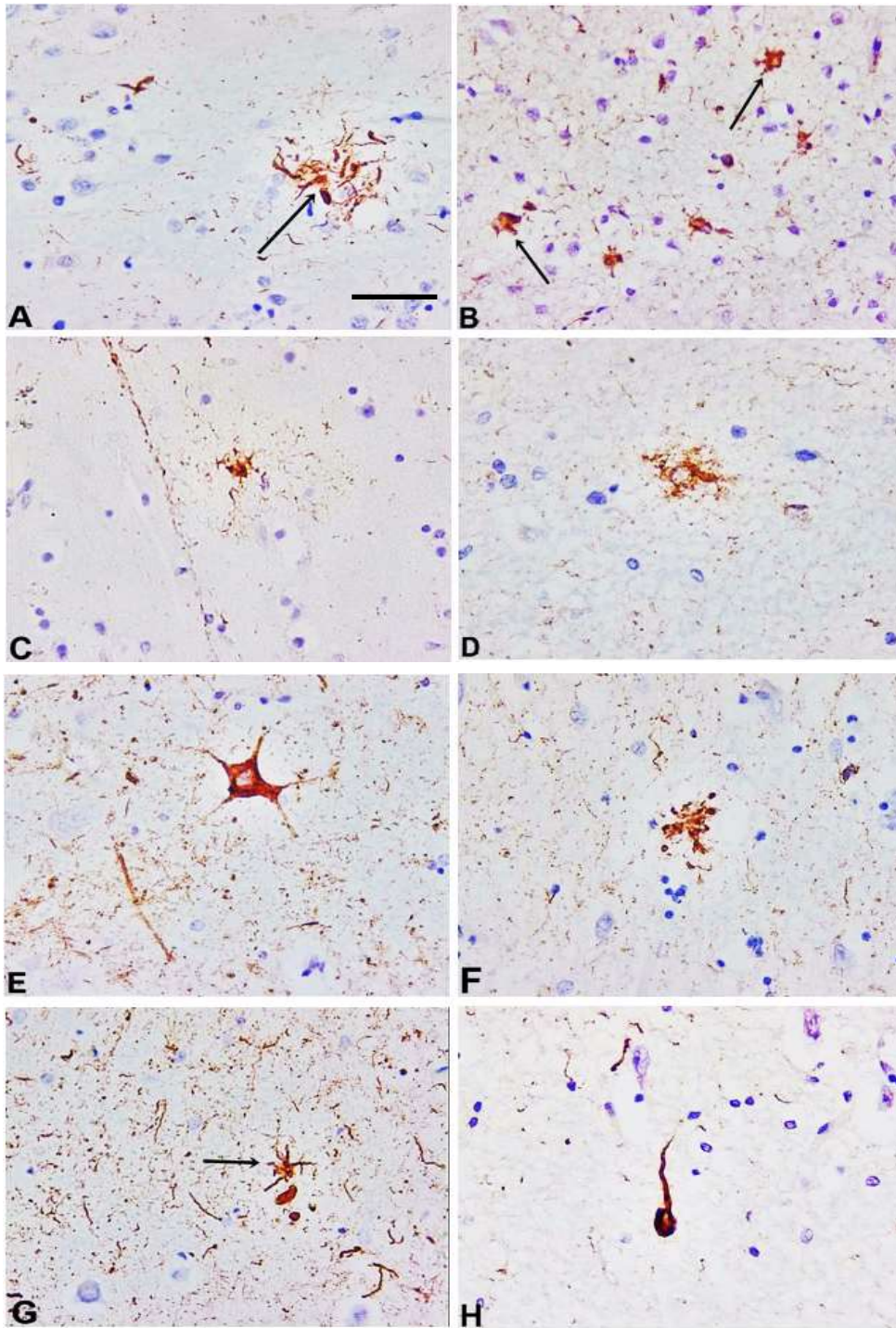
Figure 2.3 Glial cells morphologies stained by AT8 antibody.
Tufted astrocyte in the TC (A); thorn-shaped astrocyte in TC (B); fuzzy astrocyte with fine granular processes in TC (C); ramified astrocyte in MEC (D); stellate astrocyte in CA1 (E); globular astroglial inclusion (F); microglial cell in CA4 (G) and coiled body in the hippocampal WM (H); Magnification 100X; Scale bars 50μm.

For further analysis, all scores of 0, 1, 2 and 3 were dichotomized into two groups: significant pathology (all scores of 2-moderate and 3-severe) and minor pathology (all scores of 0-none and 1-mild).

All 45 cases were scored, for each key biomarker. A random selection of 10% of the cases were scored by an independent scorer (Dr Gemma Lace-Costigan) in order to check reliability. Inter-rater agreement was tested using Cohen's kappa to compare the scores in the three brain regions–for each marker used for staining–from the two observers. A high level of agreement was found (kappa=0.94), with respect to all six antibodies used for the staining.

2.3   Double labelling immunofluorescence staining

Similarly to the conventional immunohistochemistry, the brain sections were firstly dewaxed by immersion into histoclear pots for 10 mins, followed by sequencial rehydration in 100%, 100%, 95% and 75% ethanol, for 5 mins each. Then, the brain sections required antigen retrieval by heat in the PT module (Thermo Scientific), for a 20 mins cycle at 98°C. After this step, three washes of 10 mins each with 100mM glycine buffer were introduced to reduce the non-specific staining due to autofluorescence of the brain tissue. For amplified results and a better signal of the staining, an avidin-biotin complex was selected. The avidin-biotin complex (ABC) is a highly sensitive method for immunohistochemical detection with biotinylated secondary antibodies. Avidin is a 65kDa protein, found in the egg whites of birds, reptiles and amphibians which shows strong affinity for biotin, a water

soluble vitamin (vitamin B_7 or vitamin H) having four biotin binding sites which makes the interaction ideal for detection of antibodies. The avidin-biotin complex is one of the strongest non-covalent interaction between a protein and a ligand as they bind really quickly to each other and do not seem to get affected by changes in temperature or pH or by other organic solvents.

Prior to the avidin and biotin incubations, several extra steps were required including a 15 mins incubation with egg white (containing casein) in ddH20, followed by a 15mins incubation in 2% skimmed milk in PBS buffer, both steps at RT. The avidin and biotin blocking steps were included to saturate any available avidin and biotin binding sites, exposed and potentially being able to generate false positive results. All sections were blocked, using 1.5% horse normal blocking serum from the Vectastain ABC kit, for 30min at room temperature. The sections were then incubated with primary rabbit antibodies against LAMP2A (1:500) and LC3 (1:1000) for 1 hour at RT followed by washes with PBS buffer. Biotinylated secondary antibody from the rabbit Vectastain ABC kit was used to incubate the sections for 30mins at RT. After three washes with PBS buffer, avidin-Red Texas dye conjugate (Sigma,-Aldrich) was applied to all the sections in the dark, for 30mins at RT followed by an additional blocking step with horse serum for 30mins at RT. The second primary antibody, mouse monoclonal AT8, was then applied on the sections (1:750) for 1h at RT, followed by a 30mins incubation with biotinylated secondary antibody from the mouse Vectastain ABC kit. Sections were then incubated with avidin-green dye conjugate (Thermo Scientific) for 30mins at RT, away from the sunlight. An additional step for

further non-specific staining reduction due to autofluorescence was required, thus 0.1% Sudan Black B reagent (Abcam) diluted in 70% ethanol was used to incubate all the sections for 30 minutes, which were then washed with PBS and mounted with aqueous ProLong Antifade mounting media (Thermo Fisher) (no dehydration required).

Zeiss Zen Software in correlation with a multi-headed Carl Zeiss microscope allowed computer controlled image capturing for the double labelling studies. Magnifications used included 200x and 400x.

Five cases from each Braak group (Braak 0-II, n=5; Braak III-IV, n=5; and Braak V-VI, n=5) were randomly selected and double-stained for each marker LC3 (n=15) and LAMP2A (n=15). Therefore, a total of 15 sections were stained against LAMP2A and a total of 15 sections were stained against LC3. Images were captured in each CA4 and CA1 subregions for each individual case. After capturing, the red and the green channel images (of each region/case) were merged in order to assess the protein expression of the autophagy markers and the co-localisation with AD related tau protein. Five random fields of view from the chosen regions CA4 and CA1 were selected and mean values for autophagy marker vs AD protein were obtained. Individual cells within the selected fields of view were then analysed to explore the MA and CMA markers levels (red channel) and the tau protein levels across all three Braak stage groups and the same cell area was kept for the two channels to reduce variability among the results. For accuracy, five selections of background with no fluorescence were selected around each cell that was analysed to give final *corrected total cell fluorescence* (CTCF) values. LAMP2A, LC3 and AT8 positive cells, in both

subregions CA4 and CA1, were then quantified, in all cases, in order to assess the co-localisation of the two autophagy markers and tau protein. The degree of co-localisation was then explored with increasing Braak staging to assess its variation with disease progression.

2.4 <u>Statistical analysis</u>

Statistical analysis was initially performed on GraphPad software (Inc., San Diego, CA, USA) or on SPSS 22/24 software. Chi-square test was performed to evaluate the variation in MA and CMA markers across Braak stage groups and the regional variation of LAMP2A, LC3, Beclin-1, Hsp70, AT8 and beta-amyloid across all hippocampal subregions. This test was also used to assess the relationship between the autophagy positively stained astrocytes and oligodendrocytes across the different Braak stages in order to explore glial autophagy changes at different stages of disease. CA4 and CA1 were chosen as regions of interest as CA4 is associated with tau/beta-amyloid in late stages of AD and CA1 is associated with tau/beta-amyloid in early stages of AD. Chi-square test explored if different autophagy markers varied across various pathologies including astrocytes and NTh. Chi-square test also assessed autophagy markers positively stained lesions such as the axons, neurophil threads, vacuoles and intracellular inclusions across Braak stages. Chi-square tests were also used to assess the co-localisation of the two autophagy markers with AT8 marker with Braak staging and to evaluate the variation between CA4 and CA1 staining of LAMP2A and LC3 as well as AT8 in individual neurons of the hippocampal subregions.

2.5 Human skin-derived fibroblasts

2.5.1 Cells

Commercially available fibroblasts were purchased from NHCDR and Coriell Cell Biorepositories. The cells purchased from Coriell were found within NIA (National Institute of Aging) Aging Cell Culture repository catalogue and all details can be found at https://www.coriell.org/. Skin-derived fibroblasts were collected from arm/calf from patients with sporadic AD (no known family history) and familial AD (FAD) with PSEN mutations and age-matched controls. Skin-derived fibroblasts were cultured and characterized by Coriell before shipping. Cells from nine individual cases: three from sporadic AD cases, three from familial AD cases and three age-matched controls, were used in this study.

Table 2.3 Skin-derived fibroblasts used in this study

	Coriell catalog ID	Age	Gender
Controls	ND35044	77	male
	ND36320	71	female
	ND29178	66	male
Sporadic AD	AG09019	76	female
	AG07375B	71	male
	AG08517	66	female
Familial AD	AG08711	34	female
	AG06840	56	male
	AG06848	56	female

2.5.2   Growth conditions *in vitro*

The fibroblasts were grown in until passage 14 in T75 flasks, at 37°C, 5% CO_2 and 21% O_2 and fed with MEM w/ Earle's Salts media (Labtech), supplemented with penicillin/streptomycin (Labtech), 200mM L-glutamine (Thermo Fisher), 20% foetal bovine serum (Scientific Laboratory Supplies), 10% non-essential amino acids and 10% vitamins (Scientific Laboratory Supplies). Media changes were performed every 2-3 days until cells reached 70-80% confluency (Figure 2.8).

2.5.3   Cell trypsinization

Once the cells reached 70-80% confluency (Figure 2.4), they were subcultured by trypsinization, using 0.25% trypsin/EDTA (Scientific Laboratory Supplies), for 2-3 mins at 37°C. Trypsinization was stopped by addition of 3-4 fold volume of FBS containing media, followed by centrifugation for 4 mins at 400xg to obtain a pellet of the cells. The pellet was washed twice in sterile PBS before being resuspended in fresh media for passaging at a ratio of 1:3. Alternatively trypsinized cell may have been harvested for freezing by resuspending the collected pellet in sterile freezing buffer (10 % DMSO in FBS-Pierce) and rapid transfer to a Mr Frosty (Thermo Scientific) in a -80 freezer for 24-48hrs. Cells were then transferred to liquid nitrogen for long term storage.
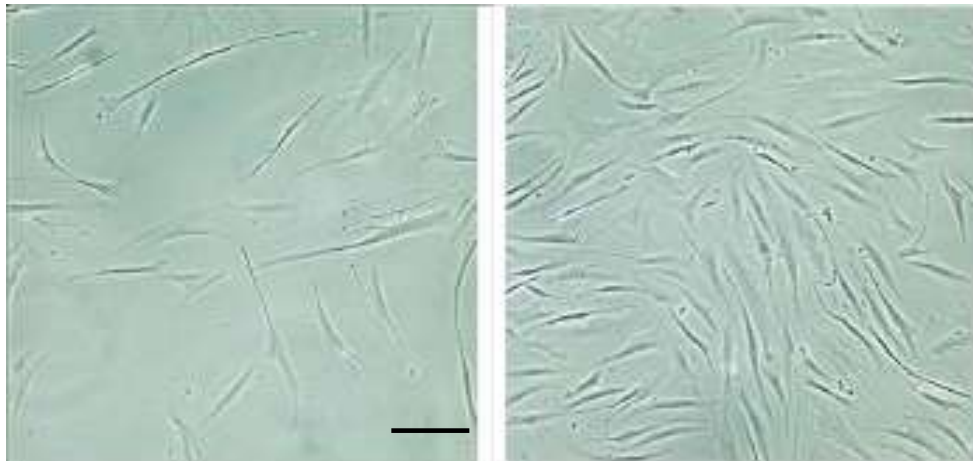
Figure 2.4 Fibroblasts confluency. Fibroblasts confluent at approximately 30-40% in the flask (left) and at over 70%, being ready to be split (right). Magnification 400x. Scale bar 100 μm

2.5.4   Protein extraction

Cells were grown until passage 14 and experiments were performed on cell lysates from passages 10–12. Protein extraction was performed at each passage for all control and AD cells, by trypsinization (as previously described in 2.5.3), followed by centrifugation for 4 mins at 400xg to obtain a pellet and lastly, additional washes of the pellet with sterile PBS, to wash away the media (as previously described in 2.5.3). Once the pellet was clean, 150µl radioimmunoprecipitation assay buffer (RIPA) (Thermo Scientific), supplemented with Halt™ Protease and Phosphatase Inhibitor Cocktail (Thermo Scientific) was added to lyse the cells, while gently pipetting up and down, on ice. This allowed cell membranes lysis and exposure of the cellular content, which protected proteins from degradation during the extraction process.

2.6   Western blotting

2.6.1   Bradford assay

Known concentrations of bovine serum albumin (BSA, Thermo Scientific) were used to generate a standard curve to determine unknown protein concentration in the cell homogenates by Bradford assay. This assay is a commonly used method, a colorimetric protein method of determining the concentration in a solution using the Commassie blue absorbance properties. Under acidic conditions, the initial form of Commassie blue

which is red/brown becomes blue by binding to the proteins that are being assaye (Butt, 2013).

For each cell lysate sample, 2.5µl of protein lysate of unknown concentration (section 2.5.4) was mixed with 997.5µl dH_2O to make up an end volume of 1000µl. 100µl from each sample was added to a 96 well plate with equal volumes of Commassie blue reagent (Thermo Scientific). MultiSkan FC plate reader was used to read the absorbance values of the Bradford samples, at 595nm wavelength, giving values for both unknown samples and known concentration standards, which were then used to plot a standard curve. The linear equation $y=ax+b$ of the standard curve was used to establish the concentration of unknown protein samples and the results were adjusted depending on the dilution factors used.

2.6.2   Homogenates preparation

Prior to running the proteins through the gel, the homogenates were treated with active sample buffer (SB) which was prepared by adding 200µl dithiothreitol (DTT, Scientific Laboratory Supplies) to 800µl 2xSample buffer (100mM Tris-HCl pH 6.8, 4% SDS, 0.02% bromophenol blue (purchased from Scientific Laboratory Supplies), 20% glycerol (Scientific Laboratory Supplies). DTT is a denaturing agent and its role is to break down the disulphide bonds between protein-protein. SDS is a denaturing anionic detergent that converts the folded form of proteins into linear chains of amino acids, giving them a negative charge. This is because the linearized proteins need an even charge as they have to separate based on their size

only, migrating from the negative electrode to the positive electrode. The glycerol gives enough density to the samples so they sink, while bromophenol blue is a tracking dye enabling the sample loading in the wells as well as checking how far the proteins have travelled through the gel, before the electric current is stopped.

Samples were then boiled in equal volumes of active 2x sample buffer for 5 mins to help further unfolding of the proteins and bring them to their primary structure. Samples were centrifuged for 15s in a bench top microcentrifuge and stored at -20°C until ready to use for Western blotting.

2.6.3   SDS polyacrylamide gel electrophoresis

The first experiments aimed to optimise LC3 (Novus), LAMP2A (Abcam), Beclin-1 (Abcam) and Hsp70/Hsc70 (Santa Cruz Biotechnology) antibodies using the cell homogenates from the skin-derived fibroblasts. A 12% SDS optimal gel was chosen for LC3 antibody (Table 2.4) as LC3 protein's molecular weight is 15-17kDa, being found in two forms: 15kDa cytosolic (LC3I) and 17kDa membrane bound (LC3II). This means, the LC3 bands would be captured 3/4 down the gel to avoid it being 'pushed' off the end of the gel during electrophoresis. The resolving gel was firstly made, which is 2/3 of the total length gel, by adding distilled water, 30% polyacrylamide, 1.5M Tris pH 8.8, 10% SDS, 10% ammonium persulfate (APS-purchased from National Diagnostics) and TEMED. Gel polymerization is initiated by APS and TEMED, forming cross-links between acrylamide molecules that result in pores of specific size, depending on the acrylamide amount used.

Then, the stacking gel was made by adding distilled water, 30% polyacrylamide (Sigma), 0.5M Tris pH 6.8, 10% SDS, 10% APS and TEMED (Sigma). The SDS-PAGE gel uses two types of layers which have different functions. The stacking gel is more acidic and has a pH of 6.6, packing and concentrating the proteins together in one band and being ready to move towards the positive electrode. Then, the migration of the proteins continues in the resolving gel, which has a higher pH of 8.6, where pores get smaller, therefore proteins in the samples are able to separate according to their size into bands of specific molecular weights. Similarly to 12% gel for LC3 antibody, a 7.5% gel was used to optimise LAMP2A (105kDa), Beclin-1 (60kDa) and Hsp70 (70kDa) antibodies (Table 2.4) as these proteins have higher molecular weights, thus their size is bigger needing a lower polyacrylamide % of the gel.

SDS gel electrophoresis and protein transfer were performed using mini-PROTEAN Tetra Cell System attached to a PowerPac HC Power supply by Bio-Rad. The nine samples (3 controls and 6 AD samples) were loaded in lanes 2-10 of the gel at 0.2A per gel and constant 150V, with 10μl of the hyperladder (molecular weight marker, Thermo Scientific) loaded in lane 1. All wells were balanced with 1x SB to ensure equal volumes. 10X electrolyte buffer (25 mM Tris, 192 mM glycine, 0.1% SDS) was used to fill up the electrophoresis tank which was placed on a tray filled with ice to keep the temperature low. The gel was then run for 1h 30 mins (LAMP2A, Hsp70 and Beclin-1) and for 1h 45min (LC3) to allow differentiation of the two LC3 bands (Table 2.4). Once the running finished, the gel was washed

in cold (4°C) transfer buffer (25 mM Tris base, 192 mM glycine, 20% methanol) for 15min on a shaker to remove any excess electrolyte buffer.

2.6.4   Wet transfer of the proteins

The proteins in the gel were then transferred to a nitrocellulose membrane (Sigma) in cold transfer buffer (4°C). The Biorad Trans-Blot system was used for 1h at 100V to perform the transfer. Then, the membrane was washed in TBS-T for 3 x 10min to remove the transfer buffer.

2.6.5   Immunostaining of autophagy markers

The membranes were blocked in 1% BSA with 5% (Marvel) skimmed powdered milk made up in TBS-T, for 30 min (Hsp70 and Beclin-1) and for 1h (LAMP2A, LC3) at room temperature, on a rocker (Table 2.4), followed by incubation with primary antibody diluted into blocking solution, 1:3000 (LC3 antibody); 1:1000 (LAMP2A, Beclin-1 and Hsp70) for 1h at room temperature (Table 2.4). The membranes were rinsed in TBS-T for 3 x 10min and blocked for a second time in the same blocking solution for 30 mins at room temperature, on a rocker. After blocking step, membranes were incubated with secondary antibodies. LC3 and LAMP2A membranes were incubated with secondary goat anti-mouse HRP conjugated antibody (Goat pAb to Rb IgG; Abcam) diluted into blocking solution, 1:5000 for 30min at room temperature, while Beclin-1 and Hsp70 membranes were incubated in goat anti-mouse secondary antibody (Abcam), diluted in

blocking solution 1:5000, for 30 mins, at room temperature. Lastly, the membranes were washed in TBS-T for 5 x 10min.

2.6.6 Enhanced chemiluminescence

The Thermo Scientific ECL kit (SuperSignal West Femto Maximum Sensitivity Substrate; as per manufacturer instructions) was used to visualize the proteins in a G: Box Chemi XX6 (Syngene). Software G: Box Chemi XX6 GeneSys was used to capture images at exposure times 5 sec (LAMP2A), 10 sec (Hsp70), 1 min (Beclin-1) and 3mins (LC3) (Table 2.4).

Table 2.4 Optimal conditions of Western blotting experiments. These conditions were chosen for the four antibodies LAMP2A, Hsp70, LC3 and Beclin-1 to give the best bands resolution with minimal non-specific staining and background.

Experimental condition	LAMP2A	Hsp70	LC3	Beclin-1
Protein concentration (µg)	20	10	20	10
Gel %	7.5	7.5	12	7.5
Gel running time	1h30min	1h30min	1h45min	1h30min
Blocking incubation time	1h	30min	1h	30min
Primary antibody incubation	1:1000	1:1000	1:3000	1:1000
Exposure time	5 sec	10 sec	3 mins	1 min

2.6.7 Stripping and reprobing for beta-actin (loading control)

Membranes were washed 3 x for 10min in TBS-T and incubated in stripping buffer (62.5mM Tris HCl, pH 2.2, 0.1% SDS, 1% Tween20) for 10 min at room temperature to remove the previously used antibodies from the membrane. The membranes were then incubated in blocking solution 1% BSA and 5% skimmed milk made up in TBS-T, for 30min at room temperature. Primary antibody monoclonal mouse beta-actin (Thermo Fisher) was added directly into blocking solution, at a dilution of 1:5000, for 1h at room temperature, followed by three washes in TBS-T for 3 x 10min and blocked again for 30 min. Secondary anti-mouse HRP conjugated antibody was added into blocking solution at 1:5000 and incubated for 30min and washed with TBS-T for 3x 10min. SuperSignal West Femto Maximum Sensitivy substrate reagent (Thermo Scientific) were added to the membrane to visualise bands as previously described.

2.6.8 Protein quantification and statistical analysis

The protein bands were then quantified by analysis in ImageJ software in order to determine a relative protein ratio of each protein of interest compared to the loading control beta-actin. Ratios were also corrected to the background and for LC3, due to presence of two isoforms, LC3-I and LC3-II, each isoform was corrected to beta-actin, then a final ratio LC3-I/LC3-II was obtained to reflect the autophagic flux rate in the cells.

All relative ratios were then plotted on graphs and protein amounts in the sporadic AD cells and the mutated AD cells were compared to the protein amounts in the control fibroblasts.

Paired T-test was used to assess the variation of autophagy markers expression in the skin-derived fibroblasts between the control cases, sporadic cases and PSEN mutated cases. Error bars on graphs represent the standard error and statistical significance is denoted by asterisks with p-values as following: $*p<0.05$ and $**p<0.01$.

Chapter 3   RESULTS: Autophagy in human brain tissue

3.1   <u>Immunohistochemistry of human brain tissue</u>

This chapter will explore the variation of staining distribution of autophagy markers in the three brain regions – the hippocampus, the frontal cortex and the occipital cortex – and will look in-depth at each subregion of these three regions to evaluate how autophagy proteins vary across these areas. Staining distribution will be assessed based on the number of the cells stained positive, as well as based on the immunoreactive intensity at a cellular level. These variations will also be investigated in each Braak stage group in order to evaluate how they change with disease progression. Overall MA and CMA markers staining will then be compared in the three brain regions to identify which pathways becomes more susceptible in AD. Immunoreactivity of autophagy markers will also be evaluated in axons, neuropil threads, intracellular inclusions and glial cells such as oligodendrocytes and astrocytes. Overall, in the hippocampus, LAMP2A staining levels were found the highest in the subiculum and the entorhinal cortex, and the lowest in CA1 and CA3 sugregions. Hsp70 staining levels were also found the lowest in CA1 subregions. For MA markers, LC3 and Beclin-1, the staining distribution was reduced in DG, CA1 and CA3, and was more increased in CA1/S and EC subregions. In the hippocampus, only LC3 was found to significantly decrease with advancing AD ($p < 0.001$).

In the frontal cortex, LAMP2A and Hsp70 staining levels were the lowest in layers II, IV and VI, and the highest in layers III and V. Very similar results were seen for the MA markers, LC3 and Beclin-1. No autophagy marker was found to significantly decrease with advancing disease, however, Beclin-1 was significantly increased in the high Braak group ($p<0.001$).

In the occipital cortex, variation of LAMP2A staining distribution between the subcortical layers was less noticeable. Hsp70 staining varied more than LAMP2A with increasing levels seen in layer III and decreased levels seen in layer IV. Similar distribution of both MA markers were seen in the occipital cortex, with layers II and IV having the lowest levels, and layers III and IV having the most staining. In this brain region, both Hsp70 and LC3 were found to significantly decrease with increasing Braak ($p=0.02$). These results were based on both the number of the cells stained and on the immunereactive intensity.

Overall CMA markers were distributed less than MA markers in the hippocampus and the occipital cortex, whereas in the frontal cortex, the staining levels of CMA markers were more abundant than the MA markers. In terms of immunopositivity of autophagy markers in the glial cells, no significances were found for CMA proteins, however LC3 positive oligodendrocytes were found to significantly increase with advancing AD in both the hippocampus and the frontal cortex ($p<0.01$). On the other hand, LC3 positive astroyctes significantly decreased in Braak V-VI ($p=0.03$). Beclin-1 positive oligodendrocytes were also found to increase with increasing Braak ($p<0.001$).

Moreover, in the hippocampus, a significant increase with higher Braak cases was seen in Beclin-1 positively-stained neurophil threads (p=0.02). In the frontal cortex, significant decreases were seen in LAMP2A positively stained intracellular inclusions (p=0.002) and in Beclin-1 positively-stained axons (p=0.04).

3.1.1 Variation of neuronal staining distribution in the hippocampus

The first set of graphs describe the percentage of cases in the cohort with any staining (mild, moderate, severe) based on the number of the cells stained (0–3 rating scale), for LAMP2A, LC3, Hsp70 and Beclin-1 in each hippocampal region (Figure 3.1 and 3.2).

The majority of cases demonstrated similar degree of staining in the hippocampus. Thus, LAMP2A positivity was found in 90% of cases, LC3 in 80% of cases, Beclin-1 in 94% of cases and Hsp70 positive staining was seen in 72% of cases. There was a similar level of positive staining across most hippocampal subregions. DG subregion was the only area to present less staining for both LC3 and Hsp70 (68% of cases) compared with all other hippocampal subregions.

Beclin-1 staining is the most present in the hippocampus region (Figure 3.2B, followed by LAMP2A staining (Figure 3.1A), while LC3 (Figure 3.2A) and Hsp70 (Figure 3.1B) staining had slightly lower levels of positivity. All cases (100%) demonstrated Beclin-1 positivity in the LEC subregion, followed by 95% of cases demonstrating staining in CA4, CA1 and CA1/S. A total of 93% of cases had Beclin-1 staining in DG, CA3, CA2, S and MEC

subregions (Figure 3.2B). LAMP2A positive staining was found in less than 90% of cases, with CA3 region having the lowest value (84%) (Figure 3.1A). LC3 staining levels were found lower compared with LAMP2A and Beclin-1. LC3 positivity was found in 68% of cases in DG region, followed by the subiculum (72%) (Figure 3.2A). LC3 staining was found in 80% cases in the hippocampus, with the most staining found in CA4 (84%) and CA1/S (84%); and it was least prevalent in DG (68%). Hsp70 staining was found the lowest in the hippocampus (72%) in comparison to other autophagy markers. A mild variation was observed across the hippocampus, when looking at Hsp70 staining with 65% cases found positive in LEC, followed by 68% in DG (Figure 3.1B). Most subregions had around 70% Hsp70 positivity, while CA4 and CA2 had the highest prevalence of the marker, 81% (Figure 3.1B). Overall, DG subregion seemed to have the lowest autophagy proteins distribution, followed by CA3. On the other hand, EC and CA4 were the areas with the most autophagy marker staining in the hippocampal neurons. Based on overall high prevalence of authophagy marker staining across the hippocampal regions, it was decided to dichotomise the data to allow analysis of cases demonstrating only significant staining attaining scores of moderate/severe staining compared to minimal/absent staining (both 0–3 and -/+/++/+++ rating scales).
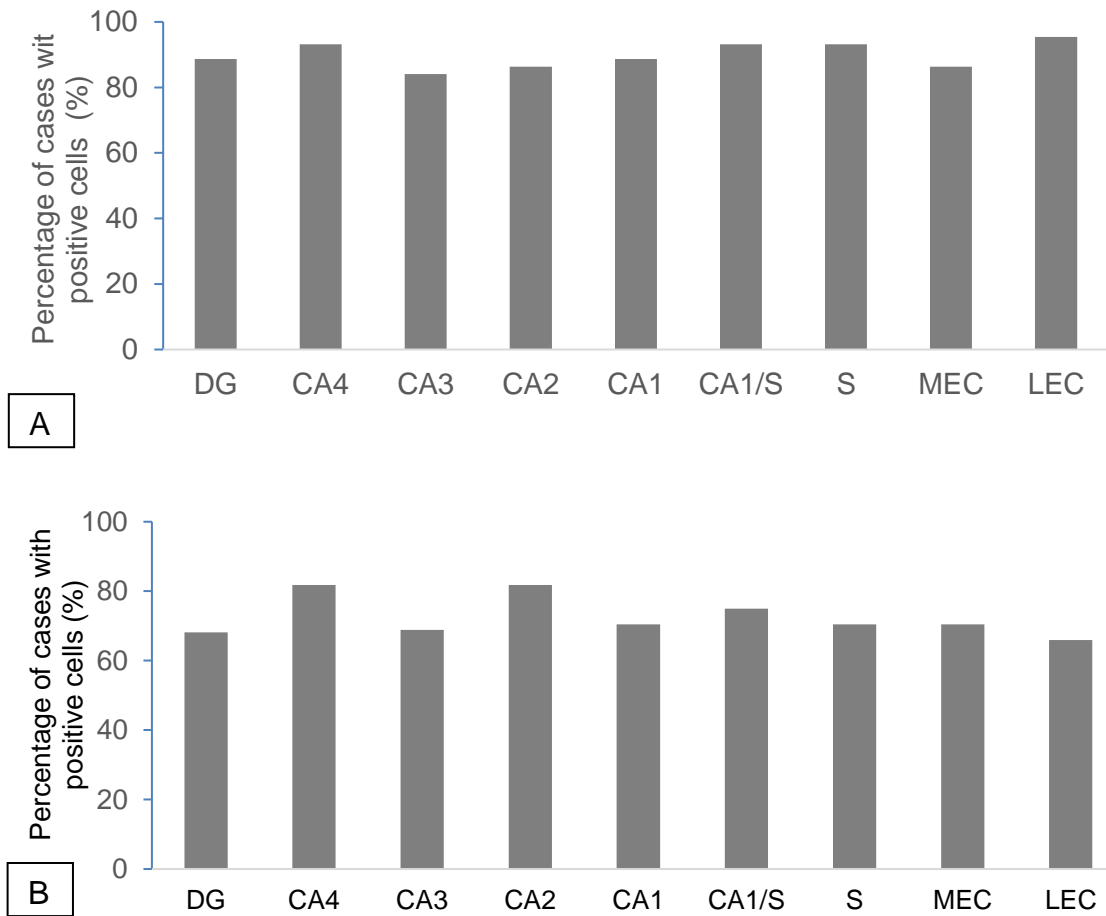
Figure 3.1 Chaperone-mediated autophagy markers across the hippocampal subregions. LAMP2A (A) and Hsp70 (B) staining, expressed in the hippocampal subregions, by the proportion of cases with positive staining, according to the number of the cells stained; (0–3 rating scale).
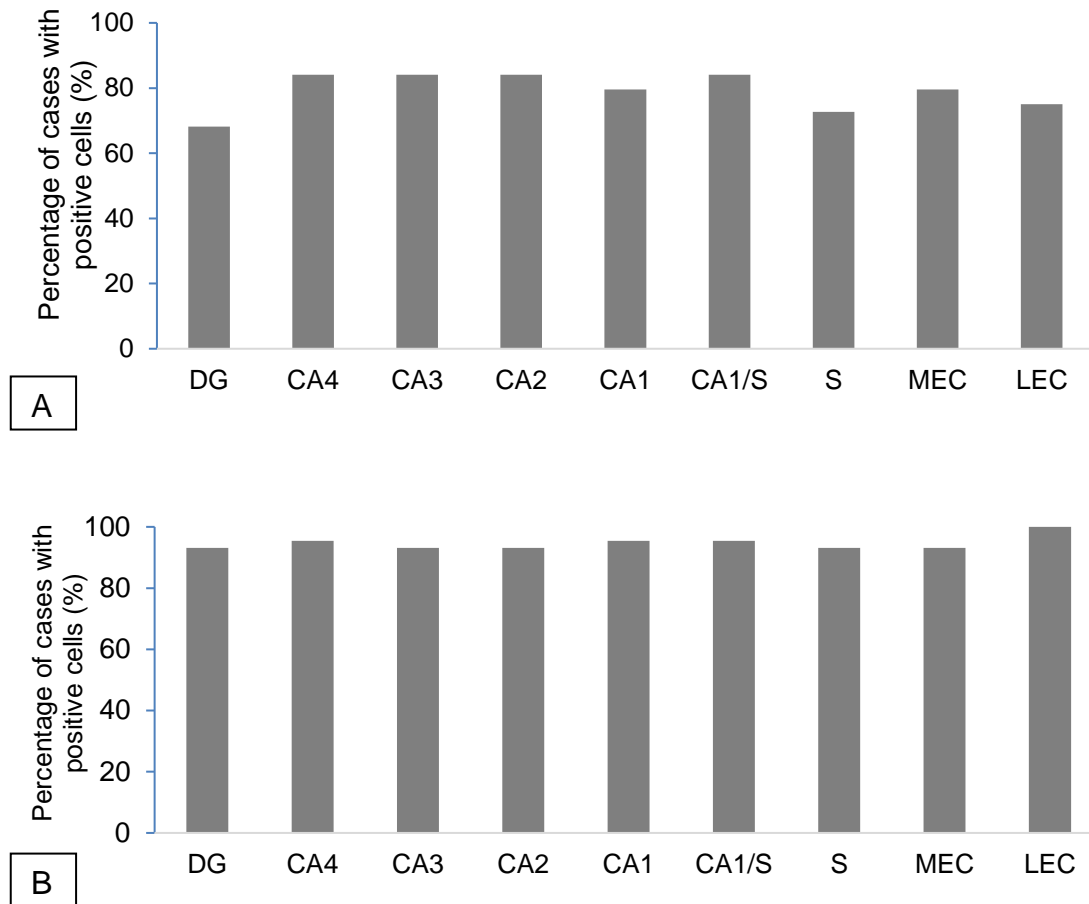
Figure 3.2 Macroautophagy markers across the hippocampal subregions. LC3 (A) and Beclin-1 (B) staining, in the hippocampal subregions, represented by the proportion of cases with positive staining, according to the number of the cells stained; (0–3 rating scale).

The number of cases that demonstrated any staining for the autophagy markers did not significantly vary across the cohort, within the hippocampus subregions, therefore, for a better understanding of the results, the staining scores were dichotomised into two groups: significant staining of autophagy markers (scores of 2 and 3) and minimal staining (scores of 0 and 1). Graphs were then generated based on the significant scores of autophagy

markers in the hippocampus subregions (2 and 3; ++ and ++), therefore the graphs show the percentage of the cases that express each of the four autophagy markers (Figure 3.3 and 3.4). Dichotomised data showed a more evident variation across the hippocampal subregions when compared with the non-dichotomised results (Figure 3.1 and 3.2). Stratification of dichotomised results into the three Braak groups demonstrated a degree of regional variation in LAMP2A staining, seen in Braak V-VI (Figure 3.3A). Staining levels of LAMP2A were found the lowest in CA3 (53%) compared with the highest amounts of staining in LEC (92%) and the subiculum (100%) (Figure 3.3A). Dichotomised results show that Hsp70 positive staining was the lowest in CA1, across all three Braak groups (38%, 40% and 23%, respectively); the lowest value was seen in Braak V-VI (Figure 3.3B). The highest levels of Hsp70 staining were found in MEC (75%) and LEC (75%) in Braak 0-II, in CA2 and CA1/S (60%) in Braak III-IV and lastly, in CA2-4 (61%) and MEC (61%) in Braak V-VI (Figure 3.3B).

For the MA markers, the most evident regional variation was observed for LC3 staining, in Braak III-IV, with the lowest staining seen in DG (33%), followed by the subiculum (40%) compared with the highest staining presence in CA2 (80%) (Figure 3.4A). In Braak 0-II, similar levels of staining were seen across most hippocampal regions, except DG which scored the lowest value of 56% (Figure 3.4A). DG was also found with the lowest level of LC3 staining (53%) in Braak V-VI, while CA1/S region had 84% positively stained cases (Figure 3.4A).

Beclin-1 staining demonstrated similar levels of staining across most hippocampal regions, with minimal regional variation (Figure 3.4B).

Differences were only observed in Braak 0-II as DG had the lowest staining levels (63%), compared with LEC (100%); Braak V-VI showing CA1 with the lowest Beclin-1 staining (69%), compared to MEC,LEC (92%) (Figure 3.4B). These results demonstrated a regional variation of Hsp70 (CMA) and LC3 (MA) staining across the hippocampal subregions, mostly associated with Braak III-IV and Braak V-VI.
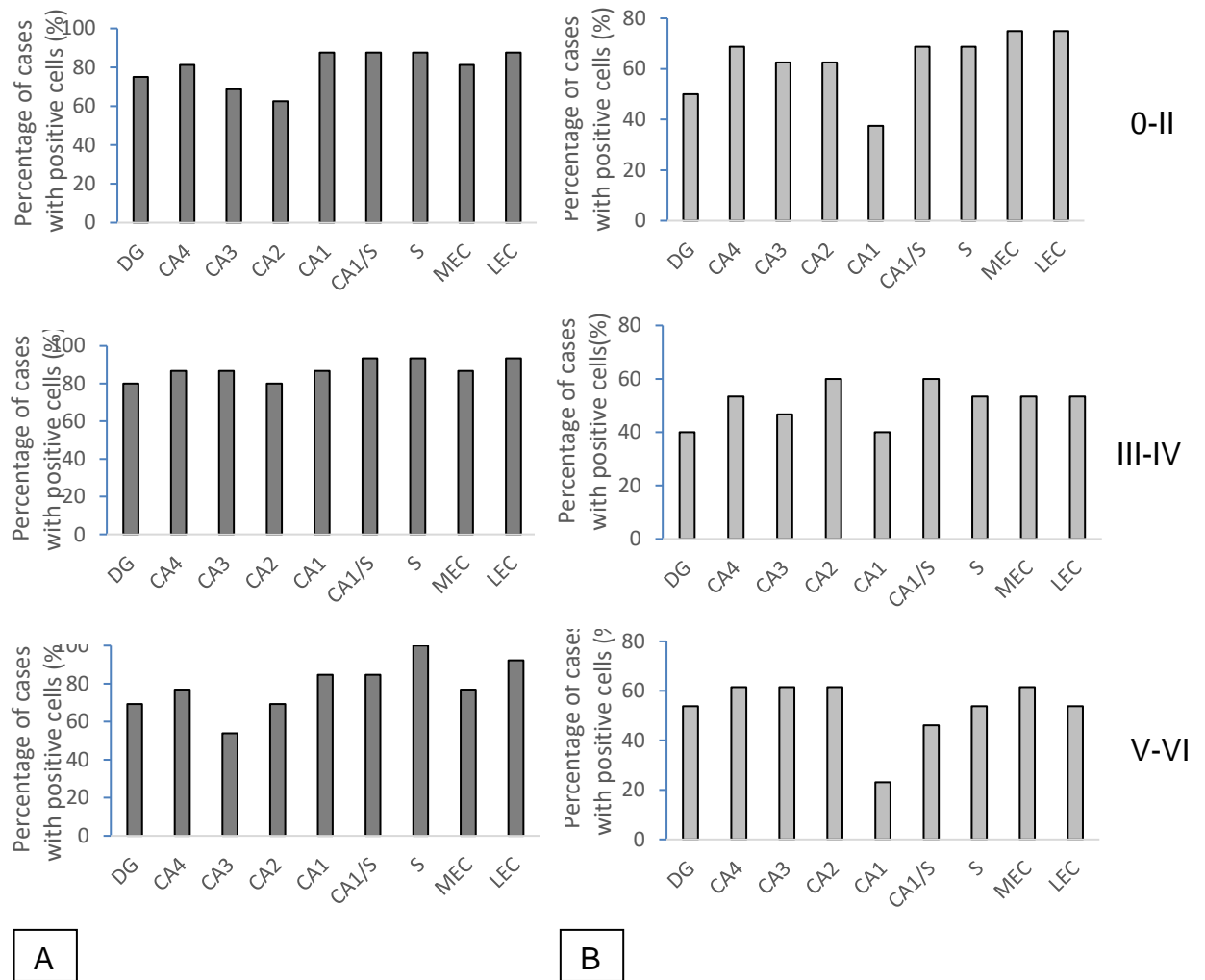
Figure 3.3 Chaperone-mediated autophagy markers in the hippocampal subregions across Braak stages (Braak 0-II, Braak III-IV, Braaak V-VI). LAMP2A (A) and Hsp70 (B) significant staining, expressed across the hippocampal subregions, represented by the total percentage of all cases with dichotomised scores of 1 (significant staining), based on the number of the cells stained; (0–3 rating scale).
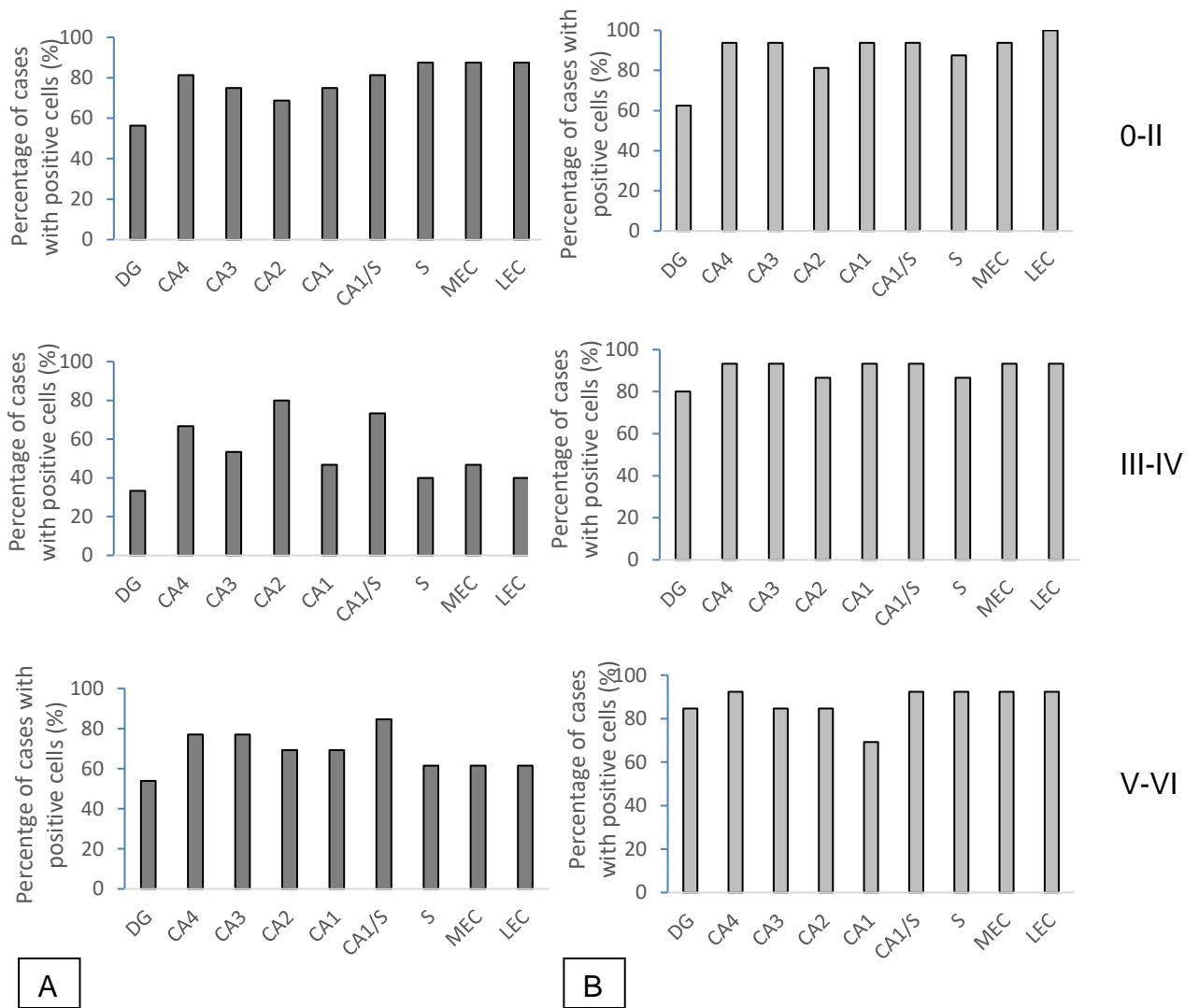
Figure 3.4 Macroautophagy markers in the hippocampal subregions across Braak stages (Braak 0-II, Braak III-IV, Braaak V-VI). LC3 (A) and Beclin-1 (B) significant staining, expressed across the hippocampal subregions, represented by the total percentage of all cases with dichotomised scores of 1 (significant staining), based on the number of the cells stained; (0–3 rating scale).

Following assessment of the number of the cells stained, consideration of intensity of staining (-/+/++/+++ rating scale) was performed as described in section 2.2.3. All autophagy markers had similar staining across all hippocampal regions with no noticeable differences (Figure 3.5 and 3.6). DG had the lowest staining levels, seen in Hsp70 (CMA) and LC3 (MA) staining present in 68% cases (Figure 3.5B and 3.6A). However, most subregions demonstrated positive staining in above 70% of cases. The intensity graphs did not depict significant regional variation in the autophagy markers and as a result, the staining scores were dichotomised into two groups as previously described (-/+ scores in the not significant group and ++/+++ in the significant group).
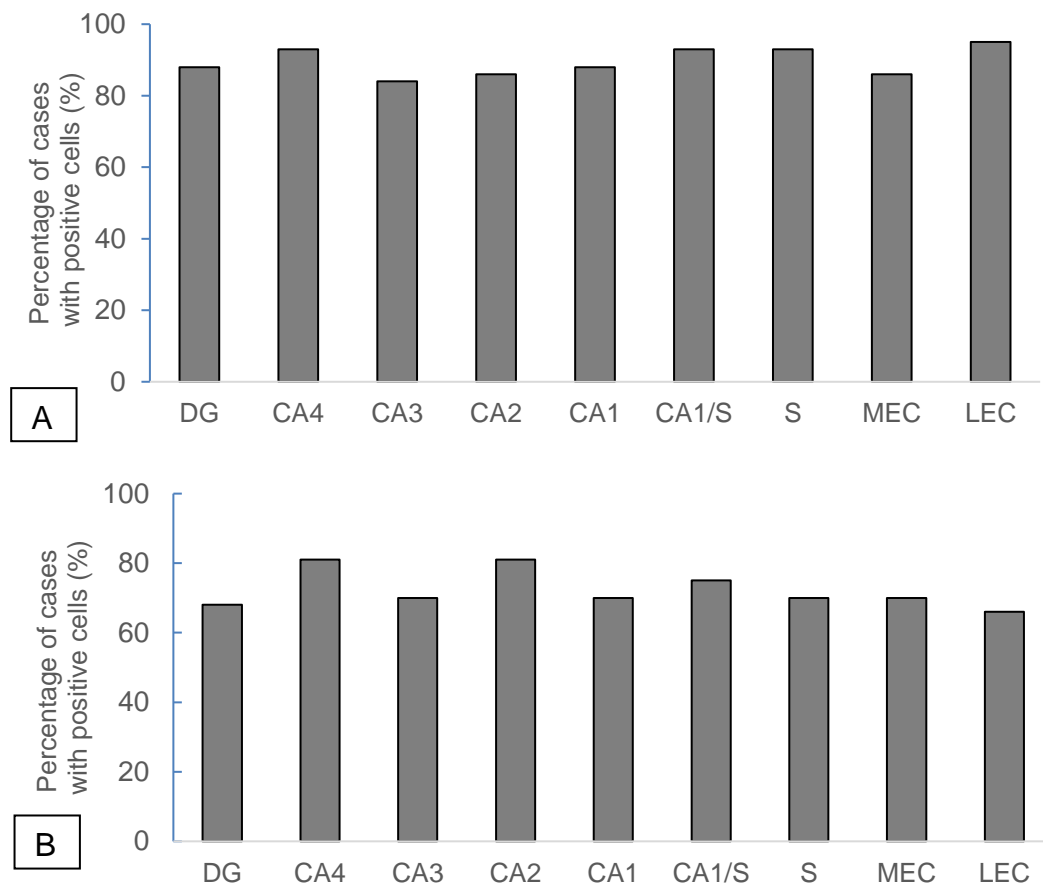
Figure 3.5 Chaperone-mediated autophagy markers across the hippocampal subregions. LAMP2A (A) and Hsp70 (B) staining, expressed in the hippocampal subregions, by the proportion of cases with positive staining, based on the cells intensity; (-/+/++/+++ rating scale).
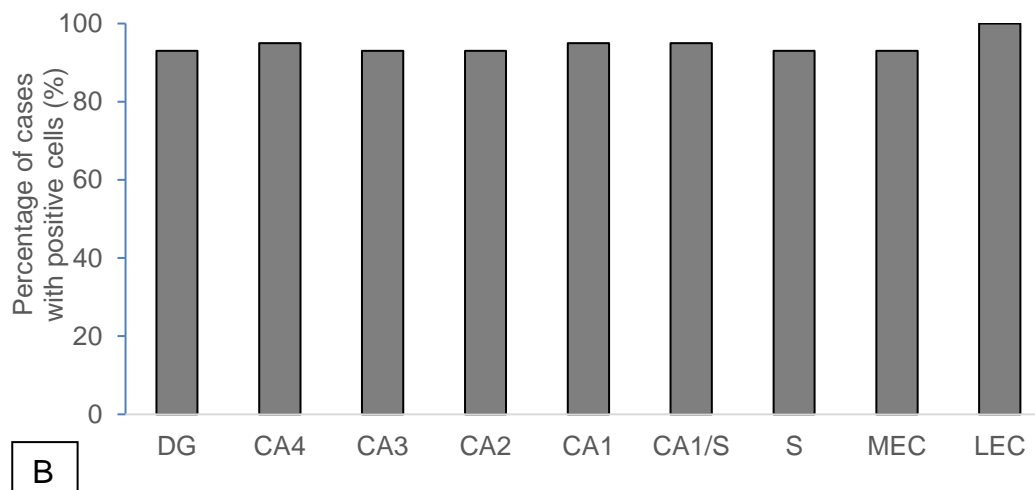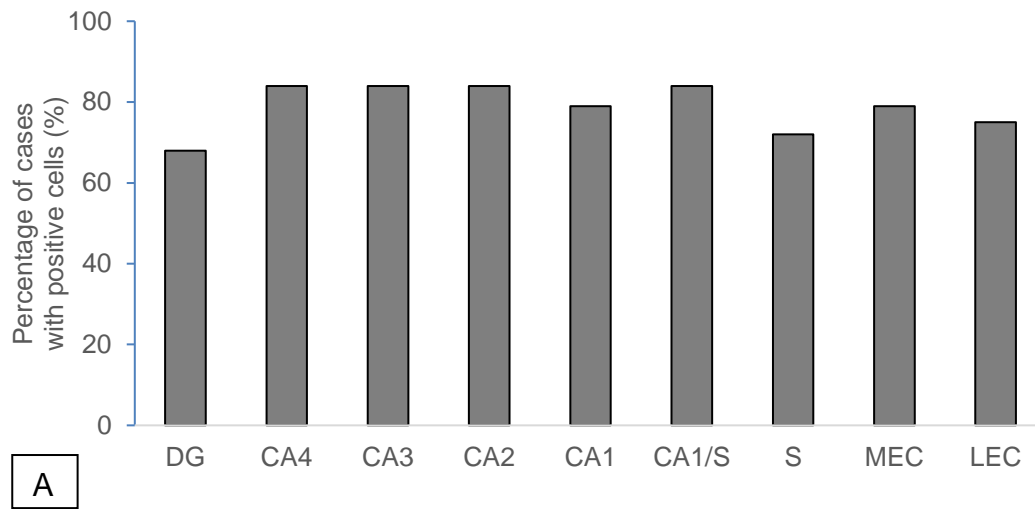
Figure 3.6 Macroautophagy markers across the hippocampal subregions. LC3 (A) and Beclin-1 (B) staining, expressed in the hippocampal subregions, by the proportion of cases with positive staining, based on the cells intensity; (-/+/++/+++ rating scale).

After dichotomisation, based on the staining intensity, a more evident regional variation was observed across all hippocampal regions in the autophagy markers levels (Figure 3.7 and 3.8). Hsp70 staining variation was higher than LAMP2A staining variation across all three Braak groups (Figure 3.7 and 3.8). Nevertheless, LAMP2A staining was found the lowest in CA3 and CA2 (33%), compared with the highest in CA1/S (73%), followed by the subiculum and MEC (66%) in Braak 0-II (Figure 3.7A). In Braak III-IV, the same subregion, CA2, had the lowest LAMP2A staining (60%), whereas all cases demonstrated significant LAMP2A staining (100%) (Figure 3.7A). Levels of LAMP2A decreased in CA2, from Braak III-IV to Braak V-VI (46%), with CA2 being the region with the lowest staining levels across all Braak groups (Figure 3.7A). Very low levels of Hsp70 staining were seen in CA1 subregion in Braak 0-II (6%) and Braak V-VI (15%) (Figure 3.7B). Higher levels of Hsp70 staining were observed in the subiculum (50%) in Braak 0-II and in CA4 and CA2 (54%) in Braak V-VI (Figure 3.7B). In Braak III-IV, Hsp70 staining was found the lowest in CA3 (13%), compared with the highest staining in CA2 (53%) (Figure 3.7B). There was also a regional variation in both MA markers across all Braak groups (Figure 3.8). LC3 staining was found the lowest in CA3 (26%), compared with CA1/S (80%) in Braak 0-II (Figure 3.8A). In Braak III-IV, LC3 positive staining was only found in 13% of cases in the subiculum and CA1 compared with 46% in CA1/S, whereas in high Braak, LC3 staining was the lowest in LEC (23%) and the highest in CA2 (61%) (Figure 3.8A). Beclin-1 staining was found very low in DG (6%), compared with CA1/S (60%) in

Braak 0-II (Figure 3.8B). In Braak III-IV, Beclin-1 staining was present in 26% in LEC compared with 73% in CA4, whereas in high Braak, LC3 staining was the lowest in CA1 (30%) and the highest in CA1/S (77%) (Figure 3.8B). These results demonstrated a regional variation of all autophagy markers staining across the hippocampal subregions, in all Braak groups.
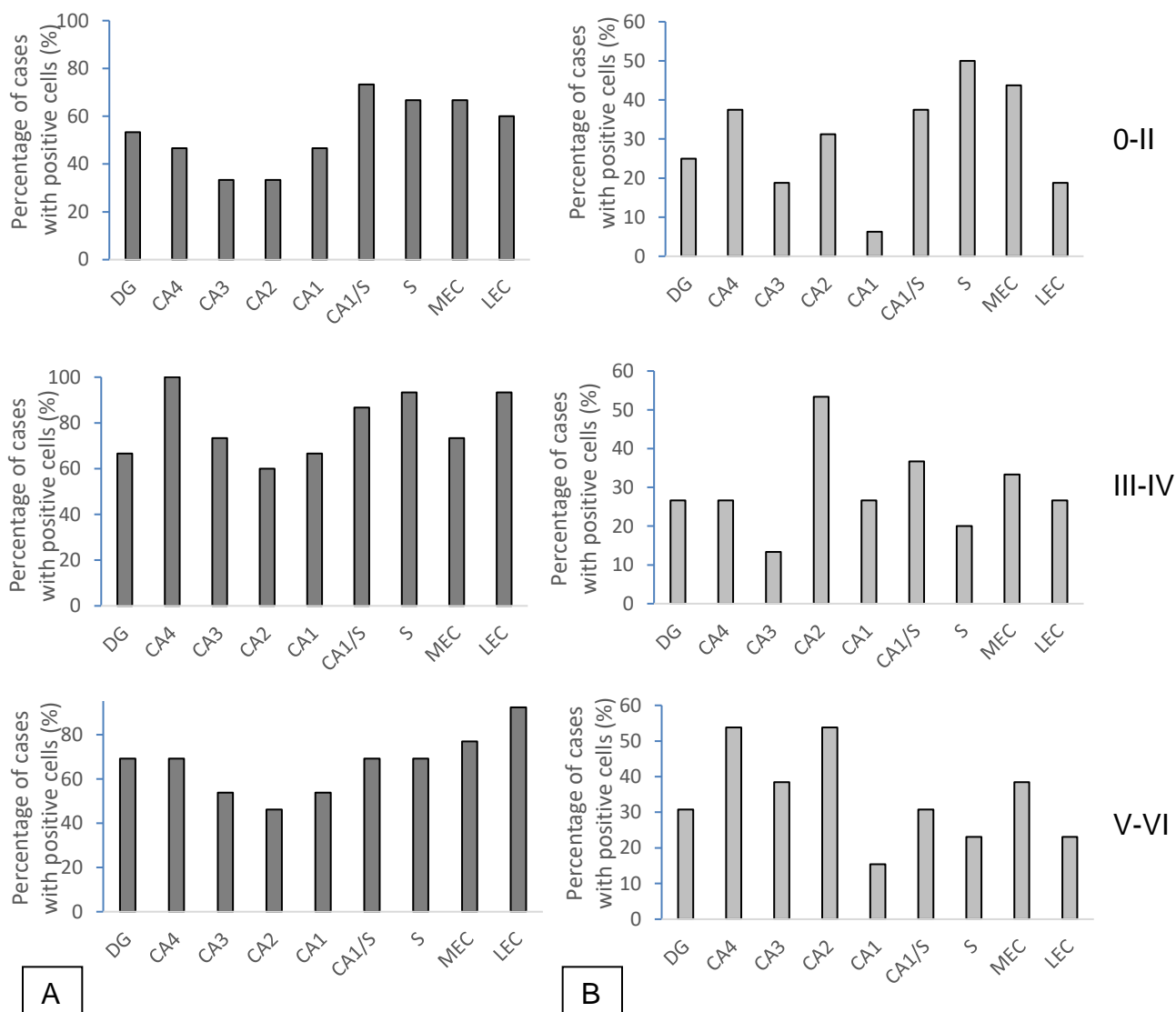
Figure 3.7 Chaperone mediated autophagy markers in the hippocampal subregions across Braak stages (Braak 0-II, Braak III-IV, Braaak V-VI). LAMP2A (A) and Hsp70 (B) significant staining, expressed across the hippocampal subregions, represented by the total percentage of all cases with dichotomised scores of 1 (significant staining), based on the cells intensity; (-/+/++/+++ rating scale).
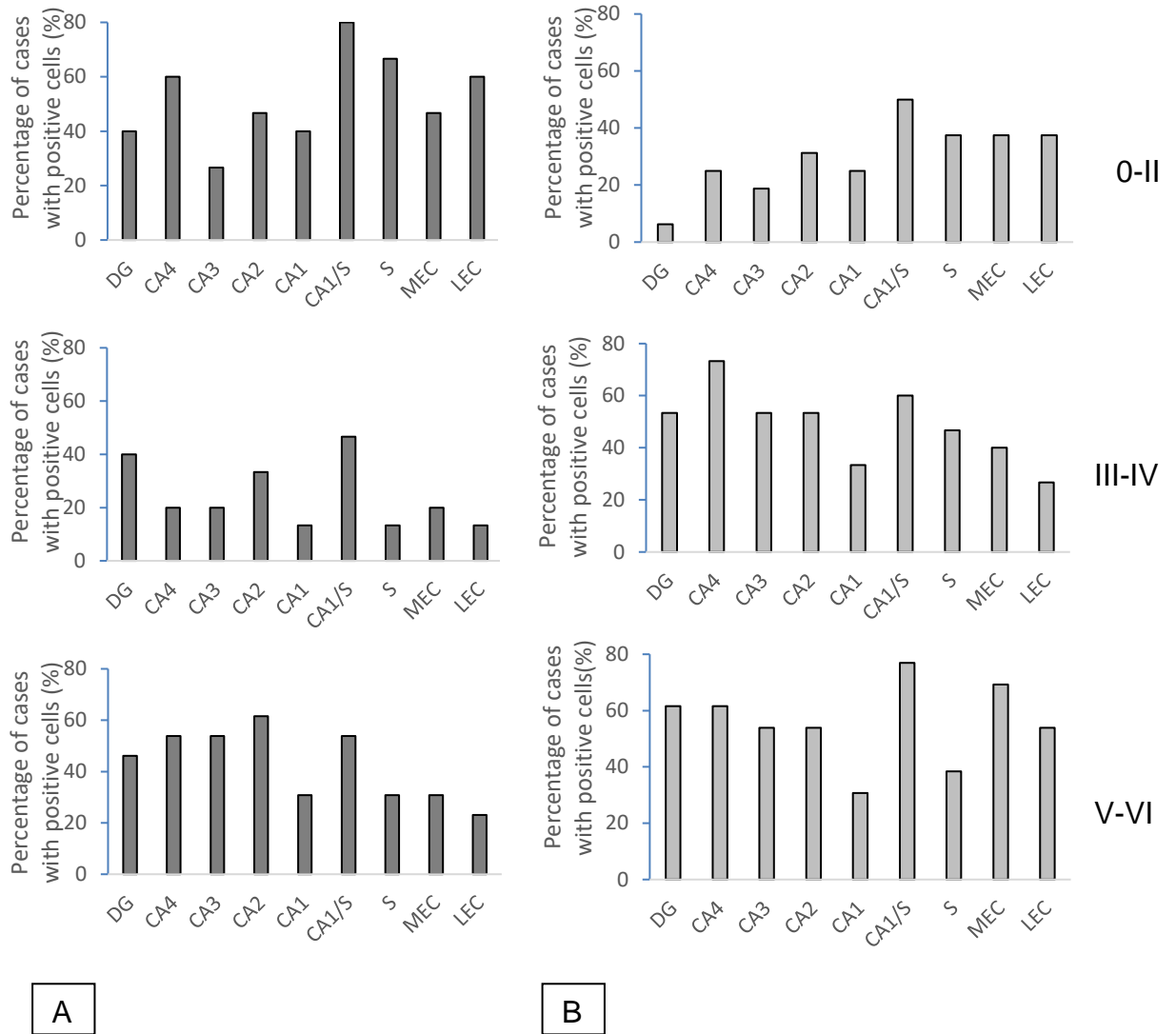
Figure 3.8 Macroautophagy autophagy markers in the hippocampal subregions across Braak stages (Braak 0-II, Braak III-IV, Braaak V-VI). LC3 (A) and Beclin-1 (B) significant staining, expressed across the hippocampal subregions, represented by the total percentage of all cases with dichotomised scores of 1 (significant staining), based on the cells intensity; (-/+/++/+++).

Next, we looked at the overall moderate/severe staining of MA and CMA autophagy markers in the hippocampus to explore how the markers distribution change with disease progression (scores of 2 and 3 considered; 0-3 rating scale). LC3 staining levels were found to decrease significantly in Braak III-IV cases (Figure 3.9).

Hippocampal cells stained by LC3 were present in 78% of the cases in Braak 0-II, dropping to 53% in Braak III-IV and an increase in high Braak (68%) (Chi square test, $p<0.001$) (Figure 3.9 and 3.10). Hsp70 hippocampus levels showed a slower decline rate, with no statistical significance, from 63% in low Braak, to 51% and 53%, respectively, in late stages of the disease (Chi square test, $p=0.09$) (Figure 3.9 and 3.10). Beclin-1 and LAMP2A staining was similar across the Braak stages, being present in the majority of the cases (Chi square test, $p=0.7$ and $p=0.13$, respectively) (Figure 3.9).
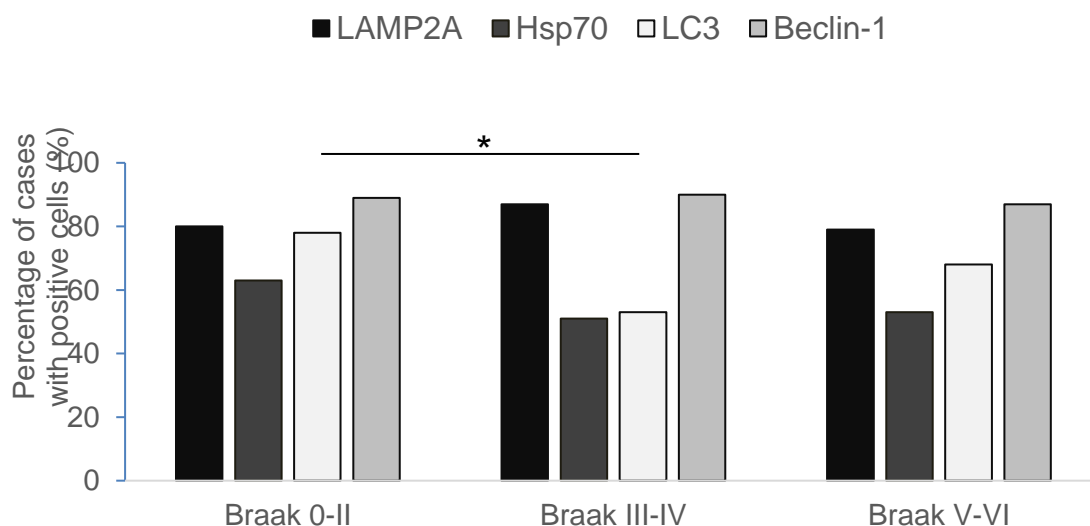
Figure 3.9 Autophagy markers staining across all Braak stages in the hippocampus. Scores were based on the number of the cells stained; (0–3 rating scale); *$p<0.05$

	Braak 0-II	Braak III-IV	Braak V-VI
LC3			
Hsp70			
LAMP2A			
Beclin-1			
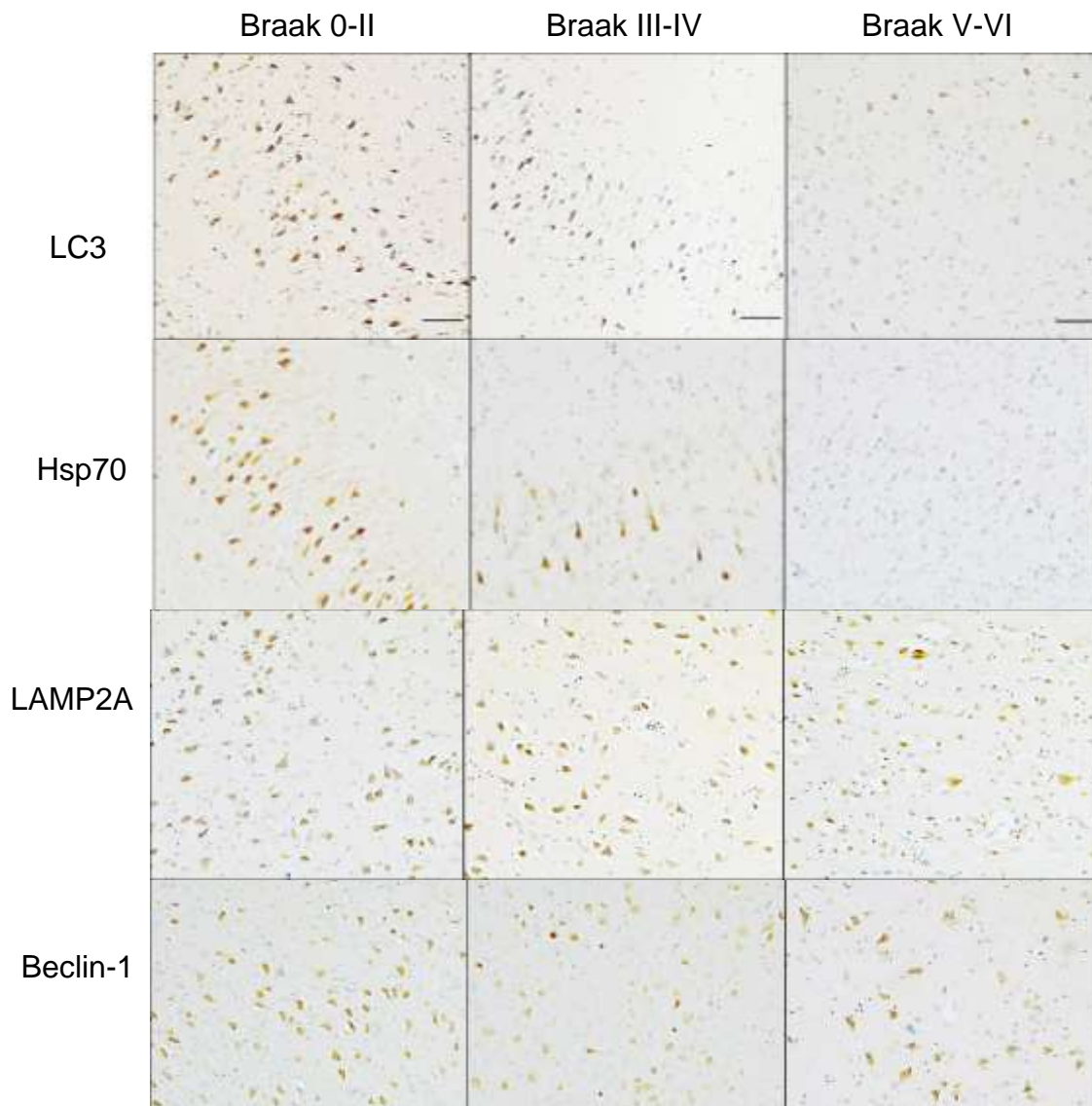
Figure 3.10 Immunohistochemical representation of all autophagy markers distribution across all Braak stages in the hippocampus. Hsp70 and LC3 markers demonstrated a decrease of staining in Braak III-IV and Braak V-VI, whereas LAMP2A and Beclin-1 were abundant across all Braak groups. Magnification 100x; Scale bars represent µm.

3.1.2   Variation of neuronal staining distribution in the frontal cortex

Next, the study aimed to explore if autophagy marker distribution varied in the different cells of the frontal cortex, an area of the brain that gets affected in later stages of disease (Scahill, 2002). Therefore, positive intracellular staining of the four autophagy markers was scored and assessed.

A high number of cases were stained by LAMP2A (83%), LC3 (67%), Hsp70 (90%) and Beclin-1 (82%). Similar levels of staining were reported across all subcortical layers of the frontal cortex with no significant variation (Figure 3.11). As previously described, based on the high prevalence of staining across the layers in the frontal cortex, the data was dichotomised to allow analysis of cases demonstrating significant staining attaining scores of moderate/severe staining (2/3 in the 0-3 rating scale; ++/+++ in the -/+/++/+++ rating scale) compared with minimal or absent staining (0/1 in the 0-3 rating scale; -/+ in the -/+/++/++ rating scale).
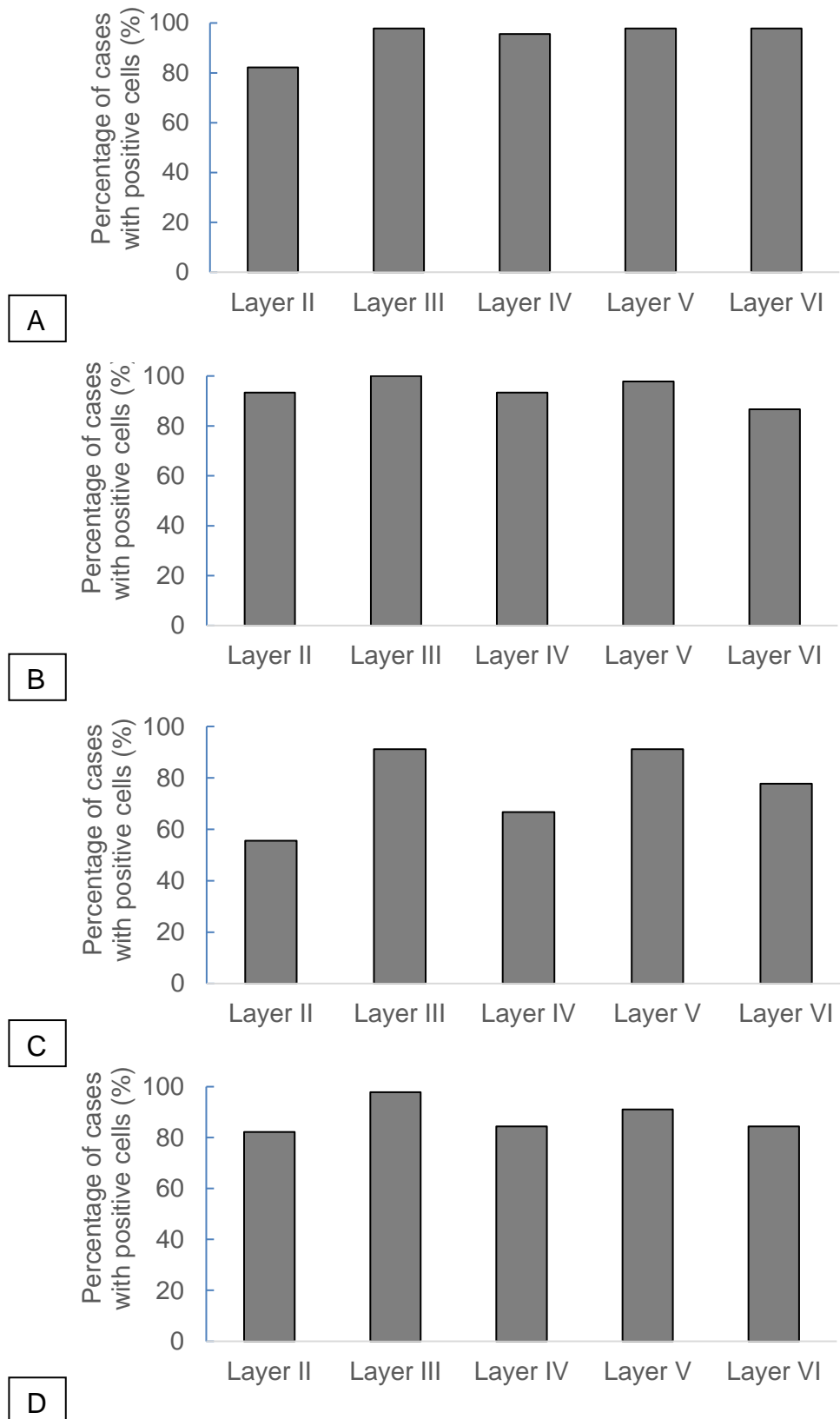
Figure 3.11 MA and CMA markers staining across the frontal cortex layers. LAMP2A (A), Hsp70 (B), LC3 (C) and Beclin-1 (D) staining across the frontal cortex subcortical layers. Bar charts represent the proportion of cases based on the number of the cells stained; (0–3 rating scale).

Moderate/severe scores (2/3 in the 0-3 rating scale; ++/+++ in the -/+/++/+++ rating scale) were used to illustrate the variation in the distribution of autophagy markers across different subcortical layers of the frontal cortex.

Overall, there was a minimal variation of CMA markers across the frontal cortex layers, with similar staining levels in each layer. Layers II and IV had slightly lower staining than layers III and V, which have the highest staining levels (Figure 3.12). In Braak 0-II, LAMP2A distribution was found the lowest in layer IV (70%), compared with the highest in layer V (94%). Hsp70 staining varied less across the layers, presenting the lowest staining seen in layer II (70%)

Figure 3.12A). In both Braak III-IV and Braak V-VI groups, LAMP2A was found the lowest in layer IV and II (60%) and the highest in layer III and V (84% and 86%, respectively) (Figure 3.12A). A more evident variation of Hsp70 positive staining was seen with increasing Braak staging, therefore the lowest staining, in Braak III-IV, was found in 66% cases (layer IV) compared with 93% cases (layers III and V) (Figure 3.12B). Similarly, Hsp70 staining was reported the

lowest in 46% cases (layer VI) compared with 77% cases (layer III) (Figure 3.12B). Neuronal staining varied more for the MA markers, across all Braak stages. Beclin-1 staining levels were found quite similar across all layers, in Braak 0-II (Figure 3.13B). However, in Braak 0-III, LC3 staining was found the lowest in layer IV (23%) and the highest in layer V (58%) (Figure 3.13A). Distribution of LC3 decreased with increasing Braak, resulting in only 13%

cases with positive staining (Braak III-IV) (Layers II, IV and VI), compared with 46% cases in Layer III (Figure 3.13A). Interestingly, Beclin-1 exhibited a higher degree of variation in Braak III-IV, with the lowest staining level in layer IV (13%) and the highest in layer III (73%) (Figure3.13B). In high Braak, Beclin-1 staining was reported the lowest staining in layer IV (53%) and the highest in layer III, with all cases demonstrating Beclin-1 positivity (100%) (Figure 3.13B).
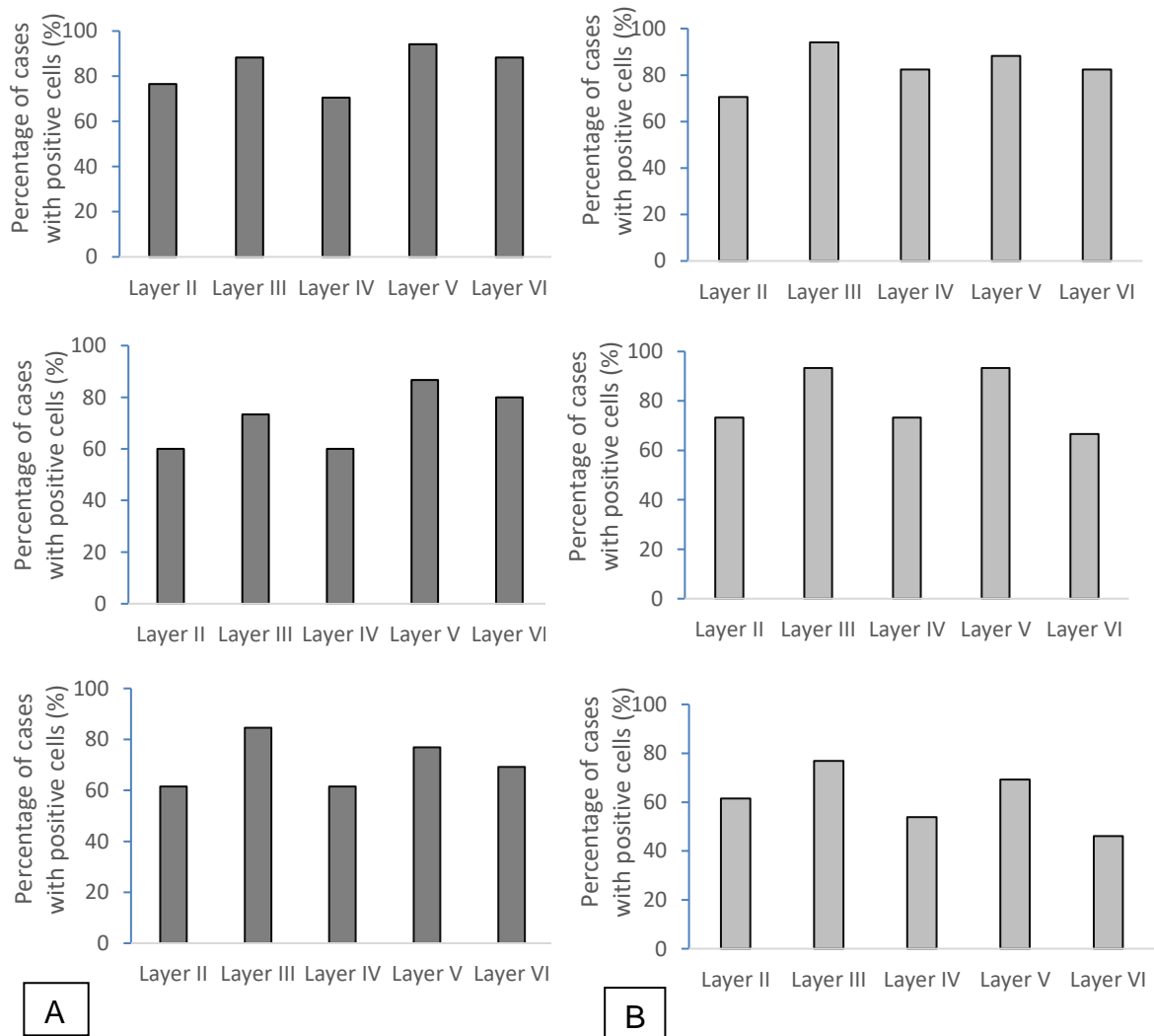
Figure 3.12 Chaperone-mediated autophagy markers in the frontal cortex subcortical layers across Braak stages (Braak 0-II, Braak III-IV, Braaak V-VI). LAMP2A (A) and Hsp70 (B) significant staining, expressed across the layers. Bar charts represent the total percentage of all cases with dichotomised scores of 1 (significant staining), based on the number of the cells stained; (0–3 rating scale).

These results demonstrated a regional variation in MA markers staining, as well as Hsp70 (in mid and high Braak groups) across the frontal cortex cellular layers.
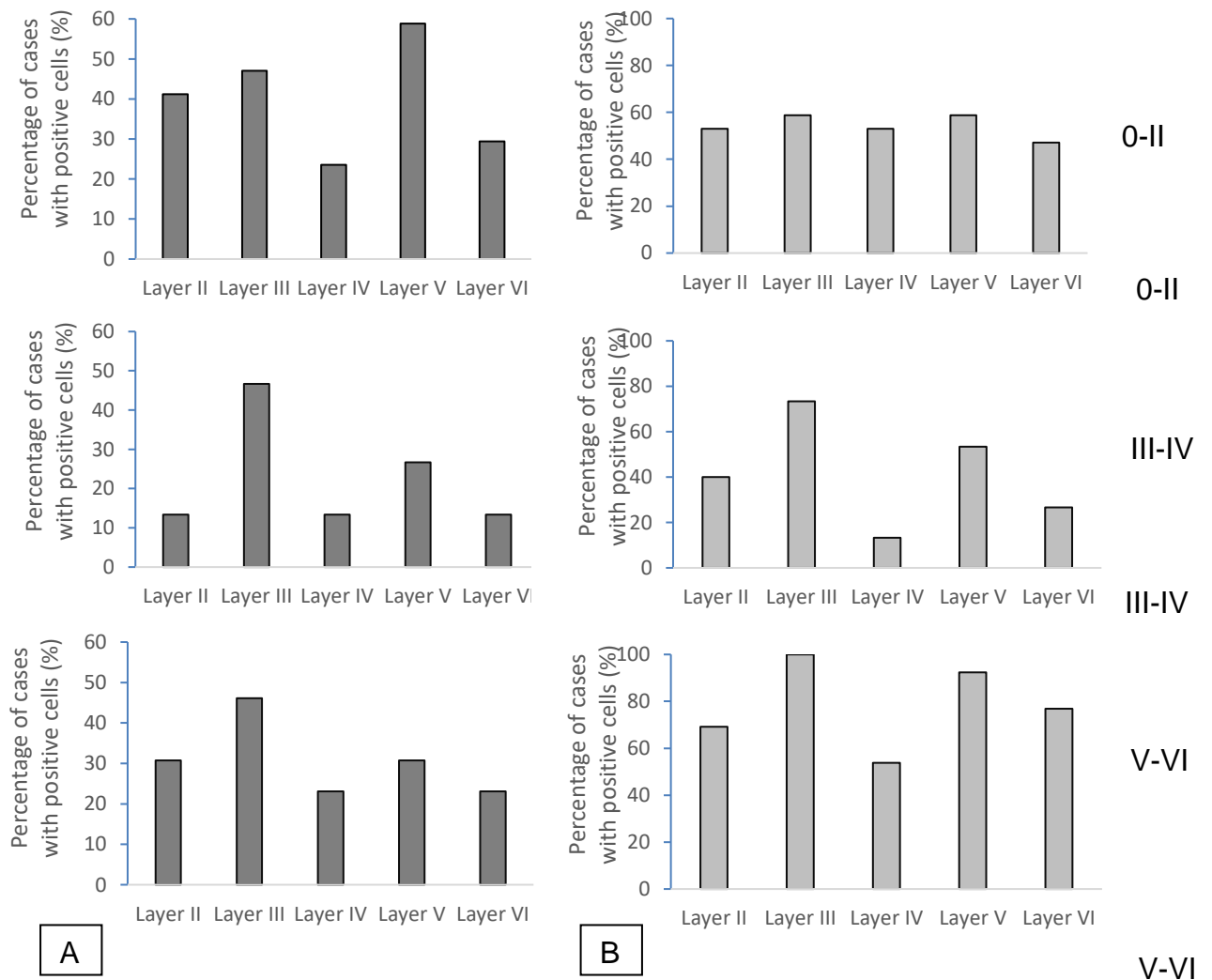
Figure 3.13 Macroautophagy markers in the frontal cortex subcortical layers across Braak stages (Braak 0-II, Braak III-IV, Braaak V-VI). LC3 (A) and Beclin-1 (B) significant staining, expressed across the layers. Bar charts represent the total percentage of all cases with dichotomised scores of 1 (significant staining), based on the number of the cells stained; (0–3 rating scale).

Following assessment of the number of the cells stained (0-3 rating scale), intensity of staining was assesed in the frontal cortex, as described in section 2.2.3. Significant staining (++/+++) of CMA markers across Braak stages demonstrated minimal variation across the layers in this brain region (Figure 3.14). The only variance seen in LAMP2A staining was found in Braak V-VI, as the CMA marker was present in 38% cases (layer II) when compared to 54% cases (layers III-VI) (Figure 3.14A). Variation of Hsp70 staining across the subcortical layers increased with increasing Braak staging. The variation was the most noticeable in Braak V-VI, with the lowest staining in layer VI (46%) and the highest in layer III (84%) (Fogure 3.14B). The frontal cortex layers demonstrated an evident variation in LC3 staining across all Braak stages (Figure 3.15A). In Braak 0-II, LC3 staining was found the lowest in layer IV (23%) and the highest in layer V (58%), whereas in Braak III-IV, LC3 distribution dropped to 13% in layers II, IV and VI and to 46% in layer III (Figure 3.15A). Very similar to Braak 0-II, LC3 staining in Braak V-VI was seen in 23% cases in layer IV and in 54% in layer III (Figure 3.15A). Beclin-1 staining demonstrated some variation between layers II (53%) and layer III (41%) when compared with the rest of the layers (above 80%), with minimal variation in Braak III-IV (Figure 3.13B). Interestingly, in Braak V-VI, Beclin-1 staining was seen in only 30% cases in layer III and in all cases (100%) in layer VI (Figure 3.15B).

These results demonstrate that, although the degree of variation is not as high as seen in the hippocampus, MA markers in the frontal cortex were found in various amounts across the subcortical layers layers of this brain regions. Also, LAMP2A, LC3 and Beclin-1 markers staining decreased with increasing Braak.
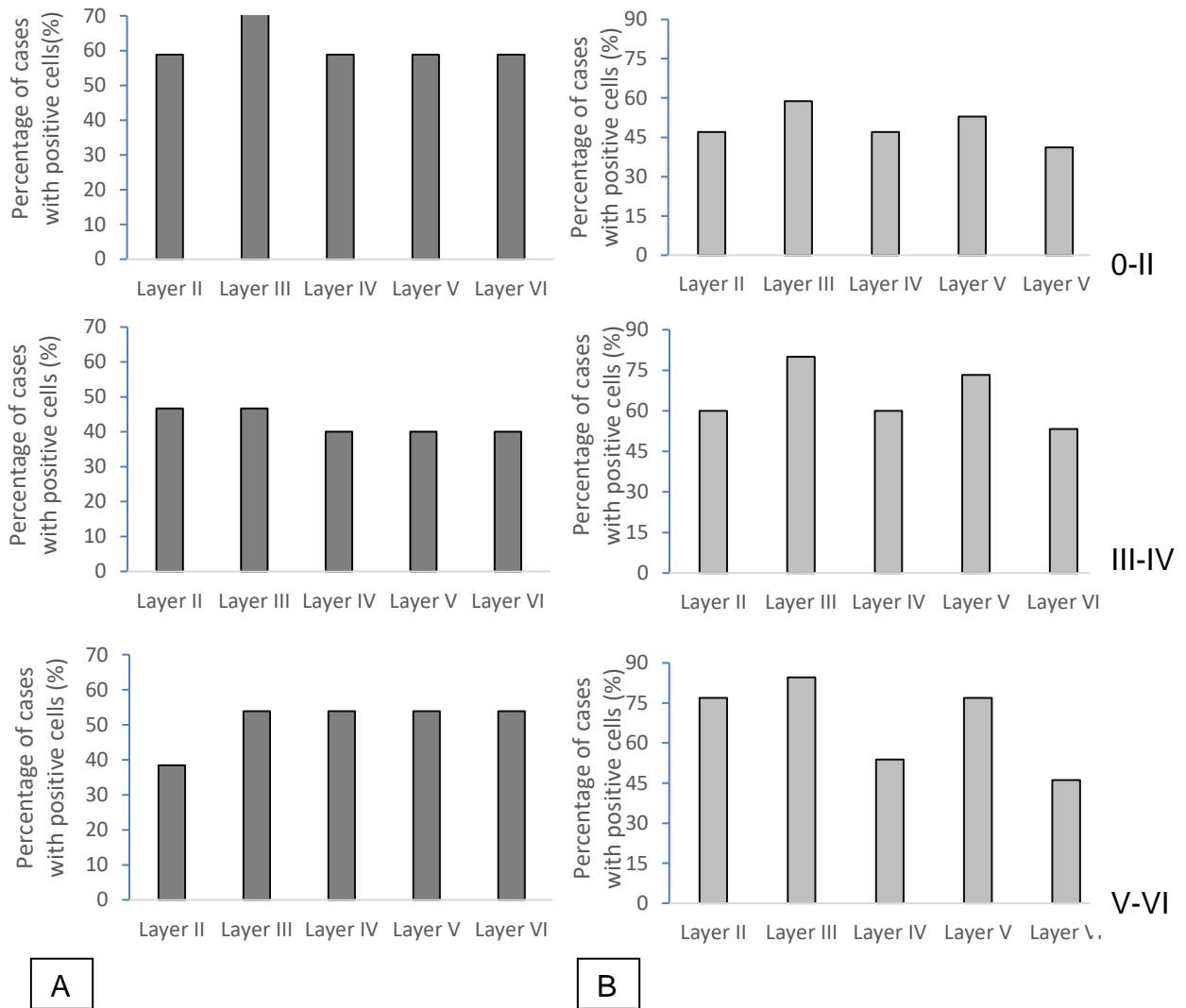
Figure 3.14 Chaperone-mediated autophagy markers in the frontal cortex subcortical layers across Braak stages (Braak 0-II, Braak III-IV, Braaak V-VI). LAMP2A (A) and Hsp70 (B) significant staining, expressed across the layers. Bar charts represent the total percentage of all cases with dichotomised scores of 1 (significant staining), based on the intensity of the cells stained; (-/+/++/+++ rating scale).
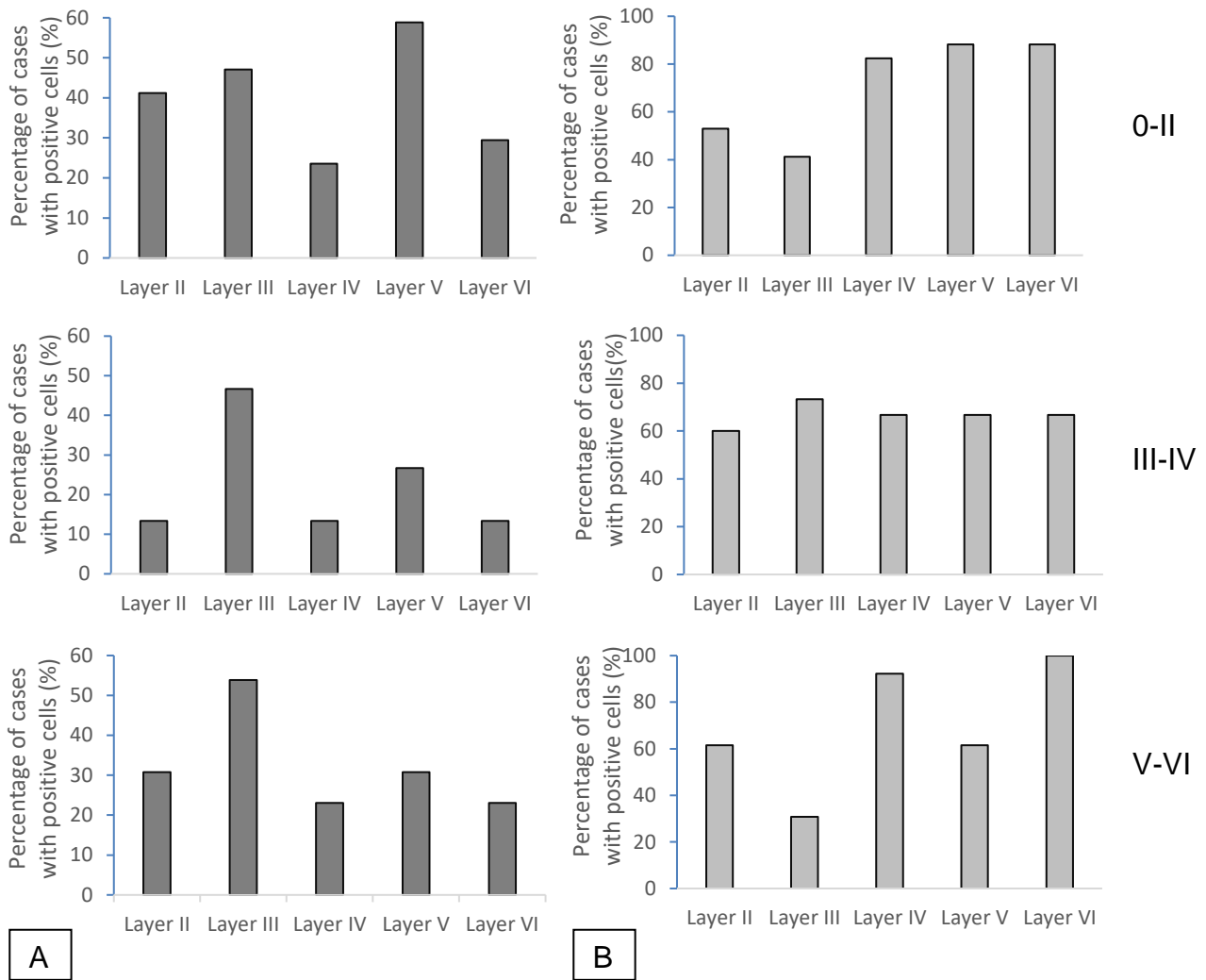
Figure 3.15 Macroautophagy markers in the frontal cortex subcortical layers across Braak stages (Braak 0-II, Braak III-IV, Braaak V-VI). LC3 (A) and Beclin-1 (B) significant staining, expressed across the layers. Bar charts represent the total percentage of all cases with dichotomised scores of 1 (significant staining), based on the intensity of the cells stained; (-/+/++/+++ rating scale).

We, then, investigated the overall moderate/severe (scores of 2/3; 0-3 rating scale) staining of MA and CMA autophagy markers in the frontal cortex to explore how the markers distribution change with disease progression. Beclin-1 staining was found to increase significantly between the three Braak groups (Figure 3.16).

LAMP2A staining was reported in 48% cases in Braak 0-II, decreasing to 42% in both Braak III-IV and Braak V-VI with no statistical significance (Chi square test, $p=0.48$) (Figure 3.16). Also, Hsp70 staining demonstrated a decline from Braak 0-II (50%) to Braak III-IV (47%) and to Braak V-VI (41%) with no statistical significance (Chi square test, $p=0.35$) (Figure 3.16). Both LC3 and Beclin-1 markers distribution decreased from Braak 0-II (25% and 36%) to Braak III-IV (13%, and 25%), however the staining was found to increase significantly in Braak V-VI to 18% (LC3) and 56%, respectively (Chi square test, $p=0.05$ and $p<0.001$) (Figure 3.16).
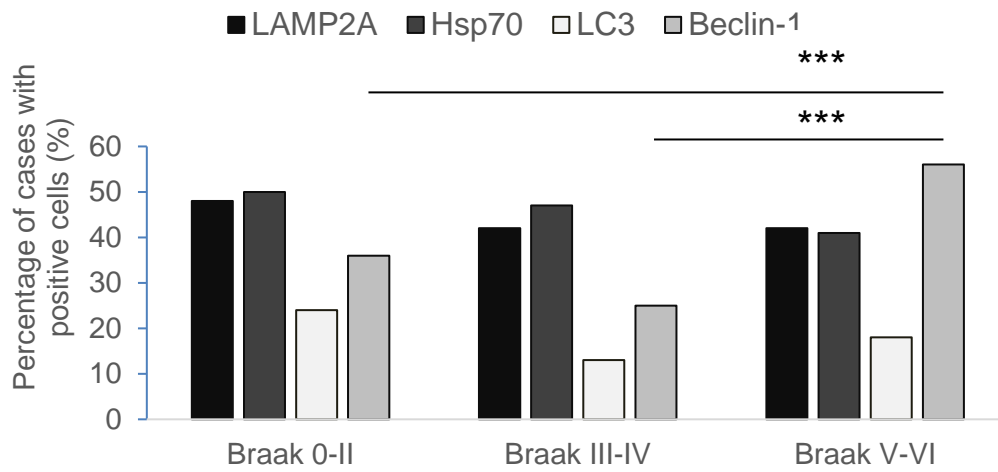
Figure 3.16 Autophagy markers staining across all Braak stages in the frontal cortex. Scores were based on the number of the cells stained; (0–3 rating scale); ***p<0.001
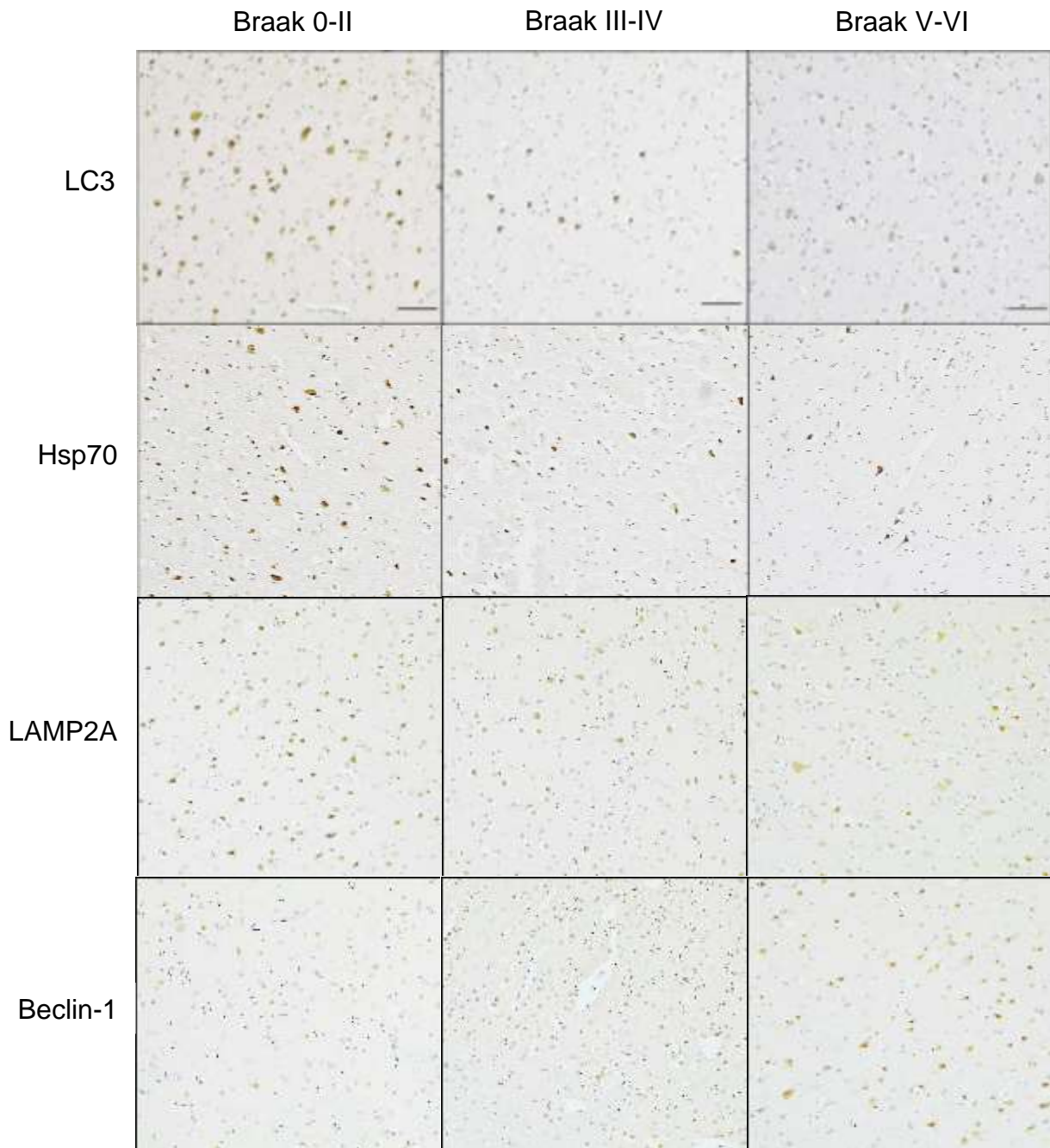
Figure 3.17 Immunohistochemical representation of all autophagy markers distribution across all Braak stages in the frontal cortex. LAMP2A, Hsp70 and LC3 demonstrated a decrease of staining in the frontal cortex layers across the Braak stages whereas Beclin-1 increased from Braak 0–II to Braak V-VI. Magnification 100x; Scale bars represent 100 μm.

3.1.3 Variation of staining distribution in the occipital cortex

The next aim was to explore if there was variation in autophagy marker distribution across the cell layers of the occipital cortex. This brain region did not exhibit a high degree of regional variation in LAMP2A, Hsp70 and Beclin-1 staining across all subcortical layers, however there was some variation for LC3 marker (Figure 3.18). Therefore, positive intracellular staining of the four autophagy markers was scored and assessed.
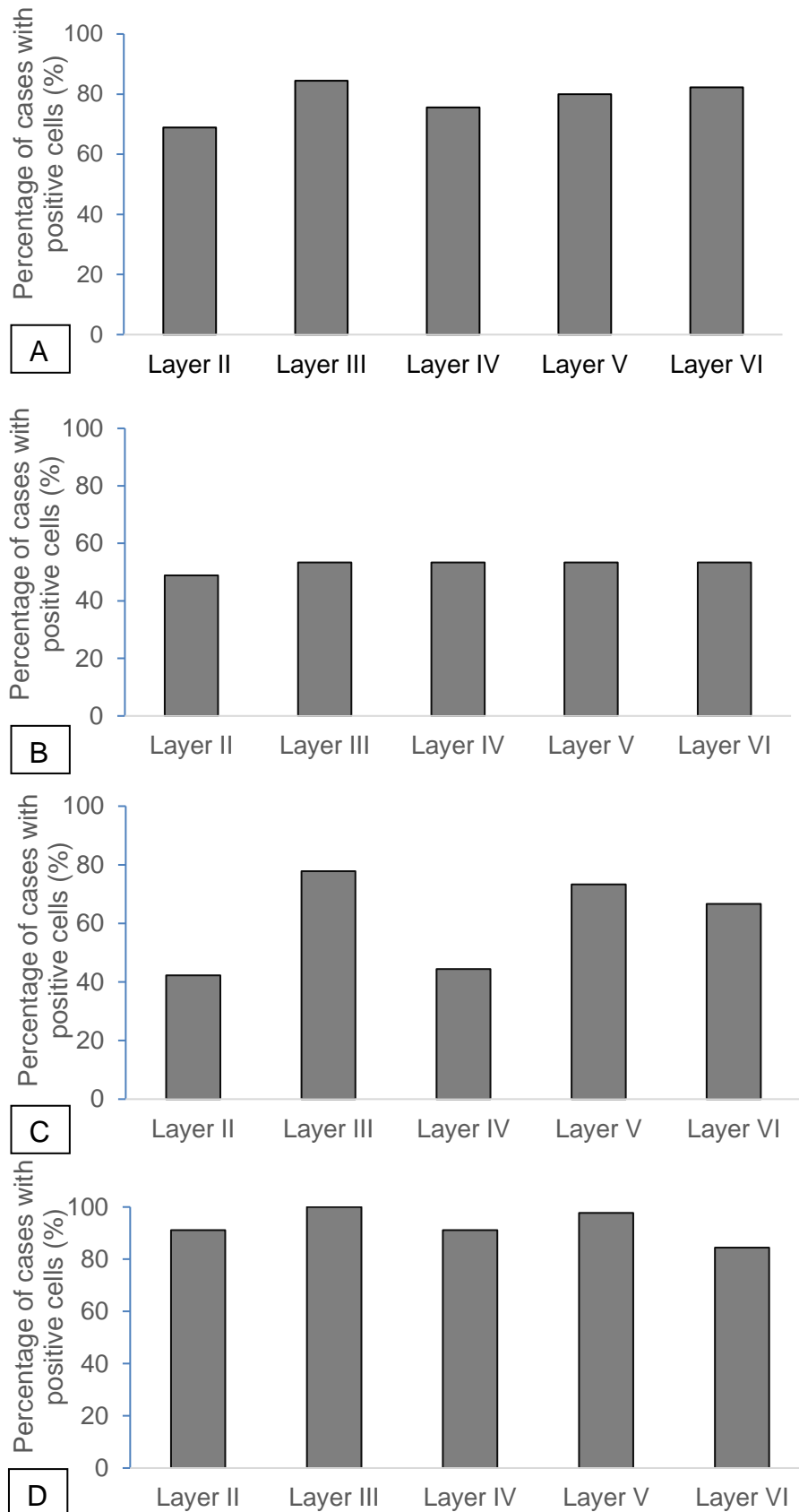
Figure 3.18 MA and CMA markers staining across the occipital cortex layers. LAMP2A (A), Hsp70 (B), LC3 (C) and Beclin-1 (D) staining based on the number of the cells stained; (0–3 rating scale).

As previously described, all occipital cortex scores were also dichotomised into significant staining (2/3 in the 0-3 rating scale) and minimal/absent staining (0/1 in the 0-3 rating scale), based on the number of the cells stained by all autophagy markers. Overall, the results suggested a lower amount of autophagy markers staining compared with the other brain regions, the hippocampus and the frontal cortex. The majority of cases were stained by Beclin-1 (91%), also demonstrating similar levels of staining across all subcortical layers (Figure 3.18D). LAMP2A (75%) and Hsp70 (56%) had no variation across the layers (Figure 3.18A and 3.18B), except LC3 staining (51%) which exhibited some variation (Figure 3.18C).

After data was dichotomised, regional variations were seen in Braak III-IV (LAMP2A, Hsp70, LC3 markers staining) and in Braak 0-II (LAMP2A, LC3 staining) (Figure 3.19 and 3.20). Beclin-1 staining had similar levels of staining across all cellular layers, except in Braak V-VI, where the lowest staining was found layers II and IV (61%) compared with layer II (84%) (Figure 3.20B). In Braak 0-II, LC3 staining varied from 23% (layer II) to 53% (layer V), whereas in Braak III-IV, the lowest staining was seen in layer IV (33%) and the highest staining was seen in layers III and V (53%) (Figure 3.20A). The lowest LAMP2A staining in both Braak 0-II and Braak III-IV was reported in layer II (32% and 35%, respectively) and the highest LAMP2A staining was detected in layer V (58% and 53%, respectively) (Figure 3.19A). Hsp70 only varied in Braak III-IV, with the highest marker distribution seen in layer III (67%), compared with layer IV (33%) (Figure 3.19B). Overall, Hsp70 and LC3 markers were reported to significantly decrease with increasing Braak staging.
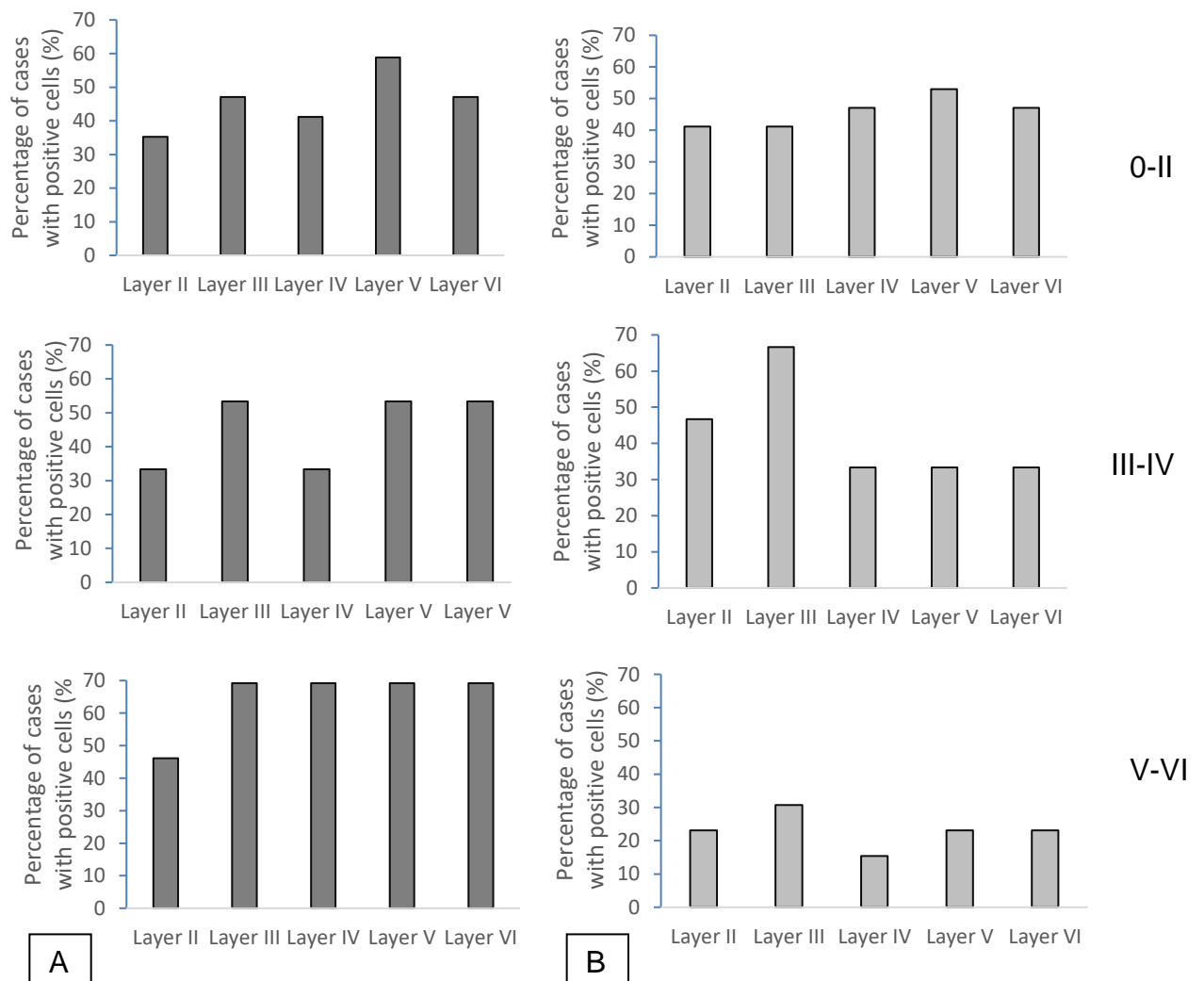
Figure 3.19 Chaperone-mediated autophagy markers in the occipital cortex subcortical layers across Braak stages. LAMP2A (A) and Hsp70 (B) significant staining, expressed across the layers. Bar charts represent the total percentage of all cases with dichotomised scores of 1 (significant staining), based on the number of the cells stained; (0–3 rating scale).
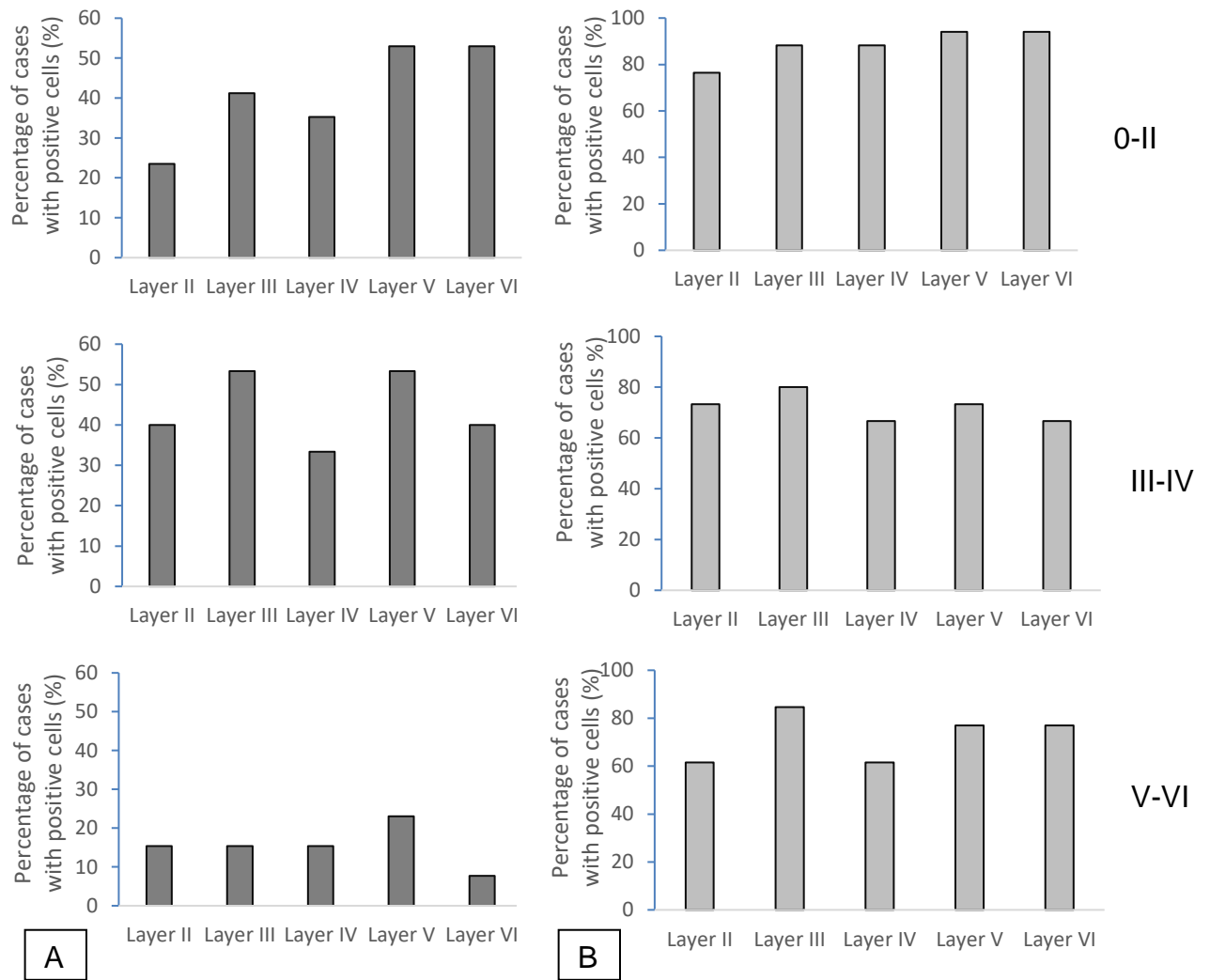
Figure 3.20 Macroautophagy markers in the occipital cortex subcortical layers across Braak stages. LC3 (A) and Beclin-1 (B) significant staining, expressed across the layers. Bar charts represent the total percentage of all cases with dichotomised scores of 1 (significant staining), based on the number of the cells stained; (0–3 rating scale).

As previously described, the intensity of positive staining was assesed using the occipital cortex scores. There was no regional variation of LAMP2A staining in the occipital cortex, with similar levels seen across the layers (Figure 3.21A). Moderate/severe (++/++ scores) Hsp70 staining was absent in all layers in Braak 0-II, Braak III-IV and in layer II in Braak V-VI (Figure 3.21B). Despite the very low levels of staining seen in Braak V-VI, there was no regional variation across layers III-VI (Figure 3.21B). LC3 staining varied across the layers in all Braak groups, with the lowest levels in layers II and IV and the highest levels in layers III, V, VI (Figure 3.22A). Similar patterns were seen in Beclin-1 staining, with variation in Braak III-IV and Braak V-VI (Figure 3.22B).

Overall, these results demonstrate minimal regional variation compared with the results associated with the other two brain regions.
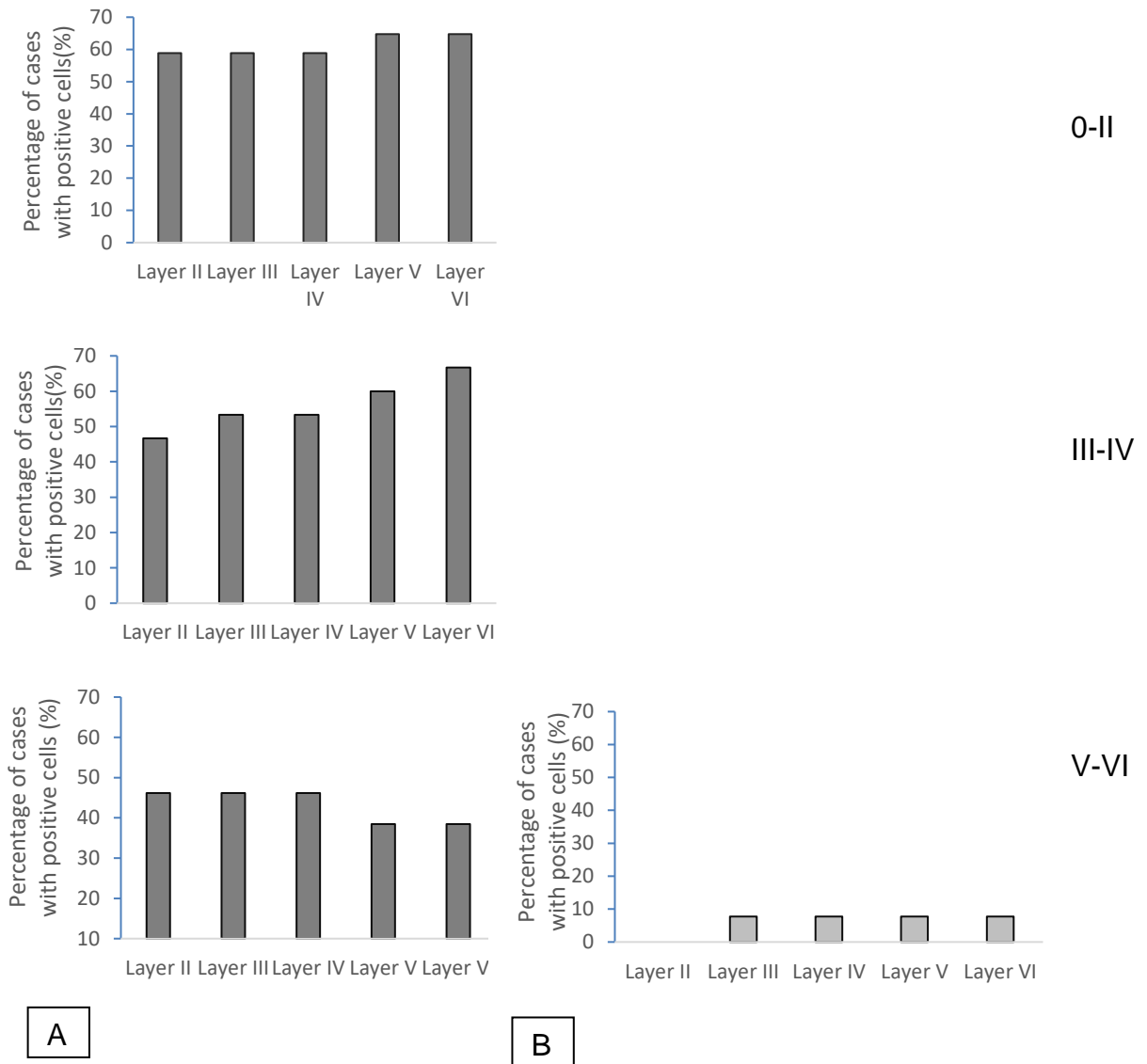
Figure 3.21 Chaperone-mediated autophagy markers in the occipital cortex subcortical layers across Braak stages. LAMP2A (A) and Hsp70 (B) significant staining, expressed across the layers. No significant Hsp70 staining seen in Braak 0-II and Braak III-IV groups. Bar charts represent the total percentage of all cases with dichotomised scores of 1 (significant staining), based on the intensity of the cells stained; (-/+/++/+++ rating scale).
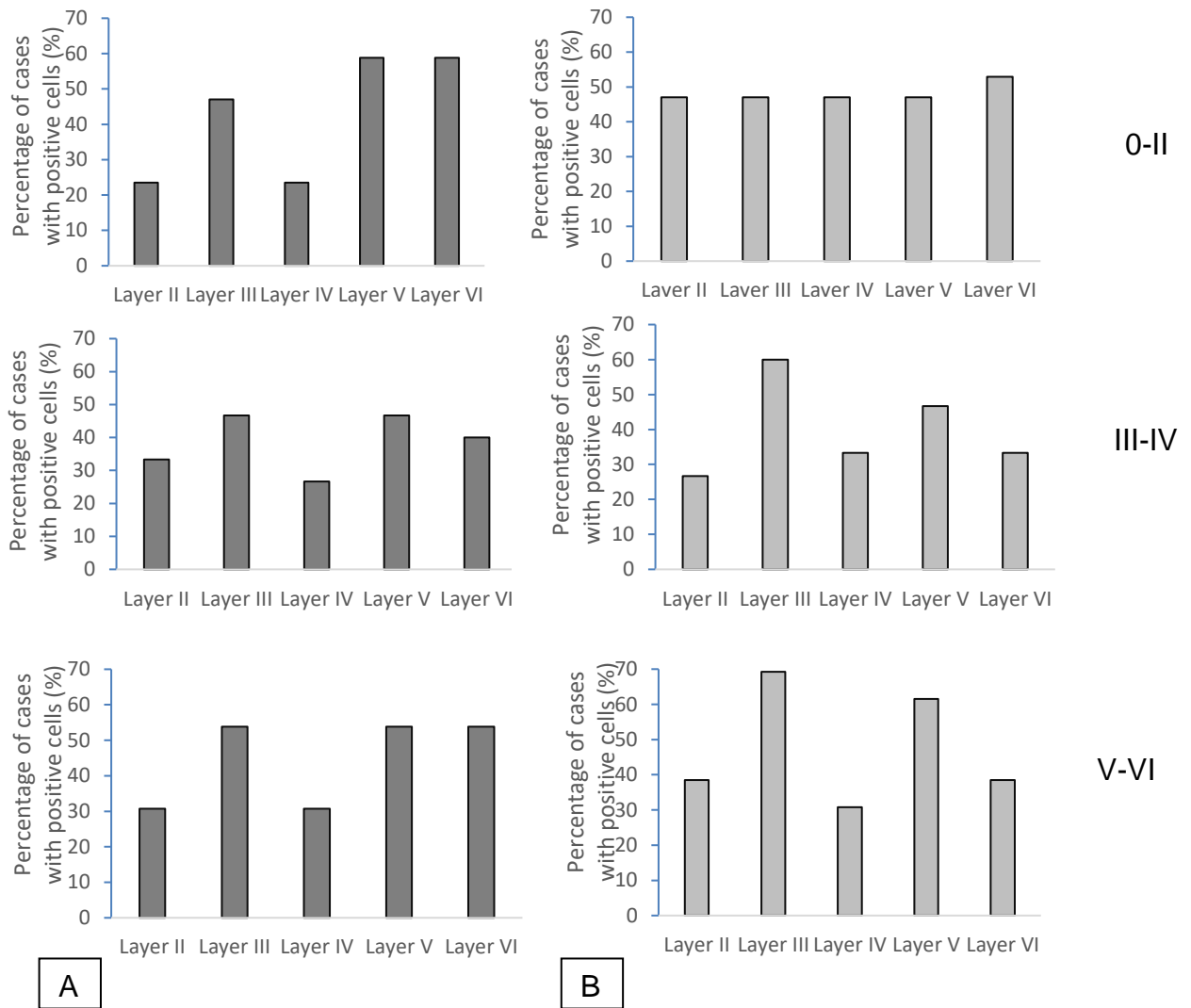
Figure 3.22 Macroautophagy markers in the occipital cortex subcortical layers across Braak stages. LC3 (A) and Beclin-1 (B) significant staining, expressed across the layers. Bar charts represent the total percentage of all cases with dichotomised scores of 1 (significant staining), based on the intensity of the cells stained; (-/+/++/+++ rating scale).

We then analysed the overall moderate/severe staining (scores of 2/3; 0-3 rating scale) of MA and CMA autophagy markers in the occipital cortex. The staining levels of LC3 and Hsp70 were found to significantly decrease with advancing Braak staging (Figure 3.23).

In the occipital cortex, LAMP2A staining had a linear increase, being present in 27% cases in Braak 0-II and in 40% cases in Braak V-VI (Chi square test, p=0.07). All other autophagy markers were found to linearly decrease across the three Braak stages (Figure 3.23). Therefore, Beclin-1 declined from 54% in early stages by 45% in mid and late stages with no statistical significance (Chi square test, p=0.05), while both Hsp70 and LC3 followed similar decreasing trends, from approximately 25% in Braak 0-II and Braak III-IV to around 10% in late stages (Chi square test, p=0.02) (Figure 3.23).
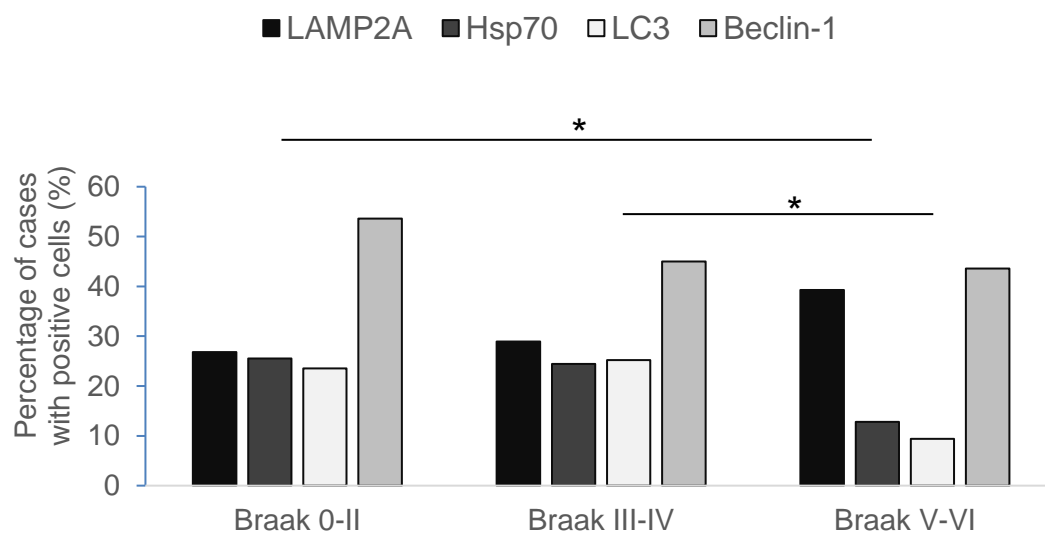
Figure 3.23 Autophagy markers staining across all Braak stages in the occipital cortex. Scores were based on the number of the cells stained; (0–3 rating scale); *p<0.05
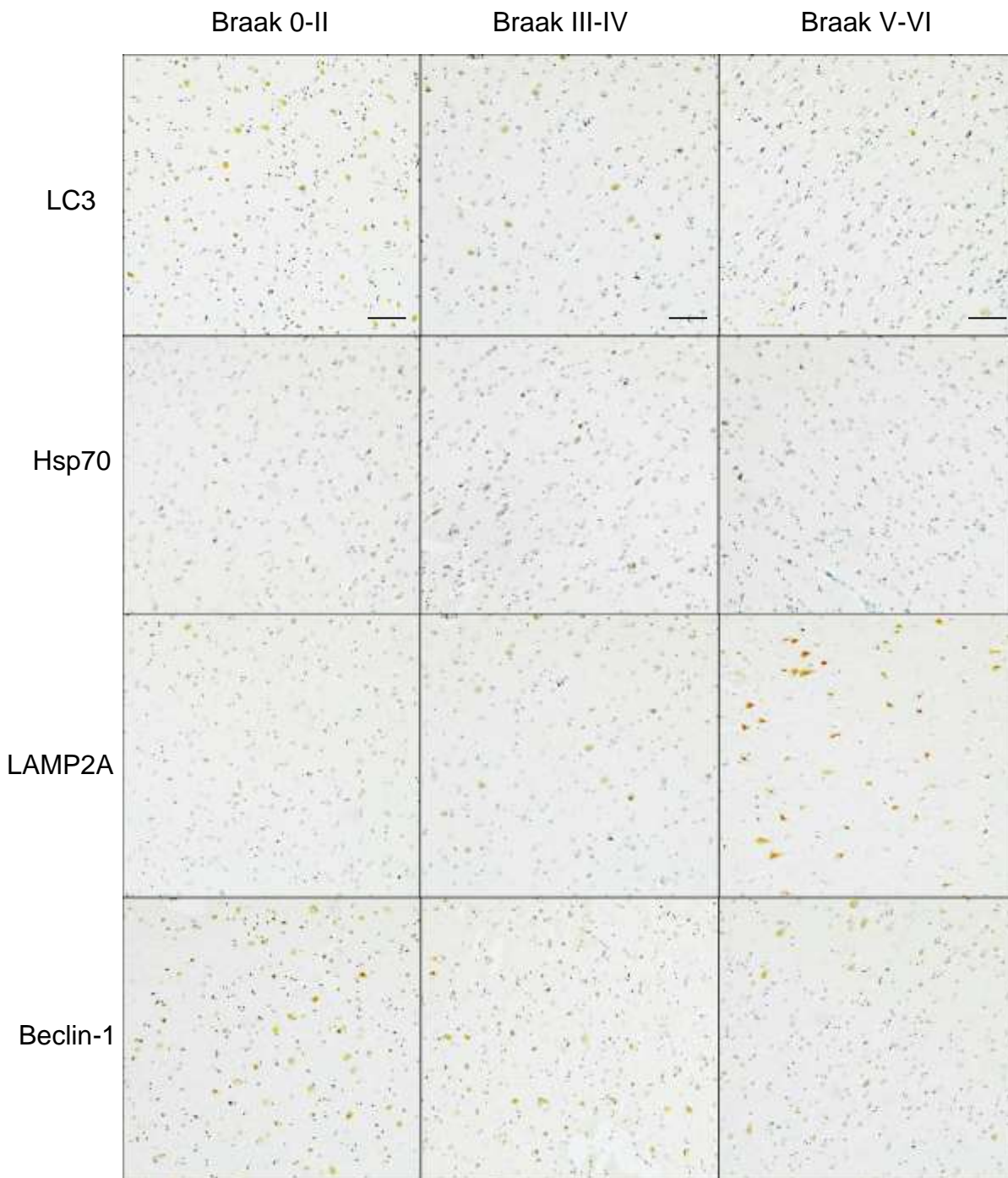
Figure 3.24 Immunohistochemical representation of all autophagy markers distribution across all Braak stages in the occipital cortex. Hsp70, LC3 and Beclin-1 markers were found to decrease with increasing Braak stage whereas LAMP2A was found to increase in Braak V-VI. Magnification 100x; Scale bars in A-F represent 100 μm.

3.1.4 Comparison of MA and CMA

Next, we segregated the overall autophagy scores into MA and CMA staining to allow comparison of MA and CMA preference in each brain region assessed. In the hippocampus, the total CMA marker levels (moderate/severe staining of both LAMP2A and Hsp70 proteins) were 11% lower than the total MA marker levels (moderate/severe staining of both LC3 and Beclin-1 proteins) (Figure 3.25). In the frontal cortex, CMA overall staining was reported to be 41% higher when compared with MA expression (Figure 3.25). Similar to the hippocampus, in the occipital cortex, the total CMA expression levels were 22% lower than the total MA levels (Figure 3.25).

Therefore, these results suggest that the hippocampus had a similar distribution of MA and CMA markers (77% and 70%, respectively) whereas in the frontal cortex, CMA staining (68%) was more predominant when compared with MA staining (40%) and in the occipital cortex, MA staining (51%) was higher than CMA staining(40%) (Figure 3.25).
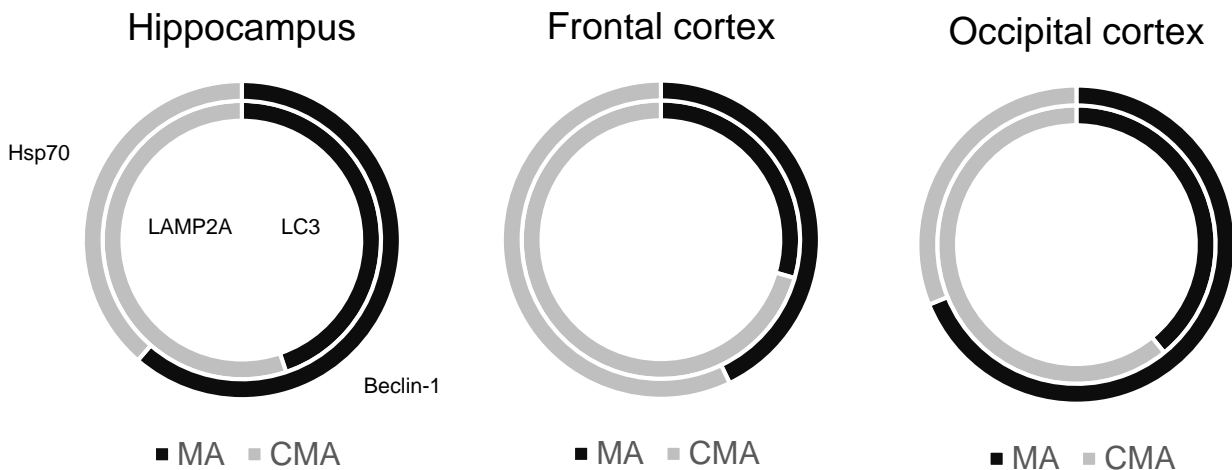
Figure 3.25 Comparison between MA and CMA. A diagram illustrating the proportion of cases with moderate to severe staining of MA proteins (LAMP2A and Hsp70) in contrast with CMA proteins (LC3 and Beclin-1) in each of the three brain regions. Scores were based on the number of the cells stained; (0–3 rating scale).

3.1.5 Regional comparison of autophagy marker distribution across all Braak groups

A generalised regional comparison of autophagy markers distribution between all three brain regions: the hippocampus, the frontal and the occipital cortex was generated by collecting all moderate/severe scores in each Braak group. There is a noticeable variation in the overall autophagy markers staining between the three brain regions. Overall, all markers were decreased in the frontal and the occipital cortex when compared to the hippocampus in all Braak stages (Figure 3.25).

In Braak 0-II, CMA marker levels were similar in the hippocampus and the frontal cortex when compared with the occipital cortex (Figure 3.25). Therefore, LAMP2A staining was very prevalent in the hippocampus (80%) and the frontal cortex (71%), when compared with the lower levels in the occipital cortex (40%) (Figure 3.25). Hsp70 marker had the highest levels in the hippocampus (63%) and the frontal cortex (62%) and the lowest in the occipital cortex (38%) (Figure 3.25). LC3 distribution pattern between the brain regions varied and although the hippocampus identified 93% cases with Hsp70, the other two brain regions had a much lower staining of this marker (35%) (Figure 3.25). Beclin-1 positivity was reported the highest in the occipital cortex (80%), followed by the hippocampus (77%) and the lowest was seen in the frontal cortex (50%) (Figure 3.25).

In Braak III-IV, the occipital cortex was still the brain region with lowest LAMP2A and Hsp70 markers staining (43% and 36%, respectively), when compared with the other two regions (Figure 3.25). LAMP2A was found in higher proportion in the hippocampus (87%) when compared with the frontal cortex (63%), whereas Hsp70 staining was more abundant in the frontal cortex (71%) rather than the hippocampus (51%) (Figure 3.25). Hippocampal LC3 staining was found in half of the cases (53%), followed by staining in the occipital cell layers (38%) and lastly, the frontal cells presented LC3 staining in fewer cases (19%) (Figure 3.25). On the other hand, Beclin-1 stained the hippocampal cells in almost all cases (90%), compared to the frontal cortex (67%) and the occipital cortex (37%) (Figure 3.25).

Lastly, in Braak V-VI, the occipital cortex had the lowest staining levels of all autophagy markers (Figure 3.25). LAMP2A had similar distribution across both

the frontal (61%) and the occipital (59%) cortices, when compared with the hippocampus (78%) (Figure 3.25). Hsp70 (19%) and LC3 (14%) marked the lowest levels of staining in the occipital cell layers, whereas the other two brain regions presented higher proportions (53-87%), suggesting a high degree of regional variation between the brain regions (Figure 3.25). Beclin-1 was found prevalent in all regions: the hippocampus (87%), the frontal cortex (71%) and the occipital cortex (65%) (Figure 3.25).

Overall, these results suggest that both MA and CMA markers distribution exhibit a regional variation between the three brain regions, which get involved at different stages of disease. CMA markers, but mostly MA markers were the most present in the hippocampus region when compared to the other two brain regions. Moreover, the results suggest that the regional variation becomes more evident with increasing Braak.
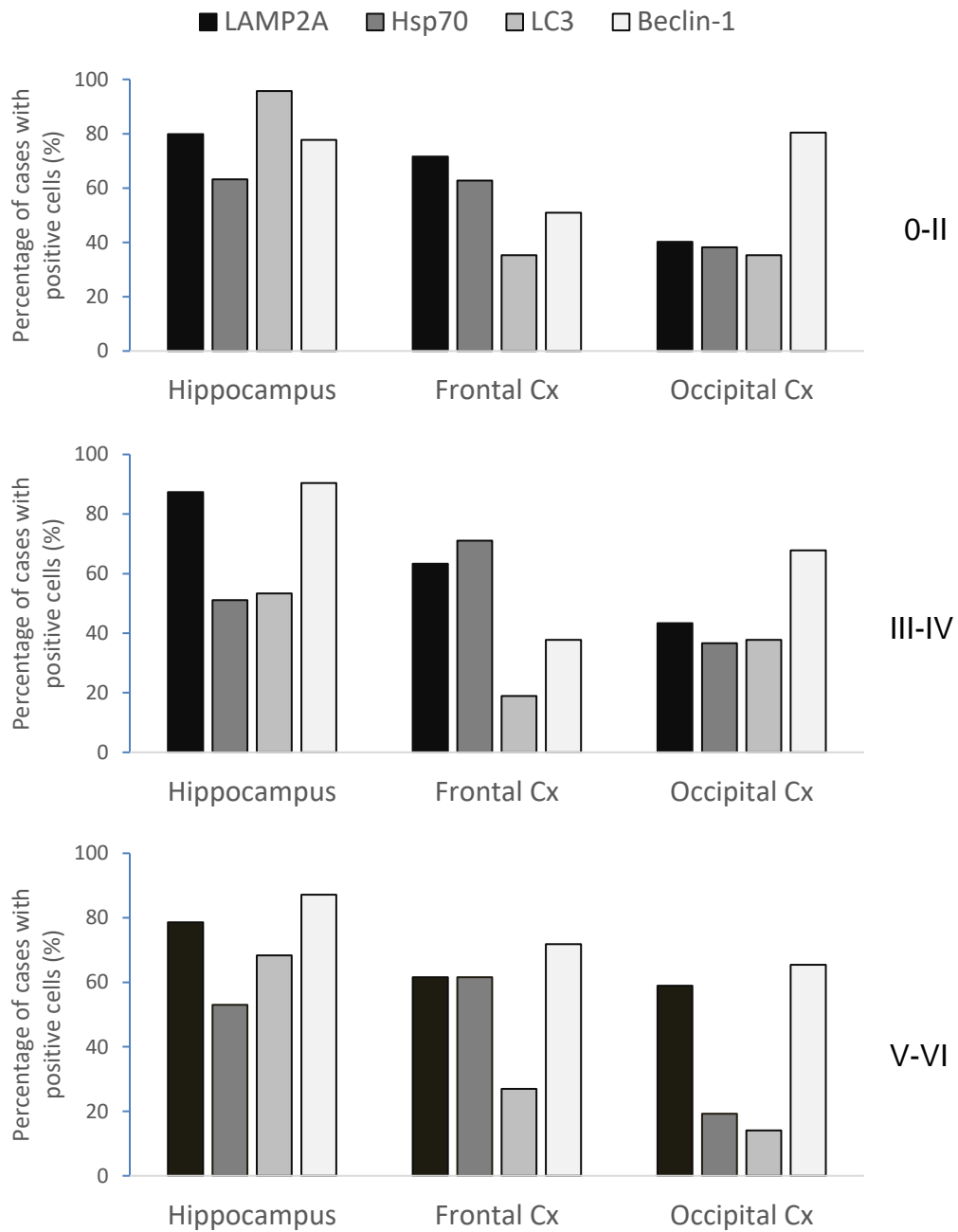
Figure 3.26 Comparison of autophagy markers distribution across the three brain regions in each Braak group (Braak 0-II, Braak III-IV, Braak V-VI). Bar charts represent percentage of cases with moderate/severe staining of each autophagy marker based on the number of cells stained; (0–3 rating scale).

Moreover, to allow a generalised comparison of autophagy markers across the Braak groups, each case was given a significant or minimal staining score. This meant each case had a single score for each of the three brain regions, allowing to understand how each autophagy marker gets involved in each brain region across the Braak groups. In other words, each case received either a score of 0 (absent/mild staining) or a score of 1 (moderate/severe staining) for each autophagy marker in each brain region. Then, the three brain regions scores were added up so that each individual case would have either a total score of 0 (no brain region significantly stained), a score of 1 (one brain region had significant staining), a score of 2 (two brain regions had significant staining) or a score of 3 (all three brain regions had significant staining). The total scores for regional involvement of each autophagy marker were then represented as proportions, suggesting that there was no variation in LAMP2A staining (p=0.9, Chi-square test) across Braak stages, whereas variations were seen in the other markers staining (Figure 3.27). Hsp70 and LC3 total scores proportion showed a decline with increasing Braak groups, suggesting that in mid and late stages of disease, the regional involvement of Hsp70 and LC3 in the brain regions was reduced. No statistical significance was identified (Figure 3.27) (p=0.1 and p=0.5, respectively, Chi-square test). Beclin-1 distribution demonstrated a different pattern as the total scores for regional variation increased in higher Braak stages, suggesting that Beclin-1 significant brain regions in higher Braak groups (p=0.5, Chi-square test) (Figure 3.27).
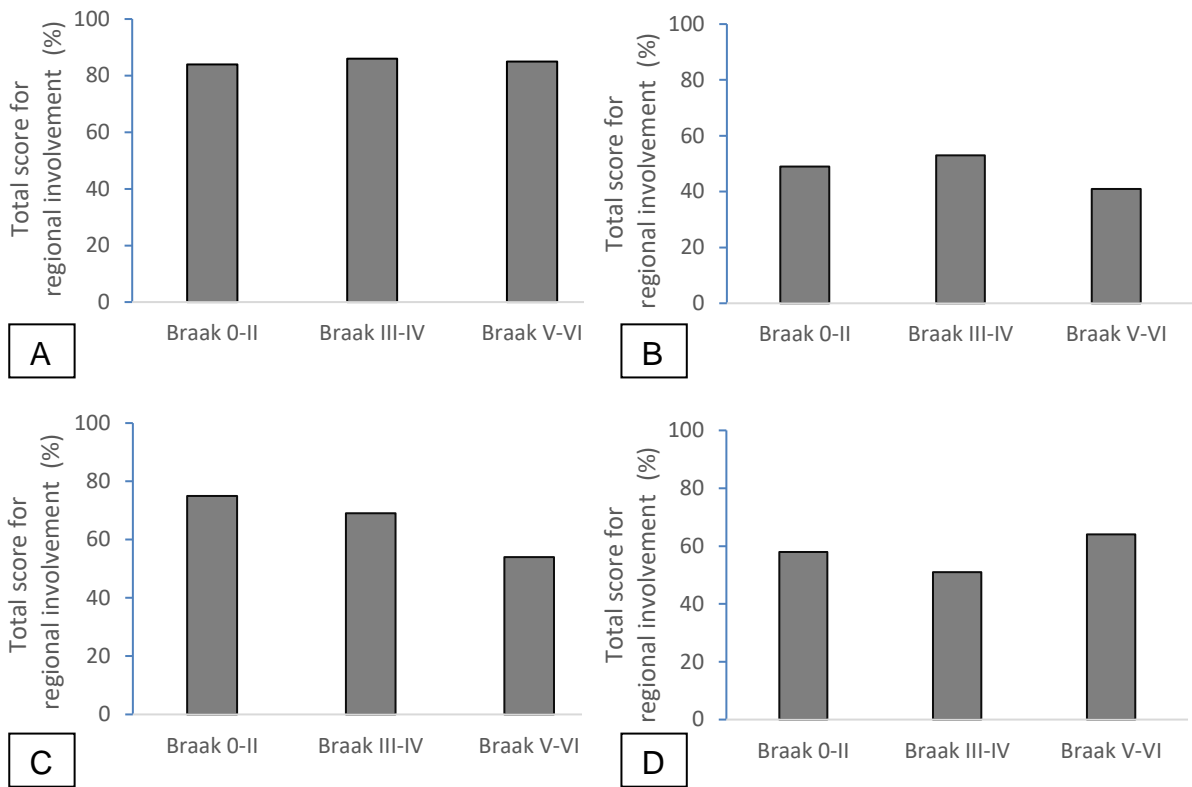
Figure 3.27 Autophagy marker distribution across the Braak groups.
Bars represent the total score of significant (moderate/severe) staining for regional involvement of each marker (A-LAMP2A; B-Hsp70; C-LC3; D-Beclin-1) across all Braak stages; Scores were based on the number of the cells stained; (0–3 rating scale).

3.1.6 <u>Axons and neuronal inclusions distribution of autophagy markers</u>

In sections 3.1.1-3.1.5, we described the neuronal staining, which has been the main focus when assessing the levels of autophagy marker staining across different stages of AD, in the three brain regions. However, other neuronal structures within the brain areas were noted to be positively stained by LAMP2A, Hsp70, LC3 and Beclin-1 (Figure 3.28). These structures included axons, neuropil threads and neuronal inclusions (Figure 3.28).
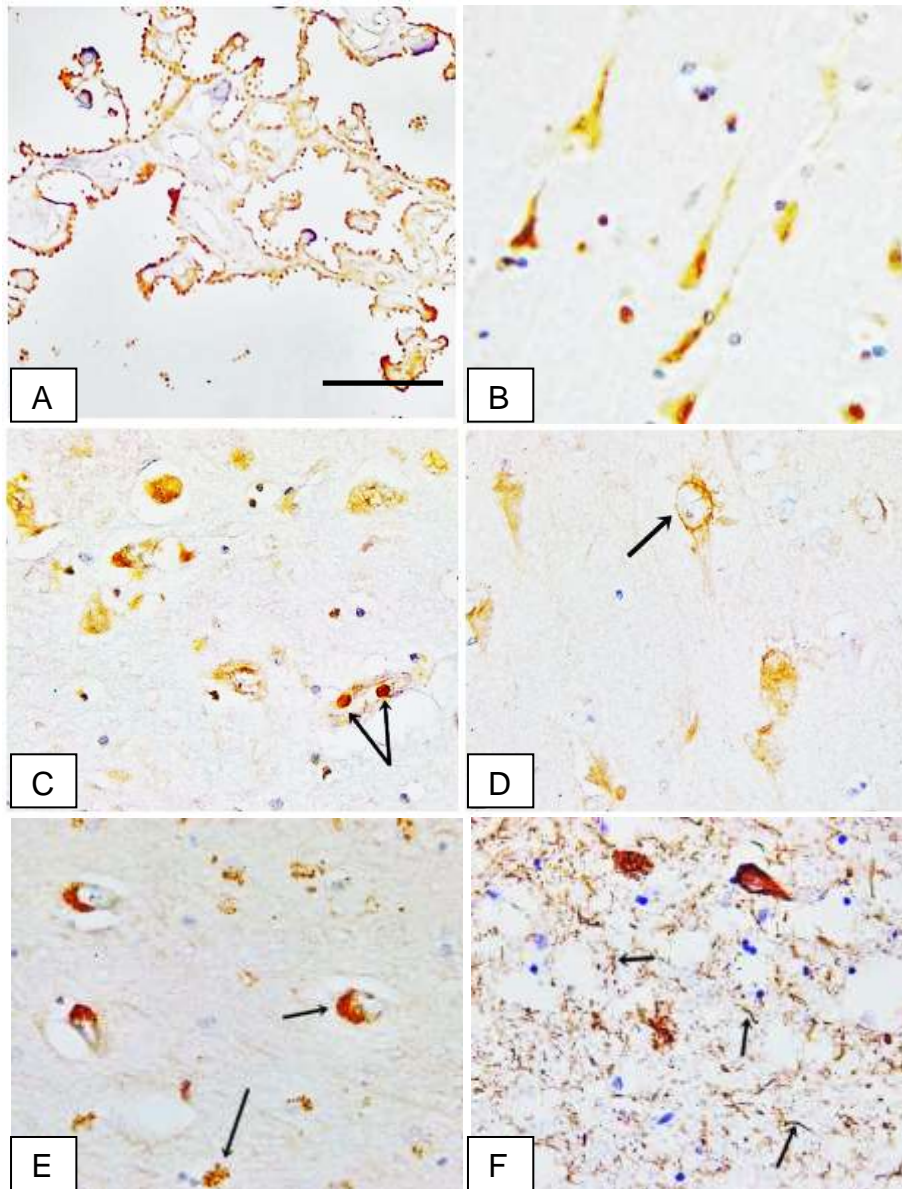
Figure 3.28 Distribution of other neuronal structures stained by autophagy markers. A- LAMP2A positivity in the choroid plexus epithelium; B-axonal staining; C-intracellular inclusions within CA4 neurons; D-presence of vacuoles in positively CA4 pyramidal stained cells; E- Intracellular and extracellular cluster of granules in CA1 cells; F-Neuropil threads. Magnification 100x. Scale bar 50 µm

Autophagy markers were assessed in axons, neuropil threads and intracellular inclusions in each of the three Braak groups to assess variation in distribution with disease progression.

Overall, LC3 protein expression level in these structures was found the most abundant, while LAMP2A expression was found the lowest (Figure 3.29A). The axons within the grey matter of the hippocampus were stained by LAMP2A in 56% of the cases in Braak 0-II, decreasing by 10% in Braak V-VI (Chi-square test, p=0.85) (Figure 3.29A). Similarly, LC3 positive axons staining decreased across the three stages from 86-87% cases in Braak 0-II and Braak III-IV to 75% in Braak V-VI (Chi-square test, p=0.54) (Figure 3.29C). For Hsp70 and Beclin-1 axonal staining, a increase was observed across the AD stages from around 44% cases, in Braak 0-II, expressing both Hsp70 and Beclin-1 proteins in the axons of the hippocampal areas, to approximately 70% in Braak V-VI (Chi-square test, p=0.12 for both Hsp70 and Beclin-1) (Figure 3.29B and 3.29D). The neurophil threads (NTh) stained by Hsp70 and Beclin-1 proteins increased across the Braak stages, from 25% in Braak 0-II, to 47% in Braak III-IV and 53% (Hsp70), 58% respectively (Beclin-1) in late stages of AD demonstrating a statistically significant association with disease progression (Chi-square test, *p=0.02, respectively) (Figure 3.29B and 3.29D). The cases with LC3 stained NTh decreased in number, from 56% in Braak 0-II to 33% in Braak III-IV (Chi-square test, p=0.11) and increased back to 50% in late stages (Figure 3.29C). NTh expressing LAMP2A were found the lowest, decreasing from 12% in Braak 0-II to only 6% in Braak III-IV (Chi-square test, p=0.52) (Figure 3.29A). Similarly to LC3 stained threads, the number of Nth stained by LAMP2A increased back to late stages (15%) (Figure 3.29C). Interestingly,

hippocampal LC3 positive cells were found to have the highest presence of vacuoles, with around 60% in early and late AD stages and a drop in their number (46%) in mid AD stages (Chi-square test, p=0.24) (Figure 3.29C). Intracellular inclusions within the hippocampal neurons were also stained by the autophagy biomarkers for MA and CMA and a decrease in presence was seen across the three stages of AD (Figure 3.29) No significant change in any autophagy immunoreactive axons with Braak stage. Only positive Beclin-1 NTh was found significantly increased as Braak stage increases (Chi-square test, p=0.02). However, no statistically significant differences were seen in the autophagy markers positively stained inclusions across the Braak groups (Chi-square test, p=0.67, p=78, p=0.34, p=0.78).
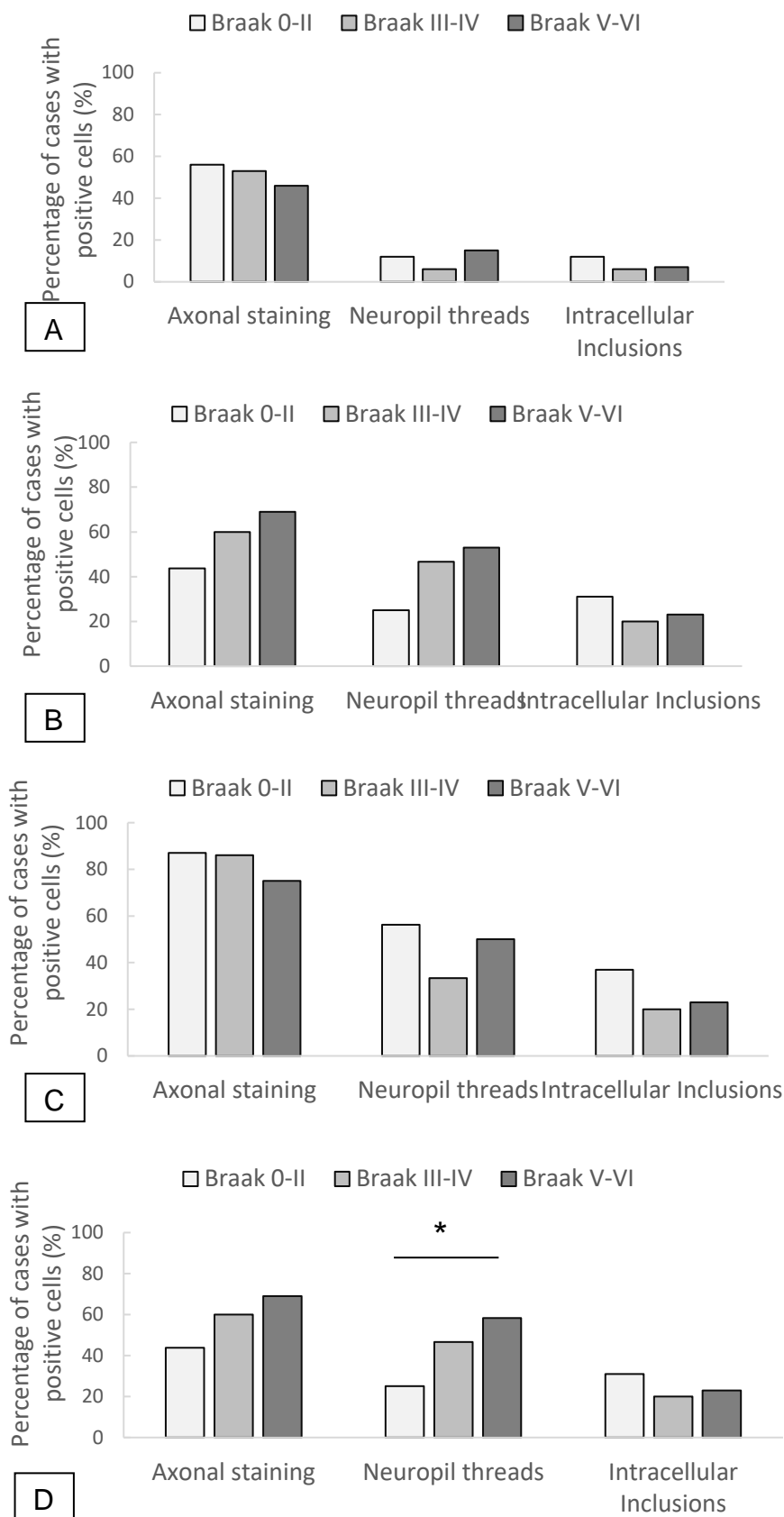
Figure 3.29 Distribution of other neuronal structures stained by autophagy markers. (A-LAMP2A; B-Hsp70; C-LC3; D-Beclin-1) in the hippocampus across the Braak stages *p<0.05,

The same structures stained by the autophagy markers, which were seen in the hippocampus, were also observed in the frontal cortex (Figure 3.30). Overall, Hsp70 marker stained more structures, such as threads, axons and inclusions, then the other autophagy marker (Figure 3.30B). LC3 positive structures were found two-fold less present in the frontal cortex layers compared with the hippocampus (Figure 3.30C). LAMP2A and Beclin-1 positivity within these structures were found at similar levels (Figure 3.30A and 3.30D).

The number of immunoreactive axons, stained by all autophagy markers, decreased with increasing Braak stage in a linear trend with the most noticeable decline seen with Beclin-1 staining decreasing from 44% (Braak 0-II) to 18% (Braak V-VI) (Chi-square test, **p=0.04) (Figure 3.30D).

In the frontal cortex, neurophil threads (NTh) were stained by LAMP2A, Hsp70 and LC3 but not by LC3. LAMP2A and Hsp70 stained threads were found to increase in a linear pattern across the Braak stages (Figure 3.30A and 3.30B). Therefore, in Braak V-VI, cases with Hsp70 associated threads were twice as many seen in Braak 0-II group with a strong association with disease progression (Chi-square test, p<0.001). There were no NTh found in the LC3 positive cases across the Braak stages (Figure 3.30C).

A total of 17% of the early Braak cases demonstrated LAMP2A positive cytoplasmic intracellular inclusions (Chi-square test, p=0.002) (Figure 3.30A), however there were no inclusions observed in the mid and late-staged cases. Similarly, there were intracellular inclusions in only 6% of the LC3 in the 0-II Braak group and they were completely absent in later Braak groups (Figure 3.30C). A decrease in the frequency of cases with Hsp70 positive intracellular

inclusions was observed as well with 23% cases in Braak 0-II demonstrating this feature and only 8% in the Braak V-VI group (Figure 3.30B).
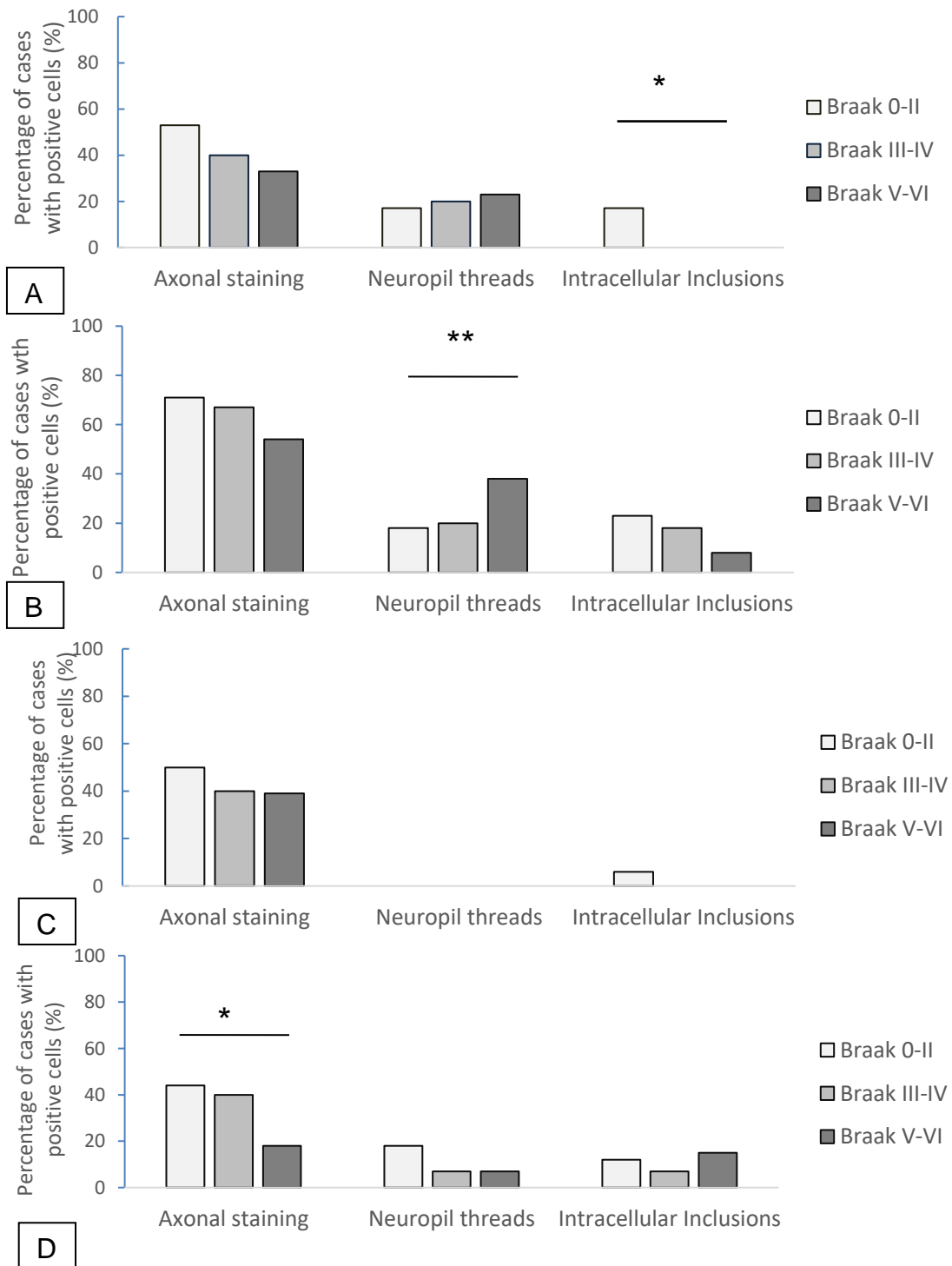
Figure 3.30 Distribution of other neuronal structures stained by autophagy markers. (A-LAMP2A; B-Hsp70; C-LC3; D-Beclin-1) in the frontal cortex across the Braak stages *p<0.05, **p<0.001

In order to understand the cellular distribution in more detail of autophagy markers, neuronal staining was divided into diffuse staining and granular staining (Figure 3.31). Diffuse staining was used to describe staining characterized by the even spread of positive stain, dispersed across both the cytoplasm or/and the nucleus, with no clear punctate-like structures being evident. On the other hand, the granular staining was used to describe non-uniform and granular (small, punctate inclusions) staining (Figure 3.31).
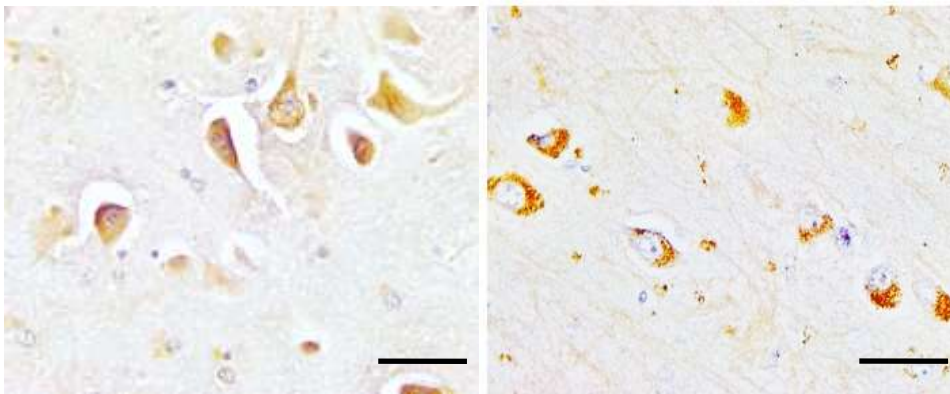
Figure 3.31 Diffuse cellular staining (left) by LAMP2A antibody and granular cellular staining (right) by LC3 antibody in the hippocampus. Magnification 100x; Scale bars 50 μm

No significant changewas seen in the granular staining of the hippocampus for any of the autophagy markers. No significant change in the diffuse staining in the frontal cortex with any of the autophagy markers, except Hsp70, which was found to decrease (Figure 3.32).
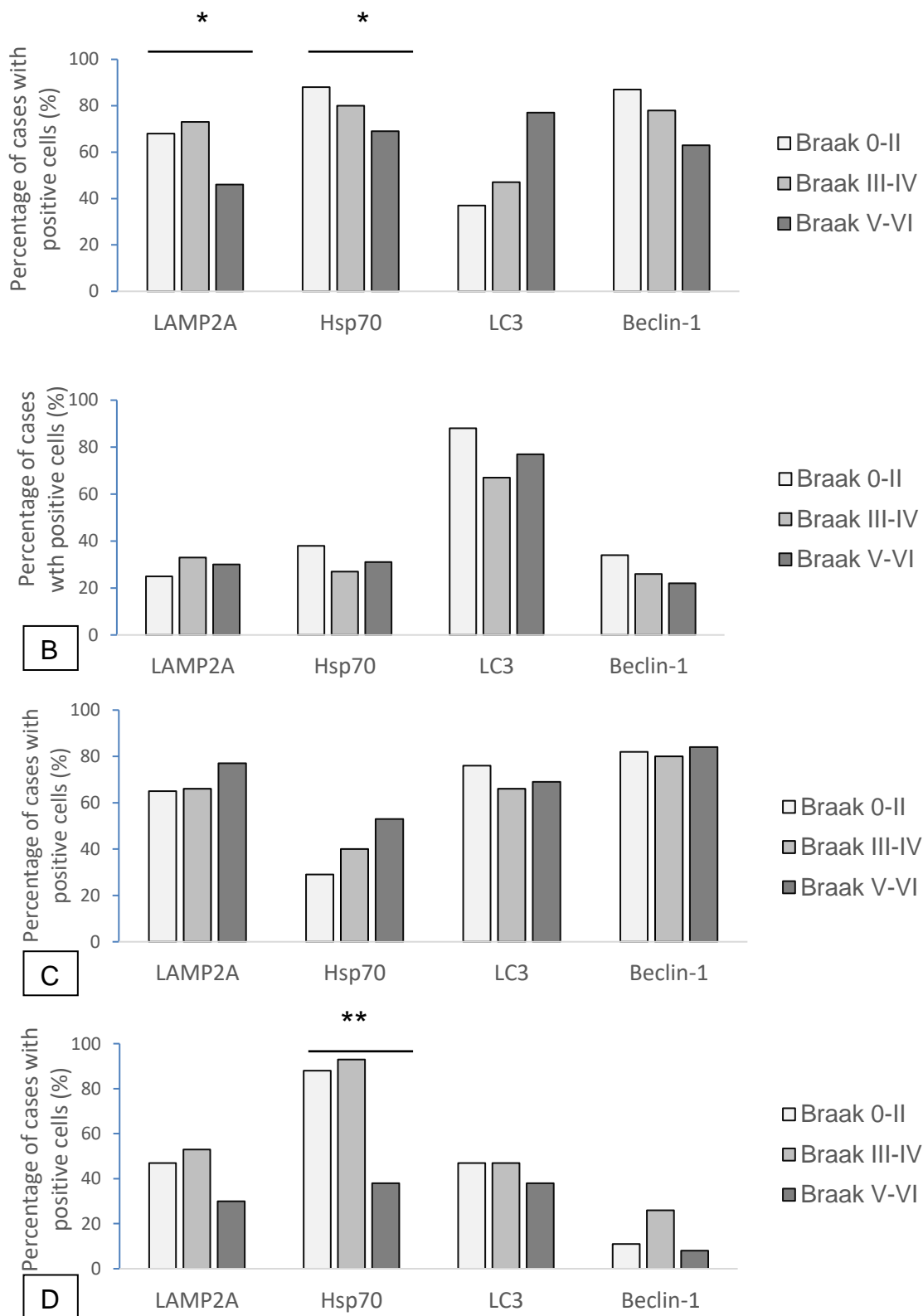
Figure 3.32 Diffuse and granular staining. Proportion of cases with diffuse and granular staining across the Braak stages in the hippocampus (A, B) and in the frontal cortex (C, D). *p<0.05; **p<0.01

3.1.7 <u>Distribution of autophagy markers in glial cells</u>

Autophagy markers positivity was also found in the glial cells (namely the astrocytes and oligodendrocytes, Figure 3.33) of the deep white matter of the hippocampus and the frontal cortex and in the subpial region of the hippocampus.
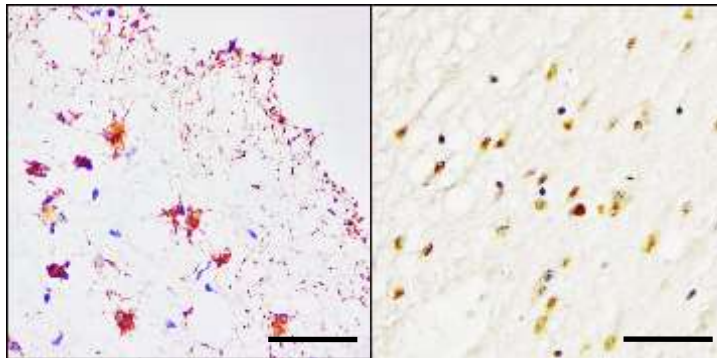
Figure 3.33 Glial cells (astrocytes-left and oligodendrocytes-right) distribution in the hippocampus. Magnification 400x; Scale bars 50 μm

Analysis explored the prevalence of any glial cells positivity (either astrocytes or oligodendrocytes) in the hippocampus, the frontal cortex and the occipital cortex across the Braak groups. Overall, oligodendrocytes stained by the MA and CMA markers were mostly seen in Braak 0-II, decreasing by 33% in Braak III-IV and increasing by 25% in Braak V-VI (Figure 3.34A). Looking at particular autophagy proteins, the most noticeable oligodendrocytes changes, related to progression of AD, were the linear decreases of both CMA proteins, from 76% and 69% in early disease stages to 54% and 46%, respectively, in late stages with no statistically significant differences (Chi-square test, p=0.24,

p=0.16) (Figure 3.34A). LC3 positive oligodendrocytes dropped by half from early to mid Braak stages, and increased back to 58% in Braak V-VI, demonstrating a statistically significant difference (Chi-square test, p=0.007). A stronger variation was seen in the Beclin-1 oligodendrocytes, which increased in number, being found in almost all cases with severe AD (92%) (Chi-square test, p<0.001) (Figure 3.34A).

Astrocytes distribution in the hippocampus was very similar in all three stages of the disease with maximum 8% difference between Braak 0-II and Braak III-IV variation (Figure 3.40B). Astrocytes recruiting LAMP2A, Hsp70 and Beclin-1 were all increasing with AD progression, in particular in Braak III-IV with LAMP2A astrocytes being present in almost all cases (92%) (Figure 3.34B). On the other hand, glial cells stained by LC3 protein decreased from 50% in Braak 0-II, to 33% in Braak III-IV and 41% in Braak V-VI (Figure 3.34B). No statistically significant differences were observed in the positively stained astrocytes with increasing Braak staging.
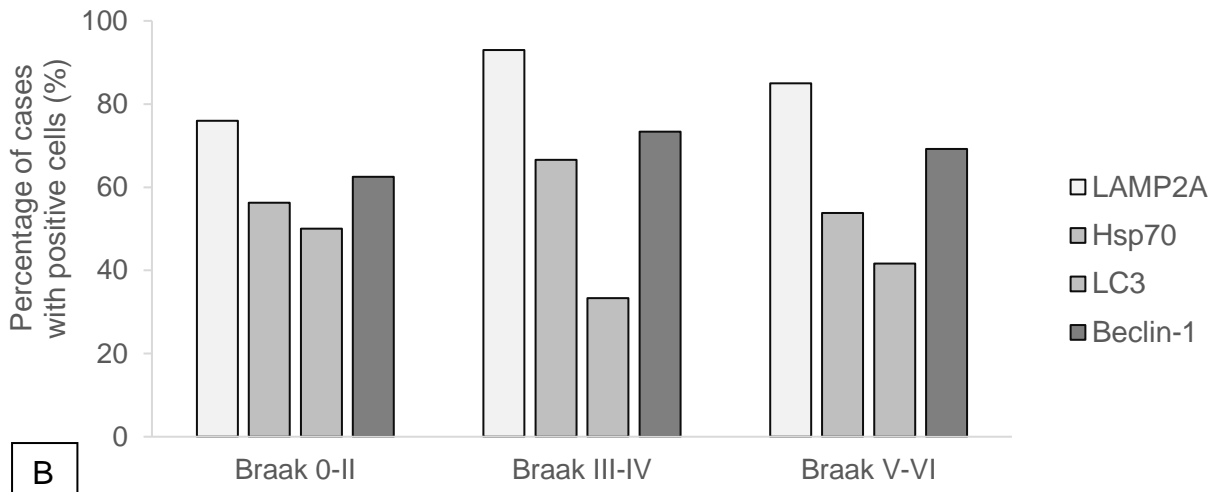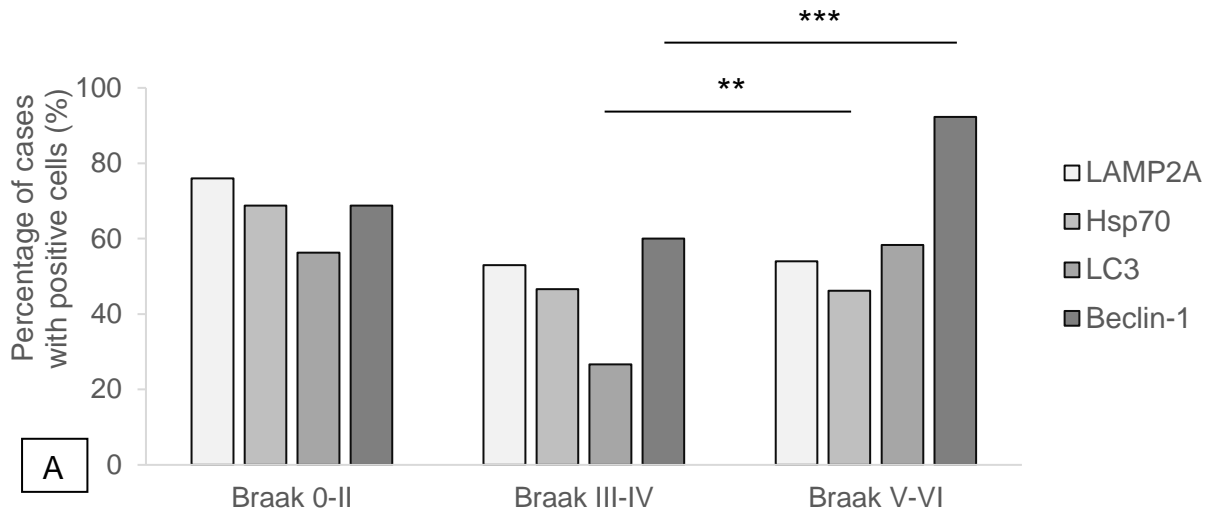
Figure 3.34 Distribution of oligodendrocytes (A) and astrocytes (B) across the Braak groups in the hippocampus **p<0.05, ***p<0.001

In the frontal cortex, no significant difference in either astrocytes or oligodendrocytes expression autophagy markers was found, except a significant decrease in LC3 in oligodendrocytes as Braak stage increases.
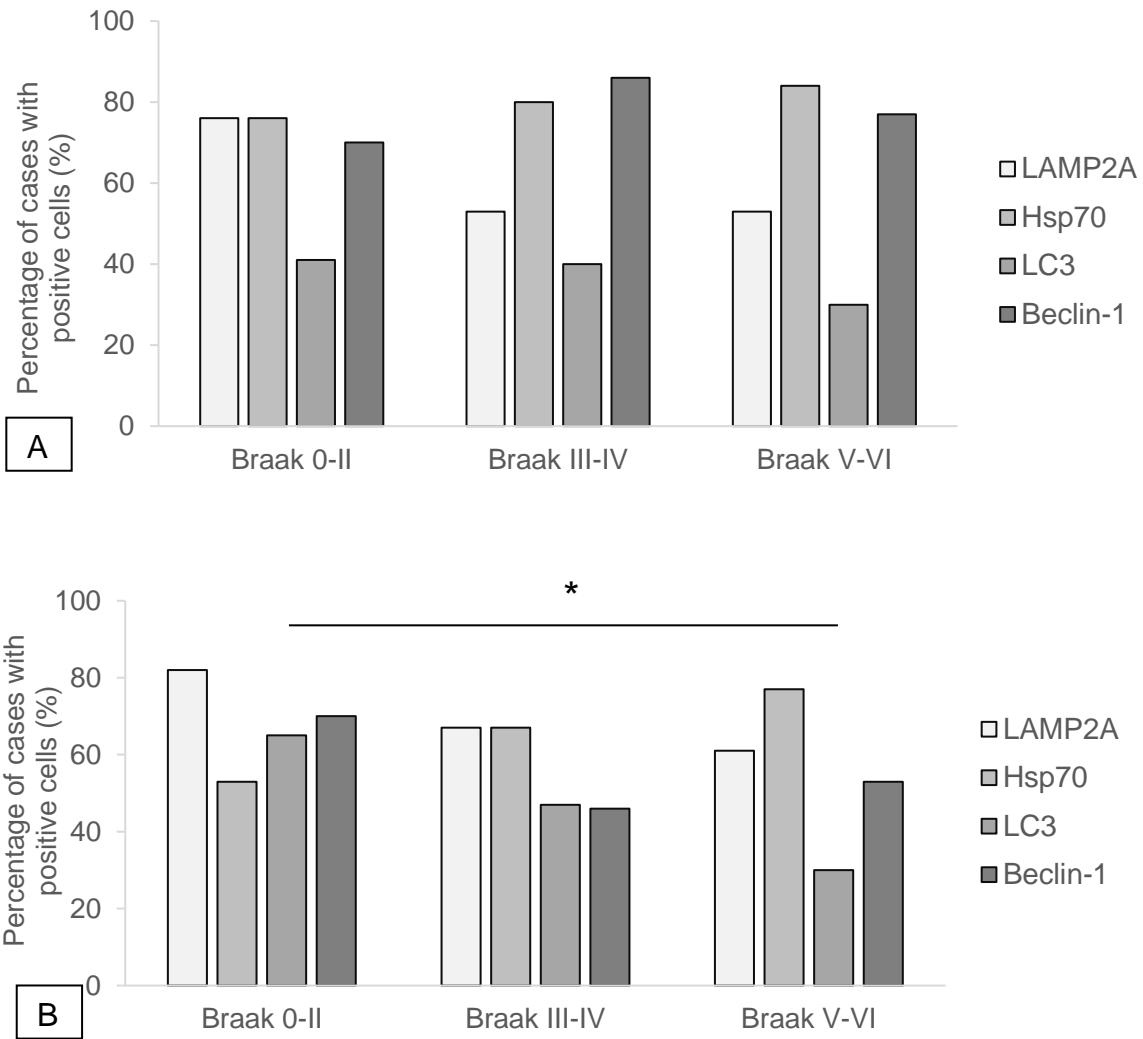
Figure 3.35 Distribution of astrocytes (A) and oligodendrocytes (B) across the Braak groups in the frontal cortex *p<0.05

In the occipital cortex, no significant difference in either astrocytes or oligodendrocytes expression autophagy markers was found, except a significant decrease in LC3 in astrocytes as Braak stage increases.
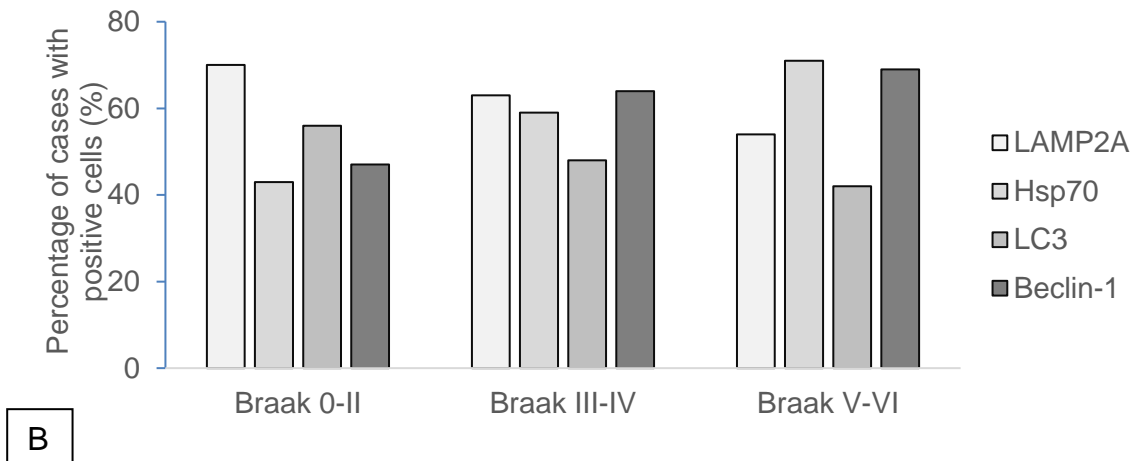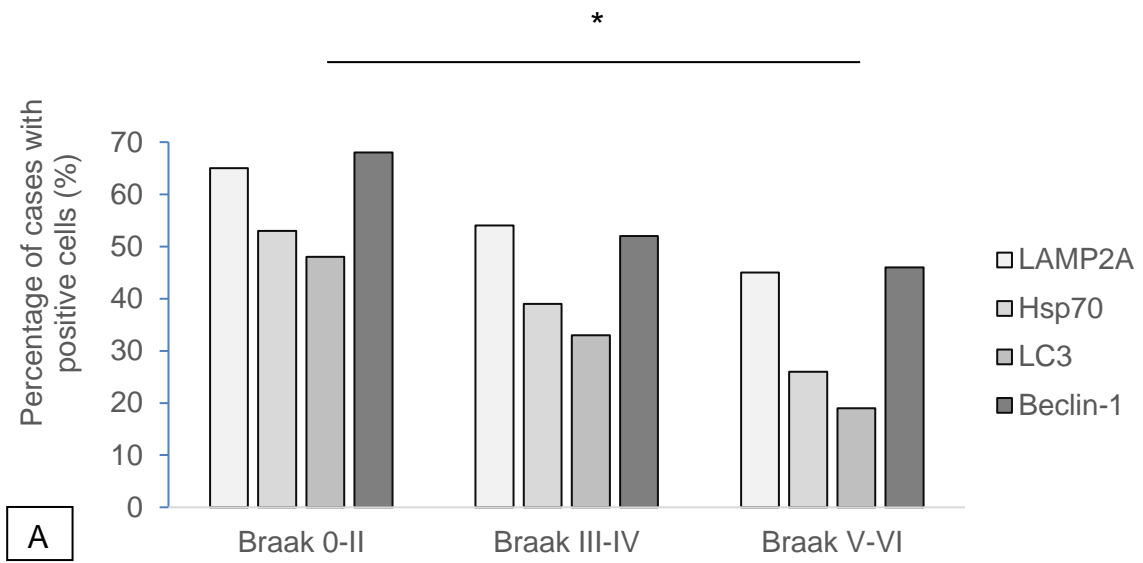
Figure 3.36 Distribution of astrocytes (A) and oligodendrocytes (B) across the Braak groups in the occipital cortex *p<0.05

3.1.8 <u>Autophagy markers vs tau and β-amyloid pathology</u>

In the previous sections of Chapter 3, the staining of all four autophagy markers
has been assessed in relation to variation in the three brain regions assessed,
in relation to Braak stage, with respect to the type of neuronal staining (diffuse,
granular) and its presence in other interesting structures and glial cells.

In this section, MA and CMA related protein staining will be assessed in relation
to AT8 positive structures and β-amyloid plaques to allow an exploration of how
autophagy markers relate to abnormal protein accumulation.

As previously mentioned in section 3.1.5, each case was given a significant or
minimal staining score. This meant each case had a single score for each of the
three brain regions, therefore receiving either a score of 0 (absent/mild staining)
or a score of 1 (moderate/severe staining) for each autophagy marker in each
brain region. Similarly, AT8 staining scores were dichotomised into minimal and
significant staining and each case received a single score of 0 or 1 for each
brain region. Then, for each brain region, the single score of each autophagy
marker was compared to the AT8 single score in each individual case.

First, the hippocampus was assessed and Chi-square tests were done to
explore the relationship between significant staining of each autophagy marker
and significant AT8 pathology in each Braak group, allowing the understanding
of the relationship between the autophagy markers and AT8 pathology and how
it varies with disease progression. Statistical analysis demonstrated a significant
negative association of LAMP2A, LC3 and Beclin-1 markers to AT8 pathology in
Braak 0-II groups (p=0.01, p=0.03, p=0.006, Chi-square test). In the frontal

cortex, significant associations were also found in Braak 0-II groups. In this brain region, stronger associations were identified between the CMA markers LAMP2A and Hsp70 when compared with AT8 marker (p<0.001; p<0.001, Chi-square test) whereas MA markers LC3 and Beclin-1 demonstrated less strong associations with AT8 staining (p=0.02, p=0.01, Chi-square test). All these associations between the increased immoreactive profile of the autophagy markers and the minimal AD pathology were found negative. Interestingly, LC3 and AT8 demonstrated a significant positive association in Braak III-IV (p=0.01, Chi-square test). In the occipital cortex, the only significant positive association seen in Braak 0-II group was found between Beclin-1 and AT8 (p<0.001, Chi-square test). Braak III-IV positive associations were seen when LAMP2A and LC3 significant scores were compared with significant AT8 (p=0.001, p=0.006, Chi-square test). The occipital cortex was the only brain region in which negative significant associations were found in the Braak V-VI group when Hsp70 (p=0.02, Chi-square test) and LC3 (p=0.009, Chi-square test) were related to AT8 significant staining.

Chi-square tests were also performed to assess the relationship between the autophagy markers staining and β-amyloid pathology, based on the dichotomised scores which were given to each case in each brain region. Stronger variations were more predominant in the brain regions when autophagy marker staining was related to β-amyloid pathology. In the hippocampus, LAMP2A was found to be negatively associated with β-amyloid pathology in all Braak groups (p=0.03, p=0.03, p<0.001, Chi-square test) whereas Hsp70 negative association to β-amyloid was found significant only in Braak 0-II stage (p<0.001, Chi-square test). The relationship between LC3 and

β-amyloid staining was also statistically significant in Braak 0-II (p<0.001, Chi-square test) and Braak III-IV (p=0.03, Chi-square test) and was found negative. In the frontal cortex, significant associations were identified in Braak 0-II for all autophagy markers LAMP2A, Hsp70, LC3, Beclin-1 (p<0.001, 0<0.001, p=0.02, p=0.01, Chi-square test). Lastly, the occipital cortex was the brain region with the most predominant variation between the autophagy markers staining and β-amyloid staining. The relationship of both CMA markers to pathological β-amyloid demonstrated a statistically significant relationship in Braak 0-II stages (p=0.001, p=0.01, Chi-square test), which was found negative. Significance of relationship between MA marker LC3 and β-amyloid was identified in Braak 0-II (p=0.001, Chi-square test) and Braak V-VI (p=0.02, Chi-square test), whereas Beclin-1 significant staining was strongly associated with β-amyloid in Braak 0-II (p<0.001, Chi-square test) and in Braak III-IV (p=0.001, Chi-square test). All associations were negative.

These results demonstrate that the majority of the associations between all autophagy markers when compared with tau and β-amyloid pathologies are negative, meaning that they follow opposite trends. Also, the stronger the association, the higher the variation in scores between the autophagy marker staining and the AT8 and β-amyloid staining. Also, there were more variations between autophagy markers and AT8 pathology in the frontal and the occipital cortices, rather than in the hippocampus. In addition, both the relationships of autophagy markers staining with AT8 staining and with β-amyloid staining varied the most in the occipital cortex.

3.2 Immunofluorescence double labelling of human brain tissue

Previous research has demonstrated that CA1 is an early site of abnormal protein accumulation in AD, whereas CA4 only becomes affected in late stages of disease (Braak *et al*, 1991; Lace *et al*, 2009; Serrano-Pozo, 2011). Therefore, CA4 and CA1 subregions were explored in detail to allow investigation of how autophagy markers are dissembled in regions differently affected in disease. In section 3.1.1, we showed the regional variation of all four autophagy markers staining and found that overall staining levels were lower in CA1 compared with CA4 (Figures 3.37 and 3.38). In this section, we will look at individual neurons within CA4 and CA1, to assess the co-localization degree of LC3 and LAMP2A autophagy markers with pathological tau protein.
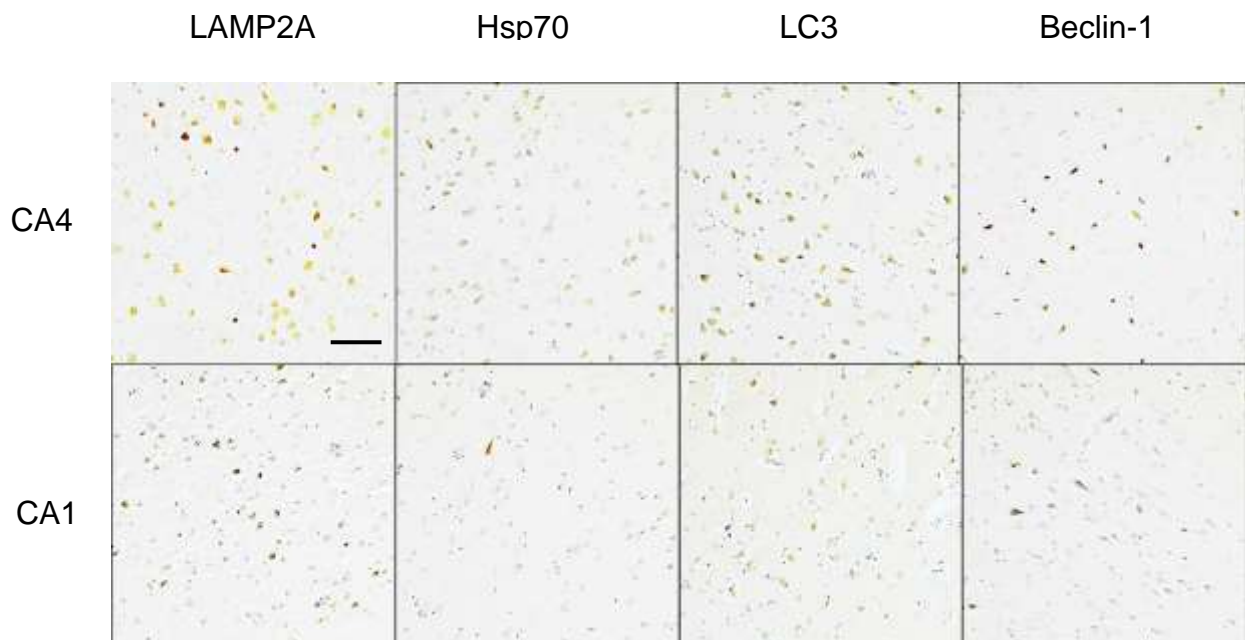
Figure 3.37 Immunohistochemical staining of all autophagy markers in hippocampal subregions CA4 and CA1. Magnification 100x. Scale bar 100 µm

In section 3.1.1, we looked at the autophagy markers stained in CA4 and CA1 (both 0-3 rating scale and -/+/++/+++ rating scale), in relationship to all other hippocampal subregions, however, in this section, we only looked at the number of the cells stained in CA4 and CA1. An overall decrease in the number of the cells stained by Hsp70, LC3 and Beclin-1 was observed in CA1, compared to CA4 (Figure 3.38A). Significant Hsp70 staining was found in 69% cases in CA4, compared to 38% in CA1 in Braak 0-II and in 50% cases in CA4, compared to 38% in CA1 in Braak III-IV (Figure 3.38A). In high Braak, half of the cases had significant Hsp70 staining (50%) in CA4 and only 19% cases presented staining in CA1 region (Figure 3.38A). LC3 staining was also found to differ between the two regions with lower levels of staining in CA1 when compared to CA4. The variation of LC3 staining, seen in Braak III-IV group, which was found in 63% cases (CA4) and 44% cases (CA1), is more evident than the variation seen in Braak V-VI, where LC3 is seen in 63% (CA4) and 50% (CA1) (Figure 3.38A). Beclin-1 staining varied only in Braak V-VI, being present in 75% cases (CA4) and 56% (CA1) (Figure 3.38A). An overall decrease was also found in the intensity of cellular staining of all autophagy markers, observed in CA1 when compared to CA4 (Figure 3.38B). LC3 staining was found variable between the two regions in all three Braak groups, with the most noticeable variation in Braak V-VI, present in 44% cases (CA4) and 25% (CA1) (Figure 3.38B). LAMP2A and Beclin-1 staining demonstrated a variation between CA4 and CA1 in both Braak III-IV and Braak V-VI groups, however most significant differences were seen in Braak III-IV for both markers. LAMP2 staining was found in a very high number of 94% cases in CA4 compared to 63% cases in CA1, whereas Beclin-1 was seen in 67% cases in CA4 and 31% cases in CA1 (Figure 3.38B).

Significant variation of Hsp70 was also reported in Braak 0-II and Braak V-VI groups with very low levels seen in CA1: 6% respectively 13% cases presenting Hsp70 (Figure 3.38B). Therefore, these results suggest a variation between CA4 and CA1 hippocampal regions across all Braak groups (Figure 3.38). Besides the variation of staining between CA4 and CA1, a decrease in the number of the cells stained by all autophagy markers was reported with increasing Braak stages in both CA4 and CA1 (Figure 3.38B). Moderate/severe LAMP2A and LC3 decreased from being present in 81% cases (Braak (0-II) to 63% cases (Braak V-VI) in CA4. Also, LC3 staining decreased from 75% to 50% in CA1 (Figure 3.38). Beclin-1 staining, which was present in almost all cases in both subregions, declined to 75% in CA4 and to 56% in CA1 (Figure 3.38A).
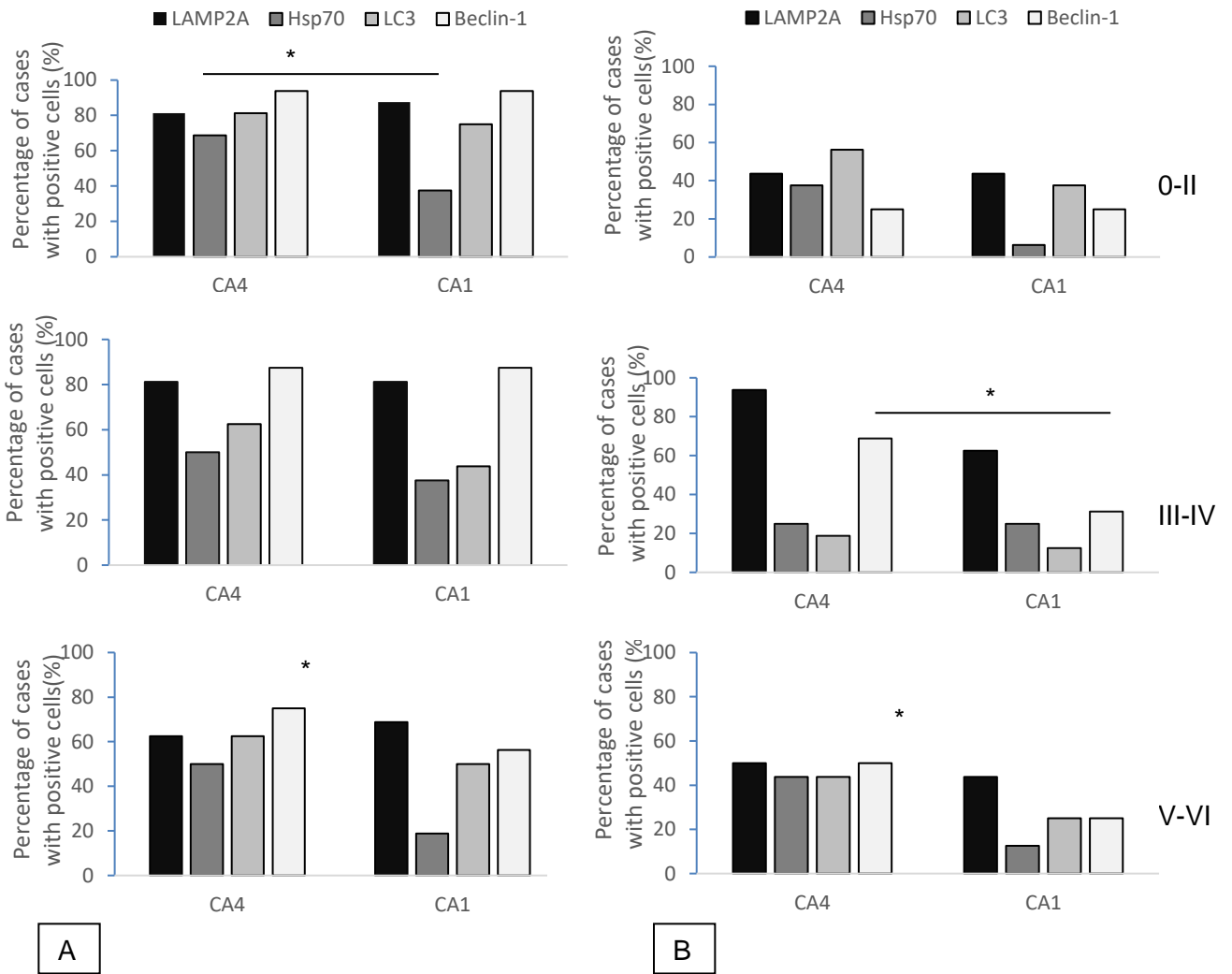
Figure 3.38 Autophagy protein levels in CA4 and CA1. Levels of MA and CMA markers staining in the hippocampal regions of interest, CA4 and CA1, across all Braak groups. Bar charts express percentage of cases with moderate and severe staining, based on the number of the cells stained (A) and on the cells intensity (B). *p<0.05

To assess if autophagy markers co-localize with intracellular accumulation of abnormal tau protein, the double-labelling immunofluorescence technique was used (Figure 3.39). LAMP2A and LC3 markers were selected for use because they demonstrated the least background staining. Aditionally, LC3 was previously shown to be largely associated with granular staining in the hippocampus (Figure 3.32) whereas LAMP2A was similar across different Braak stages.

For the double-labelling staining, tau protein was chosen rather than beta-amyloid in order to explore its relationship to autophagy markers in individual neurons. In section 3.1, autophagy marker distribution was assessed based on cellular staining and tau protein is known to be found intracellularly rather than extracellularly like beta-amyloid, which would link tau better to the autophagy markers investigation in this study. There are also studies which explore beta-amyloid burden in the frontal cortex and one study on AD mice suggests a neuronal loss in 10 months old APP/PS1K1 mice compared to 2 month old APP/PS1K1 mice, while the amyloid-plaque load in old mice was found low (Lemmens, 2011). Therefore, tau pathology is considered to be more relevant to the autophagy impairment, hence choosing tau protein for the double-labelling studies.

The expression levels of the proteins of interest were analysed in individual cells in both CA4 and CA1 hippocampal subregions across all Braak stages, since there are areas to be known differentially affected at each stage of disease.

Red channel
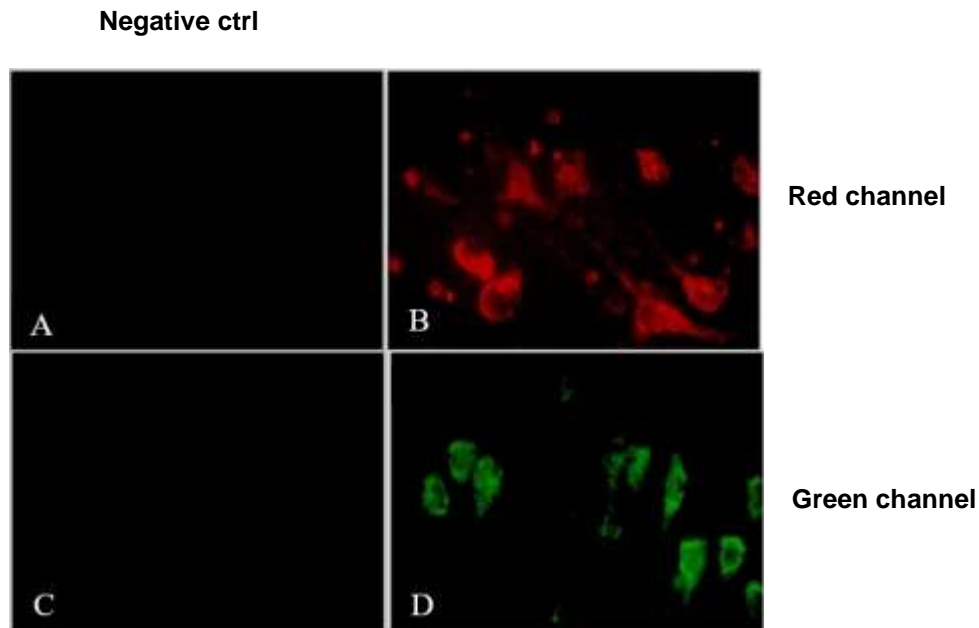
Green channel

Figure 3.39 Optimisation of double-labelling technique A) Negative control in the red channel; B) Positive control-red channel (LC3 antibody); C) Negative control in the green channel and D) Positive control-green channel (AT8 antibody).

The images below represent co-localisation of the autophagy markers LAMP2A and LC3 with pathological AT8 marker through double-labelling staining AT8 in the hippocampal subregions CA4 and CA1 (Figure 3.40-45).

These images suggest that in Braak 0-II and Braak III-IV, all AT8 positive cells were also LAMP2A positive (Figure 3.40 and 3.41), therefore the two markers co-localize, whereas in Braak V-VI, many AT8 positive cells were LAMP2A negative (Figure 3.42). The images also suggest that in Braak 0-II, all AT8 positive cells were also LC3 positive and that many LC3 positive cells were AT8 negative (Figure 3.43). In Braak III-IV and Braak V-VI, all LC3 positive cells were also AT8 positive and many AT8 positive cells were observed to be LC3 negative (Figure 3.44, 3.45).

We then looked at all cases stained (LAMP2A, n=15; LC3, n=15) and quantified all LAMP2A/LC3 positive cells and all AT8 positive cells in both CA4 and CA1, assessed the co-localisation LAMP2A-AT8 and LC3-AT8 (meaning when LAMP2A/LC3 co-localized with AT8) and expressed them as percentage (LAMP2A/LC3 % to AT8 positive staining) to assess how co-localisation varied with disease progression in both CA4 and CA1 (Figure 3.40). The results demonstrated that in CA1, co-localisation of LAMP2A with AT8 decreased significantly in Braak V-VI ($p < 0.001$, Chi-square test), whereas in CA4, the increase, which was seen only in Braak III-IV was not found to be significant ($p = 0.2$, Chi-square test). On the other hand, co-localisation of LC3 with AT8, in both CA1 and CA4, decreased drastically from being present in almost all cases in Braak 0-II to being present in only half of the cases ($p < 0.001$, $p < 0.001$, Chi-square test).
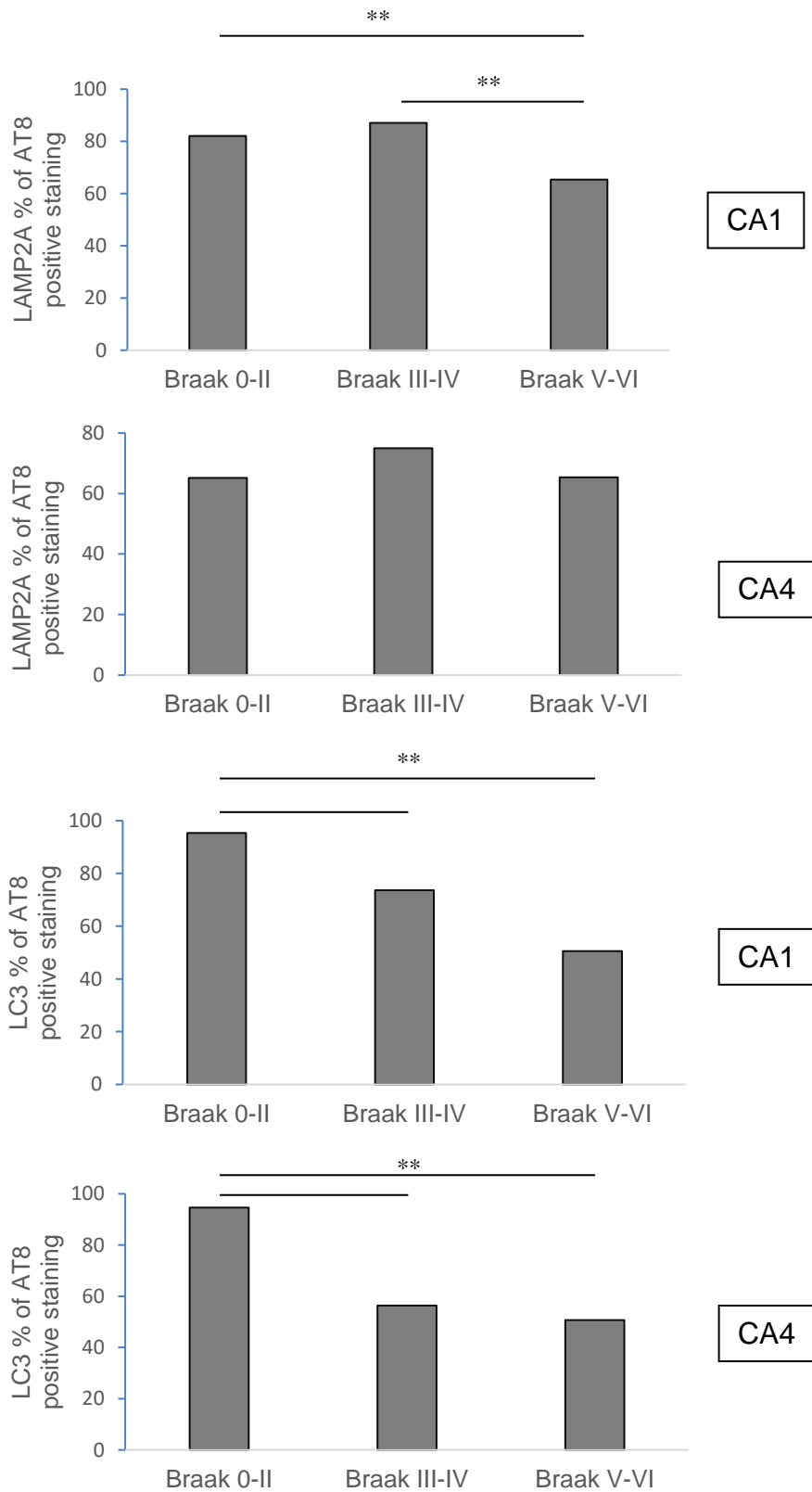
Figure 3.40 Co-localisation of autophagy markers LAMP2A/LC3 with AT8 in individual neurons of hippocampal subregions CA4 and CA1; **p<0.001
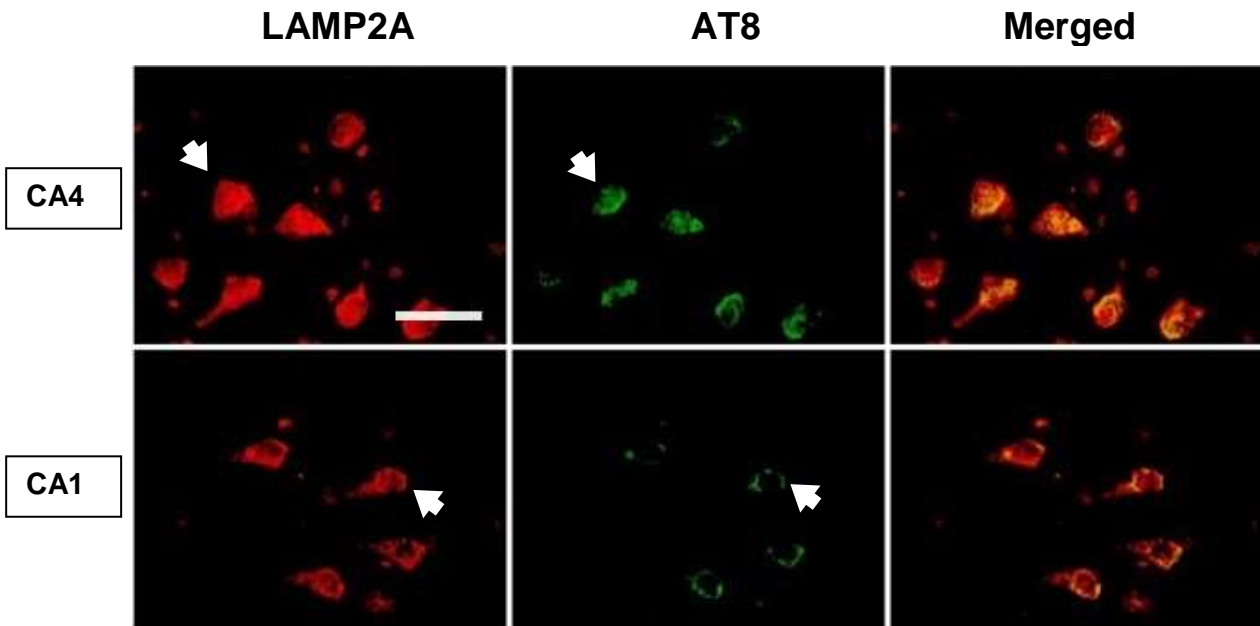
Figure 3.41 Double-immunofluorescent labelling of hippocampal CA4 and CA1 with LAMP2A (red) and AT8 (green) in a Braak 0-II case. These images suggest that all AT8 positive cells are also LAMP2A positive (arrow); images captured at 400x magnification; scale bar 50µm.
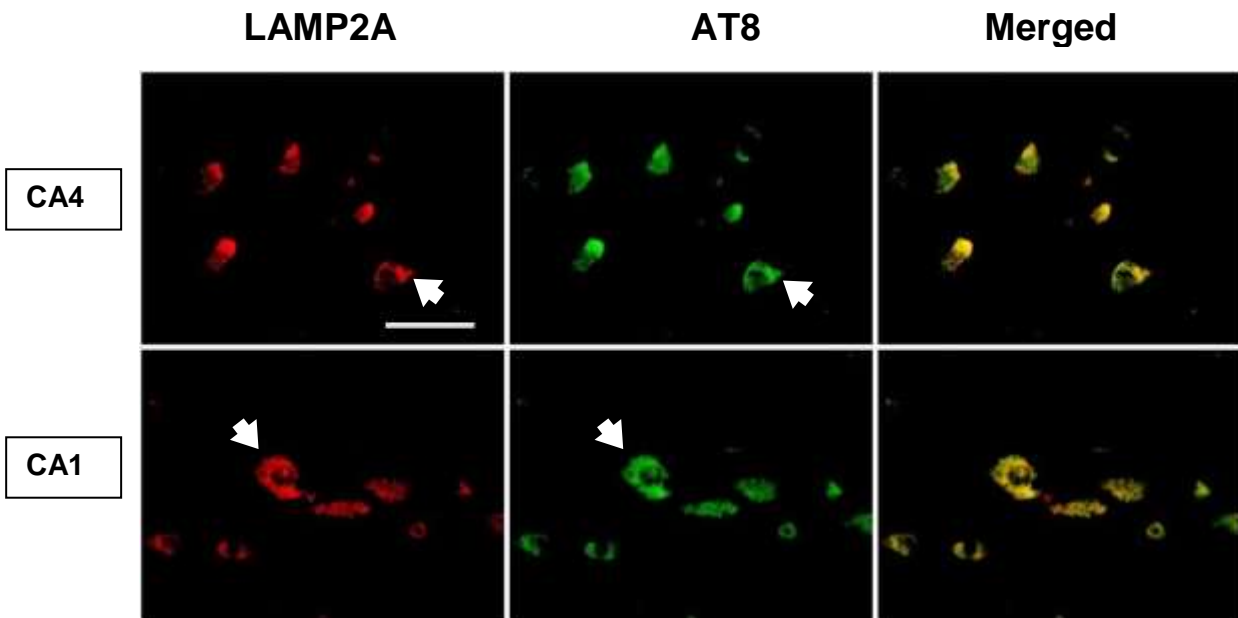
Figure 3.42 Double-immunofluorescent labelling of hippocampal CA4 and CA1 with LAMP2A (red) and AT8 (**green) in a Braak III-IV case**. These images suggest that all AT8 positive cells are also LAMP2A positive (arrow); images captured at 400x magnification; scale bar 50µm.
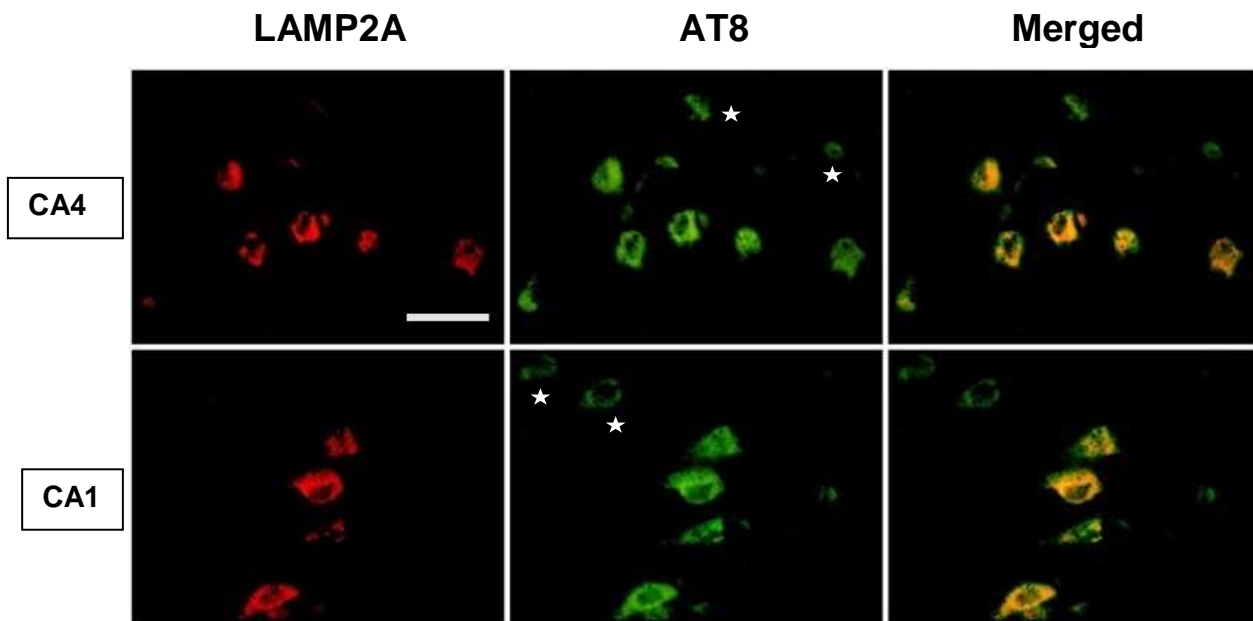
Figure 3.41 Double-immunofluorescent labelling of hippocampal CA4 and CA1 with LAMP2A (red) and AT8 (green) in high Braak V-VI. These images suggest that many AT8 positive cells are LAMP2A negative (star); images captured at 400x magnification; scale bar 50µm.
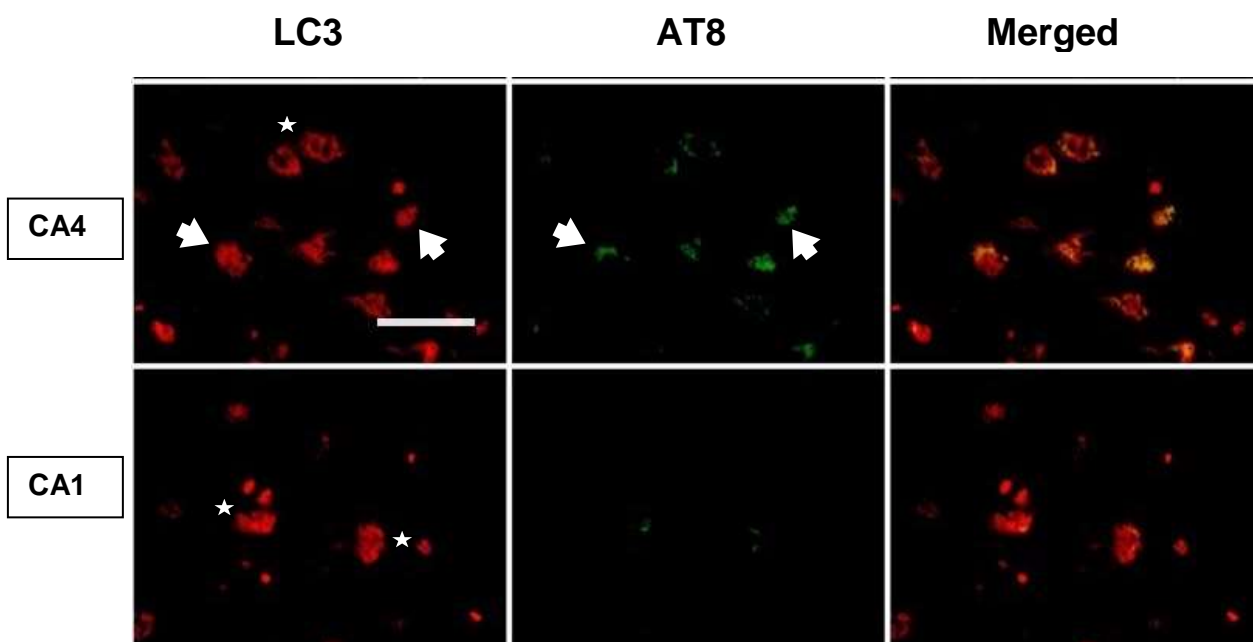
Figure 3.42 Double-immunofluorescent labelling of hippocampal CA4 and CA1 with LC3 (red) and AT8 (green) in low Braak 0-II. These images suggest that all AT8 positive cells are also LC3 positive cells (arrow) and that many LC3 positive cells are AT8 negative (star); images captured at 400x magnification; scale bar 50µm.
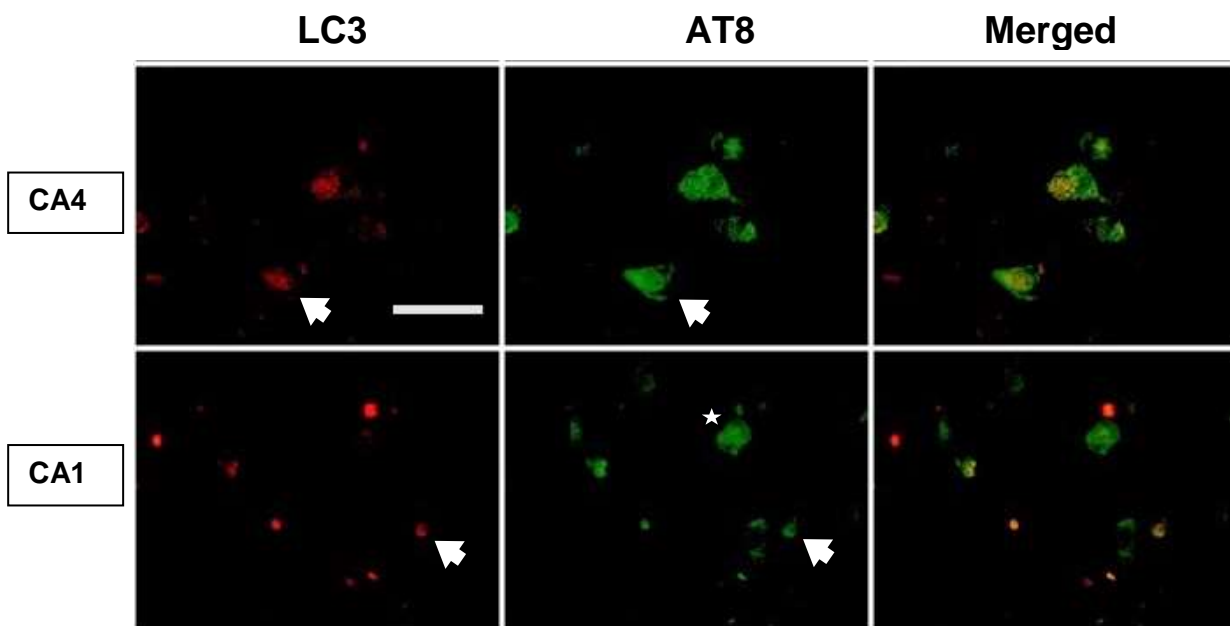
Figure 3.43 Double-immunofluorescent labelling of hippocampal CA4 and CA1 with LC3 (red) and AT8 (green) in mid Braak III-IV. These images suggest that all LC3 positive cells are also AT8 positive cells (arrow) and that some AT8 positive cells are LC3 negative (star); images captured at 400x magnification; scale bar 50µm.
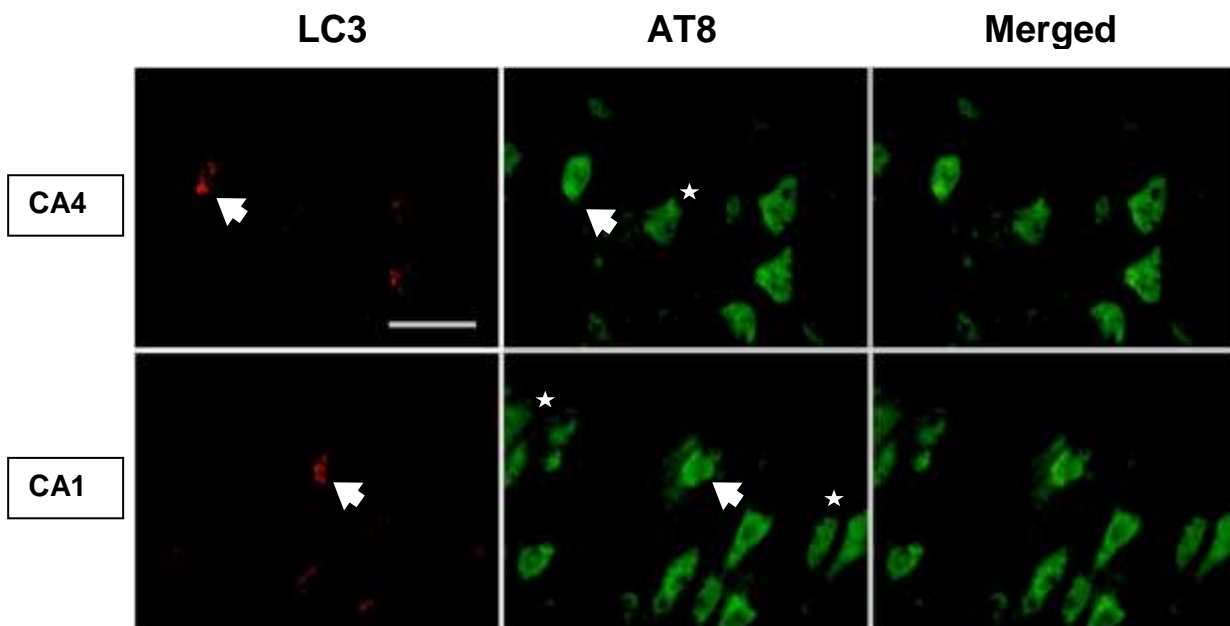
Figure 3.44 Double-immunofluorescent labelling of hippocampal CA4 and CA1 with LC3 (red) and AT8 (green) in Braak V-VI. These images suggest that all LC3 positive cells are also AT8 positive cells and that many AT8 positive cells are LC3 negative; images captured at 400x magnification; scale bar 50µm.

3.3   Western-blot analysis of skin-derived fibroblasts

Studies using skin-derived fibroblasts (as described in section 1.5.2) suggest that they may be a potentially useful model of neurodegenerative disease, particularly to use in throughput screening assays which are used to assess the efficacy of new drug therapies. As described in section 1.5.5, previous research has reported the genetic and protein expression profile in AD skin derived fibroblasts and studies have shown same of the cellular changes in brain cells are also evident in AD skin-derived fibroblast (Citron *et al.*, 1994, Magini *et al.*, 2010, Ramamoorthy *et al.*, 2012; Mocali, 2014). However, it is unclear if changes in autophagy markers can be detected in these cells.

In this chapter, MA and CMA biomarker levels were explored in AD skin fibroblasts and in comparison to normal skin fibroblasts of individuals of same age (age matched controls). After cells have been successfully grown *in vitro*, proteins were extracted and assessed via Western Blotting.

3.4   Optimisation

For each antibody, experiments aimed to optimize the gel percentage, amount of protein loaded, blocking method, primary antibody dilution and optimal temperature (Figure 3.47-53). The optimal gel percentage was chosen to capture the bands of interest such as the two LC3 bands. (Figure 3.47)
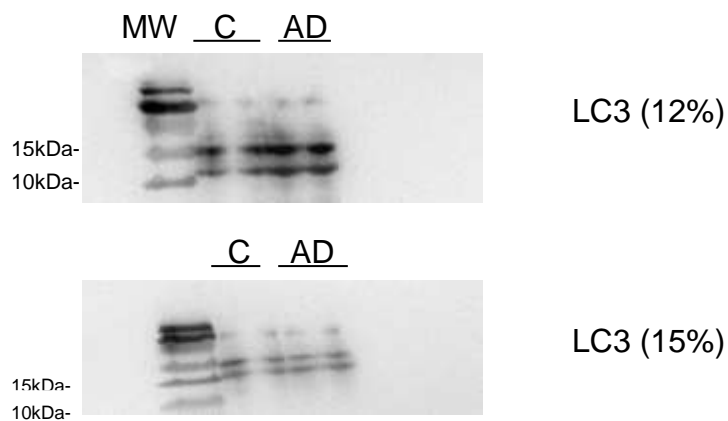
Figure 3.47 Example of optimisation by trying different gel percentages: 12% (top) and 15% (bottom) on LC3 antibody. MW=molecular weight ladder, C=control fibroblast, AD=disease fibroblast

For each antibody, a range of protein concentrations were loaded (10µg, 15µg and 20µg). An example is shown in Figure 3.48, where LAMP2A bands demonstrated poor signal when 10µg were loaded on the gel while, 20µg of protein loaded, showed better results (Figure 3.48).
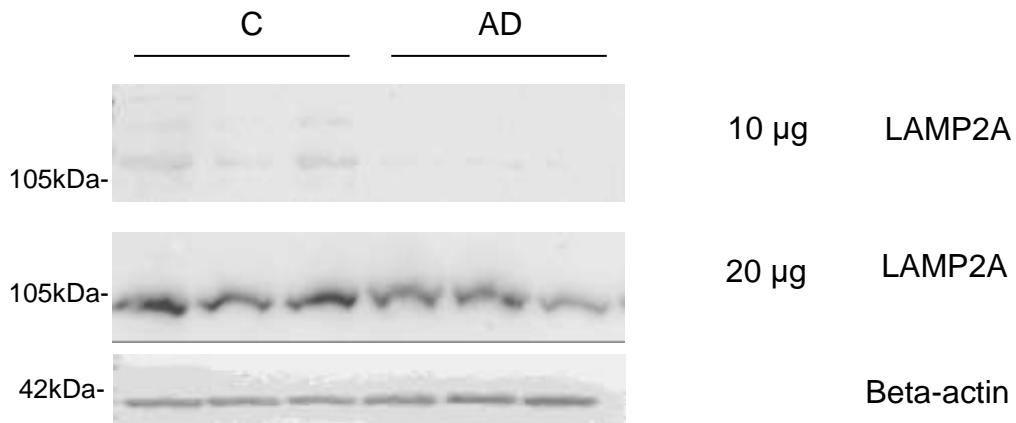
Figure 3.48 Example of optimisation. Various protein concentrations were tested in order to achieve better intensity for optimal bands resolution. After loading 10µg of protein, LAMP2A bands showed poor signal (top), while 20µg of protein seemed to improve the resolution of the bands (bottom). C-control fibroblasts, AD-disease fibroblasts.

Some antibodies (LAMP2A, Hsp70 and LC3) blotting resulted in noisy background due to non-specific binding to the membrane (Figure 3.49A) and this was resolved by adding 5% non-fat dry milk and 1% BSA to the blocking solution (Figure 3.49B).
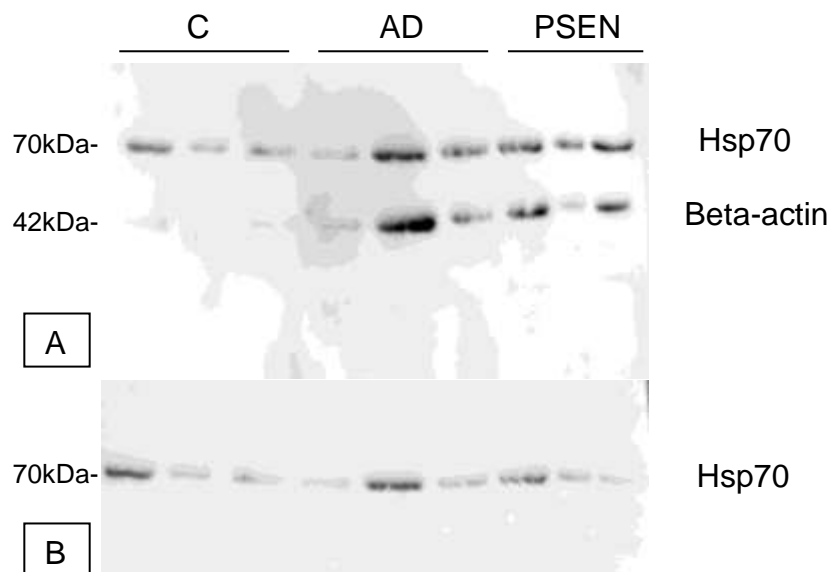
Figure 3.49 Example of optimisation of the blocking method. A) Before treatment and B) After treatment

171

Also, some antibodies expressed multiple non-specific bands on the membrane (Figure 3.50A). One example was LAMP2A optimisation to reduce the multiple bands to one single specific band at 105kDa by increasing the blocking time from 30min to 1h (Figure 3.50B).
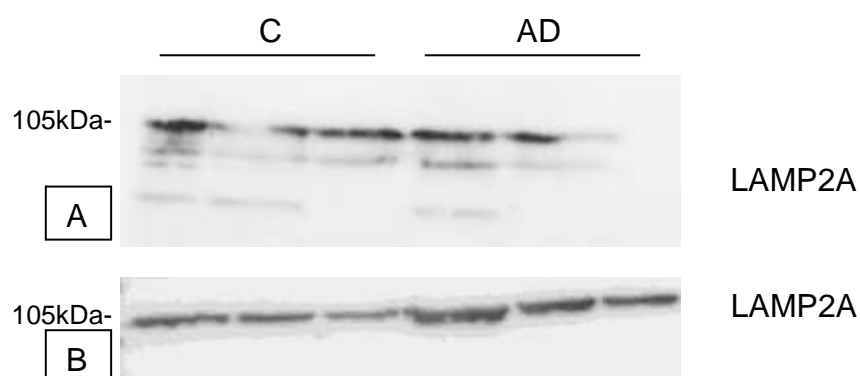
Figure 3.50 Example of optimisation. A) Presence of multiple non-specific LAMP2A bands and B) One specific LAMP2A band after increased blocking time.

Another important step of the optimisation was to choose the optimal antibody dilution for each protein of interest, in order to give the best staining of the protein with minimum background and after incubation with a series of experimental dilutions of the antibodies (1:500, 1:1000) (Figure 3.51), the optimal dilution for each antibody was as follows: LAMP2A (1:1000), LC3 (1:3000), Beclin-1 (1:1000) and Hsp70 (1:1000).
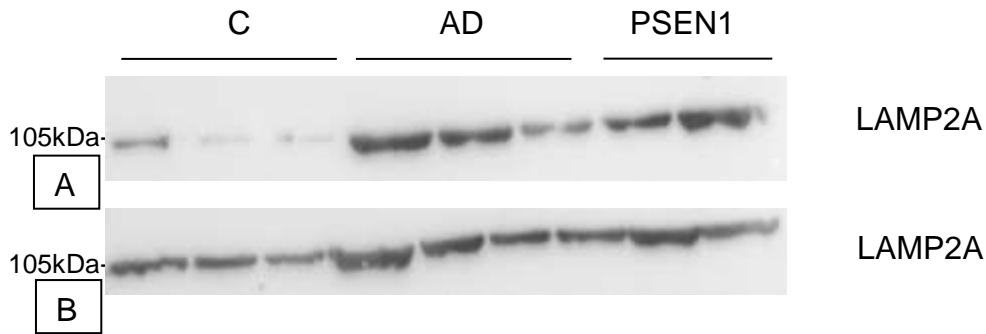
Figure 3.51 Example of antibody dilution optimisation. The image shows LAMP2A optimisation: A) 1:500 and B) 1:1000. C-control fibroblasts, AD-disease fibroblasts, PSEN1-mutated fibroblasts

Due to lab temperature variability during the experimental studies, blotting bands demonstrated poor resolution therefore optimisation included antibody incubation temperature control. When performing a Western blotting, environmental factors are crucial and in this case, a constant temperature was kept to give consistent results. Before optimisation, gels were run at room temperature which varied each day, giving poorly resolved bands, either fuzzy, dispersed or fragmented bands (Figure 3.52). Therefore, all gels were run at 4°C, in the cold room, followed by the transfer of the proteins onto the membrane at the same temperature.
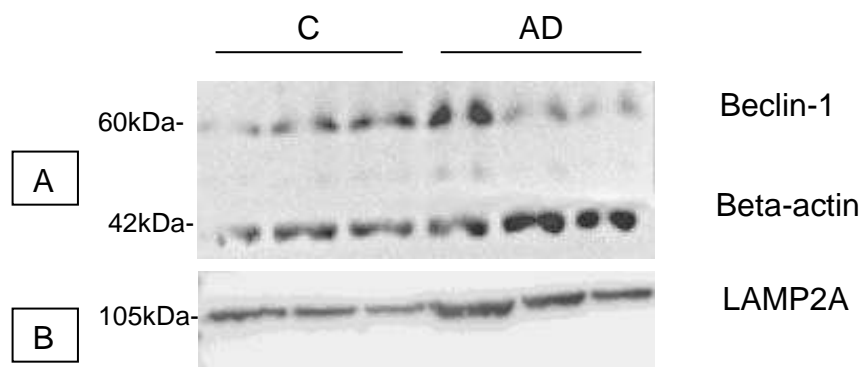
Figure 3.52 Example of optimisation of temperature control.
A) Fragmented or fuzzy bands due to variability of room temperature and B) Compact bands due to constant temperature

Lastly, the final step for achieving the best staining results was by choosing the optimal exposure time, after reading the membranes in the G-box. Subsequential exposure times starting from a few seconds up to a maximum of 10 mins have been tried on all antibodies and an example is seen below (Figure 3.53), where a 5 mins exposure of the LC3 bands demonstrated better results (optimal intensity) than a 3 mins exposure.
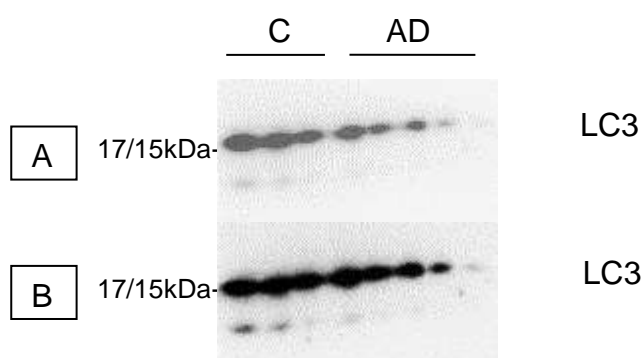
Figure 3.53 Different exposure times of LC3 bands: A) 3 mins and B) 5 mins

Overall, it was found that the optimal protein concentration was 15μg for Hsp70 and Beclin-1 and 20μg for LAMP2A and LC3, respectively (Table 2.4). Also, the optimal gel percentages were 7.5% (LAMP2A, Hsp70 and Beclin-1) and 12% (LC3) (Table 2.4). The blocking solution made of 1% BSA and 5% milk in TBS-T required optimal times of 30 mins (Hsp70, Beclin-1) and 1h (LAMP2A, LC3) (Table 2.4). The gel running time required 1h30 mins (LAMP2A, Hsp70 and Beclin-1) and 1h (LC3) to allow differentiation of the two LC3 bands (Table 2.4). The best antibody

dilutions were found to be 1:1000 (LAMP2A, Hsp70 and Beclin-1) and 1:3000 (LC3). Lastly, the exposure times chosen were 5 sec (LAMP2A), 10 sec (Hsp70), 1 min (Beclin-1) and 3mins (LC3) (Table 2.4).

3.5   Autophagy markers expression in the fibroblasts

After numerous and extensive optimisation experiments, optimal results were chosen to represent the autophagy marker levels of expression in the skin fibroblasts, grown *in vitro*.

Semi-quantification of the levels of all proteins of interest were normalised against housekeeping beta-actin, which acted as a loading control. This is to minimize variations resulting from experimental errors such as inconsistent sample preparation, uneven sample loading on the gel, incomplete transfer of the proteins. Nine samples from different patients were used in this study comprising of 3 sporadic AD cases (AD1-3), genetically mutated AD cases having a mutation in the presenilin gene (PSEN1-3) and 3 control cases which represent age matched controls or healthy ageing subjects.

LAMP2A expression was found very low in the fibroblasts derived from patients with sporadic AD or from the age matched control subjects (Figure 3.58). Although LAMP2A cellular levels were found very low, the CMA marker expression in the control cells (C) were relatively the same as the expression in the sporadic AD cells with no statistical significant difference (p=0.47, paired T-test) (Figure 3.58). In the genetically mutated

cells (PSEN), LAMP2A was found much higher when compared to the AD sporadic cells or the control cells, with a statistically significant difference between the control vs PSEN group, respectively the AD group vs the mutated cells group (p=0.006, p=0.0006, paired T-test) (Figure 3.58).
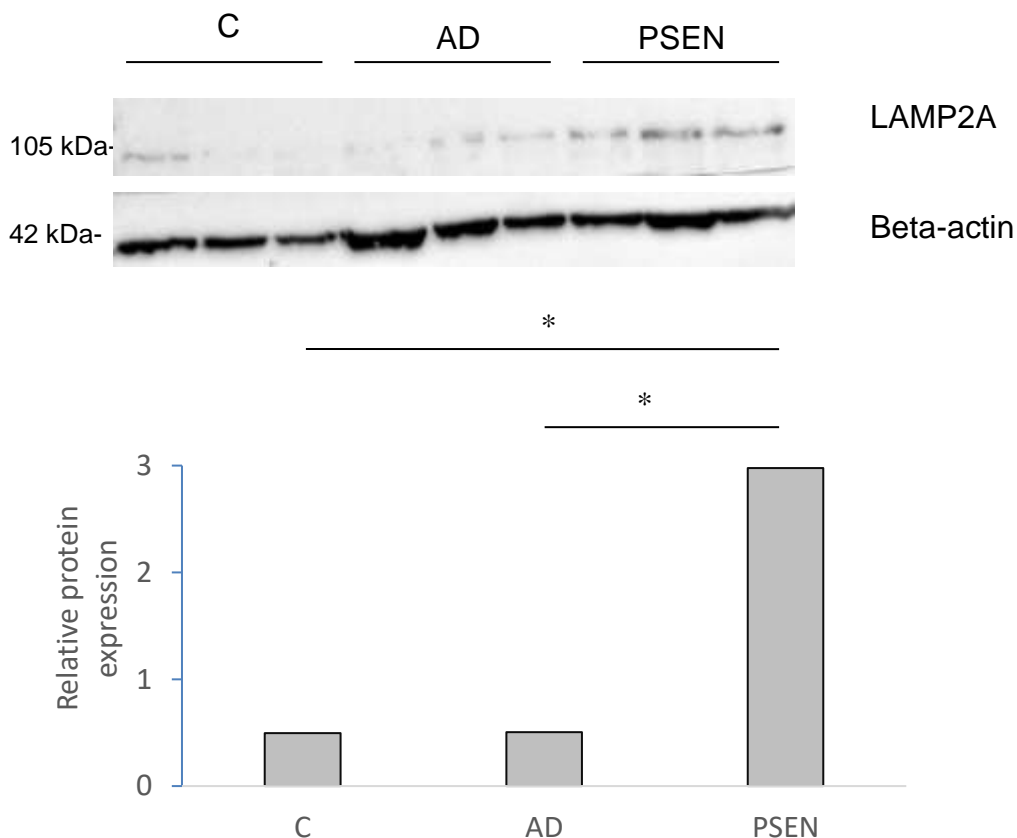
Figure 3.54 LAMP2A relative expression in the fibroblasts. LAMP2A expression observed in the sporadic AD group (AD) and in the presenilin mutated group (PSEN) compared to LAMP2A expression levels in the control group (C) *p<0.05

Overall Hsp70 expression in the control cells is higher by 15% than the expression in the sporadic AD cells, with a noticeable lowest expression in case AD3 (Figure 3.59). There is no statistically difference between control and disease expression of the CMA marker (paired T test, p=0.33). Looking

at the levels of Hsp70 expression in the presenilin mutated cells, the levels are 24% higher compared to the control levels, however no statistically significant difference (Figure 3.59) (paired T test, p=0.17). When comparing Hsp70 expression in the sporadic AD cases and the genetically mutated AD cases, the mutated genes have by 36% more cellular Hsp70 (paired T test, p=0.16).
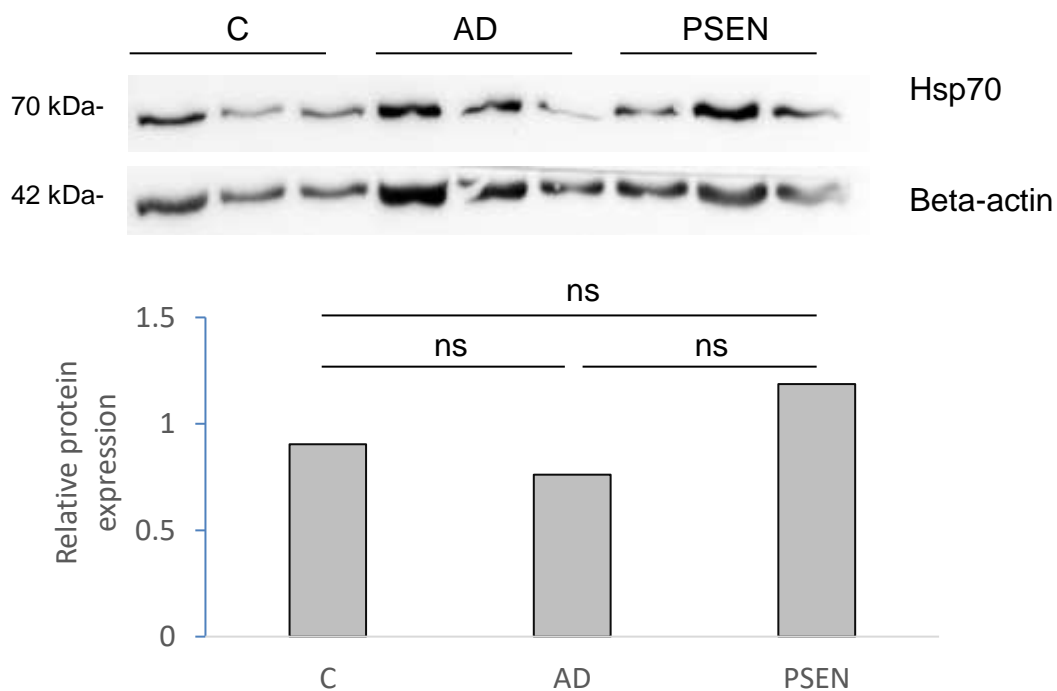
Figure 3.55 Hsp70 relative expression in the fibroblasts. Hsp70 expression observed in the sporadic AD group (AD) and in the presenilin mutated group (PSEN) compared to Hsp70 expression levels in the control group (C). ns=not significant

LC3-I/LC3-II ratio was the highest in the sporadic AD group when compared to both the control group and the PSEN group, with no statistically significant difference found (p=0.23, p=0.16, paired T test) (Figure 3.60). Also, LC3-I/LC3-II ratio found in the control group was slightly higher than in

the mutated PSEN cells with no significant difference (p=0.27, paired T test) (Figure 3.60).
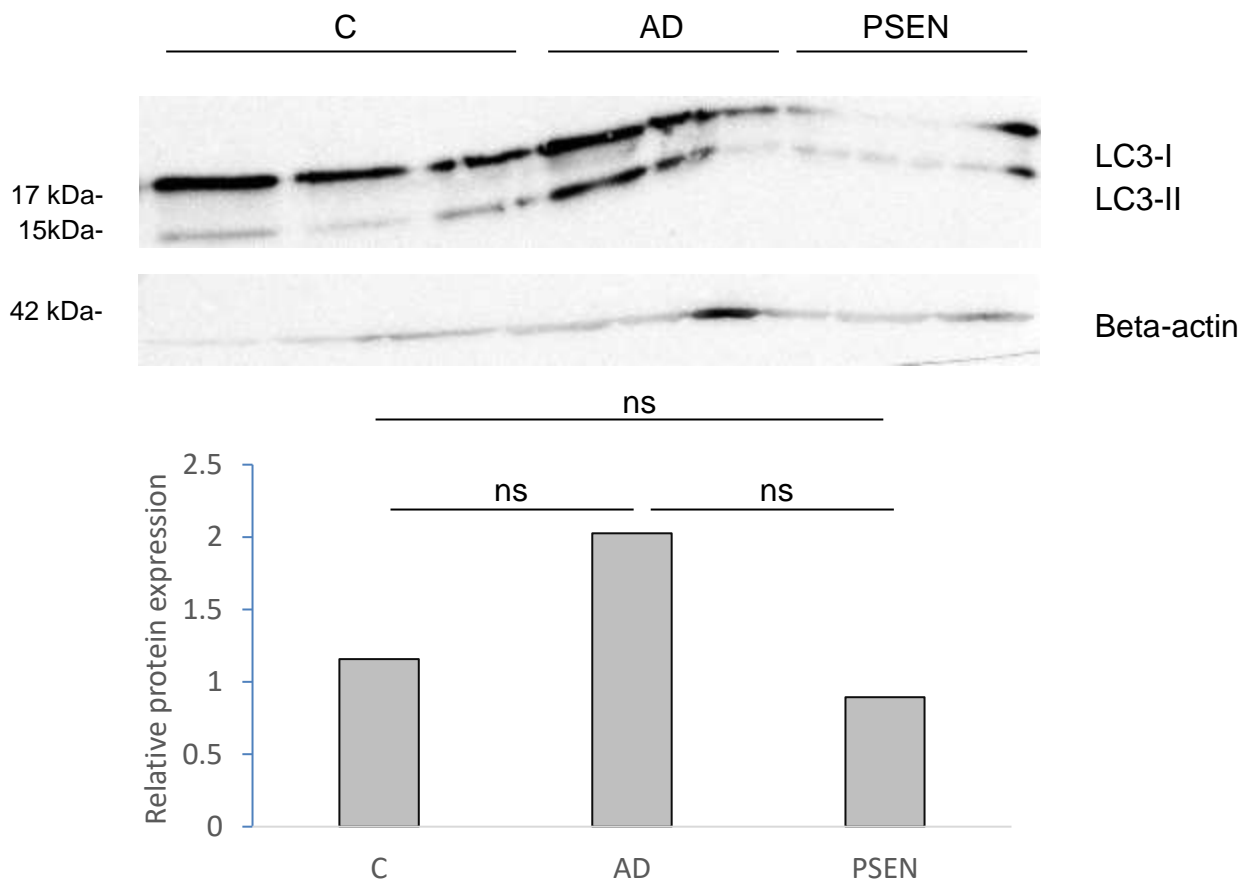
Figure 3.56 LC3 relative expression in the fibroblasts. LC3 expression observed in the sporadic AD group (AD) and in the presenilin mutated group (PSEN) compared to LC3 expression levels in the control group (C). The LC3 ratio represents the autophagic flux rate of MA; ns=not significant

Beclin-1 overall expression was found the highest in the mutated group when compared to the control group, demonstrating a statistically significant difference (p=0.04, paired T test) (Figure 3.61)

Also, the MA marker was found to be more expressed in the sporadic AD group when compared to the control group (p=0.1, paired T test) (Figure 3.61).
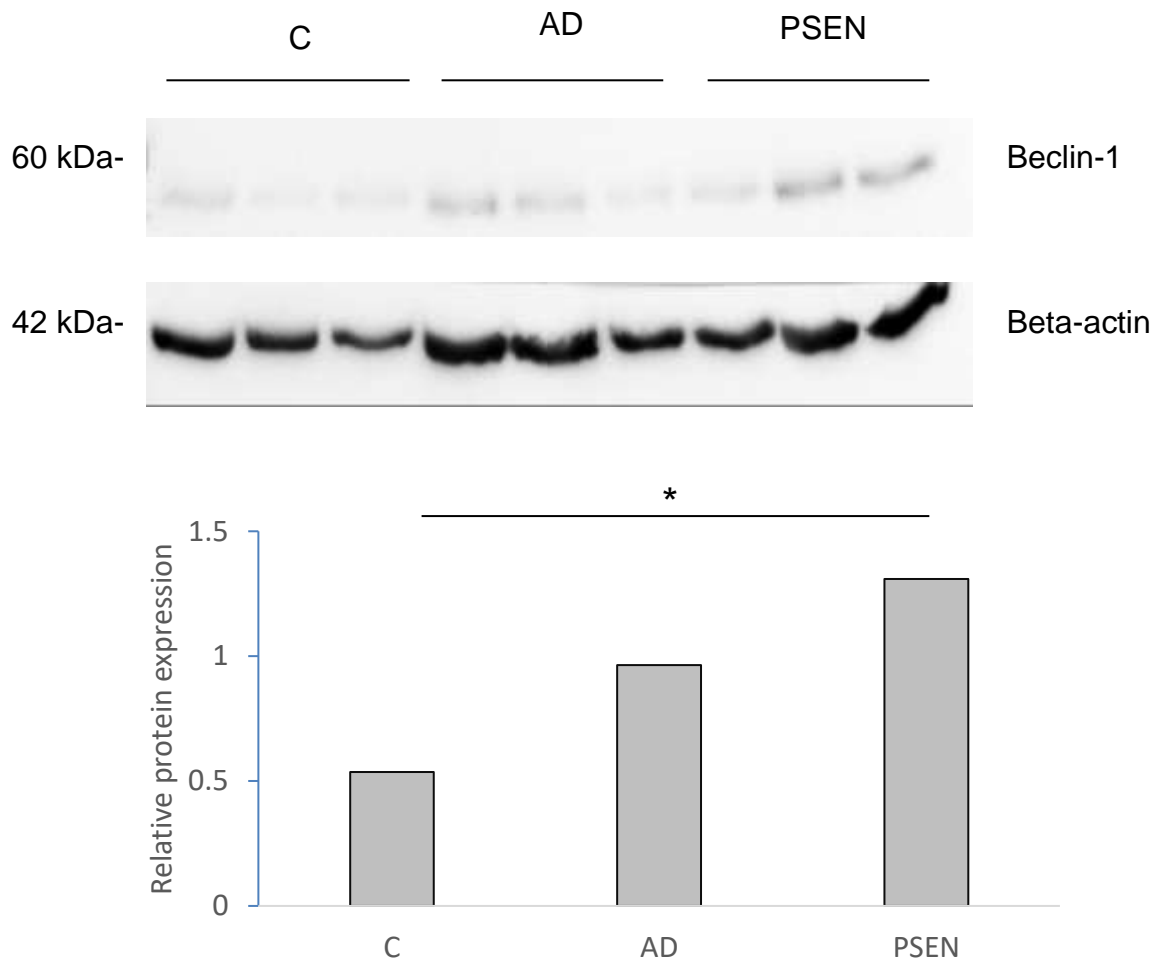
Figure 3.57 Beclin-1 relative expression in the fibroblasts. Beclin-1 expression observed in the sporadic AD group (AD) and in the presenilin mutated group (PSEN) compared to Beclin-1 expression levels in the control group (C) *p<0.05

Next, we explored the variability of all autophagy marker expression between the three cases of each group (C1-C3 control cases, sporadic AD1-AD3 cases and genetically mutated PSEN1-PSEN3 cases) to assess the potential use of fibroblasts as a diagnostic tool in the disease (Figure 3.62). The results demonstrate that the lowest variability of autophagy marker expression was seen between the control cases, whereas a higher degree of variability was seen between the AD cases and the PSEN cases (Figure 3.62).
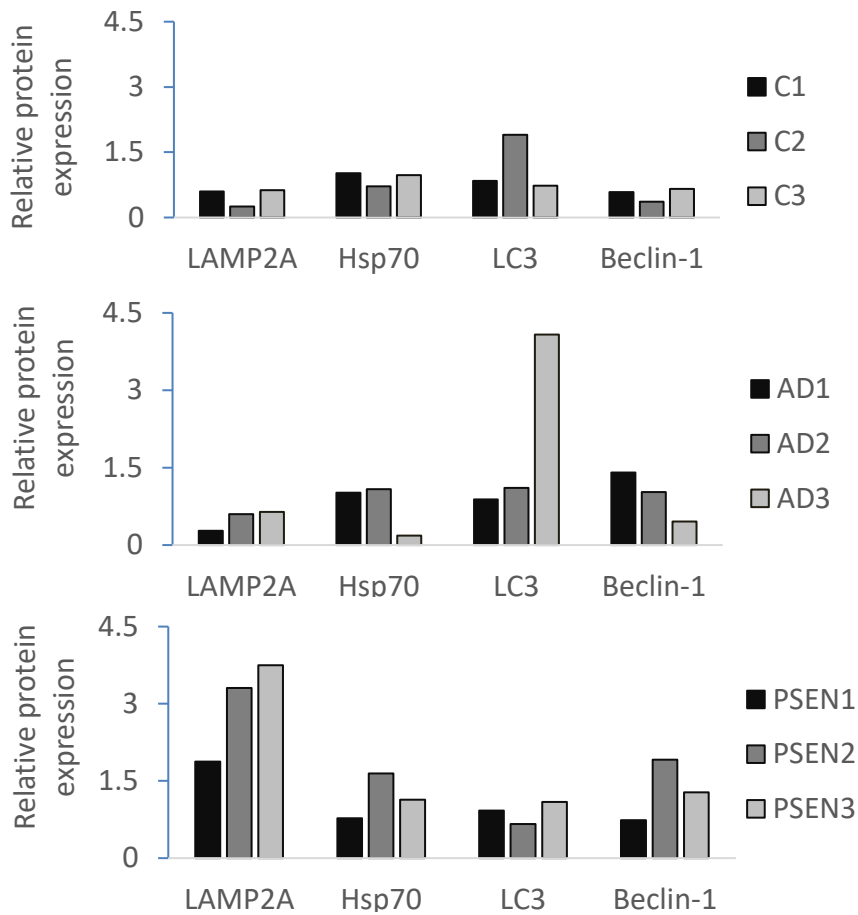
Figure 3.58 Autophagy markers expression in each case of the three groups. Different variabilities of autophagy marker expression between cases of control group (C1-C3), sporadic AD group (AD1-AD3) and genetically mutated group (PSEN1-PSEN3)

These results demonstrate that LAMP2A, Hsp70 and Beclin-1 were the highest expressed in the genetically mutated fibroblasts however, there is a high variation of the autophagy markers expression between these cases. On the other hand, LC3 was the highest expressed in the sporadic AD fibroblasts, however there was also an evident variation of LC3 expression between the three sporadic cases. The control groups showed the least varied expression of the autophagy markers between the control cases, with low levels of Hsp70 and LC3 and very low levels of LAMP2A and Beclin-1 in the control cells.

Chapter 4   Discussion

4.1   General discussion

Regional variation

The aim of this project was to explore variations in autophagy-related proteins in AD, with consideration of regional changes, variation with respect to different stages of disease and relationship to AD associated abnormal proteins such as tau protein. The following section will consider and explore the implications of this study results and how this relates to the current field of AD research.

LC3 and Hsp70 markers decreased with increasing Braak, in all brain regions, suggesting that there might be evidence of autophagy activity declining in the presence of more AD pathology. It is interesting to explore if this is potentially a cause or a consequence of build-up of abnormal proteins in AD. There is a lot of evidence based on research studies that links impairments of autophagy to neurodegenerative disorders such as AD, PD or ALS resulting in failure of abnormal proteins clearance and this has been previously described in detail in section 1.4 (Nixon, 2005; Nikon, 2007; Pickford, 2008; Son, 2012).

We understand that there might be an impairment in the autophagy pathways, due to decreased levels of autophagic proteins with increasing Braak staging. However, there is minimal evidence in the existing research on autophagy variation across different brain regions and subregions. In

AD, tau and beta-amyloid pathology is known to have a specific deposition pattern according to the region (Braak *et al*, 1997; Lace *et al*, 2009; Liu, 2012; Calignon, 2012, Whittington, 2017).

The results described in section 3.1 support a regional variation in the expression and intensity of staining in the three brain regions. The research initially focused on subdivisions of the hippocampus, a brain region involved in memory formation and an early site of neurodegeneration (Braak *et al*, 1997).

A high prevalence of all autophagy markers, in particular LAMP2A and Beclin-1, was observed in the hippocampus across most subregions. However, a regional variation was noticeable, with respect to both the number of cells and the intensity of the staining, but no association with Braak stage. The hippocampus demonstrated the most abundant levels of staining for all autophagy markers, in comparison to the frontal and occipital cortices, showing a decrease in Hsp70 and LC3 markers with increasing Braak, except LAMP2A and Beclin-1, which were found similar throughout the Braak stages. This is interesting because this region is impacted earliest in AD with respect to abnormal protein accumulation and cell loss (Dhikav, 2011; Serrano-Pozo, 2011). A recent study used natural ageing rat models to investigate autophagy changes in the hippocampus in order to determine the ideal age for treating neurodegeneration (Yu *et al*, 2017). They looked at levels of autophagy-related proteins such as LC3II, Beclin-1 and ULK via Western blotting and results showed that hippocampal autophagy marker levels were found very high in adult rats (5 months age) and even higher in old rats (18 months), however, the levels

declined considerably in the oldest group of rats (24 months) (Yu *et al*, 2017). Other studies on post-mortem human brain tissue, which examined autophagy levels in hippocampal CA1 pyramidal cells, suggested that autophagy induction and autophagosome formation were upregulated in early staged AD subjects (Bordi, 2016), which could explain the hippocampal abundant autophagy markers in our findings. They also found that the elevated levels of autophagy were maintained with disease progression, despite progressive impairment of substrate clearance via lysosomes (Bordi, 2016), which might explain our results as LAMP2A and Beclin-1 distribution had no variation across the Braak groups and remained high.

Through immunohistochemistry, we showed that in the hippocampus, Beclin-1 marker was found abundant in all Braak groups, with a minimal decrease in CA1 in Braak V-VI, when compared with CA4, which has been previously demonstrated in knockout Beclin-1 mice, leading to apoptotic CA1 neuronal death (McKnight, 2014).

As previously described in section 1.3.1, Beclin-1 is involved in the initiation of MA, being of the most important activator marker. As literature suggests, increased induction of MA may lead to failure of lysosomal substrate clearance in neurodegeneration and increased neuritic dystrophy, causing impaired MA that could result in pathogenesis (Liu, 2014; Bordi, 2016; Guo, 2016). This is supported by studies on impaired autophagy which suggested that abundant dystrophic neurites, which are a specific AD neuropathological feature, were found to be filled with autophagy-related vacuoles containing incomplete digested cellular

components, as well as β-amyloid and neurofibrillary tangles (Nixon *et al*, 2005).

~~We found that a~~Although Beclin-1 was high in all Braak groups, LC3 was significantly decreased with AD progression. These results could suggest that there is an excessive rate of MA initiation in early stages of disease, however in later stages, LC3 decreased, therefore the autophagic flux decreases causing failure of the MA system. Therefore, we believe that these results suggest an impairment in MA pathway. Lower levels of LC3 in late stages could indicate that after initiation of the pathway through Beclin-1, the MA deficit could be associated with LC3 causing incomplete formation of autophagosomes, hence accumulation of abnormal clearance of AD deposits.

Based on the number of the cells stained in the hippocampus, Beclin-1 staining demonstrated minimal variation, which was only seen in DG and CA1 subregions, with increasing Braak. LAMP2A marker was also highly prevalent with similar levels across all subregions; minimal variation was seen in CA2 and CA3 across the Braak groups. The variation of MA markers across Braak groups identified a decrease in subregions such as DG, CA1, the entorhinal cortex and the subiculum, whereas CMA markers across Braak groups described a decrease mainly in CA1, as well as in CA2 and CA3. Considering the existing literature, previously described in section 1.2, on differential involvement of the hippocampal subregions in the disease, we assume that both autophagy pathways might become impaired at early stages of tau deposition.

Overall, CA1 and DG regions had the lowest level of autophagy markers, while EC, CA4 and the subiculum regions had the highest amount of MA and CMA markers. This could explain the relationship between autophagy impairment and AD progression as tau pathology is deposited differently across the hippocampal subregions (Lace et al, 2009; Serrano-Pozo, 2011). CA1 is known to demonstrate abnormal tau accumulation early in AD, therefore LC3 and Hsp70 decreased levels might suggest autophagy deficits in this region. CA4 is known to have minimal tau pathology at early stages and here, we found that this region was rich in autophagy markers staining. On the other hand, other brain subregions known to demonstrate tau pathology such as the EC and subiculum (Lace et al, 2009) showed a high presence of autophagy proteins. This may suggest that some cell populations trigger autophagy marker recruitment in the attempt to clear pathological tau.

Strong regional variation in Hsp70 staining was shown as a result of CA1 low levels of staining and CA4 high levels of staining Therefore, to further investigate if autophagy markers were found in individual cells harbouring abnormal tau deposits, double labelling immunofluorescence was performed. Our findings, suggest that in Braak 0-II and Braak III-IV groups, LAMP2A positive cells within CA1 were also AT8 positive, suggesting their co-localization. However, in Braak V-VI, many AT8 positive cells within CA1 were LAMP2A negative, suggesting that the rate of co-localization declines in late stages of disease. This could indicate an impairment of CMA pathway, therefore abnormal intracellular proteins such as tau fail to be degraded. Moreover, our results suggest that LC3 and AT8 co-

localization rate was very high in the Braak 0-II group; In CA4, all AT8 positive cells were found to be LC3 positive. This suggests the importance of MA pathway to stay upregulated in the normal ageing brains to clear abnormal protein accumulations. Although LC3 and AT8 were both found positive in the same individual cells within both CA4 and CA1, in Braak III-IV, the co-localization rate dropped when compared withto Braak 0-II, which could suggest that MA becomes impaired in moderate stages of AD when tau burden increases. Moreover, in Braak V-VI, many AT8 positive cells were found LC3 negative with rates of co-localization declining significantly by half when compared with Braak 0-II suggesting that in late stages of AD, there might be a failure of MA to clear abnormal tau.

The dual staining results of LC3/LAMP2A vs AT8 confirmed the immunohistochemical findings that AT8 increased with increasing Braak staging and that LAMP2A, but especially LC3 decreased with increasing Braak suggesting an impairment in both MA and CMA. Therefore, although there is a degree of co-existence of LAMP2A/LC3 with AT8, it varies with Braak staging and this could be due to failure of LAMP2A/LC3 targeting and degrading tau protein. There was also a variation between CA4 and CA1 region, mostly seen in the LC3/AT8 staining suggesting that MA is more likely to get impaired due to defective autophagosome formation.

As previously discussed in section 1.4, numerous studies suggest that lysosomal-based autophagy pathways including MA and CMA are involved in the clearance of AD deposits such as tau and Aβ, suggesting that both protein degradation pathways could be important in

neurodegeneration (Wang, 2009; Wang, 2012; Lee, 2013). Researchers have used various mechanisms to either promote or inhibit autophagy in order to assess tau production and relate it to the protein clearance pathways. It was shown that using 3-methyladenine, an inhibitor of autophagy, supressing autophagosome formation, results in excessive tau aggregates (Wang, 2009). *In vivo* and *in vitro* studies showed that using methylene blue to induce autophagy, promoted tau clearance and reduced toxic forms such as insoluble and hyperphosphorylated tau (Congdon, 2012). Other studies describe that cells expressing the repeat domain of tau FTDP-17 mutant ΔK280 or P301S, which were treated with disaccharide trehalose, an autophagy enhancer, demonstrated a reduction of tau aggregates via immunohistochemistry and western blotting (Kruger, 2012; Schaeffer, 2012). There are also genetic studies on transgenic mice expressing mutant tau which have demonstrated that manipulating mTor pathway related genes can reduce the pathological tau (Caccamo, 2013). All these studies contribute as evidence of tau being degraded by autophagy systems, therefore understanding the relationship of autophagy proteins in the process of tau degradation in disease is crucial. Also, this could be linked to our findings as in Braak 0-II group, the co-localization of LC3 and AT8 markers was seen in almost all cases.

In section 1.4, we extensively described the link between impaired autophagy and neurodegeneration which is believed to result in the build-up of abnormal tau aggregates. Nixon and collegues, was one of the first to observe a significant high number of autophagic vacuoles within the lysosome of AD neurons, which were suggested to be an accumulation of

immature vacuoles due to incomplete macroautophagy in AD (Nixon *et al.*, 2005). In another key study, researchers found that the AD-damaged neurons, containing neurofibrillary tangles, showed high autophagic levels in the cell bodies, measured by immunoblotting and immunofluorescent labelling (Yu *et al*, 2005). Therefore impaired macroautophagy was suggested due to incomplete development of macroautophagic vacuoles, which affected their transport to the lysosomes, resulting in faulty tau degradation. This links with our findings showing that although in Braak 0-II and Braak III-IV groups, all AT8 positive cells were also LC3 positive, in Braak V-VI (late stages of AD), most of the AT8 positive cells were found LC3 negative, suggesting a possible impairment in MA and a defective clearance of tau in late stages of the disease. This could also indicate that impairment of autophagy is a late change that occurs due to the system becoming overly stressed, rather than an early disease change which is crucial in understanding which stage is the most suitable for therapeutic intervention to rescue autophagy.

When looking at the regional variation of the autophagy markers in CA4 and CA1 subregions, their distribution was higher in CA4 when compared with CA1, with a significant difference seen in Hsp70 marker. Existing studies describe the importance of Hsp70, a major component of the Hsp70 family, in stabilizing lysosomal function and ensuring cytoprotection by inhibiting protein aggregation (Ge, 2008; Zhu, 2012). Cleavage of carbonylated Hsp70 by calpain enzyme in CA1 neurons has been shown to lead to ischemia and neuronal death through lysosomal rupture in the hippocampal CA1, whereas in the motor cortex, Hsp70 expression in the

absence of active calpain has neuroprotective properties (Yamashima, 2012; Zhu, 2012). Calpains are calcium-activated proteases, found in high levels in the brain (Liu, 2008) and have been described to play a role in neurodegeneration (Vosler, 2008). Studies have shown that once activated, calpain levels increase significantly when compared with healthy ageing brains and are found in the neurofibrillary tangles of AD and tauophathies related brains (Taniguchi *et al,* 2001; Adamec, 2002; Yamashima, 2004).

Chaperone proteins such as heat-shock proteins are specialized in cellular protection from oxidative stress, maintaining homeostasis (Mayer, 2005; Hall, 2013). One of the most important of the chaperone protein family and is Hsp70 and along with other chaperones (Hsp60, Hsp27, etc) play a crucial role in protein misfolding by stopping the abnormal protein aggregation seen in AD (Lu, 2014). Research has shown that Hsp70 acts as a regulator in neurodegeneration, assisting protein folding and being involved in repair mechanisms of faulty proteins therefore Hsp70 has been investigated as a potential therapeutic agent in AD (Franklin, 2005; Meriin, 2005; Hoshino, 2011; Doyle, 2013). Studies in transgenic AD mouse model have showed that overexpression of Hsp70, after intranasal administration of exogenous Hsp70, demonstrated neuroprotection properties by reducing Aβ formation and accumulation in these murine species (Bobkova, 2014). Exogenous Hsp70 was also shown to have similar effects in cell models such as SK-N-SH neuroblastoma cells, reducing Aβ42 cytotoxicity (Yurinskaya, 2015). There is also evidence in transgenic mice and AD human brains, which demonstrates that Hsp70

enhances tau binding to microtubule and promotes tau solubility, therefore reducing insoluble and hyperphosphorylated tau which can suppress neurofibrillary tangles formation (Dou, 2003).

Considering all the existing evidence that Hsp70 is neuroprotective in AD and that Hsp70 was found to decrease in CA1 with AD progression, we could suggest that in this hippocampal subregion, there is compromised neuroprotection at late stages of the disease, which could indicate animpairment of CMA and tau excessive build-up in CA1 neurons.

Studies on Hsp70 cleavage by calpain could support our findings demonstrating a significant reduction in CA1 Hsp70 levels across all Braak groups, when compared with CA4, Hsp70 reduction may lead to lysosomal dysfunction, causing a possible CMA impairment and abnormal accumulation of phosphorylated tau. Studies could further explore these findings by assessing the levels of calpain in the brain sections.

As previously described, CA4 and CA1 hippocampal regions were chosen to explore regional variation in the expression of autophagy markers in relation to tau deposition Only LC3 marker decreased with increasing Braak in both CA4 and CA1 suggesting a possible impairment of MA .

Lack of significant Beclin-1 staining variation in Braak III-IV suggests that autophagy initiation may not be impacted at moderate stages of AD, considering that other proteins (PI3K-III, Atg14, Vps34; see section 1.3.1) are also involved in autophagy initiation. Previous studies on rat models, showed that induction of AD-related cerebral hypoperfusion in the animals, increased Beclin-1 significantly in hippocampal CA1 neurons (Liu, 2015). Similarly, another study on vascular dementia rat models, suggests that

Beclin-1 was elevated in hippocampal CA1 cells due to neuronal injury (Liu, 2014). This evidence suggests that Beclin-1 might not be related to impaired MA and abnormal accumulation of tau in CA1, when compared to the other autophagy proteins.

Hsp70 and LC3 markers were found higher in CA4, whereas in CA1, their levels were very low across all Braak groups, in particular in Braak III-IV and Braak V-VI. This suggests their poor involvement in the autophagic process for the clearance of tau deposits, found in a high numberin CA1. These findings offer an insight to understand the regional variation of autophagy impairment in specific subregions of the hippocampus, which is crucial for developing a highly selective and effective treatment to restore autophagy functions.Our results prove a regional variation of LC3 in relationship with Braak stages and further studies could explore LC3 related to tau pathology in the hippocampal CA4 and CA1.

Our study then focused on investigating variations in autophagy-related proteins in the frontal cortex. It is already known that each subcortical layer has specific functions within the central nervous system, mediating nerve impulses from the cerebral cortex to other regions, having distinct connections within the cortex and with other structures (Rubenstein, 2011). The six layers stratification has been described since over a century ago by pioneers Brodmann and Meynert, featuring morphological and anatomical distribution in size and shape of pyramidal and granular cell bodies within each layer (Brodmann, 1909). Only in the recent years, it has become evident that the layer stratification plays a crucial role, not just anatomically speaking, but also because functional differences depend on

specific subcortical layers that have particular cell types, based on animal model research (Morishima *et al*, 2011; Oberlaender *et al*, 2012; Narayanan *et al*, 2015). The most recent review on subcortical stratification describes these changes important in synapse activity and neuronal excitability via neurotransmitters such as adenosine, dopamine and acetylcholine (Radnikow, 2018). These neuromodulation chemicals can be released from axons of afferent neurons that come from other cortex regions (neurons in cortical layers II and III), from the thalamus (neurons in cortical layer IV) or from the brain stem (neurons in cortical layer V). They can also be released from axons of efferent neurons which leave to the thalamus (layer VI), to the brain stem and spinal cord (layer V) or other cortical regions (layers II and III) (Thomson, 2010; Mitchell, 2015; Miller, 2017).

A regional variation in the autophagy markers staining was observed across the subcortical cellular layers of the frontal cortex. A noticeable variation was seen across layer II-VI associated with LAMP2A, LC3 and Beclin-1 staining. Layer I or the molecular layer was excluded when assessing the regional variation in neurons as it has few cell bodies and mainly axons and dendrites of neurons from the deeper layers (Krause 2005) and the main interest was in the layers rich in pyramidal, granular and polymorphic neurons.

The regional variation seen across the frontal cortex layers was due to higher distribution of autophagy markers in layer III and V and lower distribution in layers II and IV.

Interestingly, these findings could be linked to abnormal tau protein based on its preferential deposition in the deeper subcortical layers III-V. There are numerous studies demonstrating how tau preferentially deposits within the cortical layers and how various layers get more affected in neurodegeneration. One recent immunohistochemical study revealed reduced cell volume by nearly 40% of large pyramidal cells in layers III and V in the frontal cortex in patients with vascular dementia, mixed AD and post-stroke patients when compared with non-dementia control subjects, suggesting the susceptibility of these two layers in neurodegeneration (Foster, 2014). Other studies suggest that, in contrast with pThr tau pathology (tau neuronal inclusions) involvement in the superficial layers of the hippocampus, the frontal cortex has the most prominent pathology including dystrophic neurites in the deeper layers as shown in ALS cases (Moszczynski, 2017). Although, tau pathology is mainly associated with the limbic regions such as the hippocampus, hence higher levels of AT8, pathological tau is seen in the deeper layers of the frontal cortex in cases of AD, vascular dementia, ALS, MSA, DLBD, FTLD (Moszczynski, 2017). This could explain tau propagation starting from the hippocampus and arriving to the layers III, IV and V of anterior cingulate cortex through thalamic projections and ultimately propagating to the frontal cortex (Moszczynski, 2017). These studies could relate neuritic dystrophy and high tau pathology found in deeper layers to our findings which suggest that distribution of autophagy markers was the highest in layers III, V whereas the lowest was in layer II. This suggest that tau might

co-localize with autophagy markers in individual neurons within the cellular layers, as a result of autophagy markers tagging tau for degradation.

Interestingly, the only marker found to vary significantly with increasing Braak was Beclin-1. The MA marker distrubtion increased in advanced stages of AD. In the frontal cortex, excessive induction has been demonstrated to have neurotoxic effects and leads to AD pathology and neurodegeneration. Layer IV demonstrated lower levels of staining, in particular in the MA markers staining, but studies suggest that deep layer IV, along with layers V and VI present tau burden (Calignon, 2012).

Human studies that used late staged AD brains, in which LC3-II expression (isoform actively involved in MA) was significantly decreased in the frontal cortex of AD patients, compared to age-matched controls suggesting an impairment in MA (Qiu, 2016), however most studies fail to demonstrate how these impairment varies according to the cell layer stratification.

There are also studies exploring the beta-amyloid plaque burden and the neuronal loss according to the cortical stratification in the frontal cortex and one study on AD mice suggests a neuronal loss in deep layers V-VI of 10 months old APP/PS1K1 mice compare to two month old APP/PS1K1 mice, while the amyloid-plaque load in old mice was found low in layers V and VI (Lemmens, 2011). This could suggest two important things: that the deep layers are mainly affected by tau pathology rather than beta-amyloid plaques and that the regional variation found in our results could associate tau pathology to be more relevant to the autophagy impairment, hence choosing tau protein for the double-labelling studies. In addition,

autophagy marker distribution, assessed based on cellular staining, and tau protein distribution were are found intracellularly rather than extracellularly like beta-amyloid

These findings suggest that despite some degree of variation between the frontal cortex subcortical layers, no significant decreases in the autophagy markers distribution was asscociated with advancing disease. The only significant variation was the upregulated Beclin-1 marker in advanced stages of AD. Therefore, the frontal cortex is not thought to be linked to impairments in CMA and MA. High distribution of Beclin-1 remains a question to whether the MA marker, involved in initiation of the pathway, contributes to increasing AD pathology or whether it is highly recruited to initiate MA in the attempt to rescue the protein clearance mechanisms.

As previously described, tau pathology originates in the limbic structures, starting with EC, spreading to the entire hippocampal regions, then to the temporal cortex and the frontal cortex and lastly, it spreads to the other cortices (Braak, 1997; Hu, 2017).

The research investigating AD pathology deposition across the occipital cortical layers is scarce, however a study from 2015 suggests an increased number in neuropil thread, neurofibrillary tangle, amyloid plaques and dystrophic neurites in layer VI of the primary visual cortex, in cases of Braak VI when compared with fewer AD pathology lesions in cases of Braak IV or lower (Rahimi, 2015).

Another paper describes how the occipital cortex has no AD pathology until Braak IV stage with evident tau pathology like neurofibrillary tangles

and neurophil threads, in Braak V and VI and this could be supported by our findings in the AT8 staining in the occipital cortex (Pikkarainen, 2009).

In our study, only Hsp70 and LC3 markers were found to significantly decrease with increasing Braak. These findings suggest a possible impairment of the autophagy pathways in the occipital cortex as levels of LC3 and Hsp70 decrease with increasing Braak staging.

The already existing studies on human brain tissue and transgenic mice support some of our results in which MA marker LC3 and CMA marker Hsp70 decrease with increasing Braak stages The most significant declines were seen in LC3 and Hsp70, in the hippocampus and the occipital cortex We know that LC3 and Hsp70 are involved at different steps in MA and CMA as described in section 1.3.1 and 1.3.2, which could suggest a possible location of the deficits within the two pathways. In other words, if LC3 decreases with AD progression, but Beclin-1 maintains constant levels in the brain, it might suggest that MA deficiency is located at the autophagosome formation step, hence lower LC3, which leads to incomplete formation of the vesicles responsible for degradation. Although the first steps of MA are functional, hence constant Beclin-1 levels, the incomplete formation of the autophagosomes, due to insufficient levels of LC3, could lead to faulty degradation that results in abnormal tau accumulation. Incomplete autophagosome formation could be supported by Yu *et al*, study in which they discovered numerous immature vacuoles to contain abundant APP molecules and presenilin-1, linking AD pathology to incomplete and dysfunctional MA (Yu *et al.*, 2005).

As previously mentioned, increased induction of MA could result in failure of lysosomal substrate clearance in neurodegeneration and increased neuritic dystrophy, causing impaired MA that could result in pathogenesis (Liu, 2014; Bordi, 2016; Guo, 2016). On the other hand, Beclin-1 upregulation, despite decreased levels of LC3, could indicate a compensatory mechanism as a response to the system becoming faulty. This could be supported by previous studies suggesting that upregulation of autophagy induction is believed to be a compensatory attempt to increase autophagic flux and cope with abnormal protein build-up since autophagosome maturation is defective in AD neurons (Orr, 2013).

This could explain our results seen in Braak V-VI group, where both Beclin-1 and tau were found very high, despite other autophagy proteins being decreased (Hsp70, LC3). On the other hand, high Beclin-1 in late stages could be explained by its involvement in tau protein clearance, however Beclin-1 is only involved in MA initiation, thus, without normal levels of LC3, MA would not successfully degrade the abnormal deposits. Considering that LC3 was found to decrease in the hippocampus and the occipital cortex, in Braak V-VI, we are inclined to believe that increased Beclin-1 contributes to pathology.

As described in detail in section 1.3.2, Hsp70 is responsible for recognition and binding of the substrate that requires degradation, before it reaches the lysosome therefore. A deficit of Hsp70, due to low levels seen in the occipital cortex, could lead to an accumulation of abnormal proteins in the cytosol, including pathological tau. This cytosolic accumulation of tau could precede the formation of neurofibrillary tangles (Brion, 1998). We

mentioned before that Hsp70 has been extensively described to have neuroprotection roles by inhibiting protein aggregations and help refolding misfolded proteins, by stabilizing the functioning of the lysosome and by reducing the oxidative stress (Ge, 2008; Zhu, 2012; Leak, 2015: Morozov, 2017). Considering these, we could link decreasing Hsp70 levels with disease progression, in the occipital cortex to be a factor in CMA impairment that leads to excessive accumulation of abnormal proteins.

We suggest that MA and CMA pathways become impaired as autophagy proteins, Hsp70 and LC3, decrease with increasing Braak and we found a regional variation of autophagy markers distribution within each brain region. We conclude that in the hippocampus, the autophagy markers were found the lowest in CA1, a region associated with early deposition of tau (Lace *et al*, 2009; Serrano-Pozo, 2011) and the level of these markers decreased in CA1 with advancing disease. On the other hand, the autophagy markers distribution was higher in CA4, a region associated with late tau deposition (Lace *et al*, 2009; Serrano-Pozo, 2011). In the frontal and the occipital cortices, layers II and IV were associated with the lowest rates of staining, whereas autophagy markers were more predominant in deeper layers III, V, VI, which have been previously associated with tau deposition (Moszczynski, 2017). These findings are crucial as they give an insight of the relationship between autophagy proteins and pathological tau which could be essential in developing in a highly specific therapeutic target.

Overall, we could speculate that both autophagy pathways are impaired as rates of LC3 and Hsp70, key markers in MA and CMA, were reduced with advancing AD.

Summary of MA and CMA impairment

In conclusion, we understand that both MA and CMA might get impaired. LC3 decreased levels were found in both the hippocampus and the occipital cortex, with increasing Braak staging, therefore we speculate that defective MA might be related to insufficient levels of LC3, while defective CMA might get impaired due to Hsp70 deficits in the occipital cortex. LC3 is responsible for autophagosome formation and maturation, therefore a deficit at this step might indicate that the impairment is related to immature autophagosome accumulation and incomplete degradation of abnormal proteins, resulting in abnormal deposits in the AD neurons. Hsp70 deficits could suggest that there is insufficient chaperone proteins in the cytosol that specifically recognize and bind the subtrates for degradation, hence accumulation of abnormal tau in the neurons (section 1.3.2)

Currently, there are potential AD therapeutic drugs that alter different stages of the autophagy mechanism (Zhang, 2011), but in order for them to work, it is essential to target the right pathways and deficits at the right stage of disease. Switching on macroautophagy has been shown to increase the neuropathology in transgenic mice brains in SOD1G93A mouse models, worsening symptoms and accelerating neurodegeneration (see section 1.1.7) (Zhang, 2011).

As mentioned before, AD pathology originates in the limbic structures, starting with EC, spreading to the entire hippocampal regions, then to the temporal cortex and the frontal cortex and lastly to all other cortices (Hu, 2017). When comparing the results of our autophagy protein levels across all three brain regions, the hippocampus, followed by the frontal cortex had the highest amounts of staining, which could suggest one important thing. This could be a result of these regions being largely associated with tau and beta-amyloid pathology when compared with the occipital cortex (Serrano-Pozo, 2011). Since these regions are known to be largely impacted in AD pathogenesis, cells in these regions have been shown to have oxidative stress, inflammation, disruption of Ca^{2+} channels, egeneration of xcess reactive oxygen speacies (Di, Bona, 2010; Tan, 2012; Manoharan, 2016), which is known to initiate autophagy (Essick, 2010). The generally higher levels of autophagy markers may reflect the need for a functioning waste disposal system.

The two pathways of autophagy were compared in each brain region showing that MA marker levels were higher than CMA in the hippocampus and in the occipital cortex, while the CMA marker levels were higher in the frontal cortex. Results have also revealed that when comparing the overall levels of MA with CMA across the Braak stages, CMA rates were lower in the hippocampus, compared with the frontal cortex, in all Braak groups, whereas in the frontal cortex, MA is much lower than CMA, in both Braak 0-II and Braak III-IV groups. However, a change was seen in Braak V-VI, where MA and CMA levels become similar in the frontal cortex. These patterns suggest that in this brain region, the two pathways might work

together via compensatory mechanisms in late stages of disease in the attempt to rescue the imbalances.

These findings are important for the future research in order to identify which autophagy pathway should be therapeutically targeted at different stages. Also, differences between the levels of MA and CMA activity in each brain region, could suggest that they exhibit compensatory mechanisms. In other words, if MA becomes defective, CMA compensatory mechanisms will try and rescue the protein degradation system in order to antagonize the adverse effects caused by the MA impairment the other way around. Studies have shown that both lysosomal pathways compensate each other to promote cell survival in hepatocytes after cell injury (Wang, 2010; Chava, 2017). It was shown that CMA is upregulated in rat cell line RALA255-10G in order to compensate impaired MA after hepatocyte injury and cirrhotic liver (Wang, 2010; Chava, 2017). Moreover, studies in cancer have showed that genetically suppression of MA upregulates CMA levels in order to degrade aberrant p53 tumour suppressor (Vakifahmetoglu-Norberg, 2013).

Studies in neurodegeneration have also shown that there is a functional relationship between the two pathways and disruption of one of them leads to upregulation of the other one (Massey, 2006; Cuervo, 2014). More specifically, cell model studies, including mouse fibroblasts, have showed that CMA can compensate for MA, but not the opposite, suggesting that highly selective mechanisms of CMA are essential in stress responses (Massey, 2006). There is also a review paper which describes how the two machineries interact with each other in the

202

mammalians systems and how they counteract at a molecular level (Wu, 2015). These could relate to our findings as we observed that in the frontal cortex, in the Braak V-VI group, overall MA levels increased and became similar to the CMA levels, suggesting that CMA might have compensated to rescue impaired MA in this brain region, at late stages of disease.

These findings suggest that according to the brain regions affected in the disease, therapeutic targets should focus on specific pathways. In other words, therapeutics for rescuing autophagy, should target CMA impairment in the hippocampus across all stages of disease as our findings suggest that CMA levels were decreased in this brain region when compared with the MA levels. Regarding the frontal cortex, therapeutics should aim to target MA impairment in early and moderate stages (Braak 0-II and Braak III-IV) as our results indicated lower MA levels in these stages. Considering the existing literature which describes that it is easier for MA to compensate CMA activity, rather than the opposite, we tend to believe that targeting the hippocampus would be ideal for therapeutics. This means drugs could aim to enhance CMA activity in this brain region at any stage of disease. However, it would be ideal to target CMA impairments at the earliest stages, considering that our findings indicated lower levels of CMA compared to MA in Braak 0-II.

Studies on neurodegenerative mouse models have already tested MA activator drugs such as rapamycin, spermidine, carbamazepine and tamoxifen which have showed therapeutic potential, improving behaviour, enhancing learning and memory and slowing down the loss of motor

203

function (Wang, 2012). Other studies have showed that rapamycin had neuroprotective properties, facilitating the clearance of aberrant proteins and reducing tau and beta-amyloid in the AD brains (Cai, 2013). There are also studies which contradict these findings, suggesting that treatment with rapamycin on ALS mouse models, can increase neuropathology in the brain and worsen the symptoms (Zhang, 2011). More recent studies on neuronal cell lines suggest the therapeutic potential of spermidine which is shown to be neuroprotective by suppressing caspase 3 protease to cleave Beclin-1, essential in the well-functioning of MA (Yang, 2017). Moreover, Choi *et al*, showed that spermidine had anti-inflammatory effects on lipopolysaccharide treated murine microglia, therefore inhibiting inflammation (Choi *et al*, 2012). Despite these studies, there are also controversial researchers which contradicts the potential therapeutic of this drug in preventing or delaying the progression of AD as Lewandowski *et al*, showed a link between spermidine pathway and α-synuclein toxicity in the pathogenesis of PD by using a yeast model expressing α-synuclein (Lewandowski, 2010). Trehalose, an mTOR activator of autophagy was also tested on human mutant P301S tau transgenic mouse models however, the treatment failed to activate autophagy in the mice spinal cord and had no improvement effects on these mice motor impairments (Schaeffer, 2012). A more recent study on Tg2576 transgenic AD mouse model showed that oral administration of trehalose had no effect on MA, due to no variation of LC3I/II ratio western blotting results and had no cognitive improvement on the mice (Portbury, 2017). Considering all studies investigating the beneficial points of autophagy activation by using

enhancers, we tend to believe that these drugs offer therapeutic potential in rescuing autophagy in AD, however we also need to consider the amount of studies which fail to prove efficacy of these drugs in some of the AD modelsThus, this field requires a better understanding of how these drugs would successfully promote protein clearance in the AD brains. Moreover, most studies on therapeutic intervention to rescue autophagy focus on MA, and there is a gap in research, regarding the drugs that would successfully target impaired CMA.

Glial cells

The white matter, which largely consists of myelinated axons of the neurons and the glial cells, stained positively for all autophagy markers in the three brain regions, We considered the glial cells stained by the autophagy markers as the white matter is directly linked to cognition, distribution of action potentials, and information exchange between different brain regions, which are all affected in AD (Fields, 2008; Zhang, 2009). Immunohistochemistry and imaging studies suggest that white matter abnormalities seen in AD are due to impaired myelin and oligodendrocytes, which result in demyelination causing pathology and impaired cognition (Nasrabady, 2018).

Glial cells are very important components of the nervous system as they perform various functions from sustaining neurons by maintaining homeostasis, providing nutrients and oxygen to the cells and protecting against threats, pathogens and oxidative stress (Greener, 2015; Jäkel,

2017). Different types of astrocytes are known to exist (Sun, 2012), though short, thick protoplasmic star-shaped astrocytes were found to be very abundant in the subpial regions, in most of the cases.

Autophagy is described to be impaired not only in neurons but also in glial cells, however the role of autophagy in glial cells and the role of glia in defective MA in AD is not very well understood (Nikoletopoulou, 2015). There are studies that link glial cells and autophagy pathways and one example is a study on a parkinsonian mouse model that suggests that Gaucher disease (lysosomal storage disorder) specific mutation leads to impaired autophagy and activation of astrocytes in the AD brains (Osellame, 2013). Another *in vivo* study linking defective lysosomal function to glial cells explains that deletion of sulphatase modifying factor 1 (SUMF1) gene in both neurons and glial cells caused severe lysosomal dysfunction, impaired autophagy, neuronal loss and inflammation suggesting that astrocytes play a very important part in the disease progression (Di Malta, 2012).

Mutations of the lipid phosphatase FIG4 that regulates PI $(3,5)P_2$, a signalling lipid, have been associated with ALS, spongiform degeneration of the brain and Charcot-Marie-Tooth disease (Chow, 2009). Studies on transgenic mouse models reported that mutations in PI $(3,5)P_2$ cause accumulations of excessive LC3II, LAMP2 and p62 proteins in the murine neurons and astrocytes (Ferguson, 2009). Double-labelling studies identified astrocytes to be abundant in p62 protein, suggesting a link of glial cells and MA as p62 is involved in recognition and binding to substrate for degradation (Ferguson, 2009). Other studies, showed that

exposure to toxic compounds (trimethyltin) induces MA not just in neurons but also in glia cells, supressing the autophagic flux and overexpressing LC3 and p62 (Fabrizi, 2015).

 There is a study reviewing how microglia and astrocytes surface receptors mediate degradation of beta-amyloid through phagocytosis (Ries, 2016). The same review explains that although there are some studies in which glial cells activation may have damaging effects on the neurons in AD, there is plenty of evidence that supports their neuroprotective function and removal of beta-amyloid (Ries, 2016).

Therefore, there is a lot of evidence that links glial cells and autophagy which is why we considered the glial cells stained by autophagy markers.

Glial cells have been extensively linked to neurodegeneration and studies suggest that while neurons die in the presence of toxic protein accumulations in late stages, glial cells including astrocytes and microglia are resistant to toxicity and moreover, they become highly activated in the attempt to destroy neurons harbouring tau (Jana, 2010). There is a lot of research that describes glial cells contribution to neurodegeneration through neuroinflammatory mechanisms which are commonly seen in AD brains (Sofroniew, 2010; Kahlson, 2015; Leyns, 2017). Glial cells secretion of proinflammatory cytokines such as interleukins and tumour necrosis factor alpha exacerbate tau pathology facilitating neurodegeneration (Leyns, 2017). It has been suggested that suppressing excessive inflammation by inhibiting active glial cells in AD may reduce the production of proinflammatory factors which could reduce neurotoxicity, therefore, there are numerous clinical trials using glial cells as therapeutic

targets to develop drugs that could prevent or slow AD (Lopategui, 2014). On the other hand, there is a recent study which suggests that glial cells showed rescuing effects in a *Drosophila* model of AD expressing toxic beta-amyloid, which resulted in engulfment of Aβ peptides by the glial cells (Ray, 2017). Some researchers still debate whether glia are good, acting as immune cells of the nervous system and degrading abnormal proteins and pathogens, or whether glial cells contribute to neurotoxicity and pathogenesis in neurodegeneration (Mena, 2008; Jana, 2010; Tejera and Heneka, 2015). For example, a review paper describing the role of glial cells in PD, suggests that astrocytes have neuroprotective properties as they remove toxic deposits and free radicals in the brain, whereas microglia, release proinflammatory cytokines and protein complements, promoting inflammation in the brain (Mena, 2008). On the other hand, Verkhratsky et al, suggests that astrocytes are also a contributor to neuroinflammation, therefore promoting neurodegeneration, however, astrocytes become highly activated in late staged of AD (Verkhratsky, 2010). Early stages of AD changes are associated with deterioration of astroglia, which disrupts the connection between the synapses, thus the neurons, cause an imbalance in the neurotransmitter homeostasis and as a result it leads to neuronal death due to high toxicity. Later on, astrocyte in advanced stages, become highly activated and contribute to the neuroinflammatory part of neurodegeneration (Verkhratsky, 2010). The astrocytes can also cause damage inhibiting the axon regeneration with nitric oxide TNF-α leading to no recovery and exacerbation of the clinical pathology (Verkhratsky, 2010).

For a long time, astrocytes were primarily considered to protect the neurons, clearing beta-amyloid peptides, yet more and more research has shaped their role into inflammation and neurodegeneration in AD which is thought to be due to release of neurotoxins and inflammatory factors, as well their initial functional loss (Birch, 2014; Rodríguez-Arellano, 2016). Considering that studies suggest glial cells, specifically astrocytes, play a role in clearance and degradation of beta-amyloid, we could potentially link the role of glia in autophagy in the attempt to clear tau and beta-amyloid.

In our study, positively stained astrocytes and oligodendrocytes, located in the white matter and in the subpial region, were reported in a high number across the Braak groups, suggesting possible involvement of glia in MA and CMA

Our results suggest prevalent autophagy markers in glia cells, however, there was no difference in autophagy markers in astrocytes, with increasing Braak staging, in the hippocampus and the frontal cortex. The only difference observed was with astrocytes expression of LC3 decreasing in the occipital cortex as the disease advances. Moreover, there was no difference in expression associated with oligodendrocytes across Braak stages in the frontal cortex and the occipital cortex, but a difference was seen with LC3 and Beclin-1 positive oligodendrocytes, which decreased in Braak III-IV and then increased in the hippocampus at Braak V-VI.

There are studies that demonstrate a substantial damage to the white matter of the AD brains, causing a decrease of oligodendrocytes as the disease advances and leading to cognitive impairment (Braak et al.,

2000). According to Roth, cell culture experiments on neonatal rat oligodendrocytes show that malfunctioning of oligodendrocytes is due to the toxic effect of Aβ in advanced staged of AD (Roth, 2005). They tested fibrilogenic Aβ *in vitro* resulting in a substantial reduction of the oligodendrocytes. On the other hand, they have also tested pro-inflammatory molecules such as lipopolysaccharide and IFNγ cytokine, along with active astrocytes presence and noted that these reduced the damage caused by Aβ (Roth, 2005). This might support our findings suggesting that Aβ might have a direct negative effect on the presence of oligodendrocytes, as they decrease with increasing Braak stages in the in the frontal cortex (LC3 staining), while astrocytes could become activated to compensate the AD neurotoxicity and reduce the damage on the neurons. There is also evidence demonstrating a link of autophagy and oligodendrocytes suggesting that oligodendroglial precursor cells, NG2 can degrade beta-amyloid in transgenic AD mice model and in NG2 rat cell lines via double-labelling and western blotting studies (Li, 2013).

It is still not clear why glia recruit autophagic markers and it would be interesting to develop an *in vitro* cell model to see if glia can degrade tau and beta-amyloid in MA and CMA. Research on MA and CMA in glial cells and their role in AD is very scarce, however there is some research on ubiquitin proteasome system which describes the involvement of glia in neurodegeneration, suggesting that the ubiquitin proteasome system is more effective in removing abnormal proteins in glia (Jansen, 2014). If glia pathology will be demonstrated to relate to impaired autophagy, it could impact the novel therapeutic strategies and the approaches to a beneficial

treatment, directly targeting the glial cells.The benefits of glia inflammation are that astrocytes, in a high number, can release neuroprotective factors, preventing oxidative stress, apoptosis and excitotoxic damage (Choudhury and Ding, 2015). A high number of astrocytes can also contribute to the environment maintenance, restricting free radicals release and reducing excitotoxicity via glutamate intake (Zhang, 2010). MA and CMA activities have been shown to decline with age as the lysosome function is affected by the ageing process (Cuervo, 2008; Martinez-Lopez, 2015; Carmona-Gutierrez, 2016), resulting in accumulation of oxidised proteins and free radicals, normally seen in brain tissue of old organisms (Pajares, 2018), therefore these products could contribute to decreases of astrocytes in late stages of disease.

Oligodendrocytes are involved in axon sheath myelination and are extremely important as the myelin layer which covers the axons of the neurons allow quick and efficient transmission of signals through the nervous system which become defective in AD (Mitew, 2010; Carmeli, 2013). Compared with astroglia, oligodendrocytes have lower rates of reaction to stress however they can both be activated at the same time (Bradl, 2010). These two types of glia might be related as studies suggest that active astrocytes induce activation of oligodendrocytes, which are recruited in a high number in the attempt to produce new myelin for the damaged neurons in order to restore signal transmission (Bradl, 2010). As previously described, glial cells have been linked to autophagy and although this field of research is very novel, glia are believed to get activated in AD brains via compensatory mechanisms, as autophagy

pathways become defective and fail to clear abnormal proteins. Our findings suggest that Beclin-1 and LAMP2A positive glia were very abundant in the brain regions Beclin-1 positive glia significantly increase in Braak V-VI, suggesting the potential role of glia in autophagy. Therefore, in Braak V-VI, the glial cell numbers was increased in despite the neuronal autophagy markers decreasing in the presence of abundant tau/beta-amyloid. This might suggest that although MA and CMA in neuronal cells gets defective and fails to clear the abnormal proteins, glia, which are more resistant to stress conditions such as neurotoxicity and neurodegeneration, become activated to rescue autophagy and promote degradation via endocytosis.

Axons and neuronal inclusions distribution of autophagy markers

Axonal staining was found relatively high in all brain regions, however it was found to significantly decrease across the Braak stages for Beclin-1 only. Autophagy role in axonal related pathologies is still unclear. A study from 2006 used GFP–LC3 transgenic mice (C57BL/6J) to produce LC3 tagged with a protein that emitted green fluorescence (GFP) to show that autophagy is switched on in axonal dystrophies. Numerous autophagosomes of macroautophagy pathway tagged with LC3 bound GFP started accumulating in the axons (Wang, 2006), which might explain our findings of very high LC3 positive axonal staining seen in the hippocampus. Also, the same study investigated microtubule-associated protein 1B (MAP1B) which is known to interact with LC3, on a high scale,

within the central nervous system. It bounds to both forms of LC3, free cytosolic LCI and membrane-bound LC3II at a significant level in the axonal swelling that are specific to axonal dystrophy, resulting in high prevalence of LC3 related autophagosomes in the axon terminals (Wang, 2006).

There is an interesting paper describing how axonal transport is disrupted in degradative organelles such as lysosome which causes an Alzheimer's like-axonal dystrophy (Lee, 2012). Neuritic dystrophy, specific in AD, is characterized by accumulation of autophagic vacuoles that contain incomplete digested proteins and these accumulate in the swelled axons, explaining a possible link between defective protein degradation and disrupted axonal transport (Lee, 2012). We only found Beclin-1 axonal staining to significantly decrease, which could suggest a disruption of the axonal transportation in the lysosomes, which are crucial for the well-functioning of autophagy and this disruption is associated with late stages of AD which may lead to impaired autophagy and lysosomal dysfunction in AD. In other words, the misallocation of autophaghic components and vacuoles could be associated with disease change and that the cellular distribution of autophagy markers changes with disease progression which may suggest axonal transport deficits.

Surprisingly, the choroid plexus was positively stained by both LC3 and LAMP2A, mostly in Braak V-VI. The epithelium of the choroid plexus, found in the four brain ventricles has numerous functions, being at the interface of the brain blood and the cerebrospinal fluid, which is being produced by the epithelial cells (Strazielle, 2000). The choroid plexus is

known to be involved in inflammation responses when various proteins such as lipocalin 2 are produced by the choroid plexus epithelial cells (Marques et al., 2008). Released proteins might also interact to autophagy markers which might upregulate autophagy and explain the LAMP2A and LC3 levels of expression in the epithelial cells of the choroid plexus (Toyonaga, 2016).

The intracellular inclusions that were found within the neurons, mostly associated with hippocampal LC3 staining, are known to be abnormal ubiquitin related protein aggregates that require well-functioning autophagy clearance (Yue, 2009). Our results showed that intracellular inclusion stained by LAMP2A, decreased with Braak staging, in the frontal cortex. It has been previously described in a study that deletion of macroautophagy regulatory proteins Atg 5 and Atg7 in mice Purkinje cells block the neuronal autophagy resulting in cytoplasmic imbalance, abnormal protein accumulations and inclusion bodies formations (Yue, 2009). Moreover, transgenic mouse models express axonal dystrophies which could be directly related to the blocking of macroautophagy due to lack of Atg 5 or Atg7 (Nishiyama, 2007).

In the hippocampus, the presence of the granular staining was mostly found in the LC3 positive cells which was shown to be associated with the presence of the autophagy markers in the axon, however, no association was seen in regards to the LC3 positive intracellular inclusions. Our results could relate to studies suggesting that the granules and the cluster of grains might be stress granules derived from the endoplasmic reticulum, representing unfolded protein mechanisms due to their responsive state to

stress kinases (Thakur et al., 2007). Other studies suggest that these granules, which positively stain for ubiquitin and other autophagy markers (LC3, p62, LAMP1), indicate their involvement in MA and ubiquitin proteasome system and an increased granule accumulation can suggest incomplete formation of the autolysosome, hence failure of degradation systems (Funk et al., 2011).

One of the major limitations of human pathological studies is that data provides just a 'snapshot' of protein expression and pathogenesis. Therefore, it is difficult to establish the sequence of pathogenic events or changes in autophagy staining. However, a general overview of pathology in the sections was based on the different tau and beta-amyloid deposition in the Braak III-IV and Braak V-VI groups, which was mainly used to relate it to the changes seen in the autophagy markers across the groups. However, the staining may give an indication of the molecular events that may be going on inside the cell at the time of death.

The limitations of this study include the subjectivity of immunohistochemical scoring interpretation.This scoring approach is highly subjective and might mask potential differences in expression, therefore, a quantitative approace such as assessing the percentage area of staining with size exclusion to assess neuronal staining might be more useful for future studies.

Variable activity of antibodies staining is thought to be mainly influenced by environmental factors such as pH or laboratory temperatures. Antibody specificity is always an issue and the question is whether the antibodies are detecting the appropriate proteins of interest. The antibodies of these

study have been well described in the chapter 2 and have been previously used in other studies and were recommended by staff at the Manchester Brain Bank. We could have also used isotype and absorption controls, however the tissue available was limited and the antibodies which were used are all well-published (see section 2).Another limitation of this study could be that the autophagy markers chosen are not exclusively indicators of MA and CMA activity although they are gold standard markers in the staining of autophagy as described in numerous studies (Yu et al, 2005; Jaeger, 2010; Kaushik, 2012; Son, 2012 Cuervo, 2013). Moreover, immunohistochemistry, when compared with Western blotting, delivers an overall staining of both isoforms of LC3, limiting LC3 ratio findings which could be crucial in investigating macroautophagix flux. It would be useful to assess the human tissue via Western blotting to explore the LC3 ratio for a better overview of the autophagic flux and this is explained, later on, in the 'Future work' section.

Another limitation of the study was the small sample size of the brain sections (n=17 Braak 0-II; n=15 Braak III-IV; n=13 Braak V-VI. This could improve considerably if we could extend the sample size for a better understanding of autophagy impairment in AD.

Autophagy in skin-derived fibroblasts

For the past decade, alterations in autophagy pathways, in numerous animal models and human autopsy tissue havea been described extensively for (Nixon, 2005; Nikon, 2007; Pickford, 2008; Son, 2012).

Nevertheless, as described in section 1.5, there are still many disadvantages of using animal models. New accurate potent models for impaired autophagy in AD are required to overcome all challenges that the research is currently facing. Of particular interest is a cell-based model such as skin fibroblasts that would allow the rapid testing of new drug compounds on patients living with AD. This model would allow periodic sample collection through biopsy followed by investigation of how different drug-based therapies might interact with protein degradation systems. Extraction of AD fibroblasts might be crucial for early detection and diagnosis of the disease through assessing dysfunctional protein mechanisms (Mocali, 2014.)

It is still unclear whether pathogenic autophagy alterations extend to peripheral cells such as skin-derived fibroblasts but the idea of using fibroblasts as a potential resource came after many of the neuronal pathological modifications that are seen in AD brains, such as toxic protein accumulation, increased oxidative stress and mitochondrial abnormalities, have also been reported in fibroblasts derived from AD patients (Citron *et al.*, 1994, Magini *et al.*, 2010, Ramamoorthy *et al.*, 2012; Mocali, 2014). If autophagy deficits are seen in these cells, they could prove invaluable in identifying and assessing new therapeutic approaches, as well as for the identification of new diagnostic biomarkers, which are scarce at the moment.

In this pilot study, we found variability of MA markers, LC3 and Beclin-1, between the control group and the sporadic group suggesting a possible impairment of MA. We also identified a variation of LAMP2A, Hsp70 and

Beclin-1 autophagy markers in the control group when compared with the presenilin mutated group. Increased expression in the presenilin group might be due to the lower age of this group, however age-matched controls with very similar age was challenging to find in the Coriell Biorepository cell bank. Studies in mouse embryonic fibroblasts show that mutations of presenilin in familial AD worsen lysosomal pathology, supporting a peripheral demonstration of deficit. They demonstrated that presenilin gene mutation leads to abnormal build-up of dysfunctional autophagosomes, an indicator of autophagy failure and that knock down mice exhibit increased LC3-II and decreased mTOR and LAMP2A (Neely, 2011). Moreover, studies in blastocysts show that lysosomal degradation systems such as MA depend on presenilin-1 protein and become defective as a mutation occurs in the PSEN gene (Lee, 2010), suggesting that in PSEN fibroblasts, we would expect impaired MA. This could link our findings that Beclin-1, involved in MA, significantly varies in the presenilin group when compared to the control group. If MA depends on presenilin-1, which is mutated in this cells, it might suggest that the pathway becomes defective by overexpressing Beclin-1 in the attempt to initiate MA which could explain our findings that show high levels of Beclin-1 in the presenilin group when compared to lower levels in the control group. Studies showed that in presenilin knockout mouse model, LC3 and p62 levels were abnormally high when compared to the control group as shown by immunhistochemical studies (Lee, 2010). Then, they treated the cells with rapamycin to induce MA and LC3 levels were found to increase in both the control cells and the mutated cells, however 6h after they

218

stopped the treatment, LC3 levels returned to normal in the control cells whereas in the presenilin mutated cells, they remained elevated (Lee, 2010). All of these suggest that impairments in MA are linked to the presenilin mutation and AD fibroblasts with mutation in the presenilin gene could become a potential tool in investigating MA defects in AD.

Nixon *et al*, reviews the role of presenilin mutations (the main cause of early onset familial AD) leading to failure of protein degradation systems (Nixon, 2011). Presenilin is known to be involved in the APP molecule cleavage by γ-secretase enzyme, however, it also plays an important part in lysosomal acidification, essential for activation of lysosomal enzymes specific to autophagy (Pasternak, 2003; Lee, 2015), therefore using presenilin mutated fibroblasts could be a good indicator of lysosomal malfunction, hence impaired autophagy. Existing studies on mice, in which presenilin gene was deleted, indicates an abnormally increased accumulation of autophagy substrates in the mice neurons and blastocytes, therefore presenilin mutations, seen in familial AD, can cause a dysfunction in lysosomal acidification, causing failure in substrate degradation and accumulation of autophagic vacuoles (Esselens *et al*, 2004; Wilson *et al*, 2004). Besides the mice studies, there is also evidence on familial AD fibroblasts showing that presenilin mutations demonstrate defective lysosomal acidification and incomplete autolysosome maturations (Lee, 2010). These studies could link lysosomal defects in presenilin mutated cells to dysfunctional removal of tau and beta-amyloid aggregates, accelerating neuronal death and leading to neurodegeneration. Induced pluripotent (Arber, 2017).

As previously discussed in section 1.5.4, induced pluripotent stem cells are a good source of generating limitless AD models for *in vitro* studies and iPSC-derived fibroblasts would allow exploring the autophagy pathways in relation to pathological changes in AD (Arber, 2017). Also, studies on iPSC-derived neurons suggest that stem cells with a genetic background could offer a source of neurons that express physiological levels of mutated genes, therefore they could be key in exploring autophagy proteins and how they relate to disease mechanisms (Wray, 2017).

A study from 2011, explained the use of familial AD fibroblasts with mutations in the PSEN 1 and PSEN2 genes, which were differentiated into iPSC leading to neurons that revealed increased Aβ accumulation, illustrating the specific pathological characteristics of familial AD (Yagi *et al.*, 2011). This study demonstrated the potential of familial AD-iPSC-derived neurons in the research of AD to identify novel therapeutic strategies. In the following year, another study which explored iPSC in both familial AD and sporadic AD, revealed that in some of the sporadic cases, the cells showed increased Aβ generation and tau hyperphosphorylation (Israel *et al.*, 2012). The same study also emphasized the importance of studying AD pathology only in these iPSC-derived neurons as the initial fibroblast cells did not exhibit the same AD pathology features (Israel *et al.*, 2012). These two studies as well as other numerous studies demonstrate the potential of iPSC-derived neurons as a good AD model to explore the disease progression and to guide the drug

development in the hope of finding the cure (Zhang, 2014; Nieweg, 2015; Ortiz-Virumbrales, 2017).

The fibroblast pilot study could improve considerably as we have to consider the very small sample size of the fibroblasts (n=3 cells lines for each group) giving insufficient understanding of autophagy markers expression in the peripheral AD cells. Also, the 3 cases of presenilin mutated cells were the only ones commercially available at the start of this project. It was also challenging, considering that we aimed to find genetically mutated cells from individuals that were age-matched to controls. Moreover, there was high variability of all autophagy markers, in particular in LC3 and LAMP2A, observed between the three sporadic AD cases as well as large variability seen between the three presenilin mutated group, which suggests that the study will require more individual cases in order assess the potential of the fibroblasts as a suitable model for exploring autophagy deficits in AD.

One of the major weaknesses of using *in vitro* cell culture is that the cells environment is simulated and sometimes conditions may differ from the *in vivo* cell interactions with other types of cells and chemical compounds. Autophagy pathways are highly conserved and complex mechanisms in eukaryotic species that depending on signalling pathways, cellular stress responses, nutrient deprivation and pathogens (He, 2009) and interact with numerous other pathways such as the ubiquitin proteasome system (Park, 2013), therefore one of the limitations of this pilot study is that results might not be an accurate representation of the autophagy changes in disease, requiring drug of genetic manipulation in the future work.

4.2   Future work

Future work would aim to validate the immunohistochemical results by using fresh homogenates from the three brain regions of the same 45 cases and explore the autophagy proteins levels through Western blotting. This studies would give a full insight of all autophagy markers chosen in this study and see how they change with disease progression, but most importantly, it will give an insight on LC3 ratio in the AD brains, which will allow the identification of both LCI and LC3II isoforms in the brain sections.

Double labelling would further explore the co-localisation of not just LAMP2A and LC3 but all autophagy markers chosen in this study, related to both tau and beta amyloid. The relationship of MA and CMA would be further explored via dual staining of one marker of MA and one marker of CMA to identify the degree of co-localisation and establish potential compensatory mechanisms when one pathway becomes impaired.

The fibroblasts study would further extend to cells from more individuals to evaluate the changes in autophagy levels in these cells. Also, drug manipulation via autophagy enhancers/inhibitors could manipulate autophagy expression in order to identify which protein becomes defective in the protein degradation systems.Ideally, age-matched controls for the PSEN fibroblast samples would be necessary to depict autophagy marker levels in aged individuals.

More studies on glia cells and their role in autophagy would be useful to offer an insight of the role of astrocytes and oligodendrocytes when protein disposal systems fail to clear abnormal deposit in AD.

4.3   Conclusions

In this study, results demonstrated that MA marker LC3 and CMA marker Hsp70 decreased with increasing Braak staging, in the hippocampus and the occipital cortex, suggesting a possible impairment of both pathways. We also relate them to AD pathological protein tau. In early stages of AD, autophagy markers levels are found high, despite minimal tau pathology. In higher Braak groups, LC3 and Hsp70 autophagy markers declined as pathological tau significantly increased, suggesting that MA and CMA may fail to degrade abnormal proteins in AD. Moreover, hippocampal subregions CA4 and CA1, which have been previously described to become affected in AD, at different stages, show variation in the autophagy marker levels. We showed that in CA1–a hippocampal subregion associated with early deposition of tau/beta-amyloid– autophagy markers, LC3 and Hsp70, were considerably decreased with increasing Braak stages. In CA4 – a hippocampal subregion, associated with later tau/beta-amyloid deposition– autophagy levels were not much affected across the Braak groups. This emphasizes the significance of regional variation in autophagy changes with disease progression. Moreover, double-labelling studies investigated LC3 and LAMP2A in relation to tau protein in individual cells of both CA4 and CA1 subregions.

The main findings suggest that LAMP2A was present in cells harbouring tau and this co-localization decreased in CA1 neurons, in Braak V-VI, suggesting that CMA becomes impaired and fail to clear the abnormal tau deposits. Moreover, our results suggest that LC3 and AT8 co-localization rate was very high in the Braak 0-II group as in CA4, all AT8 positive cells were found to be LC3 positive, as well. This suggests the importance of MA pathway to stay upregulated in the normal ageing brains in order to clear abnormal protein accumulations. In Braak III-IV, the co-localization rates declined, which could suggest that MA becomes impaired in moderate stages of AD as tau burden increases, whereas in Braak V-VI, co-localization declined significantly suggesting that in late stages of AD, there is an evident failure of MA well-functioning. The importance of regional variation in autophagy marker staining is emphasized not only in the hippocampus subregions, but also across the subcortical layers of the frontal and the occipital cortices. Autophagy markers were mostly predominant in the deeper layers which were also associated with tau deposition, suggesting the involvement of autophagy proteins in the attempt to clear these deposits.

MA impairment in late stages of disease might be associated to insufficient LC3 levels, causing incomplete autophagosome formation and protein degradation, leading to abnormal tau accumulations. CMA impairment in late stages of disease could be associated to insufficient Hsp70 to recognize and bind tau for degradation, therefore this might result in cytosolic accumulation of tau aggregates. We also found that in the hippocampus, MA levels were higher than CMA levels across all Braak

groups, suggesting that deficits in the hippocampus could be associated to CMA pathway. On the other hand, in the frontal cortex, CMA levels were found higher than MA levels, in Braak 0-II and Braak III-IV however, in Braak V-VI, both MA and CMA were found to have similar levels which could emphasize activation of compensatory mechanisms by CMA in order to rescue defective MA, in the frontal cortex, in late stages of AD.

Our study also investigated autophagy marker stained glial cells and found that astrocytes and oligodendrocytes were highly activated and their number increased in higher Braak stages, suggesting that although neuronal autophagy markers dropped in late stages of disease, glia might be more resistant, becoming highly activated in order to degrade abnormal tau and beta-amyloid peptides, hence the positive staining of autophagy markers in the glial cells.

The fibroblast pilot study main findings suggested that there is a variation of LAMP2A, Hsp70 AND Beclin-1 expression between the control group and the genetically mutated group, as well as a variation of MA markers between the control group and the sporadic AD group. This suggests an impairment of MA and CMA in AD, however further research will validate if the fibroblasts could potentially become a suitable diagnostic tool in AD.

According to specific deficit locations, lysosomal and autophagic functions, which become impaired in AD neurons, can be restored by treatment with autophagy enhancers in order to promote the clearance of AD specific pathology.

REFERENCES

Adamec, E., Mohan, P., Vonsattel, J. and Nixon, R. (2002). Calpain activation in neurodegenerative diseases: confocal immunofluorescence study with antibodies specifically recognizing the active form of calpain 2. *Acta Neuropathologica*, **104**(1):92-104

Alexander, A. G., Marfil, V., & Li, C. (2014). Use of *Caenorhabditis elegans* as a model to study Alzheimer's disease and other neurodegenerative diseases. *Frontiers in Genetics*, **5**:279

Alford, S., Patel, D., Perakakis, N. and Mantzoros, C. (2017). Obesity as a risk factor for Alzheimer's disease: weighing the evidence. *Obesity Reviews*, **19**(2):269-280

Alonso, A. C., Zaidi, T., Grundke-Iqbal, I., & Iqbal, K. (1994). Role of abnormally phosphorylated tau in the breakdown of microtubules in Alzheimer disease. *Proceedings of the National Academy of Sciences of the United States of America*, **91(**12):5562–5566

Alonso, A.C., Grundke-Iqbal, I., Iqbal, K. (1996). Alzheimer's disease hyperphosphorylated tau sequesters normal tau into tangles of filaments and disassembles microtubules. *Nature medicine*, **2**(7):783-7

Alvarez-Erviti, L., Rodriguez-Oroz, M.C., Cooper, J.M., et al. (2010). Chaperone-mediated autophagy markers in Parkinson disease brains. *Archives of Neurology*, **67**:1464-1472

Anglade P, Vyas S, Javoy-Agid F, Herrero MT, Michel PP, Marquez J, *et al.* (1997). Apoptosis and autophagy in nigral neurons of patients with Parkinson's disease. *Histology and Histopathology*, **12**:25-31

Arber, C., Lovejoy, C., & Wray, S. (2017). Stem cell models of Alzheimer's disease: progress and challenges. *Alzheimer's Research & Therapy*, **9**:42

Asthana, S., Baker, L., Craft, S., Stanczyk, F., Veith, R., Raskind, M. and Plymate, S. (2001). High-dose estradiol improves cognition for women with AD: Results of a randomized study. *Neurology*, **57**(4):605-612

Avila, J., Santa-María, I., Pérez, M., Hernández, F. and Moreno, F. (2006). Tau Phosphorylation, Aggregation, and Cell Toxicity. *Journal of Biomedicine and Biotechnology*, **2006**:1-5

Avila, J., Santa-María, I., Pérez, M., Hernández, F. and Moreno, F. (2006). Tau Phosphorylation, Aggregation, and Cell Toxicity. *Journal of Biomedicine and Biotechnology*, **2006**:1-5

Babin, P. J., Thisse, C., Durliat, M., Andre, M., Akimenko, M.-A., & Thisse, B. (1997). Both apolipoprotein E and A-I genes are present in a nonmammalian vertebrate and are highly expressed during embryonic development. *Proceedings of the National Academy of Sciences of the United States of America*, **94**(16):8622–8627

Bachurin, S., Bovina, E. and Ustyugov, A. (2017). Drugs in Clinical Trials for Alzheimer's Disease: The Major Trends. *Medicinal Research Reviews*, **37**(5):1186-1225

Bäckman, L., Jones, S., Berger, A.K., Laukka, E.J., Small, B.J. (2004). Multiple Cognitive Deficits during the Transition to Alzheimer's disease. *Journal of Internal Medicine.* **256**(3):195–204

Bai, Q., & Burton, E. A. (2011). Zebrafish models of Tauopathy. *Biochimica et Biophysica Acta*, **1812**(3):353–363

Banks, W. A., Owen, J. B., & Erickson, M. A. (2012). Insulin in the Brain: There and Back Again. *Pharmacology & Therapeutics*, **136**(1):82–93

Barbazuk, W. B., Korf, I., Kadavi, C., Heyen, J., Tate, S., Wun, E., Johnson, S. L. (2000). The Syntenic Relationship of the Zebrafish and Human Genomes. *Genome Research*, **10**(9):1351–1358

Barnett, M.W., Larkman, P.M. (2007).The action potential. *Practical Neurology,* **7:**192-197

Bekris, L. M., Yu, C.-E., Bird, T. D., & Tsuang, D. W. (2010). Genetics of Alzheimer Disease. *Journal of Geriatric Psychiatry and Neurology*, **23**(4):213–227

Bell, R., Winkler, E., Singh, I., Sagare, A., Deane, R., Wu, Z., Holtzman, D., Betsholtz, C., Armulik, A., Sallstrom, J., Berk, B. and Zlokovic, B. (2012). Apolipoprotein E controls cerebrovascular integrity via cyclophilin A. *Nature*, **485**(7399):512-516

Berent-Spillson, A., Briceno, E., Pinsky, A., Simmen, A., Persad, C., Zubieta, J. and Smith, Y. (2015). Distinct cognitive effects of estrogen and progesterone in menopausal women. *Psychoneuroendocrinology*, **59**:25-36

Bielschowsky M. (1902). Die Silberimprägnation der Achsenzylinder. *Neurol. Zentralb*, (Leipzig) **13**:579–584 (In German)

Bierer, L., Hof, P., Purohit, D., Carlin, L., Schmeidler, J., Davis, K. and Perl, D. (1995). Neocortical neurofibrillary tangles correlate with dementia severity in Alzheimer's Disease. *Archives of Neurology*, **52**(1):81-88

Birch, A. (2014). The contribution of astrocytes to Alzheimer's disease. *Biochemical Society Transactions*, **42**(5):1316-1320

Birks, J. S. (2006). Cholinesterase inhibitors for Alzheimer's disease. *The Cochrane database of systematic reviews*, (1):CD005593

Blennow, K., Leon, M.J. and Zetterberg, H. (2006). Alzheimer's disease. *The lancet*, **368** (9533), 387-403

Bobkova, N.V., Garbuz, D.G., Nesterova, I., Medvinskaya, N., Samokhin, A., Alexandrova, I., Yashin, V., Karpov, V., Kukharsky, M.S., Ninkina, N.N., Smirnov, A.A., Nudler, E., Evgen'ev, M. (2014). Therapeutic effect of exogenous hsp70 in mouse models of Alzheimer's disease. Journal of Alzheimer's Disease: JAD, **38**(2):425-35

Bolós, M., Pallas-Bazarra, N., Terreros-Roncal, J., Perea, J., Jurado-Arjona, J., Ávila, J. and Llorens-Martín, M. (2017). Soluble Tau has devastating

effects on the structural plasticity of hippocampal granule neurons. *Translational Psychiatry*, **7**(12)

Boluda, S., Toledo, J. B., Irwin, D. J., Raible, K. M., Byrne, M. D., Lee, E. B., Trojanowski, J. Q. (2014). A comparison of Aβ amyloid pathology staging systems and correlation with clinical diagnosis. *Acta Neuropathologica*, **128**(4):543–550

Bona, D., Scapagnini, G., Candore, G., Castiglia, L., Colonna-Romano, G., Duro, G., Nuzzo, D., Iemolo, F., Lio, D., Pellicano, M., Scafidi, V., Caruso, C. and Vasto, S. (2010). Immune-Inflammatory Responses and Oxidative Stress in Alzheimers Disease: Therapeutic Implications. *Current Pharmaceutical Design*, **16**(6):684-691

Bordi, M., Berg, M. J., Mohan, P. S., Peterhoff, C. M., Alldred, M. J., Che, S., Nixon, R. A. (2016). Autophagy flux in CA1 neurons of Alzheimer hippocampus: Increased induction overburdens failing lysosomes to propel neuritic dystrophy. *Autophagy*, **12**(12):2467–2483

Bordi, M., Berg, M. J., Mohan, P. S., Peterhoff, C. M., Alldred, M. J., Che, S., Nixon, R. A. (2016). Autophagy flux in CA1 neurons of Alzheimer hippocampus: Increased induction overburdens failing lysosomes to propel neuritic dystrophy. *Autophagy*, **12**(12):2467–2483

Bornemann, K. D., Wiederhold, K.-H., Pauli, C., Ermini, F., Stalder, M., Schnell, L., Staufenbiel, M. (2001). Aβ-Induced Inflammatory Processes in Microglia Cells of APP23 Transgenic Mice. *The American Journal of Pathology*, **158**(1), 63–73

Boutajangout, A., M. Sigurdsson, E. and K. Krishnamurthy, P. (2011). Tau as a Therapeutic Target for Alzheimers Disease. *Current Alzheimer Research*, **8**(6):666-677

Bowen, D.M., Smith, C.B., White, P., Davison, A.N. (1976). Neurotransmitter-related enzymes and indices of hypoxia in senile dementia and other abiotrophies. Brain: a journal of neurology, **99**(3):459-96

Braak, H., Braak E. (1991). Neuropathological st, aging of Alzheimer-related changes. *Acta Neuropathology*, 82: 239-59

Bradl, M., and Lassmann, H. (2010). Oligodendrocytes: biology and pathology. *Acta Neuropathologica*, 119(1), 37-53

Brion, J. (1998). Neurofibrillary Tangles and Alzheimer's Disease. *European Neurology*, **40**(3):130-140

Brion, J.-P., Tremp, G., & Octave, J.-N. (1999). Transgenic Expression of the Shortest Human Tau Affects Its Compartmentalization and Its Phosphorylation as in the Pretangle Stage of Alzheimer's Disease. *The American Journal of Pathology*, **154**(1), 255–270

Brion, J.-P., Tremp, G., & Octave, J.-N. (1999). Transgenic Expression of the Shortest Human Tau Affects Its Compartmentalization and Its Phosphorylation as in the Pretangle Stage of Alzheimer's Disease. *The American Journal of Pathology*, **154**(1):255–270

Bu, G. (2009). Apolipoprotein E and its receptors in Alzheimer's disease: pathways, pathogenesis and therapy. *Nature Reviews Neuroscience*, **10**(5):333-344

Butt, R. H., & Coorssen, J. R. (2013). Coomassie Blue as a Near-infrared Fluorescent Stain: A Systematic Comparison with Sypro Ruby for In-gel Protein Detection. *Molecular & Cellular Proteomics : MCP*, **12**(12), 3834–3850

Cacabelos, R. (2007). Donepezil in Alzheimer's disease: From conventional trials to pharmacogenetics. *Neuropsychiatric Disease and Treatment*, **3**(3):303–333

Caccamo, A., Magrì, A., Medina, D., Wisely, E., López-Aranda, M., Silva, A. and Oddo, S. (2013). mTOR regulates tau phosphorylation and degradation: implications for Alzheimer's disease and other tauopathies. *Aging Cell*, **12**(3):370-380

Caccamo, A., Majumder, S., Richardson, A., Strong, R., Oddo, S. (2010). Molecular interplay between mammalian target of rapamycin (mTOR), amyloid-beta, and Tau: effects on cognitive impairments. *The Journal of Biological Chemistry*, **285**:13107-20

Cai, Z. and Yan, L.J. (2013). Rapamycin, Autophagy, and Alzheimer's disease. *Journal of Biochemical and Pharmacological Research*, 1(2): 84-90

Cai, Z., & Yan, L.-J. (2013). Rapamycin, Autophagy, and Alzheimer's Disease. *Journal of Biochemical and Pharmacological Research*, **1**(2):84–90

Calhoun, M., Wiederhold, K., Abramowski, D., Phinney, A., Probst, A., Sturchler-Pierrat, C., Staufenbiel, M., Sommer, B. and Jucker, M. (1998). Neuron loss in APP transgenic mice. *Nature*, **395**(6704):755-756

Cárdenas-Aguayo, M., Gómez-Virgilio, L., DeRosa, S. and Meraz-Ríos, M. (2014). The Role of Tau Oligomers in the Onset of Alzheimer's Disease Neuropathology. *ACS Chemical Neuroscience*, **5**(12):1178-1191

Carmeli, C., Donati, A., Antille, V., Viceic, D., Ghika, J., von Gunten, A., Clarke, S., Meuli, R., Frackowiak, R. and Knyazeva, M. (2013). Demyelination in Mild Cognitive Impairment Suggests Progression Path to Alzheimer's Disease. *PLoS ONE*, **8**(8):e72759

Carmona-Gutierrez, D., Hughes, A.L., Madeo, F., Ruckenstuhl, C. (2016). The crucial impact of lysosomes in ageing and longevity. *Ageing research reviews*, S1568-1637(16)30066-6

Carter, D.B. (2005). The interaction on Amyloid-beta with ApoE in Alzheimer's disease. *Subcellular Biochemistry*, **38**

Cebollero, E. and Reggiori, F. (2009). Regulation of autophagy in yeast Saccharomyces cerevisiae. *Biochimica et Biophysica Acta (BBA) - Molecular Cell Research*, **1793**(9):1413-1421

Cerf, M. E. (2013). Beta Cell Dysfunction and Insulin Resistance. *Frontiers in Endocrinology*, **4**:37

Chan, K., Wang, W., Wu, J., Liu, L., Theodoratou, E., Car, J., Middleton, L., Russ, T., Deary, I., Campbell, H., Wang, W. and Rudan, I. (2013). Epidemiology of Alzheimer's disease and other forms of dementia in China, 1990–2010: a systematic review and analysis. *The Lancet*, **381**(9882):2016-2023.

Chang, Y.-Y., & Neufeld, T. P. (2009). An Atg1/Atg13 Complex with Multiple Roles in TOR-mediated Autophagy Regulation. *Molecular Biology of the Cell*, **20**(7):2004–2014

Chava, S., Lee, C., Aydin, Y., Chandra, P. K., Dash, A., Chedid, M., Dash, S. (2017). Chaperone-mediated autophagy compensates for impaired macroautophagy in the cirrhotic liver to promote hepatocellular carcinoma. *Oncotarget*, **8**(25):40019–40036

Chen, M., Martins, R. and Lardelli, M. (2009). Complex Splicing and Neural Expression of Duplicated Tau Genes in Zebrafish Embryos. *Journal of Alzheimer's Disease*, **18**(2):305-317

Chen, P.-C., Vargas, M. R., Pani, A. K., Smeyne, R. J., Johnson, D. A., Kan, Y. W., & Johnson, J. A. (2009). Nrf2-mediated neuroprotection in the MPTP mouse model of Parkinson's disease: Critical role for the astrocyte. *Proceedings of the National Academy of Sciences of the United States of America*, **106**(8), 2933–2938

Chen, S., Townsend, K., Goldberg, T. E., Davies, P., & Conejero-Goldberg, C. (2010). MAPT Isoforms: Differential Transcriptional Profiles Related to 3R and 4R Splice Variants. *Journal of Alzheimer's Disease*, **22(**4):1313–1329

Chen, S., Townsend, K., Goldberg, T. E., Davies, P., & Conejero-Goldberg, C. (2010). MAPT Isoforms: Differential Transcriptional Profiles Related to 3R and 4R Splice Variants. *Journal of Alzheimer's Disease*, **22**(4):1313–1329

Chen, Y., Klionsky, D.J. (2009). The regulation of autophagy–unanswered questions. *Journal of Cell Science*, **124**:161-170

Choi, K.C., Kim, S.H., Ha, J.Y., Kim, S.T., Son, J.H. (2010). A novel mTOR activating protein protects dopamine neurons against oxidative stress by repressing autophagy related cell death. *The Journal of Neurochemistry*, **112**:366-76

Choi, Y. and Park, H. (2012). Anti-inflammatory effects of spermidine in lipopolysaccharide-stimulated BV2 microglial cells. *Journal of Biomedical Science*, **19**(1):31

Choudhury, G. and Ding, S. (2016). Reactive astrocytes and therapeutic potential in focal ischemic stroke. *Neurobiology of Disease*, **85**:234-244

Churcher, I. (2006). Tau Therapeutic Strategies for the Treatment of Alzheimers Disease. *Current Topics in Medicinal Chemistry*, **6(**6):579-595

Citron, M., Vigo-Pelfrey, C., Teplow, D.B., Miller, C., Schenk, D., Johnston, J., Winblad, B., Venizelos, N., Lannfelt, L., Selkoe, D.J. (1994). Excessive production of amyloid beta-protein by peripheral cells of symptomatic and presymptomatic patients carrying the Swedish familial Alzheimer disease

mutation. *Proceedings of the National Academy of Science USA,* **91**(25):11993–11997

Čolović, M. B., Krstić, D. Z., Lazarević-Pašti, T. D., Bondžić, A. M., & Vasić, V. M. (2013). Acetylcholinesterase Inhibitors: Pharmacology and Toxicology. *Current Neuropharmacology*, **11**(3):315–335

Congdon, E., Wu, J., Myeku, N., Figueroa, Y., Herman, M., Marinec, P., Gestwicki, J., Dickey, C., Yu, W. and Duff, K. (2012). Methylthioninium chloride (methylene blue) induces autophagy and attenuates tauopathy in vitro and in vivo. *Autophagy*, **8**(4):609-622

Connolly, G.P. (1998). Fibroblasts models of neurological disorders: fluorescence measurement studies. *TiPS*, **19**:171-177

Contestabile, A. (2011). The history of the cholinergic hypothesis. *Behavioural Brain Research*, **221**(2):334–340

Crum, T., Gleixner, A., Posimo, J., Mason, D., Broeren, M., Heinemann, S., Wipf, P., Brodsky, J. and Leak, R. (2015). Heat shock protein responses to aging and proteotoxicity in the olfactory bulb. *Journal of Neurochemistry*, **133**(6):780-794

Cuervo, A. and Wong, E. (2013). Chaperone-mediated autophagy: roles in disease and aging. *Cell Research*, **24**(1):92-104

Cuervo, A. M. (2008). Autophagy and aging: keeping that old broom working. *Trends in Genetics : TIG*, **24(**12):604–612

Cuervo, A., Knecht, E., Terlecky, S. and Dice, J. (1995). Activation of a selective pathway of lysosomal proteolysis in rat liver by prolonged starvation. *American Journal of Physiology-Cell Physiology*, **269**(5):C1200-C1208

Cuervo, A.M. (2004). Autophagy: many paths to the same end. *Molecular and Cellular Biochemistry*, **263**:55-72

Cuervo, A.M., Dice, J.F. (2000). Age-related decline in chaperone-mediated autophagy. *Journal of Biology and Chemistry,* **275**:31505-31513

Cuervo, A.M., Dice, J.F. (1996). A receptor for the selective uptake and degradation of proteins by lysosomes. *Science,* **273**:501-503

Cuervo, A.M., Stefanis, L., Fredenburg, R., Lansbury, P.T., Sulzer, D. (2004). Impaired degradation of mutant alpha-synuclein by chaperone-mediated autophagy. *Science*, **305**:1292-5

Cuervo, A.M., Wong, E. (2014) Chaperone-mediated autophagy: roles in disease and aging. *Cell research*, **24**:92-104

Cummings, J., Lee, G., Mortsdorf, T., Ritter, A. and Zhong, K. (2017). Alzheimer's disease drug development pipeline: 2017. *Alzheimer's & Dementia: Translational Research & Clinical Interventions*, **3**(3):367-384

D'Antonio, M., Woodruff, G., Nathanson, J. L., D'Antonio-Chronowska, A., Arias, A., Matsui, H., Frazer, K. A. (2017). High-Throughput and Cost-Effective Characterization of Induced Pluripotent Stem Cells. *Stem Cell Reports*, **8**(4):1101–1111

Danysz, W., and Parsons, C. G. (2012). Alzheimer's disease, β-amyloid, glutamate, NMDA receptors and memantine – searching for the connections. *British Journal of Pharmacology*, *167*(2):324–352

Dawkins, E. and Small, D. (2014). Insights into the physiological function of the β-amyloid precursor protein: beyond Alzheimer's disease. *Journal of Neurochemistry*, **129**(5):756-769

De Calignon, A., Polydoro, M., Suárez-Calvet, M., William, C., Adamowicz, D. H., Kopeikina, K. J., Hyman, B. T. (2012). Propagation of tau pathology in a model of early Alzheimer's disease. *Neuron*, **73**(4):685–697

DeFina, P.A., Moser, R.S., Glenn, M., Lichtenstein, J.D. and Fellus, J. (2013). Alzheimer's Disease Clinical and Research Update for Health Care Practitioners. *Journal of Aging Research*, **2013**:1-9

Dekeyzer, S., De Kock, I., Nikoubashman, O., Vanden Bossche, S., Van Eetvelde, R., De Groote, J., Acou, M., Wiesmann, M., Deblaere, K. and Achten, E. (2017). "Unforgettable" – a pictorial essay on anatomy and pathology of the hippocampus. *Insights into Imaging*, **8**(2):199-212

Deurveilher, S. and Semba, K. (2011). Basal forebrain regulation of cortical activity and sleep-wake states: Roles of cholinergic and non-cholinergic neurons. *Sleep and biological rhythms*, **9** (1), 65-70

Dhikav, V., Anand, K. (2011) Potential Predictors of Hippocampal Atrophy in Alzheimer's disease. *Drugs and Aging,* **29**(1), 1-11

Di Malta, C., Fryer, J. D., Settembre, C., & Ballabio, A. (2012). Astrocyte dysfunction triggers neurodegeneration in a lysosomal storage disorder. *Proceedings of the National Academy of Sciences of the United States of America*, **109**(35), E2334–E2342

Di, J., Cohen, L., Corbo, C., Phillips, G., El Idrissi, A. and Alonso, A. (2016). Abnormal tau induces cognitive impairment through two different mechanisms: synaptic dysfunction and neuronal loss. *Scientific Reports*, **6**(1)

Dice, J.F. (1990). Peptide sequences that target cytosolic proteins for lysosomal proteolysis. *Trends of Biochemical Science,* **15**:305-309

Dice, J.F. (2000). Degradation of intracellular proteins by microautophagy. Lysosomal pathways of protein degradation. *Landes Bioscience*; 75-84

Dobranici, L. (2010) Anticholinergic Medication Use in Patients with Alzheimer's Dementia: Results from a Romanian Longitudinal Study. *Timisoara Medical Journal*, **60**(2-3), 196-202

Dodart, J., Bales, K., Gannon, K., Greene, S., DeMattos, R., Mathis, C., DeLong, C., Wu, S., Wu, X., Holtzman, D. and Paul, S. (2002). Immunization reverses memory deficits without reducing brain Aβ burden in Alzheimer's disease model. *Nature Neuroscience*, **5**(5):452-457

Dong, H., Martin, M. V., Chambers, S., & Csernansky, J. G. (2007). Spatial relationship between synapse loss and β-Amyloid deposition in Tg2576 Mice. *The Journal of Comparative Neurology*, **500**(2):311–321

Dou, F., Netzer, W. J., Tanemura, K., Li, F., Hartl, F. U., Takashima, A., Xu, H. (2003). Chaperones increase association of tau protein with microtubules. *Proceedings of the National Academy of Sciences of the United States of America*, **100**(2):721–726

Doyle, S., Genest, O. and Wickner, S. (2013). Protein rescue from aggregates by powerful molecular chaperone machines. *Nature Reviews Molecular Cell Biology*, **14**(10):617-629

Durazzo, T. C., Mattsson, N., & Weiner, M. W. (2014). Smoking and increased Alzheimer's disease risk: A review of potential mechanisms. *Alzheimer's & Dementia : The Journal of the Alzheimer's Association*, **10**(30), S122–S145

Dysken, M., Sano, M., Asthana, S., Vertrees, J., Pallaki, M., Llorente, M., Love, S., Schellenberg, G., McCarten, J., Malphurs, J., Prieto, S., Chen, P., Loreck, D., Trapp, G., Bakshi, R., Mintzer, J., Heidebrink, J., Vidal-Cardona, A., Arroyo, L., Cruz, A., Zachariah, S., Kowall, N., Chopra, M., Craft, S., Thielke, S., Turvey, C., Woodman, C., Monnell, K., Gordon, K., Tomaska, J., Segal, Y., Peduzzi, P. and Guarino, P. (2014). Effect of Vitamin E and Memantine on Functional Decline in Alzheimer Disease. *JAMA*, **311**(1):33

Eichner, J. (2002). Apolipoprotein E Polymorphism and Cardiovascular Disease: A HuGE Review. *American Journal of Epidemiology*, **155**(6):487-495.

Eriksen, J.L., Sagi, S.A., Smith, T.E., Weggen, S., Das, P., McLendon, D.C., Ozols, V.V., Jessing, K.W., Zavitz, K.H., Koo, E.H., Golde, T.E. (2003). NSAIDs and enantiomers of flurbiprofen target gamma-secretase and lower Abeta 42 in vivo. *The Journal of Clinical investigation*, **112**(3):440-449

Esselens, C., Oorschot, V., Baert, V., Raemaekers, T., Spittaels, K., Serneels, L., Annaert, W. (2004). Presenilin 1 mediates the turnover of telencephalin in hippocampal neurons via an autophagic degradative pathway. *The Journal of Cell Biology*, **166**(7):1041–1054

Essick, E. E., & Sam, F. (2010). Oxidative stress and autophagy in cardiac disease, neurological disorders, aging and cancer. *Oxidative Medicine and Cellular Longevity*, **3**(3):168–177

Evans, D.A., Morris, M.C., Rajan, K.B. (2014) Vitamin E, Memantine, and Alzheimer Disease. *The Journal of the American Medical Association*, **311**(1):29-30

Ewald, C. Y., & Li, C. (2010). Understanding the molecular basis of Alzheimer's disease using a *Caenorhabditis elegans* model system. *Brain Structure & Function*, **214**(0):263–283

Fabrizi, Cinzia et al. Autophagy is differently regulated in astrocytes and microglia exposed to environmental toxic molecules. *Italian Journal of Anatomy and Embryology*, **167**

Farrer, L. (1997). Effects of age, sex and ethnicity on the association between Apolipoprotein E genotype and Alzheimer's Disease. *JAMA*, **278**(16):1349

Fields, D. R. (2008). White Matter Matters. *Scientific American,* **298**(3): 54–61

Fillenbaum, G. G., van Belle, G., Morris, J. C., Mohs, R. C., Mirra, S. S., Davis, P. C., Heyman, A. (2008). CERAD (Consortium to Establish a Registry for Alzheimer's Disease) The first 20 years. *Alzheimer's & Dementia : The Journal of the Alzheimer's Association*, **4**(2):96–109

Fillenbaum, G. G., van Belle, G., Morris, J. C., Mohs, R. C., Mirra, S. S., Davis, P. C., Heyman, A. (2008). CERAD (Consortium to Establish a Registry for Alzheimer's Disease) The first 20 years. *Alzheimer's & Dementia : The Journal of the Alzheimer's Association*, **4**(2):96–109

Fleminger, S. (2003). Head injury as a risk factor for Alzheimer's disease: the evidence 10 years on; a partial replication. *Journal of Neurology, Neurosurgery & Psychiatry*, **74**(7):857-862

Fontana, B., Mezzomo, N., Kalueff, A. and Rosemberg, D. (2018). The developing utility of zebrafish models of neurological and neuropsychiatric disorders: A critical review. *Experimental Neurology*, **299**:157-171

Foster, V., Oakley, A., Slade, J., Hall, R., Polvikoski, T., Burke, M., Thomas, A., Khundakar, A., Allan, L. and Kalaria, R. (2014). Pyramidal neurons of the prefrontal cortex in post-stroke, vascular and other ageing-related dementias. *Brain*, **137**(9):2509-2521

Francis PT, Palmer AM, Snape M*, et al* (1999).The cholinergic hypothesis of Alzheimer's disease: a review of progress. *Journal of Neurology, Neurosurgery & Psychiatry* **1999**(66):137-147

Franco, R., & Cedazo-Minguez, A. (2014). Successful therapies for Alzheimer's disease: why so many in animal models and none in humans? *Frontiers in Pharmacology*, **5**:146

Franklin, T., Krueger-Naug, A., Clarke, D., Arrigo, A. and Currie, R. (2005). The role of heat shock proteins Hsp70 and Hsp27 in cellular protection of the central nervous system. *International Journal of Hyperthermia*, **21**(5):379-392

Funk, G.E., Mrak, R.E. and Kuret, J. (2011). Granulovacuolar degeneration (GVD) bodies of Alzheimer's disease (AD) resemble late-stage autophagic organelles. *Neuropathology and Applied Neurobiology*, **37**(3):295-306

Funk, K., Mirbaha, H., Jiang, H., Holtzman, D. and Diamond, M. (2015). Distinct Therapeutic Mechanisms of Tau Antibodies. *Journal of Biological Chemistry*, **290**(35):21652-21662

Gama Sosa, M., De Gasperi, R. and Elder, G. (2011). Modeling human neurodegenerative diseases in transgenic systems. *Human Genetics*, **131**(4):535-563

Gan, L., Vargas, M. R., Johnson, D. A., & Johnson, J. A. (2012). Astrocyte-specific Overexpression of Nrf2 Delays Motor Pathology and Synuclein Aggregation throughout the CNS in the Alpha-synuclein Mutant (A53T) Mouse Model. *The Journal of Neuroscience : The Official Journal of the Society for Neuroscience*, **32**(49):17775–17787

Ge, P.-F., Luo, T.-F., Zhang, J.-Z., Chen, D.-W., Luan, Y.-X., & Fu, S.-L. (2008). Ischemic preconditioning induces chaperone hsp70 expression and inhibits protein aggregation in the CA1 neurons of rats. *Neuroscience Bulletin*, **24**(5), 288–296

George-Carey, R., Adeloye, D., Chan, K., Paul, A., Kolčić, I., Campbell, H. and Rudan, I. (2012). An estimate of the prevalence of dementia in Africa: A systematic analysis. *Journal of Global Health*, **2**(2)

Ghebranious, N., Ivacic, L., Mallum, J., & Dokken, C. (2005). Detection of *ApoEE2*, *E3* and *E4* alleles using MALDI-TOF mass spectrometry and the homogeneous mass-extend technology. *Nucleic Acids Research*, **33**(17):e149

Giacoppo, S., Bramanti, P., & Mazzon, E. (2017). Triggering of inflammasome by impaired autophagy in response to acute experimental Parkinson's disease: involvement of the PI3K/Akt/mTOR pathway. *Neuroreport*, **28**(15), 996–1007

Glick, D., Barth, S. and Macleod, K. (2010). Autophagy: cellular and molecular mechanisms. *The Journal of Pathology*, **221**(1):3-12

Goate, A., Chartier-Harlin, M.C., Mullan, M., et al. (1991). Segreggation of a missense mutation in the amyloid precursor protein gene with familial Alzheimer's disease. *Nature*, **349**:704-6

Goedert M., Spillantini M. G., Jakes R., Rutherford D. and Crowther R. A. (1989) Multiple isoforms of human microtubule-associated protein tau: sequences and localization in neurofibrillary tangles of Alzheimer's disease. *Neuron,* **3**:519–526

Goedert, M., Ghetti, B. (2007). Alois Alzheimer: His Life and Times. *International Society of Neuropathology*, **17**(1):57-62

Goedert, M., Jakes, R. and Vanmechelen, E. (1995). Monoclonal antibody AT8 recognises tau protein phosphorylated at both serine 202 and threonine 205. *Neuroscience Letters*, **189**(3):167-170

Goedert. M, Jakes. R, Crowther. R.A. (1999). Effects of frontotemporal dementia FTDP-17 mutations on heparin-induced assembly of tau elaments. *FEBS*, **450**(1999) 306-311

Gomez-Santos, C., Ferrer, I., Santidrian, A.F., Barrachina, M., Gil, J., Ambrosio, S. (2003). Dopamine induces autophagic cell death and alpha-

synuclein increase in human neuroblastoma SH-SY5Y cells. *Journal of Neuroscience Research*, **73**:341-50

Gotz, J. (2001). Formation of Neurofibrillary Tangles in P301L Tau Transgenic Mice Induced by Abeta 42 Fibrils. *Science*, **293**(5534):1491-1495

Götz, J., Probst, A., Spillantini, M. G., Schäfer, T., Jakes, R., Bürki, K., & Goedert, M. (1995). Somatodendritic localization and hyperphosphorylation of tau protein in transgenic mice expressing the longest human brain tau isoform. *The EMBO Journal*, **14**(7):1304–1313

Götz, J., Schild, A., Hoerndli, F. and Pennanen, L. (2004). Amyloid-induced neurofibrillary tangle formation in Alzheimer's disease: insight from transgenic mouse and tissue-culture models. *International Journal of Developmental Neuroscience*, **22**(7):453-465

Gray, S. M., Meijer, R. I., & Barrett, E. J. (2014). Insulin Regulates Brain Function, but How Does It Get There? *Diabetes*, **63**(12):3992–3997

Greener, M. (2015). Don't underestimate glial cells. *Progress in Neurology and Psychiatry*, 5-8

Groth, C., Nornes, S., McCarty, R., Tamme, R. and Lardelli, M. (2002). Identification of a second presenilin gene in zebrafish with similarity to the human Alzheimer's disease gene presenilin2. *Development Genes and Evolution*, **212**(10):486-490

Guerreiro, R., and Bras, J. (2015). The age factor in Alzheimer's disease. *Genome Medicine*, **7**(106)

Guerrero-Muñoz, M. J., Gerson, J., & Castillo-Carranza, D. L. (2015). Tau Oligomers: The Toxic Player at Synapses in Alzheimer's Disease. *Frontiers in Cellular Neuroscience*, **9**:464

Haan, M. (1999). The role of Apoe4 in modulating effects of other risk factors for cognitive decline in elderly persons. *JAMA*, **282**(1):40

Haass, C. and Selkoe, D. (2007). Soluble protein oligomers in neurodegeneration: lessons from the Alzheimer's amyloid β-peptide. *Nature Reviews Molecular Cell Biology*, **8**(2):101-112.

Haidar, M. and Timmerman, V. (2017). Autophagy as an Emerging Common Pathomechanism in Inherited Peripheral Neuropathies. *Frontiers in Molecular Neuroscience*, **10**

Hall, L., & Martinus, R. D. (2013). Hyperglycaemia and oxidative stress upregulate HSP60 & HSP70 expression in HeLa cells. *SpringerPlus*, **2**:431

Hampson, E. and Morley, E. (2013). Estradiol concentrations and working memory performance in women of reproductive age. *Psychoneuroendocrinology*, **38**(12):2897-2904

Hansen, R. A., Gartlehner, G., Webb, A. P., Morgan, L. C., Moore, C. G., & Jonas, D. E. (2008). Efficacy and Safety of Donepezil, Galantamine, and Rivastigmine for the Treatment of Alzheimer's Disease: A Systematic Review and Meta-Analysis. *Clinical Interventions in Aging*, **3**(2):211–225

Hara, T., Takamura, A., Kishi, C., Iemura, S., Natsume, T., et al. (2008) FIP200, a ULK-interacting protein, is required for autophagosome formation in mammalian cells. *Journal of Cell Biology*, **181**:497–510

Harold, D., Abraham, R., Hollingworth, P., Sims, R., Gerrish, A., Hamshere, M., Pahwa, J., Moskvina, V., Dowzell, K., Williams, *et al.* (2009). Genome-wide association study identifies variants at CLU and PICALM associated with Alzheimer's disease. *Nature Genetics*, **41(**10):1088-1093

Harrison, J. and Owen, M. (2016). Alzheimer's disease: The amyloid hypothesis on trial. *British Journal of Psychiatry*, **208**(01):1-3

Hartmann, D. (2000-2013). Functional Roles of APP Secretases. In: Madame Curie Bioscience Database. *Landes Bioscience*, 2000-2013

Hayes, E., Gavrilidis, E. and Kulkarni, J. (2012). The role of oestrogen and other hormones in the pathophysiology and treatment of schizophrenia. *Schizophrenia Research and Treatment,* **2012**(8): 2012

Hayes, E., Gavrilidis, E. and Kulkarni, J. (2018). *The Role of Oestrogen and Other Hormones in the Pathophysiology and Treatment of Schizophrenia*.

He, C., Klionsky, D.J. (2009) Regulation Mechanisms and Signalling Pathways of Autophagy. *Annual Review of Genetics*, **43**:67–93

He, Y., Zhao, X., Subahan, N.R., Fan, L., Gao, J. and Chen H. (2014). The prognostic value of autophagy-related markers beclin-1 and microtubule-associated protein light chain 3B in cancers: a systematic review and meta-analysis. *Tumour biology*, 35 (8): 7317-7326

Herrmann, A. and Spires-Jones, T. (2014). Clearing the way for tau immunotherapy in Alzheimer's disease. *Journal of Neurochemistry*, **132**(1):1-4

Hewitt, G., Carroll, B., Sarallah, R., Correia-Melo, C., Ogrodnik, M., Nelson, G., Otten, E., Manni, D., Antrobus, R., Morgan, B., von Zglinicki, T., Jurk, D., Seluanov, A., Gorbunova, V., Johansen, T., Passos, J. and Korolchuk, V. (2016). SQSTM1/p62 mediates crosstalk between autophagy and the UPS in DNA repair. *Autophagy*, **12**(10):1917-1930

Hewitt, G., Carroll, B., Sarallah, R., Correia-Melo, C., Ogrodnik, M., Nelson, G., Korolchuk, V. I. (2016). SQSTM1/p62 mediates crosstalk between autophagy and the UPS in DNA repair. *Autophagy*, **12**(10):1917–1930

Himmler A., Drechsel D., Kirschner M. W. and Martin D. W. Jr (1989) Tau consists of a set of proteins with repeated C-terminal microtubule-binding domains and variable N-terminal domains. *Molecular and Cellular Biology*, **9**:1381–1388

Hirata-Fukae, C., Li, H., Ma, L., Hoe, H., Rebeck, G., Aisen, P. and Matsuoka, Y. (2009). Levels of soluble and insoluble tau reflect overall status of tau phosphorylation in vivo. *Neuroscience Letters*, **450**(1):51-55

Hoshino, T., Murao, N., Namba, T., Takehara, M., Adachi, H., Katsuno, M., Sobue, G., Matsushima, T., Suzuki, T. and Mizushima, T. (2011).

Suppression of Alzheimer's Disease-Related Phenotypes by Expression of Heat Shock Protein 70 in Mice. *Journal of Neuroscience*, **31**(14):5225-5234

Hsiao, K.K, Borchelt, D.R., Olson, K., Johannsdottir, R., Kitt, C., Yunis, W., Xu, S., Eckman, C., Younkin, S., Price, D. (1995). Age-related CNS disorder and early death in transgenic FVB/N mice overexpressing Alzheimer amyloid precursor proteins. *Neuron*, **15**(5):1203-18

Hu, W., Wu, F., Zhang, Y., Gong, C.-X., Iqbal, K., & Liu, F. (2017). Expression of Tau Pathology-Related Proteins in Different Brain Regions: A Molecular Basis of Tau Pathogenesis. *Frontiers in Aging Neuroscience*, **9**:311

Hung, S. and Fu, W. (2017). Drug candidates in clinical trials for Alzheimer's disease. *Journal of Biomedical Science*, **24**(1)

Iba, M., McBride, J. D., Guo, J. L., Zhang, B., Trojanowski, J. Q., & Lee, V. M.-Y. (2015). Tau Pathology Spread in PS19 Tau Transgenic Mice Following Locus Coeruleus (LC) Injections of Synthetic Tau Fibrils is Determined by the LC's Afferent and Efferent Connections. *Acta Neuropathologica*, **130**(3):349–362

Iijima-Ando, K., & Iijima, K. (2010). Transgenic *Drosophila* models of Alzheimer's disease and tauopathies. *Brain Structure & Function*, **214**(2-3):245–262

Iqbal, K., Grundke-Iqbal, I., Smith, A. J., George, L., Tung, Y. C., & Zaidi, T. (1989). Identification and localization of a tau peptide to paired helical filaments of Alzheimer disease. *Proceedings of the National Academy of Sciences of the United States of America*, **86**(14):5646–5650

Irie, F., Fitzpatrick, A., Lopez, O., Kuller, L., Peila, R., Newman, A. and Launer, L. (2008). Enhanced risk for Alzheime's Disease in persons with type 2 Diabetes and APOE ε4. *Archives of Neurology*, **65**(1)

Irizarry, M.C., McNamara, M., Fedorchak, K., Hsiao, K., Hyman, B.T. (1997). APPSw transgenic mice develop age-related A beta deposits and neuropil abnormalities, but no neuronal loss in CA1. *Journal of neuropathology and experimental neurology*, **56**(9): 965-73

Israel, M. A., Yuan, S. H., Bardy, C., Reyna, S. M., Mu, Y., Herrera, C., Goldstein, L. S. B. (2012). Probing sporadic and familial Alzheimer's disease using induced pluripotent stem cells. *Nature*, **482**(7384):216–220

J.A. Hardy, G.A. Higgins. (1992). Alzheimer's disease: the amyloid cascade hypothesis, *Science*, **256**(1992):184-185

Jackson, M. and Hewitt, E. (2016). Cellular proteostasis: degradation of misfolded proteins by lysosomes. *Essays In Biochemistry*, **60**(2):173-180

Jadhav, S., Cubinkova, V., Zimova, I., Brezovakova, V., Madari, A., Cigankova, V. and Zilka, N. (2015). Tau-mediated synaptic damage in Alzheimer's disease. *Translational Neuroscience*, **6**(1)

Jaeger, P.A., Pickford, F., Sun, C.H., Lucin, K.M., Masliah, E.,Wyss-Coray, T. (2005). Regulation of amyloid precursor protein processing by the Beclin 1 complex. *PLoS One*, **5**:e11102

Jäkel, S. and Dimou, L. (2017). Glial Cells and Their Function in the Adult Brain: A Journey through the History of Their Ablation. *Frontiers in Cellular Neuroscience*, **11**

Jiang, T., Yu, J.T., Zhu, X.C., Tan, M.S., Wang, H.F., Cao, L., Zhang, Q.Q., Shi, J.Q., Gao, L., Qin, H., Zhang, Y.D., Tan, L. (2014). Temsirolimus promotes autophagic clearance of amyloid-beta and provides protective effects in cellular and animal models of Alzheimer's disease. Pharmacological Research, **81**:54–63

Joshi, P., Liang, J., DiMonte, K., Sullivan, J. and Pimplikar, S. (2009). Amyloid precursor protein is required for convergent-extension movements during Zebrafish development. *Developmental Biology*, **335**(10):1-11

Jung, C. H., Ro, S.-H., Cao, J., Otto, N. M., & Kim, D.-H. (2010). mTOR regulation of autophagy. *FEBS Letters*, **584**(7):1287–1295

Jung, C.H., Jun, C.B., Ro, S.H., Kim, Y.M., Otto, N.M., Cao, J., Kundu, M., Kim, D.H. (2009). ULK-Atg13-FIP200 complexes mediate mTOR signaling to the autophagy machinery. *Molecular Biology of the Cell*, **20**(7):1992-2003

Kahlson, M. A., & Colodner, K. J. (2015). Glial Tau Pathology in Tauopathies: Functional Consequences. *Journal of Experimental Neuroscience*, **9**(2), 43–50

Kalueff, A., Stewart, A. and Gerlai, R. (2014). Zebrafish as an emerging model for studying complex brain disorders. *Trends in Pharmacological Sciences*, **35**(2):63-75

Kamada, Y., Yoshino, K., Kondo, C., Kawamata, T., Oshiro, N., Yonezawa, K. and Ohsumi, Y. (2009). Tor Directly Controls the Atg1 Kinase Complex To Regulate Autophagy. *Molecular and Cellular Biology*, 30(4), pp.1049-1058

Kaminskyy, V. and Zhivotovsky, B. (2012). Proteases in autophagy. *Biochimica et Biophysica Acta (BBA) - Proteins and Proteomics*, **1824**(1), 44-50

Kanaan, N.M., Morfini, G., Pigino, G., LaPointe, N.E., Andreadis, A., Song, Y., Leitman, E., Binder, L.I. and Brady, S.T. (2012). Phosphorylation in the amino terminus of tau prevents inhibition of anterograde axonal transport. *Neurobiology of Ageing*, **33**(4): 826.e15–826.e30

Kanekiyo, T., Xu, H. and Bu, G. (2014). ApoE and Aβ in Alzheimer's Disease: Accidental Encounters or Partners? *Neuron*, 8**1**(4):740-754

Karabiyik, C., Lee, M. and Rubinsztein, D. (2017). Autophagy impairment in Parkinson's disease. *Essays In Biochemistry*, **61**(6):711-720

Karantzoulis, S., & Galvin, J. E. (2011). Distinguishing Alzheimer's disease from other major forms of dementia. *Expert Review of Neurotherapeutics*, *11*(11):1579–1591

Karran, E. and Strooper, B.D (2016). The amyloid cascade hypothesis: are we poised for success or failure? *Journal of Neurochemistry*, 10.1111/jnc.13632

Karran, E. and Hardy, J. (2014) A critique of the drug discovery and phase 3 clinical programs targeting the amyloid hypothesis for Alzheimer disease. *Annals of Neurolology,* **76**: 185–205

Kaushik, S., Cuervo, A.M. (2009). Methods to monitor chaperone-mediated autophagy. *Methods Enzymology,* **452**:297-324

Kayed, R. (2010) Anti-tau oligomers passive vaccination for the treatment of Alzheimer disease, *Human Vaccines*, **6**(11):931-935

Kazuhiro, I., Kazuma, M., Yuichi, M., Akira, M., Hajime, O., Ryutaro, O., Kiyonori, T., Masaya, N., Takahiko, S., Takuji. S. (2005) Structure of β-amyloid fibrils and its relevance to their neurotoxicity: implications for the pathogenesis of Alzheimer's disease. *Journal of Bioscience and Bioengineering*, **99** (5): 437-447

Kiffin, R., Bandyopadhyay, U. and Cuervo, A. (2006). Oxidative Stress and Autophagy. *Antioxidants & Redox Signaling*, **8**(1-2):152-162

Kim, J., Kundu, M., Viollet, B. and Guan, K. (2011). AMPK and mTOR regulate autophagy through direct phosphorylation of Ulk1. *Nature Cell Biology*, **13**(2):132-141

Klionsky, D.J. (2007). Autophagy: from phenomenology to molecular understanding in less than a decade. *Nature Reviews Molecular Cell Biology*, **8**:931–937

Koga, H., Cuervo, A.M. (2011).Chaperone-mediated autophagy dysfunction in the pathogenesis of neurodegeneration. *Neurobiology of disease*, **43**:29–37

Kopeikina, K. J., Hyman, B. T., & Spires-Jones, T. L. (2012). Soluble forms of tau are toxic in Alzheimer's disease. *Translational Neuroscience*, **3**(3):223–233

Korde, A. and Maragos, W. (2012). Identification of anN-Methyl-d-aspartate Receptor in Isolated Nervous System Mitochondria. *Journal of Biological Chemistry*, **287**(42):35192-35200

Kovari, E., Herrmann, F., Bouras, C. and Gold, G. (2013). Amyloid deposition is decreasing in aging brains: An autopsy study of 1,599 older people. *Neurology*, **82**(4):326-331.

Kowalska, A. (2004). The beta-amyloid cascade hypothesis: a sequence of events leading to neurodegeneration in Alzheimer's disease. *Neurologia i neurochirurgia polska*, **38**(5):405-11

Krause, W. (2005). *Krause's essential human histology for medical students*. Pathology and Anatomical Sciences, **87**

Krüger, U., Wang, Y., Kumar, S. and Mandelkow, E. (2012). Autophagic degradation of tau in primary neurons and its enhancement by trehalose. *Neurobiology of Aging*, **33**(10):2291-2305

Kurosinski, P. and Götz, J. (2002). Glial cells under physiologic and pathologic conditions. *Archives of Neurology*, **59**(10):1524

Lace, G., Savva, G.M., Forster, G., Silva, R., Brayne, C., Matthews, F.E., Barclay, J.J., Dakin, L., Ince, P.G., Wharton, S.B. (2009). Hippocampal tau pathology is related to neuroanatomical connections: an ageing population-based study. *A journal of neurology*, **132**:1324-1334

Lan, A., Chen, J., Zhao, Y., Chai, Z. and Hu, Y. (2016). mTOR Signaling in Parkinson's Disease. *NeuroMolecular Medicine*, **19**(1):1-10

Law, B. (2005). Rapamycin: An anti-cancer immunosuppressant? *Critical Reviews in Oncology/Hematology*, **56**(1):47-60

Lee, J. and Cole, G. (2007). Generation of Transgenic Zebrafish Expressing Green Fluorescent Protein Under Control of Zebrafish Amyloid Precursor Protein Gene Regulatory Elements. *Zebrafish*, **4**(4):277-286

Lee, J., Giordano,S., Zhang, J.(2012) Autophagy, mitochondria and oxidative stress: cross-talk and redox signalling. *Biochemical Journal*, **441**(2): 523–540

Lee, J., McBrayer, M., Wolfe, D., Haslett, L., Kumar, A., Sato, Y., Lie, P., Mohan, P., Coffey, E., Kompella, U., Mitchell, C., Lloyd-Evans, E. and Nixon, R. (2015). Presenilin 1 maintains lysosomal Ca2+ homeostasis via TRPML1 by regulating vATPase-mediated lysosome acidification. *Cell Reports*, 12(9), pp.1430-1444.Lee, J., Yu, W., Kumar, A., Lee, S., Mohan, P., Peterhoff, C., Wolfe, D., Martinez-Vicente, M., Massey, A., Sovak, G., Uchiyama, Y., Westaway, D., Cuervo, A. and Nixon, R. (2010). Lysosomal Proteolysis and Autophagy Require Presenilin 1 and Are Disrupted by Alzheimer-Related PS1 Mutations. *Cell*, **141**(7):1146-1158

Lee, J.-H., Yu, W. H., Kumar, A., Lee, S., Mohan, P. S., Peterhoff, C. M., Nixon, R. A. (2010). Lysosomal Proteolysis and Autophagy Require Presenilin 1 and Are Disrupted by Alzheimer-Related PS1 Mutations. *Cell*, **141**(7):1146–1158

Lee, S., Sato, Y., & Nixon, R. A. (2011). Lysosomal proteolysis inhibition selectively disrupts axonal transport of degradative organelles and causes an Alzheimer's-like axonal dystrophy. *The Journal of Neuroscience*, **31**(21):7817–7830

Lee, V., Balin, B., Otvos, L. and Trojanowski, J. (1991). A68: a major subunit of paired helical filaments and derivatized forms of normal Tau. *Science*, **251**(4994):675-678

Leimer, U., Lun, K., Romig, H., Walter, J., Grünberg, J., Brand, M. and Haass, C. (1999). Zebrafish (Danio rerio) Presenilin Promotes Aberrant

Amyloid β-Peptide Production and Requires a Critical Aspartate Residue for Its Function in Amyloidogenesis†. *Biochemistry*, **38**(41):13602-13609

Leitner, M. G. (2014). Zebrafish in auditory research: are fish better than mice? *The Journal of Physiology*, **592**(Pt 21):4611–4612

Lemmens, M. A. M., Sierksma, A. S. R., Rutten, B. P. F., Dennissen, F., Steinbusch, H. W. M., Lucassen, P. J., & Schmitz, C. (2011). Age-related changes of neuron numbers in the frontal cortex of a transgenic mouse model of Alzheimer's disease. *Brain Structure & Function*, **216**(3):227–237

Lesné, S., Koh, M., Kotilinek, L., Kayed, R., Glabe, C., Yang, A., Gallagher, M. and Ashe, K. (2006). A specific amyloid-β protein assembly in the brain impairs memory. *Nature*, **440**(7082):352-357

Levy-Lehad, E., Wasco, W., Poorkaj, P., et al. (1995). Candidate gene for the chromosome 1 familial Alzheimer's disease locus. *Science*, **269**:973-7

Lewandowski, N., Ju, S., Verbitsky, M., Ross, B., Geddie, M., Rockenstein, E., Adame, A., Muhammad, A., Vonsattel, J., Ringe, D., Cote, L., Lindquist, S., Masliah, E., Petsko, G., Marder, K., Clark, L. and Small, S. (2010). Polyamine pathway contributes to the pathogenesis of Parkinson disease. *Proceedings of the National Academy of Sciences*, **107**(39):16970-16975

Lewis, J. (2001). Enhanced Neurofibrillary Degeneration in Transgenic Mice Expressing Mutant Tau and APP. *Science*, **293**(5534):1487-1491

Leyns, C. E. G., & Holtzman, D. M. (2017). Glial contributions to neurodegeneration in tauopathies. *Molecular Neurodegeneration*, **12**:50

Li, W., Tang, Y., Fan, Z., Meng, Y., Yang, G., Luo, J. and Ke, Z. (2013). Autophagy is involved in oligodendroglial precursor-mediated clearance of amyloid peptide. *Molecular Neurodegeneration*, **8**(1):27

Liang, X.H., Jackson, S., Seaman, M., Brown, K., Kempkes, B., et al. (1999). Induction of autophagy and inhibition of tumorigenesis by beclin 1. *Nature*, **402**:672–76

Lippai, M., & Lőw, P. (2014). The Role of the Selective Adaptor p62 and Ubiquitin-Like Proteins in Autophagy. *BioMed Research International*, **2014**:832704

Liu, B., Tang, J., Zhang, J., Li, S., Yuan, M., & Wang, R. (2014). Autophagy activation aggravates neuronal injury in the hippocampus of vascular dementia rats. *Neural Regeneration Research*, **9**(13):1288–1296

Liu, B., Tang, J., Zhang, J., Li, S., Yuan, M., & Wang, R. (2014). Autophagy activation aggravates neuronal injury in the hippocampus of vascular dementia rats. *Neural Regeneration Research*, **9**(13):1288–1296

Liu, C., Kanekiyo, T., Xu, H. and Bu, G. (2013). Apolipoprotein E and Alzheimer disease: risk, mechanisms and therapy. *Nature Reviews Neurology*, **9**(2):106-118.

Liu, C.-C., Kanekiyo, T., Xu, H., & Bu, G. (2013). Apolipoprotein E and Alzheimer disease: risk, mechanisms, and therapy. *Nature Reviews. Neurology*, **9**(2), 106–118

Liu, F. and Gong, C. (2008). Tau exon 10 alternative splicing and tauopathies. *Molecular Neurodegeneration*, **3**(1):8

Liu, J., Liu, M. and Wang, K. (2008). Calpain in the CNS: From Synaptic Function to Neurotoxicity. *Science Signaling*, **1**(14):re1-re1

Liu, L., Li, C., Lu, Y., Zong, X., Luo, C., Sun, J., & Guo, L. (2015). Baclofen mediates neuroprotection on hippocampal CA1 pyramidal cells through the regulation of autophagy under chronic cerebral hypoperfusion. *Scientific Reports*, **5**

Liu, Y., Su, Y., Wang, J., Sun, S., Wang, T., Qiao, X., Run, X., Li, H. and Liang, Z. (2013). Rapamycin decreases tau phosphorylation at Ser214 through regulation of cAMP-dependent kinase. *Neurochemistry International*, **62**(4):458-467

Lopategui Cabezas, I., Herrera Batista, A. and Pentón Rol, G. (2014). Papel de la glía en la enfermedad de Alzheimer. Futuras implicaciones terapéuticas. *Neurología*, **29**(5):305-309

Louis, E.D., Bain, P.G., Hallett, M., Jankovic, J. & Vonsattel, J.P.G. (2013). What is it? Difficult to Pigeon Hole Tremor: a Clinical–Pathological Study of a Man with Jaw. *Tremor and other hyperkinetic movements*, 3: tre-03-174-4112-1

Lu, R.-C., Tan, M.-S., Wang, H., Xie, A.-M., Yu, J.-T., & Tan, L. (2014). Heat Shock Protein 70 in Alzheimer's disease. *BioMed Research International*, **2014**:435203

Lynch-Day, M. A., Mao, K., Wang, K., Zhao, M., & Klionsky, D. J. (2012). The Role of Autophagy in Parkinson's disease. *Cold Spring Harbor Perspectives in Medicine*, **2**(4), a009357

Magini, A., Urbanelli, L, Ciccarone V, Tancini B, Polidoro M, Timperio AM, Zolla L, Tedde A, Sorbi S, Emiliani C. (2010). Fibroblasts from PS1 mutated pre-symptomatic subjects and Alzheimer's disease patients share a unique protein levels profile. Journal of Alzheimer's disease, **21(**2):431-44

Majumder, S., Richardson, A., Strong, R. and Oddo, S. (2011). Inducing Autophagy by Rapamycin Before, but Not After, the Formation of Plaques and Tangles Ameliorates Cognitive Deficits. *PLoS ONE*, **6**(9):e25416

Manoharan, S., Guillemin, G. J., Abiramasundari, R. S., Essa, M. M., Akbar, M., & Akbar, M. D. (2016). The Role of Reactive Oxygen Species in the Pathogenesis of Alzheimer 's disease, Parkinson's Disease, and Huntington's Disease: A Mini Review. *Oxidative Medicine and Cellular Longevity*, *2016*, 8590578

Marin, C. and Aguilar, E. (2011). In vivo 6-OHDA-induced neurodegeneration and nigral autophagic markers expression. *Neurochemistry International*, **58**(4):521-526

Marina Aunapuu, A. (2018). *The cerebral cortex*: Sisu.ut.ee. Available online at: https://sisu.ut.ee/histology/cerebral-cortex [Accessed 2 Feb. 2018]

Marques, F., Sousa, J. C., Coppola, G., Geschwind, D. H., Sousa, N., Palha, J. A., et al. (2008). The choroid plexus response to a repeated peripheral inflammatory stimulus. *BMC Neuroscience.* **10**(135)

Martin, L., Latypova, X., Wilson, C., Magnaudeix, A., Perrin, M., Yardin, C. and Terro, F. (2013). Tau protein kinases: Involvement in Alzheimer's disease. *Ageing Research Reviews*, 12(1):289-309.Martinet, W., Schrijvers, D.M., Timmermans, H.B. and De Meyer, G.R.Y. (2013). Immunohistochemical analysis of macroautophagy. *Autophagy*, 9 (3): 386-402

Martinez-Lopez, N., Athonvarangkul, D., & Singh, R. (2015). Autophagy and Aging. *Advances in Experimental Medicine and Biology*, **847**:73–87

Massey, A. C., Kaushik, S., Sovak, G., Kiffin, R., & Cuervo, A. M. (2006). Consequences of the selective blockage of chaperone-mediated autophagy. *Proceedings of the National Academy of Sciences of the United States of America*, **103**(15):5805–5810

Mathillas, J., Lovheim, H. and Gustafson, Y. (2011). Increasing prevalence of dementia among very old people. *Age and Ageing*, **40**(2):243-249

Matsui, T., Ingelsson, M., Fukumoto, H., Ramasamy, K., Kowa, H., Frosch, M., Irizarry, M. and Hyman, B. (2007). Expression of APP pathway mRNAs and proteins in Alzheimer's disease. *Brain Research*, **1161**:116-123

Matsuzaki, T., Sasaki, K., Tanizaki, Y., Hata, J., Fujimi, K., Matsui, Y., Sekita, A., Suzuki, S., Kanba, S., Kiyohara, Y. and Iwaki, T. (2010). Insulin resistance is associated with the pathology of Alzheimer disease: The Hisayama Study. *Neurology*, **75**(9):764-770

Mayer, M. P., & Bukau, B. (2005). Hsp70 chaperones: Cellular functions and molecular mechanism. *Cellular and Molecular Life Sciences*, **62**(6):670–684

McKnight, N. C., Zhong, Y., Wold, M. S., Gong, S., Phillips, G. R., Dou, Z., Yue, Z. (2014). Beclin 1 Is Required for Neuron Viability and Regulates Endosome Pathways via the UVRAG-VPS34 Complex. *PLoS Genetics*, **10**(10):e1004626

Mena, M. and García de Yébenes, J. (2008). Glial Cells as Players in Parkinsonism: The "Good," the "Bad," and the "Mysterious" Glia. *The Neuroscientist*, **14**(6):544-560

Mercer, C.A., Kaliappan, A., Dennis, P.B. (2009). A novel, human Atg13 binding protein, Atg101, interacts with ULK1 and is essential for macroautophagy. Autophagy, **5**(5):649-62

Meriin, A. and Sherman, M. (2005). Role of molecular chaperones in neurodegenerative disorders. *International Journal of Hyperthermia*, **21**(5):403-419

Messner, B. and Bernhard, D. (2014). Smoking and Cardiovascular Disease: Mechanisms of Endothelial Dysfunction and Early Atherogenesis. *Arteriosclerosis, Thrombosis, and Vascular Biology*, **34**(3):509-515

Mietelska-Porowska, A., Wasik, U., Goras, M., Filipek, A. and Niewiadomska, G. (2014). Tau Protein Modifications and Interactions: Their Role in Function and Dysfunction. *International Journal of Molecular Sciences*, **15**(3):4671-4713

Mijaljica, D., Prescott, M. and Devenish, R.J. (2011). Microautophagy in mammalian cells: Revisiting a 40-year-old conundrum. *Autophagy*, **7**(7): 673-682

Miller, O., Bruns, A., Ben Ammar, I., Mueggler, T. and Hall, B. (2017). Synaptic Regulation of a Thalamocortical Circuit Controls Depression-Related Behavior. *Cell Reports*, **20**(8):1867-1880

Mirra, S.S., Heyman, A., McKeel, D., Sumi, S.M., Crain, B.J., Brownlee, L.M., Vogel, F.S., Hughes, J.P., van Belle, G., Berg, L. (1991). The Consortium to Establish a Registry for Alzheimer's disease (CERAD). Part II. Standardization of the neuropathologic assessment of Alzheimer's disease. Neurology, **41**(4):479-86

Mitchell, A. (2015). The mediodorsal thalamus as a higher order thalamic relay nucleus important for learning and decision-making. *Neuroscience & Biobehavioral Reviews*, **54**:76-88

Mitchell, S. L. (2015). Advanced Dementia. *The New England Journal of Medicine*, **373**(13):1276–1277

Mitew, S., Kirkcaldie, M., Halliday, G., Shepherd, C., Vickers, J. and Dickson, T. (2010). Focal demyelination in Alzheimer's disease and transgenic mouse models. *Acta Neuropathologica*, **119**(5):567-577

Mizushima, N. (2015). Nbr1, a Receptor for ESCRT-Dependent Endosomal Microautophagy in Fission Yeast. *Molecular Cell*, **59**(6):887-889.

Mocali, A., Malva, N.D., Abete, C., et al. (2014). Altered proteolysis in fibroblasts of Alzheimer patients with predictive implications for subjects at risk of disease. *International Journal of Alzheimer's Disease*, **2014**:1-8

Morgan, D., Diamond, D., Gottschall, P., Ugen, K., Dickey, C., Hardy, J., Duff, K., Jantzen, P., DiCarlo, G., Wilcock, D., Connor, K., Hatcher, J., Hope, C., Gordon, M. and Arendash, G. (2000). Aβ peptide vaccination prevents memory loss in an animal model of Alzheimer's disease. *Nature*, **408**(6815):982-985

Morishima, M., Morita, K., Kubota, Y. and Kawaguchi, Y. (2011). Highly Differentiated Projection-Specific Cortical Subnetworks. *Journal of Neuroscience*, **31**(28):10380-10391

Morozov, A., Yurinskaya, M., Mitkevich, V., Garbuz, D., Preobrazhenskaia, O., Vinokurov, M., Evgen'ev, M., Karpov, V. and Makarov, A. (2017). Heat-shock protein HSP70 decreases activity of proteasomes in human

neuroblastoma cells treated by amyloid-beta 1-42 with isomerized Asp7. *Molecular Biology*, **51**(1):143-147

Morris, G., Clark, I. and Vissel, B. (2014). Inconsistencies and Controversies Surrounding the Amyloid Hypothesis of Alzheimer's Disease. *Acta Neuropathologica Communications*, **2**(1)

Moscat, J. and Diaz-Meco, M. (2009). p62 at the Crossroads of Autophagy, Apoptosis, and Cancer. *Cell*, **137**(6):1001-1004

Moszczynski, A. J., Yang, W., Hammond, R., Ang, L. C., & Strong, M. J. (2017). Threonine[175], a novel pathological phosphorylation site on tau protein linked to multiple tauopathies. *Acta Neuropathologica Communications*, **5**:6

Mufson, E. J., Counts, S. E., Perez, S. E., & Ginsberg, S. D. (2008). Cholinergic system during the progression of Alzheimer's disease: therapeutic implications. *Expert Review of Neurotherapeutics*, **8**(11):1703–1718

Müller, U. C., & Zheng, H. (2012). Physiological Functions of APP Family Proteins. *Cold Spring Harbor Perspectives in Medicine*, **2**(2):a006288

Murayama, S. and Saito, Y. (2004). Neuropathological diagnostic criteria for Alzheimer's disease. *Neuropathology*, **24**(3):254-260

Musa, A., Lehrach, H. and Russo, V. (2001). Distinct expression patterns of two zebrafish homologues of the human APP gene during embryonic development. *Development Genes and Evolution*, **211(**11):563-567

Narayanan, R. T., Egger, R., Johnson, A. S., Mansvelder, H. D., Sakmann, B., de Kock, C. P. J., & Oberlaender, M. (2015). Beyond Columnar Organization: Cell Type- and Target Layer-Specific Principles of Horizontal Axon Projection Patterns in Rat Vibrissal Cortex. *Cerebral Cortex (New York, NY)*, **25**(11):4450–4468

Nasrabady, S., Rizvi, B., Goldman, J. and Brickman, A. (2018). White matter changes in Alzheimer's disease: a focus on myelin and oligodendrocytes. *Acta Neuropathologica Communications*, **6**(1)

Nedergaard, M., Takano, T. and Hansen, A. (2002). Beyond the role of glutamate as a neurotransmitter. *Nature Reviews Neuroscience*, **3**(9):748-755

Nelson, P. T., Alafuzoff, I., Bigio, E. H., Bouras, C., Braak, H., Cairns, N. J., Beach, T. G. (2012). Correlation of Alzheimer Disease neuropathologic changes with cognitive status: a review of the literature. *Journal of Neuropathology and Experimental Neurology*, **71**(5), 362–381

Newman, M., Ebrahimie, E., & Lardelli, M. (2014). Using the zebrafish model for Alzheimer's disease research. *Frontiers in Genetics*, **5**:189

Newman, M., Verdile, G., Martins, R. and Lardelli, M. (2011). Zebrafish as a tool in Alzheimer's disease research. *Biochimica et Biophysica Acta (BBA) - Molecular Basis of Disease*, **1812**(3):346-352

Nicoll, J.A., Roberts, G.W., Graham, D.I. (2005). Apolipoprotein E epsilon 4 allele is associated with deposition of amyloid beta-protein following head injury. Nature Medicine, **1**(2):135-7

Nieweg, K., Andreyeva, A., van Stegen, B., Tanriöver, G. and Gottmann, K. (2015). Alzheimer's disease-related amyloid-β induces synaptotoxicity in human iPS cell-derived neurons. *Cell Death & Disease*, **6**(4):e1709-e1709

Nikoletopoulou, V., Papandreou, M.-E., & Tavernarakis, N. (2015). Autophagy in the physiology and pathology of the central nervous system. *Cell Death and Differentiation*, **22**(3):398–407

Nishino, I., Fu, J., Tanji, K., Yamada, T., Shimojo, S., Koori, T., Mora, M., Riggs, J., Oh, S., Koga, Y. et al. (2000). Primary LAMP-2 deficiency causes X-linked vacuolar cardiomyopathy and myopathy (Danon disease). *Nature,* **406**:906-910

Nishiyama, J., Miura, N., Mizushima, N., Watanabe, M., Yuzaki, M. (2007). Aberrant membranes and double-membrane structures accumulate in the axons of Atg5-null Purkinje cells before neuronal death, *Autophagy 3* - 591–596

Nixon, R.A. (2013). The role of autophagy in neurodegenerative disease. *Nature Medicine,* **19**(8):983-97

Nixon, R.A. Autophagy, amyloidogenesis and Alzheimer disease. (2007) *Journal of Cell Science,* **120**:4081-91

Nixon, R.A., Wegiel, J., Kumar, A., Yu, W.H., Peterhoff, C., Cataldo, A., *et al.* (2005). Extensive involvement of autophagy in Alzheimer disease: an immuno-electron microscopy study. *Journal of Neuropathology and Experimental Neurology*, **64**:113-22

Norton, W. (2013). Toward developmental models of psychiatric disorders in zebrafish. *Frontiers in Neural Circuits*, **7**

Nunomura, A. (2006). Neuropathology in Alzheimer's disease: awaking from a hundred-year-old dream. *Science of aging knowledge environment: SAGE KE*, **2006** (8)

O'Brien, R. J., & Wong, P. C. (2011). Amyloid Precursor Protein Processing and Alzheimer's Disease. *Annual Review of Neuroscience*, **34**:185–204

Oberlaender, M., de Kock, C. P. J., Bruno, R. M., Ramirez, A., Meyer, H. S., Dercksen, V. J., Sakmann, B. (2012). Cell Type–Specific Three-Dimensional Structure of Thalamocortical Circuits in a Column of Rat Vibrissal Cortex. *Cerebral Cortex (New York, NY)*, **22**(10):2375–2391

Orr, M. E., & Oddo, S. (2013). Autophagic/lysosomal dysfunction in Alzheimer's disease. *Alzheimer's Research & Therapy*, **5**(5), 53

Ortiz-Virumbrales, M., Moreno, C., Kruglikov, I., Marazuela, P., Sproul, A., Jacob, S., Zimmer, M., Paull, D., Zhang, B., Schadt, E., Ehrlich, M., Tanzi, R., Arancio, O., Noggle, S. and Gandy, S. (2017). CRISPR/Cas9-Correctable mutation-related molecular and physiological phenotypes in

iPSC-derived Alzheimer's PSEN2 N141I neurons. *Acta Neuropathologica Communications*, **5**(1)

Osellame, L. D., Rahim, A. A., Hargreaves, I. P., Gegg, M. E., Richard-Londt, A., Brandner, S., Duchen, M. R. (2013). Mitochondria and Quality Control Defects in a Mouse Model of Gaucher Disease—Links to Parkinson's Disease. *Cell Metabolism*, **17**(6), 941–953

Pajares, M., Cuadrado, A., Engedal, N., Jirsova, Z. and Cahova, M. (2018). The Role of Free Radicals in Autophagy Regulation: Implications for Ageing. *Oxidative Medicine and Cellular Longevity*, **2018**:1-19

Pankiv, S., Clausen, T., Lamark, T., Brech, A., Bruun, J., Outzen, H., Øvervatn, A., Bjørkøy, G. and Johansen, T. (2007). p62/SQSTM1 Binds Directly to Atg8/LC3 to Facilitate Degradation of Ubiquitinated Protein Aggregates by Autophagy. *Journal of Biological Chemistry*, **282**(33):24131-24145

Panula, P., Sallinen, V., Sundvik, M., Kolehmainen, J., Torkko, V., Tiittula, A., Moshnyakov, M. and Podlasz, P. (2006). Modulatory Neurotransmitter Systems and Behavior: Towards Zebrafish Models of Neurodegenerative Diseases. *Zebrafish*, **3**(2):235-247

Panza, F., Frisardi, V., Solfrizzi, V., Imbimbo, B.P., Logroscino, G., Santamato, A., Greco, A., Seripa, D., Pilotto, A. (2011). Interacting with γ-secretase for treating Alzheimer's disease: from inhibition to modulation. *Current medical chemistry*, **18**(35):5430-47

Papinski, D. and Kraft, C. (2016). Regulation of Autophagy By Signaling Through the Atg1/ULK1 Complex. *Journal of Molecular Biology*, **428**(9):1725-1741

Parihar, M.S., Hemnani, T. (2004). Alzheimer's disease pathogenesis and therapeutic interventions. *Journal of Clinical Neuroscience*, **11**(5):456-467

Park, C., & Cuervo, A. M. (2013). Selective Autophagy: talking with the UPS. *Cell Biochemistry and Biophysics*, **67**(1):3–13

Patel, B., & Cuervo, A. M. (2015). Methods to study chaperone-mediated autophagy. *Methods (San Diego, Calif.)*, **75**:133–140

Paulson, J. B., Ramsden, M., Forster, C., Sherman, M. A., McGowan, E., & Ashe, K. H. (2008). Amyloid Plaque and Neurofibrillary Tangle Pathology in a Regulatable Mouse Model of Alzheimer's Disease. *The American Journal of Pathology*, **173**(3), 762–772

Peila, R., Rodriguez, B. and Launer, L. (2002). Type 2 Diabetes, APOE Gene, and the Risk for Dementia and Related Pathologies: The Honolulu-Asia Aging Study. *Diabetes*, **51**(4):1256-1262

Pepeu, G. and Giovannini, M. (2010). Cholinesterase inhibitors and memory. *Chemico-Biological Interactions*, **187**(1-3):403-408

Pérez, L., McLetchie, S., Gardiner, G. J., Deffit, S. N., Zhou, D., & Blum, J. S. (2016). LAMP-2C inhibits MHC class II presentation of cytoplasmic

antigens by disrupting chaperone-mediated autophagy. *Journal of Immunology (Baltimore, Md. : 1950)*, **196**(6):2457–2465

Perl, D.P. (2010) Neuropathology of Alzheimer's disease. *Mount Sinai Journal of Medicine*, **77**:32-42

Perry, E., Gibson, P., Blessed, G., Perry, R. and Tomlinson, B. (1977). Neurotransmitter enzyme abnormalities in senile dementia. *Journal of the Neurological Sciences*, **34**(2):247-265

Petersen, R., Thomas, R., Grundman, M., Bennett, D., Doody, R., Ferris, S., Galasko, D., Jin, S., Kaye, J., Levey, A., Pfeiffer, E., Sano, M., van Dyck, C. and Thal, L. (2005). Vitamin E and Donepezil for the Treatment of Mild Cognitive Impairment. *New England Journal of Medicine*, **352**(23):2379-2388

Petroff, O. (2002). Book Review: GABA and Glutamate in the Human Brain. *The Neuroscientist*, **8**(6):562-573

Pickford, F., Masliah, E., Britschgi, M., Lucin, K., Narasimhan, R., Jaeger, P.A., *et al.* (2008).The autophagy-related protein beclin 1 shows reduced expression in early Alzheimer disease and regulates amyloid beta accumulation in mice. *Journal of Clinical Investigation*, **118**:2190-9

Pikkarainen, M., Kauppinen, T. and Alafuzoff, I. (2009). Hyperphosphorylated Tau in the Occipital Cortex in Aged Nondemented Subjects. *Journal of Neuropathology and Experimental Neurology*, **68**(6):653-660

Pi-Sunyer, X. (2009). The Medical Risks of Obesity. *Postgraduate Medicine*, *121*(6), 21–33

Platt, F., Boland, B. and van der Spoel, A. (2012). Lysosomal storage disorders: The cellular impact of lysosomal dysfunction. *The Journal of Cell Biology*, **199**(5):723-734

Popelka, H., Damasio, A., Hinshaw, J., Klionsky, D. and Ragusa, M. (2017). Structure and function of yeast Atg20, a sorting nexin that facilitates autophagy induction. *Proceedings of the National Academy of Sciences*, **114**(47):E10112-E10121

Portbury, S. D., Hare, D. J., Sgambelloni, C., Perronnes, K., Portbury, A. J., Finkelstein, D. I., & Adlard, P. A. (2017). Trehalose Improves Cognition in the Transgenic Tg2576 Mouse Model of Alzheimer's Disease. *Journal of Alzheimer's Disease*, **60**(2):549–560

Prince, M., Bryce, R., Albanese, E., Wimo, A., Ribeiro, W. and Ferri, C. (2013). The global prevalence of dementia: A systematic review and metaanalysis. *Alzheimer's & Dementia*, **9**(1):63-75

Prüßing, K., Voigt, A., & Schulz, J. B. (2013). Drosophila melanogaster as a model organism for Alzheimer's disease. *Molecular Neurodegeneration*, **8**:35

Qiu, C., Kivipelto, M., Strauss, E. (2009). Epidemiology of Alzheimer's disease: occurrence, determinants, and strategies toward intervention. *Dialogues in Clinical sciences*, **11**(2): 111–128

Qiu, L., Ng, G., Tan, E. K., Liao, P., Kandiah, N., & Zeng, L. (2016). Chronic cerebral hypoperfusion enhances Tau hyperphosphorylation and reduces autophagy in Alzheimer's disease mice. *Scientific Reports*, **6**:23964

Rahimi, J., Milenkovic, I. and Kovacs, G. (2015). Patterns of Tau and α-Synuclein Pathology in the Visual System. *Journal of Parkinson's Disease*, **5**(2):333-340

Rajmohan, V., & Mohandas, E. (2007). The limbic system. *Indian Journal of Psychiatry*, **49**(2), 132–139

Ramamoorthy, M., Sykora, P., Scheibye-Knudsen, M., Dunn, C., Kasmer, C., Zhang,Y., Becker KG, Croteau DL, Bohr VA. (2012) Sporadic Alzheimer disease fibroblasts: Display an oxidative stress phenotype. *Free Radical Biology and Medicine.*15, **53**(6):1371-1380

Ray, A., Speese, S. and Logan, M. (2017). Glial Draper Rescues Aβ Toxicity in aDrosophilaModel of Alzheimer's Disease. *The Journal of Neuroscience*, **37**(49):11881-11893

Razmara, A., Duckles, S., Krause, D. and Procaccio, V. (2007). Estrogen suppresses brain mitochondrial oxidative stress in female and male rats. *Brain Research*, **1176**:71-81

Reitz, C. (2012). Alzheimer's Disease and the Amyloid Cascade Hypothesis: A Critical Review. *International Journal of Alzheimer's Disease*, ***2012***:369808

Relkin, N., Szabo, P., Adamiak, B., et al. (2005). Intravenous immunoglobulin (IVIg) treatment causes dose-dependent alterations in β-amyloid (Aβ) levels and anti-Aβ antibody titers in plasma and cerebrospinal fluid (CSF) of Alzheimer's disease (AD) patients. *Neurology*, **64**:A144

Rico, E., Rosemberg, D., Seibt, K., Capiotti, K., Da Silva, R. and Bonan, C. (2011). Zebrafish neurotransmitter systems as potential pharmacological and toxicological targets. *Neurotoxicology and Teratology*, **33**(6):608-617

Ries, M., & Sastre, M. (2016). Mechanisms of Aβ Clearance and Degradation by Glial Cells. *Frontiers in Aging Neuroscience*, **8**:160

Ro, S.H., Jung, C.H., Hahn, W.S., Xu, X., Kim, Y.M., Yun, Y.S., Park, J.M., Kim, K.H., Seo, M., Ha, T.Y., Arriaga, E.A., Bernlohr, D.A., Kim, D.H. (2013). Distinct functions of Ulk1 and Ulk2 in the regulation of lipid metabolism in adipocytes. Autophagy, 9(12):2103-14

Roberson, E., Scearce-Levie, K., Palop, J., Yan, F., Cheng, I., Wu, T., Gerstein, H., Yu, G. and Mucke, L. (2007). Reducing Endogenous Tau Ameliorates Amyloid -Induced Deficits in an Alzheimer's Disease Mouse Model. *Science*, 316(5825), pp.750-754.

Rodríguez-Arellano, J., Parpura, V., Zorec, R. and Verkhratsky, A. (2016). Astrocytes in physiological aging and Alzheimer's disease. *Neuroscience*, **323**:170-182

Rosner, M., Hanneder, M., Siegel, N., Valli, A., Fuchs, C., Hengstschlager, M. (2008) The mTOR pathway and its role in human genetic diseases. *Mutation Research*, **659**(3):284-292

Roth, A.D., Ramirez, G., Alarcon, R. and Bernhardi, R.V. (2005**).** Oligodendrocytes damage in Alzheimer's disease: Beta amyloid toxicity and inflammation. *Biological Research*, **38:**381-387

Rothman, S. (2010). How is the balance between protein synthesis and degradation achieved? *Theoretical Biology & Medical Modelling*, **7**: 25

Roy, S. and Rauk, A. (2005). Alzheimer's disease and the 'ABSENT' hypothesis: mechanism for amyloid beta endothelial and neuronal toxicity. *Medical Hypotheses*, **65**(1): 123-137

Rubenstein, J. L. R. (2011). Development of the Cerebral Cortex: Implications for Neurodevelopmental Disorders. *Journal of Child Psychology and Psychiatry, and Allied Disciplines*, **52**(4):339–355

Rubinstein, A. (2006). Zebrafish assays for drug toxicity screening. *Expert Opinion on Drug Metabolism & Toxicology*, **2**(2):231-240

Ruitenberg, A., Ott, A., van Swieten, J., Hofman, A. and Breteler, M. (2001). Incidence of dementia: does gender make a difference? *Neurobiology of Aging*, **22**(4):575-580

Rusanescu, G. and Mao, J. (2014). Notch3 is necessary for neuronal differentiation and maturation in the adult spinal cord. *Journal of Cellular and Molecular Medicine*, **18**(10):2103-2116

Rutten, J., Haan, J., Terwindt, G., van Duinen, S., Boon, E. and Lesnik Oberstein, S. (2014). Interpretation ofNOTCH3mutations in the diagnosis of CADASIL. *Expert Review of Molecular Diagnostics*, **14**(5):593-603

Sala, G., Marinig, D., Arosio, A., & Ferrarese, C. (2016). Role of Chaperone-Mediated Autophagy Dysfunctions in the Pathogenesis of Parkinson's Disease. *Frontiers in Molecular Neuroscience*, **9**:157

Sanders, D. W., Kaufman, S. K., DeVos, S. L., Sharma, A. M., Mirbaha, H., Li, A., Diamond, M. I. (2014). Distinct tau prion strains propagate in cells and mice and define different tauopathies. *Neuron*, **82**(6):1271–1288

Santana, S., Rico, E. P., & Burgos, J. S. (2012). Can zebrafish be used as animal model to study Alzheimer's disease? *American Journal of Neurodegenerative Disease*, **1**(1):32–48

Santos, R., Correia, S., Cardoso, S., Carvalho, C., Santos, M. and Moreira, P. (2011). Effects of rapamycin and TOR on aging and memory: implications for Alzheimer's disease. *Journal of Neurochemistry*, **117**(6):927-936

Saraceno, C., Musardo, S., Marcello, E., Pelucchi, S. and Luca, M. (2013). Modeling Alzheimer's disease: from past to future. *Frontiers in Pharmacology*, **4**

Sasaguri, H., Nilsson, P., Hashimoto, S., Nagata, K., Saito, T., De Strooper, B., Saido, T. C. (2017). APP mouse models for Alzheimer's disease preclinical studies. *The EMBO Journal*, **36**(17):2473–2487

Satizabal, C., Beiser, A., Chouraki, V., Chêne, G., Dufouil, C. and Seshadri, S. (2016). Incidence of Dementia over Three Decades in the Framingham Heart Study. *New England Journal of Medicine*, **374**(6): 523-532

Scahill, R., Schott, J., Stevens, J., Rossor, M. and Fox, N. (2002). Mapping the evolution of regional atrophy in Alzheimer's disease: Unbiased analysis of fluid-registered serial MRI. *Proceedings of the National Academy of Sciences*, **99**(7):4703-4707

Schaeffer, V., Lavenir, I., Ozcelik, S., Tolnay, M., Winkler, D. and Goedert, M. (2012). Stimulation of autophagy reduces neurodegeneration in a mouse model of human tauopathy. *Brain*, **135**(7):2169-2177

Scheuner, D., Eckman, C., Jensen, M., et al. (1996). Secreted amyloid beta-protein similar to that in the senile plaques of Alzheimer's disease is increased in vivo by the presenilin 1 and 2 and APP mutations linked to familial Alzheimer's disease. *Nature Medicine*, **2**:864-70

Schneider, J. L., & Cuervo, A. M. (2014). Liver Autophagy: much more than just taking out the trash. *Nature Reviews. Gastroenterology & Hepatology*, **11**(3), 187–200

Schneider, J., Arvanitakis, Z., Bang, W. and Bennett, D. (2007). Mixed brain pathologies account for most dementia cases in community-dwelling older persons. *Neurology*, **69**(24):2197-2204

Scott, R. C., Juhász, G., & Neufeld, T. P. (2007). Direct induction of autophagy by Atg1 inhibits cell growth and induces apoptotic cell death. *Current Biology : CB*, **17**(1):1–11

Selkoe, D. and Hardy, J. (2016). The amyloid hypothesis of Alzheimer's disease at 25 years. *EMBO Molecular Medicine*, **8**(6):595-608.Selkoe, D., Podlisny, M., Joachim, C., Vickers, E., Lee, G., Fritz, L. and Oltersdorf, T. (1988). Beta-amyloid precursor protein of Alzheimer disease occurs as 110- to 135-kilodalton membrane-associated proteins in neural and nonneural tissues. *Proceedings of the National Academy of Sciences*, **85**(19):7341-7345

Sengupta, U., Portelius, E., Hansson, O., Farmer, K., Castillo-Carranza, D., Woltjer, R., Kayed, R. (2017). Tau oligomers in cerebrospinal fluid in Alzheimer's disease. *Annals of Clinical and Translational Neurology*, **4**(4):226–235

Serrano-Pozo, A., Frosch, M. P., Masliah, E., & Hyman, B. T. (2011). Neuropathological Alterations in Alzheimer Disease. *Cold Spring Harbor Perspectives in Medicine:* **1**(1):a006189

Shang, L., Chen, S., Du, F., Li, S., Zhao, L. and Wang, X. (2011). Nutrient starvation elicits an acute autophagic response mediated by Ulk1

dephosphorylation and its subsequent dissociation from AMPK. *Proceedings of the National Academy of Sciences*, **108**(12):4788-4793

Sherwin, B. (2003). Estrogen and cognitive functioning in women. *Endocrine Reviews*, 24(2):133-151.

Shigetomi, E. (2004). Action Potential-Independent Release of Glutamate by Ca2+ Entry through Presynaptic P2X Receptors Elicits Postsynaptic Firing in the Brainstem Autonomic Network. *Journal of Neuroscience*, **24**(12):3125-3135

Siemers, E. R., Sundell, K. L., Carlson, C. *et al.* (2016) Phase 3 solanezumab trials: secondary outcomes in mild Alzheimer's disease patients. *Alzheimers Dementia.* **12**, 110–120

Šimić, G. (2002). Pathological tau proteins in argyrophilic grain disease. *The Lancet Neurology*, **1**(5):276

Šimić, G., Babić Leko, M., Wray, S., Harrington, C., Delalle, I., Jovanov-Milošević, N., Bažadona, D., Buée, L., de Silva, R., Di Giovanni, G., Wischik, C. and Hof, P. (2016). Tau Protein Hyperphosphorylation and Aggregation in Alzheimer's Disease and Other Tauopathies, and Possible Neuroprotective Strategies. *Biomolecules*, **6**(1):6

Sofroniew, M. and Vinters, H. (2009). Astrocytes: biology and pathology. *Acta Neuropathologica*, **119**(1):7-35

Son, J.H., Shim, J.H., Kim, K.H., Ha,J.Y., Han, J.Y. (2012). Neuronal autophagy and neurodegenerative diseases. *Experimental and Molecular Medicine*, **44**(2):89-98

Song, L., Lu, S. X., Ouyang, X., Melchor, J., Lee, J., Terracina, G., Zhang, L. (2015). Analysis of tau post-translational modifications in rTg4510 mice, a model of tau pathology. *Molecular Neurodegeneration*, **10**:14

Song-Lin Ding, S.L. (2013) Comparative anatomy of the prosubiculum, subiculum, presubiculum, postsubiculum, and parasubiculum in human, monkey, and rodent. *Journal of Comparative Neurology,* **521**(18), 4145–4162

Spencer, B., Potkar, R., Trejo, M., Rockenstein, E., Patrick, C., Gindi, R., *et al.* (2009). Beclin 1 gene transfer activates autophagy and ameliorates the neurodegenerative pathology in alphasynuclein models of Parkinson's and Lewy body diseases. *Journal of Neuroscience*, **29**:13578-88

Sperling, R. A., Aisen, P. S., Beckett, L. A. *et al.* (2011) Toward defining the preclinical stages of Alzheimer's disease: recommendations from the National Institute on Aging-Alzheimer's Association workgroups on diagnostic guidelines for Alzheimer's disease. *Alzheimers Dementia.* **7**:280–292

Spillantini, M. G., Crowther, R. A., Jakes, R., Hasegawa, M., & Goedert, M. (1998). α-Synuclein in filamentous inclusions of Lewy bodies from Parkinson's disease and dementia with Lewy bodies. *Proceedings of the*

National Academy of Sciences of the United States of America, **95**(11):6469–6473

Spilman, P., Podlutskaya, N., Hart, M., Debnath, J., Gorostiza, O., Bredesen, D., Richardson, A., Strong, R. and Galvan, V. (2010). Inhibition of mTOR by Rapamycin Abolishes Cognitive Deficits and Reduces Amyloid-β Levels in a Mouse Model of Alzheimer's Disease. *PLoS ONE*, **5**(4):e9979

Stalder, M., Phinney, A., Probst, A., Sommer, B., Staufenbiel, M. and Jucker, M. (1999). Association of Microglia with Amyloid Plaques in Brains of APP23 Transgenic Mice. *The American Journal of Pathology*, **154**(6):1673-1684

Strazielle, N. Ghersi-Egea, J.F. (2000). Choroid plexus in the central nervous syste: biology and physiopathology. *Journal of neuropathology and experimental Neurology*, **59** (7): 561-74

Stromhaug, P.E., Reggiori, F., Guan, J., Wang, C.W., Klionsky, D.J. (2004). Atg21 is a phosphoinositide binding protein required for efficient lipidation and localization of Atg8 during uptake of aminopeptidase I by selective autophagy. *Molecular and Biology of Cell*, **15**:3553–66

Sturchler-Pierrat, C., Abramowski, D., Duke, M., Wiederhold, K.-H., Mistl, C., Rothacher, S., Sommer, B. (1997). Two amyloid precursor protein transgenic mouse models with Alzheimer disease-like pathology. *Proceedings of the National Academy of Sciences of the United States of America*, **94**(24), 13287–13292

Sun, D., and Jakobs, T. C. (2012). Structural Remodeling of Astrocytes in the Injured CNS. *The Neuroscientist : A Review Journal Bringing Neurobiology, Neurology and Psychiatry*, **18**(6), 567–588

Swerdlow, R.H. (2007). Pathogenesis of Alzheimer's disease. *Clinical Interventions in Aging*, **2**(3):347-359

Talboom, J., Velazquez, R. and Oddo, S. (2015). The mammalian target of rapamycin at the crossroad between cognitive aging and Alzheimer's disease. *npj Aging and Mechanisms of Disease*, **1**(1)

Tan, F. H. P., & Azzam, G. (2017). *Drosophila melanogaster*: Deciphering Alzheimer's Disease. *The Malaysian Journal of Medical Sciences : MJMS*, **24**(2):6–20

Tan, Y., Deng, Y., & Qing, H. (2012). Calcium channel blockers and Alzheimer's disease. *Neural Regeneration Research*, **7**(2):137–140

Tanghe, A., Annelies, T., Merchiers, P. (2010). Pathological hallmarks, clinical parallels and value for drug testing in Alzheimer's Disease of the APP [V717I] London Transgenic Mouse Model. *International Journal of Alzheimer's Disease*, **2010**:1-9

Taniguchi, S., Fujita, Y., Hayashi, S., Kakita, A., Takahashi, H., Murayama, S., Saido, T., Hisanaga, S., Iwatsubo, T. and Hasegawa, M. (2001). Calpain-mediated degradation of p35 to p25 in postmortem human and rat brains. *FEBS Letters*, **489**(1):46-50

Tanik, S., Schultheiss, C., Volpicelli-Daley, L., Brunden, K. and Lee, V. (2013). Lewy Body-like α-Synuclein Aggregates Resist Degradation and Impair Macroautophagy. *Journal of Biological Chemistry*, **288**(21):15194-15210

Tarasoff-Conway, J. M., Carare, R. O., Osorio, R. S., Glodzik, L., Butler, T., Fieremans, E., de Leon, M. J. (2015). Clearance systems in the brain—implications for Alzheimer disease. *Nature Reviews. Neurology*, **11**(8):457–470

Tarassishin, L., Yin, Y.I., Bassit, B., Li, Y.M. (2004). Processing of Notch and amyloid precursor protein by γ-secretase is spatially distinct. *Proc Natl Acad Sci U.S.A.,* **101**(49): 17050-17055.

Tejera, D. and T. Heneka, M. (2016). Microglia in Alzheimer's Disease: The Good, the Bad and the Ugly. *Current Alzheimer Research*, **13**(4):370-380

Terry, R.D. (2006). Alzheimer's disease and the Aging Brain. *Journal of Geriatric Psychiatry and Neurology*, **19** (3):125-128

Thakur, A., Wang, X., Siedlak, S.L., Perry, G., Smith, M.A., Zhu, X. (2007). C-Jun phosphorylation in Alzheimer disease. *Journal of Neuroscience*, **85**: 1668–1673

Thomson, A. M. (2010). Neocortical Layer 6, a Review. *Frontiers in Neuroanatomy*, **4**:13

Toyonaga, T., Matsuura, M., Mori, K., Honzawa, Y., Minami, N., Yamada, S., Nakase, H. (2016). Lipocalin 2 prevents intestinal inflammation by enhancing phagocytic bacterial clearance in macrophages. *Scientific Reports*, **6**:35014

Tran, S., Nowicki, M., Chatterjee, D. and Gerlai, R. (2015). Acute and chronic ethanol exposure differentially alters alcohol dehydrogenase and aldehyde dehydrogenase activity in the zebrafish liver. *Progress in Neuro-Psychopharmacology and Biological Psychiatry*, **56**:221-226

Treweek, J., Dickerson, T. and Janda, K. (2009). Drugs of Abuse That Mediate Advanced Glycation End Product Formation: A Chemical Link to Disease Pathology. *Accounts of Chemical Research*, **42**(5):659-669

Vakifahmetoglu-Norberg, H., Kim, M., Xia, H., Iwanicki, M., Ofengeim, D., Coloff, J., Pan, L., Ince, T., Kroemer, G., Brugge, J. and Yuan, J. (2013). Chaperone-mediated autophagy degrades mutant p53. *Genes & Development*, **27**(15):1718-1730

Van Eldik, L., Carrillo, M., Cole, P., Feuerbach, D., Greenberg, B., Hendrix, J., Kennedy, M., Kozauer, N., Margolin, R., Molinuevo, J., Mueller, R., Ransohoff, R., Wilcock, D., Bain, L. and Bales, K. (2016). The roles of inflammation and immune mechanisms in Alzheimer's disease. *Alzheimer's & Dementia: Translational Research & Clinical Interventions*, **2**(2):99-10

van der Kant, R. and Goldstein, L. (2018). *Cellular Functions of the Amyloid Precursor Protein from Development to Dementia*

Vargas, M. R., Johnson, D. A., Sirkis, D. W., Messing, A., & Johnson, J. A. (2008). Nrf2 activation in astrocytes protects against neurodegeneration in mouse models of familial amyotrophic lateral sclerosis. *The Journal of Neuroscience : The Official Journal of the Society for Neuroscience*, **28**(50):13574–13581

Verghese, P. B., Castellano, J. M., & Holtzman, D. M. (2011). Roles of Apolipoprotein E in Alzheimer's Disease and Other Neurological Disorders. *Lancet Neurology*, **10**(3): 241–252

Verghese, P., Castellano, J. and Holtzman, D. (2011). Apolipoprotein E in Alzheimer's disease and other neurological disorders. *The Lancet Neurology*, **10**(3):241-252

Verkhratsky, A., Olabarria, M., Noristani, H., Yeh, C., and Rodriguez, J. (2010). Astrocytes in Alzheimer's disease. *Neurotherapeutics*, **7**(4), 399-412

Vogiatzi, T., Xilouri, M., Vekrellis, K., Stefanis, L. (2008). Wild type alpha-synuclein is degraded by chaperone-mediated autophagy and macroautophagy in neuronal cells. *Journal of Biological Chemistry*, **283**:23542-56

von Arnim, C., Verstege, E., Etrich, S. and Riepe, M. (2006). Mechanisms of hypoxic tolerance in presymptomatic APP23 transgenic mice. *Mechanisms of Ageing and Development*, **127**(2):109-114

von Muhlinen N, Thurston T, Ryzhakov G, Bloor S, Randow F. (2010). NDP52, a novel autophagy receptor for ubiquitin-decorated cytosolic bacteria. Autophagy, **6**(2):288-9

Vosler, P., Brennan, C. and Chen, J. (2008). Calpain-Mediated Signaling Mechanisms in Neuronal Injury and Neurodegeneration. *Molecular Neurobiology*, **38**(1):78-100

Wang, I., Guo, B., Liu, Y., Wu, C., Yang, C., Tsai, K. and Shen, C. (2012). Autophagy activators rescue and alleviate pathogenesis of a mouse model with proteinopathies of the TAR DNA-binding protein 43. *Proceedings of the National Academy of Sciences*, **109**(37):15024-15029

Wang, Q.J., Ding, Y., Kohtz, S., Mizushima, N., Cristea, I.M., Rout, M.P., Chait, B.T., Zhong, Y., Heintz, N. and Yue, Z. (2006). Induction of Autophagy in Axonal Dystrophy and Degeneration. *Neurobiology of Disease*, **26** (31): 8057-8068

Wang, X., Blanchard, J., Grundke-Iqbal, I. and Iqbal K. (2015). Memantine attenuates Alzheimer's disease-like pathology and cognitive impairment. *PLoS ONE*, **10**(12): e0145441

Wang, Y. and Mandelkow, E. (2015). Tau in physiology and pathology. *Nature Reviews Neuroscience*, **17**(1):22-35

Wang, Y., Martinez-Vicente, M., Kruger, U., et al. (2009). Tau fragmentation, aggregation and clearance: the dual role of lysosomal processing. *Human Molecular Genetics*, **18**:4153-4170

Wang, Y., Martinez-Vicente, M., Krüger, U., Kaushik, S., Wong, E., Mandelkow, E.-M., Mandelkow, E. (2009). Tau fragmentation, aggregation and clearance: the dual role of lysosomal processing. *Human Molecular Genetics*, **18**(21):4153–4170

Wang, Y., Pan, L., Moens, C. B., & Appel, B. (2014). Notch3 establishes brain vascular integrity by regulating pericyte number. *Development (Cambridge, England)*, **141**(2): 307–317

Wang, Y., Singh, R., Xiang, Y., & Czaja, M. J. (2010). Macroautophagy and chaperone-mediated autophagy are required for hepatocytes resistance to oxidant stress. Hepatology, **52**(1):266–277

Whittington, A., Sharp, D. and Gunn, R. (2017). Spatiotemporal distribution of β-amyloid in Alzheimer's disease results from heterogeneous regional carrying capacities. *Journal of Nuclear Medicine*, pp.jnumed.**117**:194720

Wilcock, G., Gauthier, S., Frisoni, G., Jia, J., Hardlund, J., Moebius, H., Bentham, P., Kook, K., Schelter, B., Wischik, D., Davis, C., Staff, R., Vuksanovic, V., Ahearn, T., Bracoud, L., Shamsi, K., Marek, K., Seibyl, J., Riedel, G., Storey, J., Harrington, C. and Wischik, C. (2017). Potential of Low Dose Leuco-Methylthioninium Bis(Hydromethanesulphonate) (LMTM) Monotherapy for Treatment of Mild Alzheimer's Disease: Cohort Analysis as Modified Primary Outcome in a Phase III Clinical Trial. *Journal of Alzheimer's Disease*, 61(1):435-457.Wilkinson, D.G., Francis, P.T., Schwam, E., Payne-Parrish, J. (2004). Cholinesterase inhibitors used in the treatment of Alzheimer's disease: the relationship between pharmacological effects and clinical efficacy. *Drugs & Ageing*, 21(7): 453-78

Wilson, C. A., Murphy, D. D., Giasson, B. I., Zhang, B., Trojanowski, J. Q., & Lee, V. M.-Y. (2004). Degradative organelles containing mislocalized α- and β-synuclein proliferate in presenilin-1 null neurons. *The Journal of Cell Biology*, **165**(3):335–346

Wobst, H., Denk, F., Oliver, P., Livieratos, A., Taylor, T., Knudsen, M., Bengoa-Vergniory, N., Bannerman, D. and Wade-Martins, R. (2017). Increased 4R tau expression and behavioural changes in a novel MAPT-N296H genomic mouse model of tauopathy. *Scientific Reports*, **7**:43198

Wolfe, M.S. (2012). The Role of Tau in Neurodegenerative Diseases and Its Potential as a Therapeutic Target. *Scientifica*, **2012**:1-20

Wong, A.S.L., Cheung, Z.H. and Ip, N.Y. (2011). Molecular machinery of macroautophagy and its deregulation in diseases. *Biochimica et Biophysica Acta (BBA),* **1812**(11):1490-97

Wood, H. (2017). Alzheimer disease: Peripheral Aβ clearance — a therapeutic strategy for AD? *Nature Reviews Neurology*, **13**(7):386-386.

Wray, S. (2017). Modeling tau pathology in human stem cell derived neurons. *Brain Pathology*, **27**(4):525-529

Wu, H., Chen, S., Ammar, A., Xu, J., Wu, Q., Pan, K., Zhang, J. and Hong, Y. (2014). Crosstalk between macroautophagy and Chaperone-Mediated

Autophagy: Implications for the treatment of neurological diseases. *Molecular Neurobiology*, **52**(3):1284-1296

Wu, Y., Brayne, C. and Matthews, F. (2015). Prevalence of dementia in East Asia: a synthetic review of time trends. *International Journal of Geriatric Psychiatry*, **30**(8):793-801

Yagi, T., Ito, D., Okada, Y., Akamatsu, W., Nihei, Y., Yoshizaki, T., Yamanaka, S., Okano, H. and Suzuki, N. (2011). Modeling familial Alzheimer's disease with induced pluripotent stem cells. *Human Molecular Genetics*, **20**(23):4530-4539

Yagihashi, S., Mizukami, H., & Sugimoto, K. (2011). Mechanism of diabetic neuropathy: Where are we now and where to go? *Journal of Diabetes Investigation*, **2**(1):18–32

Yamashima, T. (2004). Ca2+-dependent proteases in ischemic neuronal death. *Cell Calcium*, **36**(3-4):285-293

Yamashima, T. (2012). Hsp70.1 and related lysosomal factors for necrotic neuronal death. *Journal of Neurochemistry*, **120**(4):477-494

Yang, Y., Chen, S., Zhang, Y., Lin, X., Song, Y., Xue, Z., Qian, H., Wang, S., Wan, G., Zheng, X. and Zhang, L. (2017). Induction of autophagy by spermidine is neuroprotective via inhibition of caspase 3-mediated Beclin 1 cleavage. *Cell Death & Disease*, **8**(4):e2738-e2738

Yang, Z., & Klionsky, D. J. (2009). An Overview of the Molecular Mechanism of Autophagy. *Current Topics in Microbiology and Immunology*, **335**:1–32

Yoo, M., Kawamata, H., Kim, D., Chun, H. and Son, J. (2004). Experimental Strategy to Identify Genes Susceptible to Oxidative Stress in Nigral Dopaminergic Neurons. *Neurochemical Research*, **29**(6):1223-1234

Yorimitsu, T., Klionsky, D.J. (2005). Autophagy: molecular machinery for self-eating. *Cell Death and Differentiation*, **12**:1542–52

Yu, W.H., Cuervo, A.M., Kumar, A., Peterhoff, C.M., Schmidt, S.D., Lee, J.H., *et al.* (2005). Macroautophagy--a novel Beta-amyloid peptide-generating pathway activated in Alzheimer's disease. *Journal of Cell Biology*, **171**:87-98

Yu, Y., Feng, L., Li, J., Lan, X., A, L., Lv, X., Zhang, M. and Chen, L. (2017). The alteration of autophagy and apoptosis in the hippocampus of rats with natural aging-dependent cognitive deficits. *Behavioural Brain Research*, **334**:155-162

Yue, Z., Friedman, L., Komatsu, M., Tanaka, K. (2009). The cellular pathways of neuronal autophagy and their implication in neurodegenerative diseases. *Biochimica et Biophysica Acta (BBA)- Molecular Cell Research,* 1793 (9): 1496-1507

Yurinskaya, M., Mit'kevich, V., Barykin, E., Garbuz, D., Evgen'ev, M., Makarov, A. and Vinokurov, M. (2015). Heat-shock protein HSP70 protects neuroblastoma cells SK-N-SH from the neurotoxic effects of hydrogen peroxide and the β-amyloid peptide. *Molecular Biology*, **49**(6):924-927

Zhang, D., Hu, X. M., Qian, L., O'Callaghan, J. P., & Hong, J. S. (2010). Astrogliosis in CNS Pathologies: Is There A Role for Microglia? *Molecular Neurobiology*, **41**(2-3):232-241

Zhang, D., Pekkanen-Mattila, M., Shahsavani, M., Falk, A., Teixeira, A. and Herland, A. (2014). A 3D Alzheimer's disease culture model and the induction of P21-activated kinase mediated sensing in iPSC derived neurons. *Biomaterials*, **35**(5):1420-1428

Zhang, X., Li, L., Chen, S., Yang, D., Wang, Y., Zhang, X., Wang, Z., Le, W. (2011). Rapamycin treatment augments motor neuron degeneration in SOD1 (G93A) mouse model of amyotrophic lateral sclerosis. *Autophagy*, **7**(4):412-25

Zhang, Y., Schuff, N., Du, A., Rosen, H., Kramer, J., Gorno-Tempini, M., Miller, B. and Weiner, M. (2009). White matter damage in frontotemporal dementia and Alzheimer's disease measured by diffusion MRI. *Brain*, **132**(9):2579-2592

Zhao, M., & Klionsky, D. J. (2011). AMPK-dependent phosphorylation of ULK1 induces autophagy. *Cell Metabolism*, *13*(2):119–120

Zhu, H., Yoshimoto, T., & Yamashima, T. (2014). Heat Shock Protein 70.1 (Hsp70.1) Affects Neuronal Cell Fate by Regulating Lysosomal Acid Sphingomyelinase. *The Journal of Biological Chemistry*, **289**(40):27432–27443

Zhu, H., Yoshimoto, T., Imajo-Ohmi, S., Dazortsava, M., Mathivanan, A. and Yamashima, T. (2012). Why are hippocampal CA1 neurons vulnerable but motor cortex neurons resistant to transient ischemia? *Journal of Neurochemistry*, **120**(4):574-585

Zhu, X.-C., Tan, L., Wang, H.-F., Jiang, T., Cao, L., Wang, C., Yu, J.-T. (2015). Rate of early onset Alzheimer's disease: a systematic review and meta-analysis. *Annals of Translational Medicine*, **3**(3):38

Zuroff, L., Daley, D., Black, K. and Koronyo-Hamaoui, M. (2017). Clearance of cerebral Aβ in Alzheimer's disease: reassessing the role of microglia and monocytes. *Cellular and Molecular Life Sciences*, **74**(12):2167-2201

Supplementary

Supplementary figures:
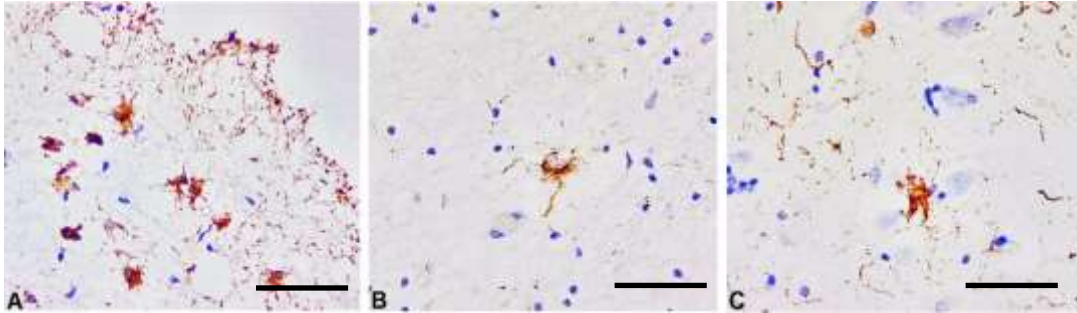
Supplementary figure 1. Astrocytes identified in different regions stained by AT8 antibody. Subpial region within LEC (A); in the white matter (B) and in the grey matter (C); Magnification 10X (A) and 100X (B, C); Scale bars 100µm (A) and 50µm (B, C).
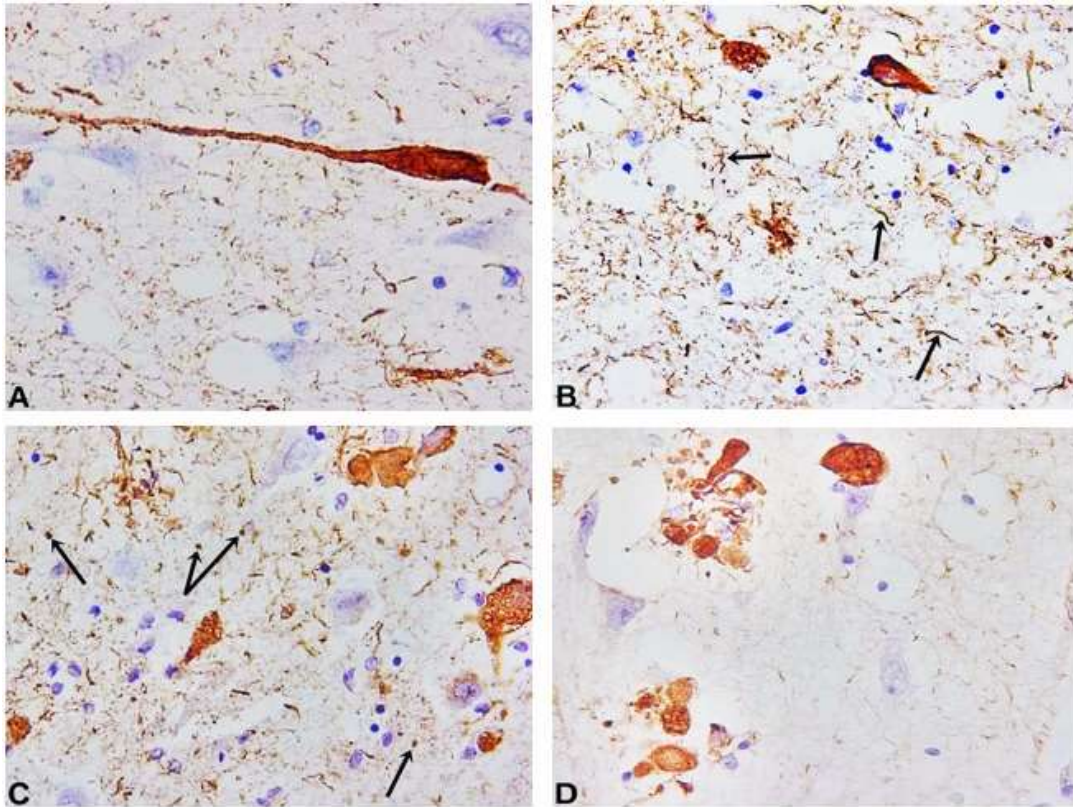
Supplemetary figure 0. Tau lesions stained by AT8 antibody. Axonal staining in CA4 (A); high background of NTh in CA1 (B) with numerous severely stained grains in CA2 (C). Many NP were observed (D); Magnification 400X; Scale bar 200µm.
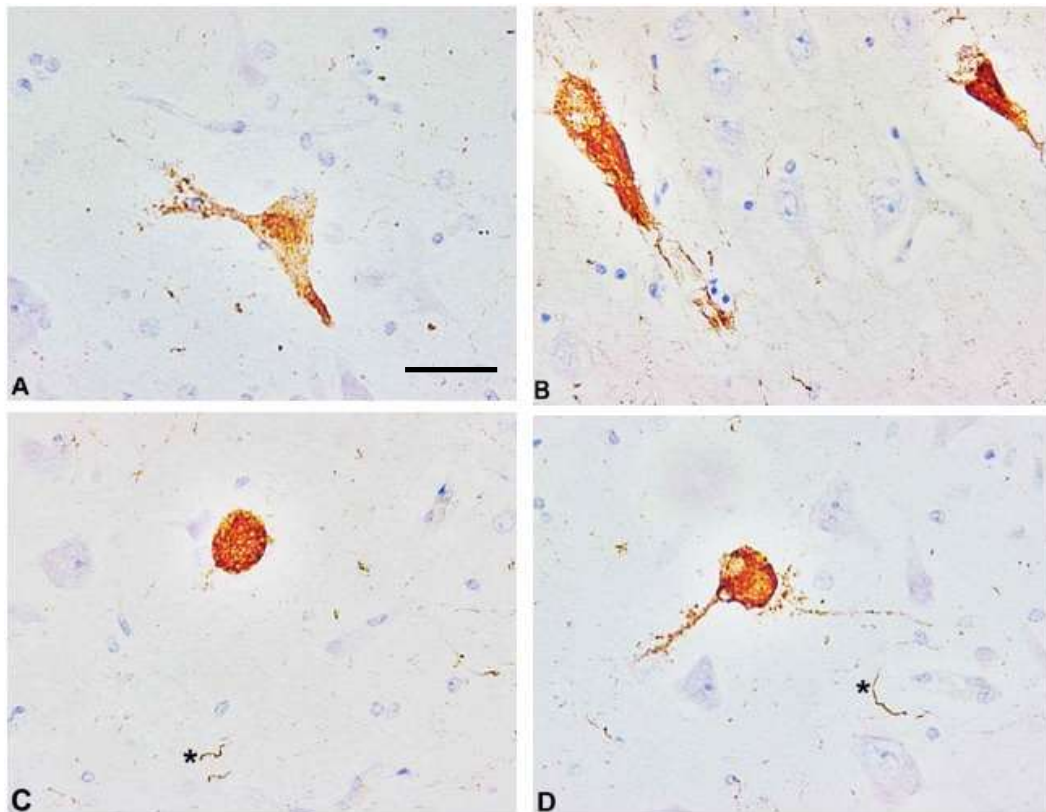
Supplementary figure 3. NFT morphologies stained by AT8 antibody.
Granular NFT in CA4 (A); flame-shaped NFT in CA2 (B), ballooned achromatic neuron in CA1 (C) and globose NFT in CA1 (D) *presence of NTh; Magnification 100X; Scale bar 50µm.
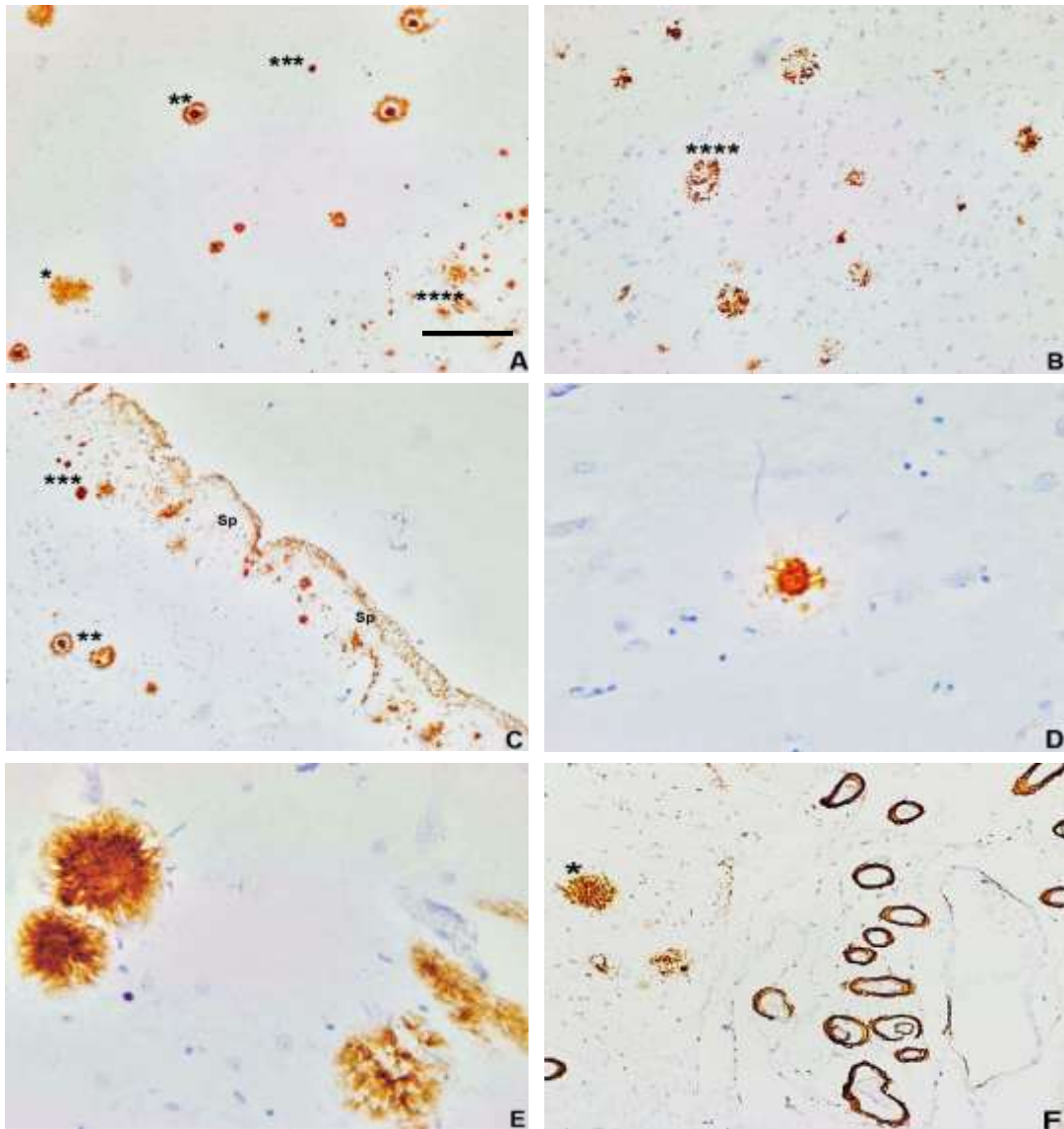
Supplementary figure 4. Aβ plaques and other morphologies stained by Aβ antibody. All types of plaques *diffuse **cored ***compact ****patchy/powdery (A) Numerous patchy/powdery plaques (B) and compact, diffuse plaques in MEC, with severe pathology in the subpial region (C). A cored plaque with the ring-like structure becoming fade while the central compact cored remains intact (D). Very large diffuse plaques with fibrillary edges (E). Advanced CAA in the collateral sulcus between LEC and TC (F); Magnification 10X; Scale bars 100μm.